Relating Ride Quality and Structural Adequacy for Pavement Rehabilitation/Design Decisions

PUBLICATION NO. FHWA-HRT-12-035 NOVEMBER 2012

U.S. Department of Transportation
Federal Highway Administration

Research, Development, and Technology
Turner-Fairbank Highway Research Center
6300 Georgetown Pike
McLean, VA 22101-2296

LTPP

FOREWORD

As the highway community transitions to a performance-based approach to managing investments in pavement infrastructure, it is vitally important that potential performance measures and inter-relationships among performance measures be thoroughly examined to assess their applicability to the challenges of managing for performance. Ride quality and structural adequacy are two key pavement performance indicators. The relationship (or lack of relationship) between the two has been a topic of frequent and continuing discussion in the pavement community for many years. Data collected through the Federal Highway Administration's Long-Term Pavement Performance (LTPP) program has created an unprecedented opportunity to examine whether there is, in fact, a meaningful and consistent relationship between ride quality and structural adequacy, and to model that relationship if it exists. There would be substantial economic and engineering benefits to the pavement engineering community if such a relationship could be identified and definitively modeled. Likewise, if no such relationship exists, the pavement engineering community could focus on proper modeling of each of the individual indicators separately in order to improve network level decision making. This study was intended to develop and document a mechanism to include both ride quality and structural adequacy values within the context of current network-level pavement management systems for highway agency implementation to ensure smooth, structurally adequate pavements. To accomplish the objective, two major activities were carried out: (1) a literature search to gather, review, and synthesize available information on relating ride quality and structural adequacy and (2) a review and assessment of data from the LTPP program to determine if such a relationship exists. LTPP data was chosen for its quality, comprehensive coverage, and robust suite of supporting information necessary to conduct a national study. This report details the study methodology and findings including presentation of a conclusion to the question – are ride and structural adequacy related?

Jorge E. Pagán-Ortiz
Director, Office of Infrastructure
Research and Development

TECHNICAL REPORT DOCUMENTATION PAGE

1. Report No. FHWA-HRT- FHWA-HRT-12-035	2. Government Accession No.	3. Recipient's Catalog No.
4. Title and Subtitle Relating Ride Quality and Structural Adequacy for Pavement Rehabilitation/Design Decisions		5. Report Date November 2012 6. Performing Organization Code
7. Author(s) Rada, G.R., Ph.D., P.E., Perera, R., Ph.D., P.E., and Prabhakar, V., P.E.		8. Performing Organization Report No.
9. Performing Organization Name and Address Fugro Consultants, Inc. 8613 Cross Park Drive Austin, TX 78754		10. Work Unit No. (TRAIS) 11. Contract or Grant No. DTFH61-08-D-00021-T-11001
12. Sponsoring Agency Name and Address Office of Infrastructure Research and Development Federal Highway Administration 6300 Georgetown Pike McLean, VA 22101-2296		13. Type of Report and Period Covered Final Report, December 2010–December 2011 14. Sponsoring Agency Code HRDI-30

15. Supplementary Notes
The task order manager was Larry Wiser. The Contracting Officer's Technical Representative (COTR) was Nadarajah Sivaneswaran (HRDI-30), the Contract Officer was Robin K. Hobbs, and the Contract Specialist was Sean Wybenga. The task order contractor was Fugro Consultants, Inc., with subcontractors Soil and Materials Engineers, Inc. and Woodward Communications, Inc.

16. Abstract
Ride quality and structural adequacy are key pavement performance indicators. The relationship between these two indicators has been a topic of frequent and continuing discussion in the pavement community, but an accepted and widely used relationship has not been identified to date. The objective of this project was to identify and verify the relationship between these two performance indicators, if any, using the Long-Term Pavement Performance (LTPP) program and other pavement performance data sources. This was done in an effort to improve the evaluation and use of pavement condition data in pavement rehabilitation and design decisions. More specifically, the project was intended to develop and document a mechanism to include both ride quality and structural adequacy values within the context of current network-level pavement management system practices for highway agency implementation to ensure smooth pavements that are also structurally adequate. Toward the accomplishment of the project objective, two major activities were carried out: (1) a literature search to gather, review, and synthesize available information on relating ride quality and structural adequacy and (2) a review and assessment of data from the LTPP program to determine if such a relationship exists. This report details those two activities as well as their major findings, observations, and conclusions. A viable relationship could not be identified.

17. Key Words Ride quality, Structural adequacy, Structural capacity, Pavement management systems, Pavement rehabilitation, Pavement design decisions		18. Distribution Statement No restrictions. This document is available to the public through the National Technical Information Service, Springfield, VA 22161.	
19. Security Classif. (of this report) Unclassified	20. Security Classif. (of this page) Unclassified	21. No. of Pages 179	22. Price N/A

Form DOT F 1700.7 (8-72) Reproduction of completed page authorized

SI* (MODERN METRIC) CONVERSION FACTORS

APPROXIMATE CONVERSIONS TO SI UNITS

Symbol	When You Know	Multiply By	To Find	Symbol
		LENGTH		
in	inches	25.4	millimeters	mm
ft	feet	0.305	meters	m
yd	yards	0.914	meters	m
mi	miles	1.61	kilometers	km
		AREA		
in^2	square inches	645.2	square millimeters	mm^2
ft^2	square feet	0.093	square meters	m^2
yd^2	square yard	0.836	square meters	m^2
ac	acres	0.405	hectares	ha
mi^2	square miles	2.59	square kilometers	km^2
		VOLUME		
fl oz	fluid ounces	29.57	milliliters	mL
gal	gallons	3.785	liters	L
ft^3	cubic feet	0.028	cubic meters	m^3
yd^3	cubic yards	0.765	cubic meters	m^3
		NOTE: volumes greater than 1000 L shall be shown in m^3		
		MASS		
oz	ounces	28.35	grams	g
lb	pounds	0.454	kilograms	kg
T	short tons (2000 lb)	0.907	megagrams (or "metric ton")	Mg (or "t")
		TEMPERATURE (exact degrees)		
°F	Fahrenheit	5 (F-32)/9 or (F-32)/1.8	Celsius	°C
		ILLUMINATION		
fc	foot-candles	10.76	lux	lx
fl	foot-Lamberts	3.426	candela/m^2	cd/m^2
		FORCE and PRESSURE or STRESS		
lbf	poundforce	4.45	newtons	N
lbf/in^2	poundforce per square inch	6.89	kilopascals	kPa

APPROXIMATE CONVERSIONS FROM SI UNITS

Symbol	When You Know	Multiply By	To Find	Symbol
		LENGTH		
mm	millimeters	0.039	inches	in
m	meters	3.28	feet	ft
m	meters	1.09	yards	yd
km	kilometers	0.621	miles	mi
		AREA		
mm^2	square millimeters	0.0016	square inches	in^2
m^2	square meters	10.764	square feet	ft^2
m^2	square meters	1.195	square yards	yd^2
ha	hectares	2.47	acres	ac
km^2	square kilometers	0.386	square miles	mi^2
		VOLUME		
mL	milliliters	0.034	fluid ounces	fl oz
L	liters	0.264	gallons	gal
m^3	cubic meters	35.314	cubic feet	ft^3
m^3	cubic meters	1.307	cubic yards	yd^3
		MASS		
g	grams	0.035	ounces	oz
kg	kilograms	2.202	pounds	lb
Mg (or "t")	megagrams (or "metric	1.103	short tons (2000 lb)	T
		TEMPERATURE (exact degrees)		
°C	Celsius	1.8C+32	Fahrenheit	°F
		ILLUMINATION		
lx	lux	0.0929	foot-candles	fc
cd/m^2	candela/m^2	0.2919	foot-Lamberts	fl
		FORCE and PRESSURE or STRESS		
N	newtons	0.225	poundforce	lbf
kPa	kilopascals	0.145	poundforce per square inch	lbf/in^2

*SI is the symbol for the International System of Units. Appropriate rounding should be made to comply with Section 4 of ASTM E380. (Revised March 2003)

TABLE OF CONTENTS

LIST OF FIGURES

LIST OF TABLES

CHAPTER 1. INTRODUCTION

1.1 PAVEMENT REHABILITATION AND DESIGN DECISIONS

State highway agencies spend billions of dollars each year on transportation infrastructure assets to meet legislative, agency, and public expectations. Pavements are a major component of those transportation assets, and pavement rehabilitation—preserving pavements to extend their service life and, more importantly, to improve motorists' safety and satisfaction—is one of the most critical, costly, and complex elements. This is especially true at a time when a large percentage of pavement networks are reaching the end of their serviceable life and pavement rehabilitation has become even more daunting given the funding constraints faced by highway agencies.

In recognition of the importance of pavement rehabilitation, Federal, State, and local policies, mandates, procedures, and initiatives are in place to help ensure pavement rehabilitation is done in a systematic, well-thought-out manner. All State transportation departments, for example, must prepare a Statewide Transportation Improvement Program (STIP), which is a multimodal, multiyear financial document listing all projects expected to be funded with Federal participation and updated periodically. Only those projects for which construction and operating funds can reasonably be expected to be available are included in STIP, and, without STIP inclusion, a project is ineligible for Federal funding.

Although the policies, procedures, mandates, and initiatives vary from one State transportation department to another, the generic approach to pavement rehabilitation decisions is similar. Decisions on pavement rehabilitation projects to be carried out in any given construction year are done centrally at the top of the department organization, where pavement rehabilitation projects compete for funding with the needs of other transportation assets, including new pavement construction. In the case of federally funded rehabilitation projects, these decisions are made as part of STIP. In addition, decisions are typically made based on work performed over the course of many years (e.g., pavement condition surveys on an annual basis or every 2 years), and those efforts enable the decisions. Moreover, these decisions generally rely on a pavement management system (PMS), which provides network-level condition scores for each pavement segment in the system and, on the basis of the score, establishes an initial action to be performed, ranging from no action to major rehabilitation or reconstruction.

After the selection of projects for pavement rehabilitation in a given construction year, the actual design of the rehabilitation is typically, but not always, turned over to districts or regions. The designs generally begin with a review of available historical data, collection of new data, and the generation of alternative rehabilitation strategies (often referred to as "pavement type selection"). The approach and level of sophistication in this design step varies from one State transportation department to another, but the principals are generally the same.

Once the various rehabilitation strategies have been defined, the final step typically entails the evaluation of those strategies and the selection of the optimal strategy using life-cycle cost analyses and other considerations. Again, the approach and level of sophistication in this evaluation step vary among State transportation departments, but the principles are generally the same.

The discussion so far has focused on the generic approach to rehabilitation decisions by State highway agencies. PMSs are at the center of those decisions. The term "PMS" was introduced in the mid-1960s to define a set of rational procedures that provide optimum pavement strategies based on predicted pavement performance, incorporating feedback regarding the various attributes, criteria, and constraints involved. Pavement management is, in essence, a coordinated systematic process for carrying out all activities related to providing pavements; it is a support tool that enables pavement engineers and managers to make better, more cost-effective decisions concerning pavement assets and their preservation. Key pavement management outcomes include the following:

- Formalization of pavement decisionmaking.
- Entire process to provide quality pavements.
- Strong emphasis on economics.
- Involvement of all associated groups—planning, design, construction, maintenance, materials, and field groups.
- Use of advanced tools and analysis techniques.

The first generation of PMSs was largely driven by pavement ride quality and distress as a direct result of the American Association of State Highway Officials (AASHO) Road Test, which introduced the concept of the Present Serviceability Rating (PSR) and the Present Serviceability Index (PSI). PSR represents the subjective rating of pavement serviceability on an arbitrary scale of 0 to 5. PSI is a more objective measure established through statistical analyses that relates the PSR to various pavement physical measurements—roughness, rutting, cracking, and patching. Without question, PSI is largely driven by pavement roughness.

With advances in technology, PMS began to move away from the present serviceability concept to the use of distress (cracking, rutting, etc.) and longitudinal roughness (typically in the form of the International Roughness Index (IRI)) as key pavement performance indicators in the decisionmaking process. Although both are important indicators that merit emphasis within the PMS process, they are not the only indicators. Structural adequacy, for example, is another important pavement performance indicator that is critical to making rational pavement rehabilitation decisions. Indeed, many State highway agencies are incorporating deflection testing as part of their routine PMS activities in recognition of the need to know about the structural adequacy of their pavements. This key pavement performance parameter and others, such as surface friction and noise, are being introduced in newer PMS generations.

1.2 RELATIONSHIP BETWEEN RIDE QUALITY AND STRUCTURAL ADEQUACY

In 1996, the U.S. Federal Highway Administration (FHWA) conducted a survey of how highway users judge roadways. The survey identified that the most important issue for highway users is roadway condition. Furthermore, studies of the AASHO Road Test showed that subjective evaluation of roadway condition by highway users is primarily judged by pavement roughness. Clearly, ride quality is a key performance indicator to highway users.

Moreover, research studies have shown that pavements that are built smooth generally have a longer service life. A study analyzing roughness trends in pavements under study by the Long-Term Pavement Performance (LTPP) program showed that with all other factors being equal, pavements follow a generally parallel trend of roughness development over time. Hence, those pavements built with better ride quality take longer to reach unacceptable levels of ride quality, and, subsequently, longer time will be required before rehabilitation.

Figure 1 shows the progression of roughness for a randomly selected set of asphalt pavements with an asphalt overlay from the LTPP database.[(1)] Each line in the figure represents a separate test section. As shown, test sections in the lower portion of the graph at an age of 0 years are also generally on the lower end of the graph toward the end of the timeline. The sections shown in the graph include sections from all over the United States and represent different environmental zones, subgrades, and rates of traffic. Accordingly, the progression of roughness would not be expected to be the same for all sections.

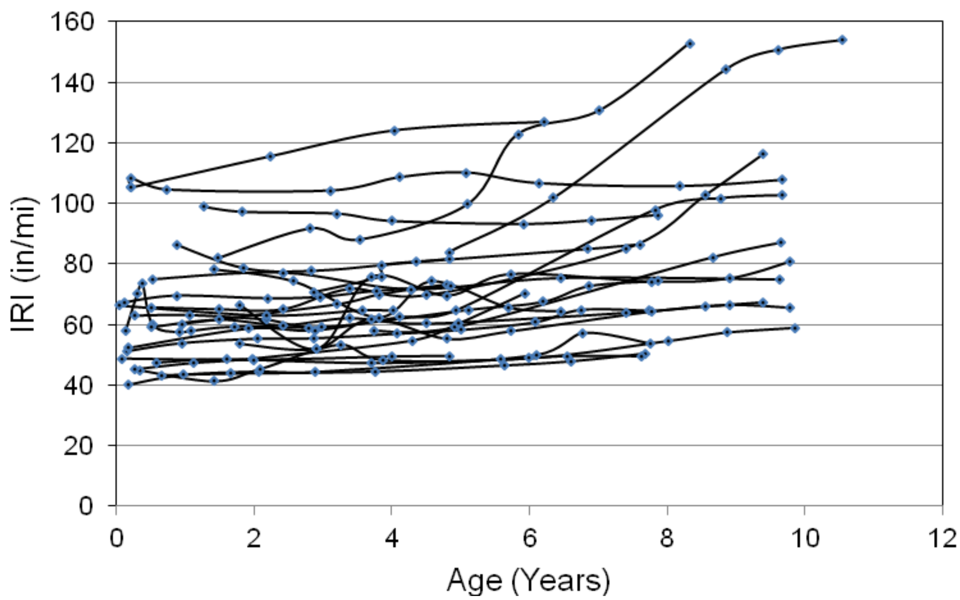

Figure 1. Graph. Progression of roughness on asphalt sections with asphalt overlay.

Prior to the development of inertial profilers, roughness data were collected using response-type roughness measuring systems, commonly referred to as roughometers (e.g., Portland Cement Association Road Meter, Mays meter, etc.). The CHLOE profilometer was used to collect roughness data in the AASHO Road Test. State highway agencies started using inertial profilers to collect network-level roughness in the 1980s. The most common measure of roughness for many years was slope variance, in large part because of the various correlations that were developed relating roughness to the American Association of State Highway and Transportation Officials (AASHTO) PSI. At present, the state of the practice in roughness data collection involves the use of inertial profilers with laser sensors, typically mounted on the front bumper at transverse locations corresponding to the wheel-paths. The roughness data shown in figure 1 were collected using this device. In addition, the index value most commonly used to represent pavement roughness is IRI.

As with roughness, nondestructive deflection testing for the structural evaluation of pavements has been used for more than half a century. Prior to the development of devices that applied a load onto the pavement surface and measured deflections at several locations, simpler devices, such as the Benkelman Beam, were used to measure the response of the pavement to a load in terms of a maximum deflection. With time and advances in technology, the pavement community started to measure multiple deflections at various radial distances from the center of the applied load (i.e., deflection basins). Since the 1980s, the most commonly used device has been the falling weight deflectometer (FWD). A number of equipment manufacturers produce or market FWDs, but all of them rely on impact loads to produce a response in the pavement similar to that produced by actual traffic loadings, which is then measured by multiple deflection sensors located at varying distances from the center of the load.

Although FWDs represent significant progress from the Benkelman Beam in terms of both quantity and quality of data gathered, FWDs are not without shortcomings. For one, they require stop-and-go rather than continuous operation. Lane closures are required, causing traffic disruptions. The amount of testing is significantly less than with continuous testing, which affects operational costs. To overcome these shortcomings, several organizations in the United States and Europe have developed devices that can continuously measure pavement deflections, such as the FHWA-funded rolling wheel deflectometer. However, FWDs presently represent the state of the practice as far as the structural capacity evaluation of pavements is concerned. Hence, further discussions in this report regarding deflections and structural adequacy are limited to FWDs.

As equipment technology has evolved, so have methods for analyzing deflection data, which allow for multiple complex algorithms to be used in real-time analysis of the deflection data. Many of the analysis techniques developed in the past, such as Boussinesq's one-layer and Burmeister's two-layer solutions, are still used today.[2,3] More complex and rational techniques have also been developed, such as finite-element solutions and dynamic analysis techniques, but because of their complexity, those procedures are most often used in research. By far, the method most often used for the analysis of deflection data is layered elastic theory, which generally works well but may have problems under certain conditions (e.g., composite pavements, thin layers, etc.). To make matters more complicated, most analysis techniques that use layered elastic solutions are heavily dependent on the user or the inputs provided. Results vary depending on the specific software used even if the inputs are all the same, and the results produced by the software require a significant amount of familiarity with the analysis technique used as well as engineering judgment.

Another factor making assessment of structural adequacy challenging is that pavement material properties change, sometimes drastically, with changes in surface and subsurface moisture and temperature conditions. Figure 2 shows changes in deflection for seven sensors at various radial distances over time at an LTPP Seasonal Monitoring Program (SMP) test section. The impact of moisture and temperature changes over time is clearly shown in this figure. Do ride quality or other performance indicators (e.g., distress and friction) change in a similar fashion?

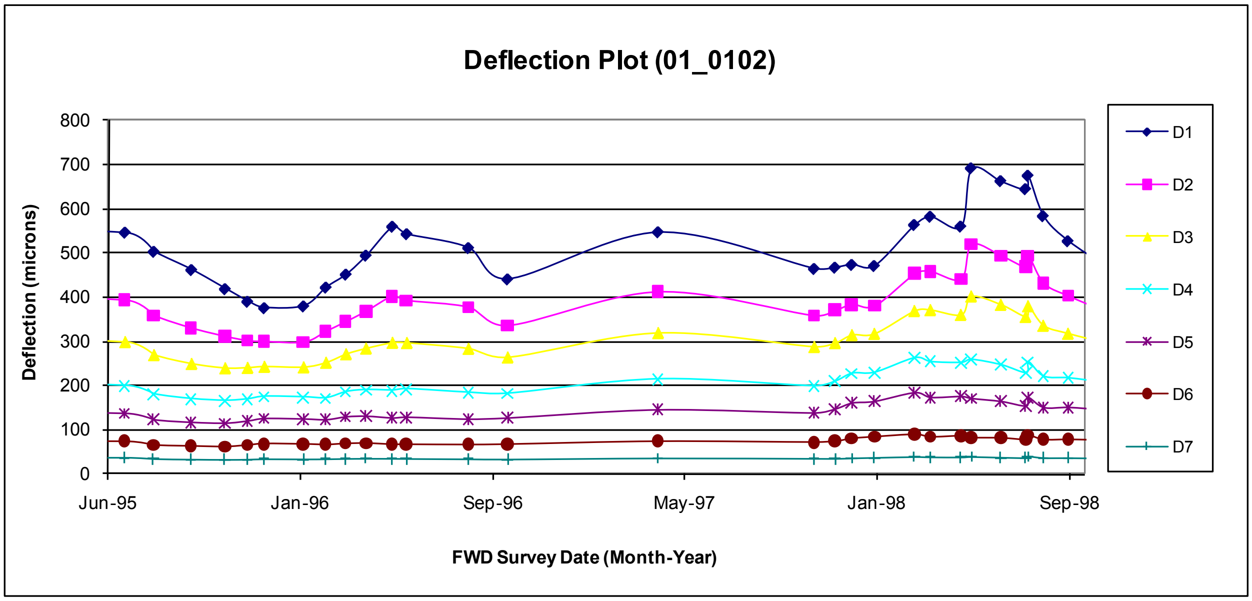

Figure 2. Graph. Changes in deflection over time at LTPP SMP test section.

In summary, ride quality and structural adequacy are key performance indicators, but the relationship between the two is a topic of frequent and continuing discussion in the pavement community. It can be argued that ride quality is not an indicator of structural strength because a pavement with low structural capacity can exist with adequate ride quality. However, if the pavement is not properly designed (for anticipated traffic, ambient conditions, etc.), distresses will likely develop quickly, which could result in an increase in roughness. It is possible that this increase in roughness could be related to structural capacity.

Alternatively, there is the case of a distressed pavement that has a high IRI value (e.g., 150 inches/mi). If a thin overly (e.g., 1.5 inches thick) is applied properly on that pavement, it will likely reduce the IRI (e.g., to 75 inches/mi). The overlay will certainly increase the structural capacity of the pavement, but only by a little. Moreover, the overlay could fail rapidly. Hence, it can be argued that there is no relationship between ride quality and structural adequacy, but there may be a relationship between deterioration of ride quality and structural adequacy of the pavement.

Table 1 shows the pavement structure of the LTPP Specific Pavement Study (SPS)-1 (new hot mix asphalt (HMA) pavement) test sections, and figure 3 and figure 4 show the roughness progression at some of the LTPP SPS-1 projects. All sections within a project appear to have close initial IRI values, but do sections that show a high rate of IRI deterioration have low structural capacity?

Table 1. Structural properties of SPS-1 test sections.

Test Section Number	HMA Thickness (inches)	Layer 2		Layer 3	
		Material	Thickness (inches)	Material	Thickness (inches)
1	7	DGAB	8	—	—
2	4	DGAB	12	—	—
3	4	ATB	8	—	—
4	7	ATB	12	—	—
5	4	ATB	4	DGAB	4
6	7	ATB	8	DGAB	4
7	4	PATB	4	DGAB	4
8	7	PATB	4	DGAB	8
9	7	PATB	4	DGAB	12
10	7	ATB	4	PATB	4
11	4	ATB	8	PATB	4
12	4	ATB	12	PATB	4
13	4	DGAB	8	—	—
14	7	DGAB	12	—	—
15	7	ATB	8	—	—
16	4	ATB	12	—	—
17	7	ATB	4	DGAB	4
18	4	ATB	8	DGAB	4
19	7	PATB	4	DGAB	4
20	4	PATB	4	DGAB	8
21	4	PATB	4	DGAB	12
22	4	ATB	4	PATB	4
23	7	ATB	8	PATB	4
24	7	ATB	12	PATB	4

— Indicates that there is no layer 3.
DGAB = Dense-graded aggregate base.
ATB = Asphalt-treated base.
PATB = Permeable asphalt-treated base.

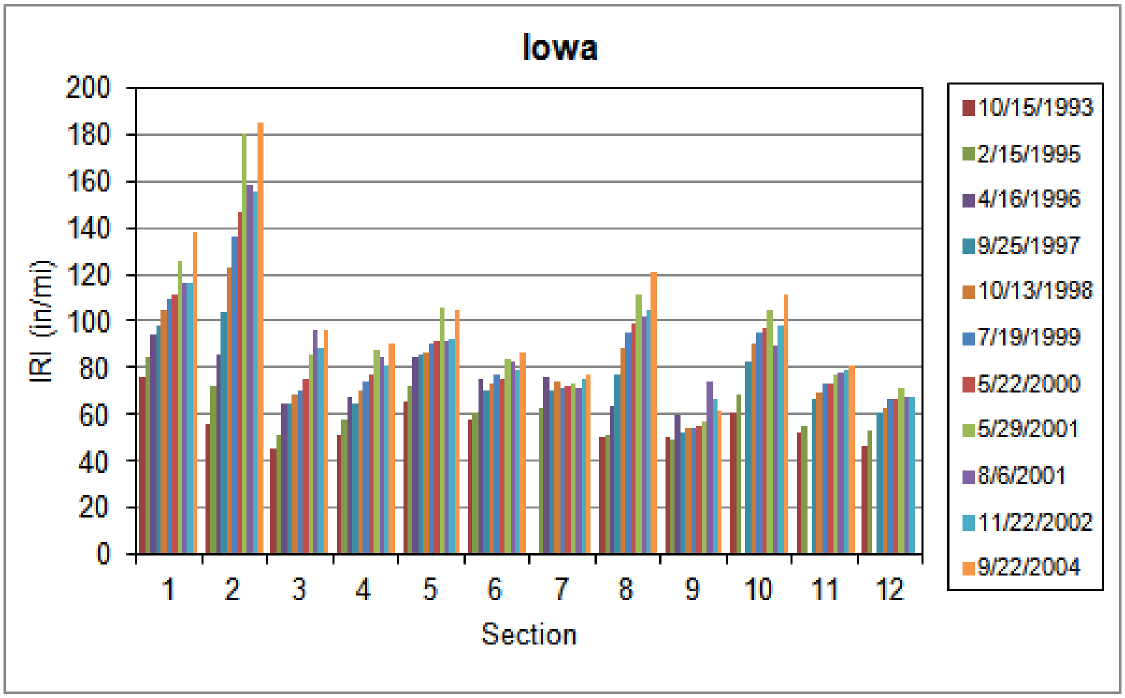

Figure 3. Graph. Changes in IRI over time for LTPP SPS-1 test sections in Iowa.

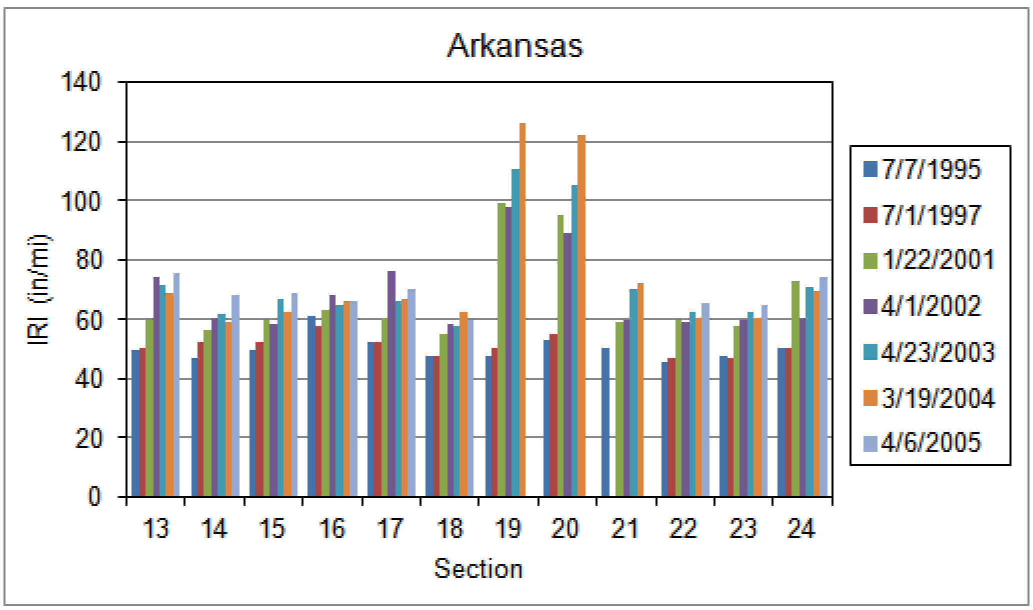

Figure 4. Graph. Changes in IRI over time for LTPP SPS-1 test sections in Arkansas.

Moreover, by looking at plots of performance over time, such as those shown in figure 5 through figure 11 for the LTPP SPS-1 test sections in Virginia and similar plots for both IRI and FWD deflections, it is possible to determine if there is a general relationship between changes in IRI and structural adequacy. The following figures are shown according to base material type—dense-graded aggregate base (DGAB), asphalt-treated base (ATB), and permeable asphalt-treated base (PATB).

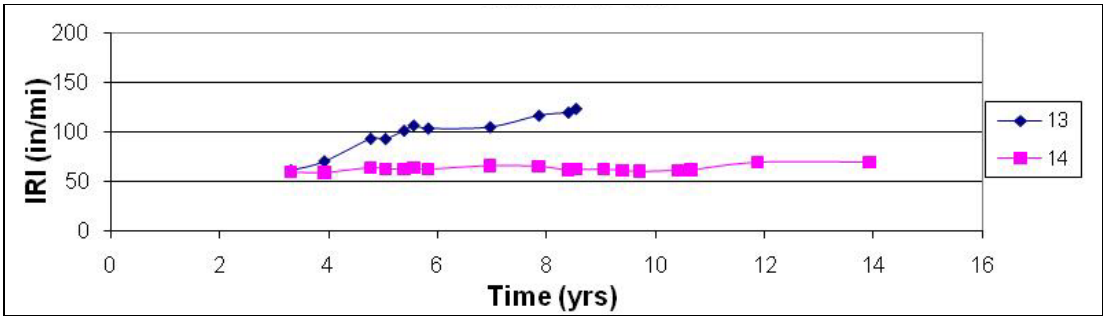

Figure 5. Graph. Changes in IRI over time for LTPP SPS-1 test sections in Virginia (DGAB).

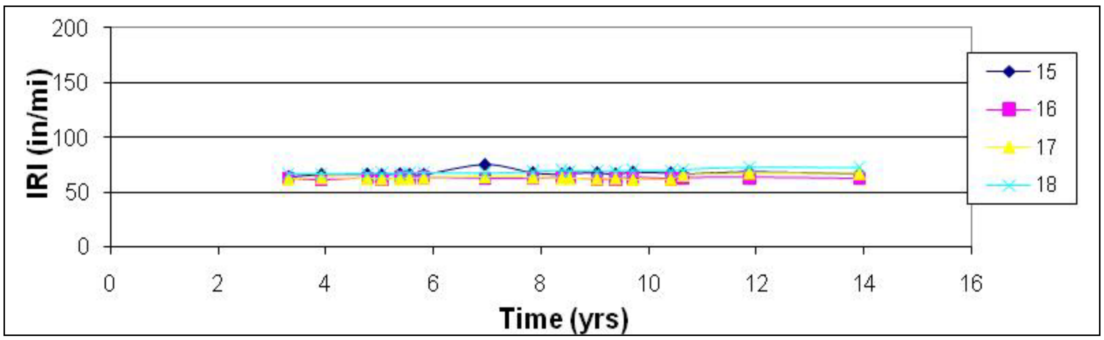

Figure 6. Graph. Changes in IRI over time for LTPP SPS-1 test sections in Virginia (ATB).

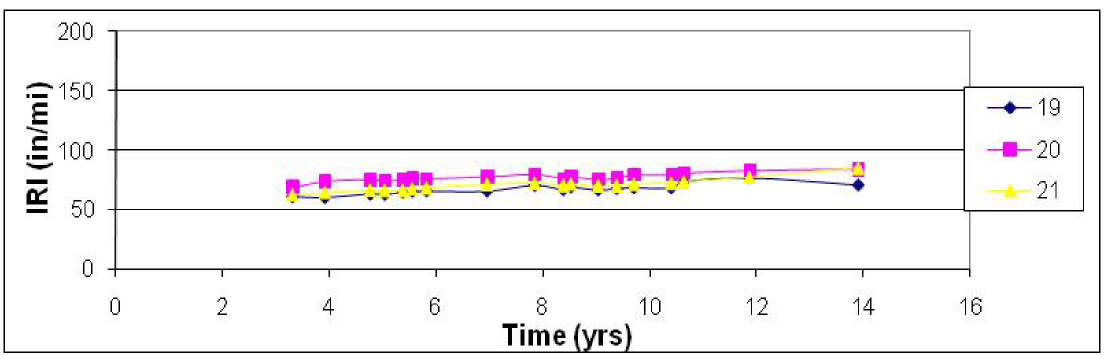

Figure 7. Graph. Changes in IRI over time for LTPP SPS-1 test sections in Virginia (PATB).

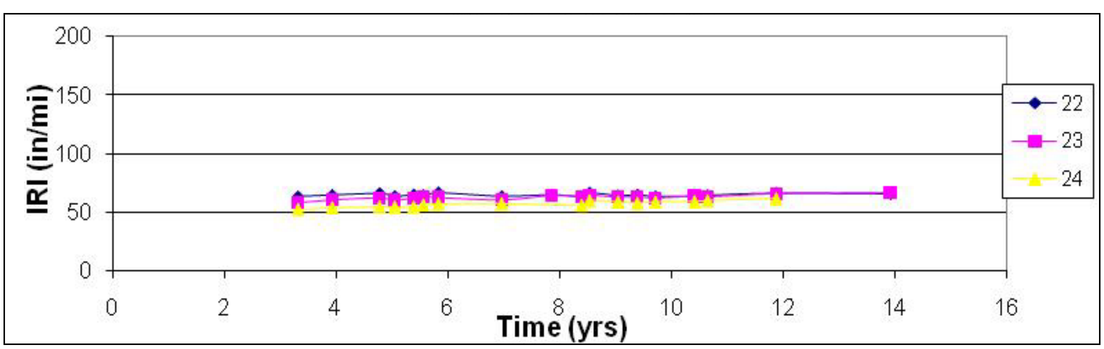

Figure 8. Graph. Changes in IRI over time for LTPP SPS-1 test sections in Virginia (ATB/PATB).

In the case of portland cement concrete (PCC) pavements, the IRI value can increase because of faulting. If FWD testing is performed at the center of the slab, the results could show that the pavement has sufficient structural capacity. Moreover, PCC pavements can be permanently curled, which can cause high IRI. In PCC pavements, center-slab FWD testing will also likely show that the pavement has suffcient structural capacity. PCC slabs can also have a convex shape, where the center of the slab is at a higher elevation compared to the joints. Because of the gap in the center of the slab, FWD testing may indicate that the pavement has a low structural capacity, but the IRI may be acceptable.

References to ride quality have focused almost entirely on IRI, but IRI is not intended to capture pavement profile frequencies known to induce dynamic loading from heavy trucks, which is more likely to be associated with pavement deterioration. It is thought that dynamic truck loadings cause accelerated pavement damage. The dynamic loads applied by heavy vehicles on pavements fall into two distinct frequency ranges: 1.5 to 4 Hz (sprung mass bounce, pitch, and roll vibration modes) and 8 to 15 Hz (unsprung mass bounce and roll). The sprung mass bounce motion is commonly referred to as “body bounce,” and the unsprung mass bounce motion is commonly referred to as “wheel hop.”

At 65 mi/h, body bounce at 2 and 2.5 Hz corresponds to spatial frequencies of 48 and 38 ft/cycle, respectively. Similarly, at 65 mi/h, axle hop at 10 and 12 Hz corresponds to spatial frequencies of 9.6 and 8 ft/cycle, respectively. On new pavements that do not have distress, dynamic loads will be mainly influenced by body bounce. As a pavement deteriorates, dynamic loads due to axle hop will occur. There is a relationship between frequency, spatial wavelength, and speed.

The magnitude of the dynamic loads applied on the pavement does not necessarily depend on the IRI level of the pavement. Instead, the wavelengths present on the roadway have a significant influence on the dynamic loads that are applied. If the dominant wavelength in the pavement is close to the spatial frequency of the truck, resonance motion will occur in the truck, resulting in high dynamic loads being imparted on the pavement.

As previously noted, a truck traveling at 65 mi/h that has a body bounce frequency of 2.5 Hz will have a spatial frequency of 38 ft/cycle. If there is significant spectral content in the roadway near this wavelength, resonance motion can occur in the truck, which can result in high dynamic loads being applied to the pavement.

Figure 9 shows a 25-ft base length continuous IRI plot of a section of roadway. Any point on this plot shows the IRI of a 25-ft-long section that is centered at that location. For example, the IRI shown at 50 ft is the average IRI from 37.5 to 62.5 ft. The overall IRI of this roadway is 73 inches/mi.

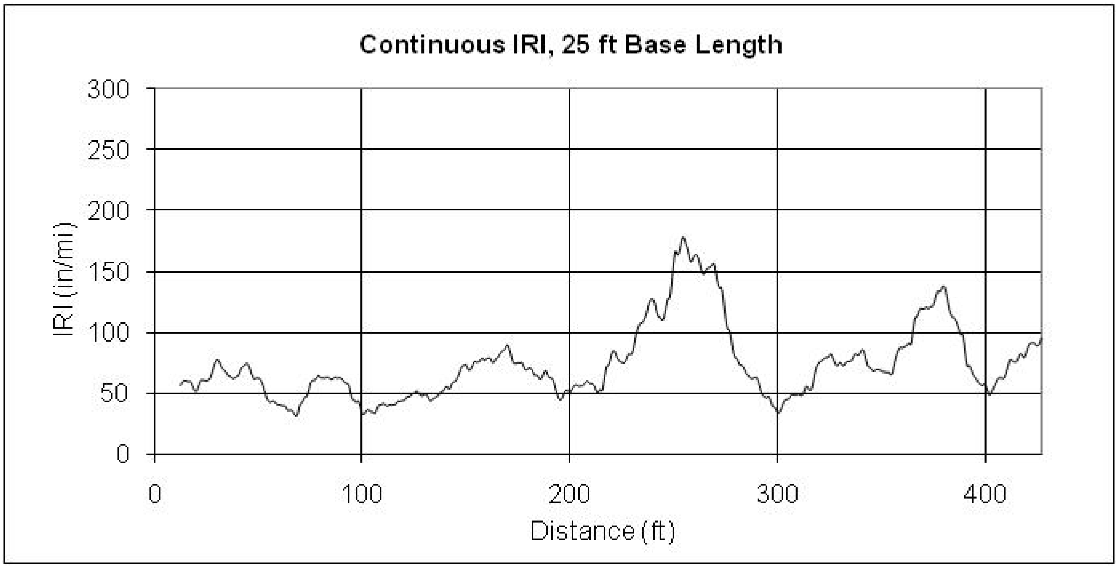

Figure 9. Graph. Continuous IRI plot of road profile.

Figure 10 shows the power spectral density (PSD) plot of the profile data. A PSD function is a statistical representation of the importance of the various wavelengths contained in the profile. The PSD plot shows that there is significant spectral content close to a wavelength of about 30 ft. This value is close to the spatial frequency of the body bounce motion of the truck and can result in high dynamic loads being applied on the pavement.

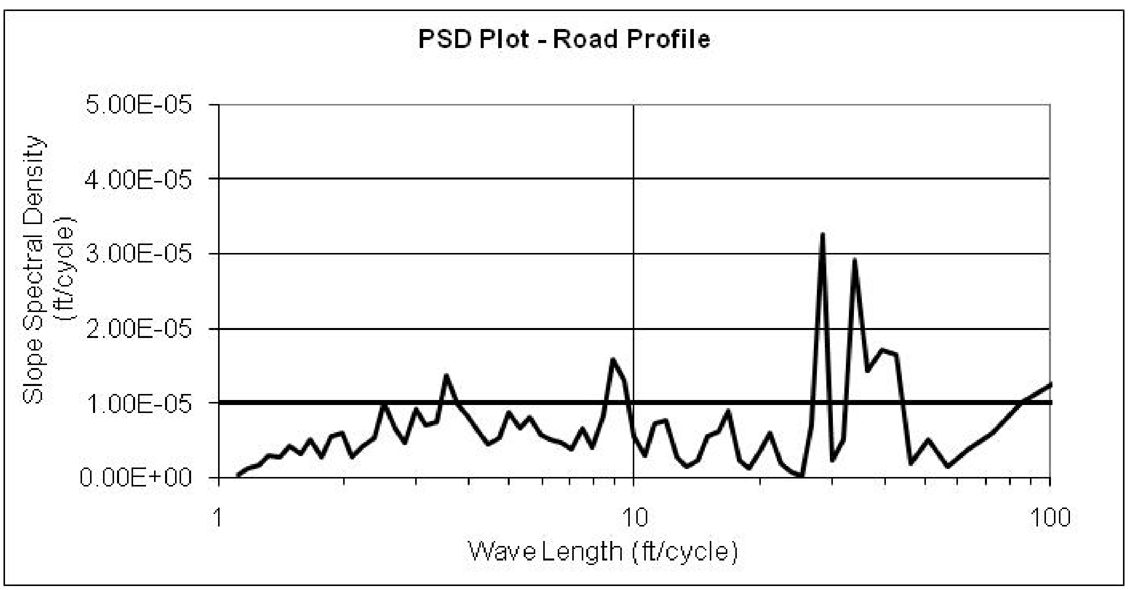

Figure 10. Graph. PSD plot of road profile.

Figure 11 shows the dynamic loads that were predicted for the leading trailer axle by a truck simulation model. The dynamic loads predicted for a truck with air suspension and for a truck with leaf suspension are shown. This pavement section is a fairly smooth pavement with an overall IRI of 75 inches/mi. However, it had wavelengths that were close to the natural frequency of the body bounce motion of the truck. This caused high dynamic loads to be applied on the pavement. There could be other pavement sections that have an IRI of 75 inches/mi that do not have significant wavelength content close to the natural frequency of the body bounce motion of this section. On such a section, the magnitude of the dynamic loads applied on the pavement is expected to be lower. Therefore, the IRI level by itself is not a predictor of dynamic loads imparted on the pavement.

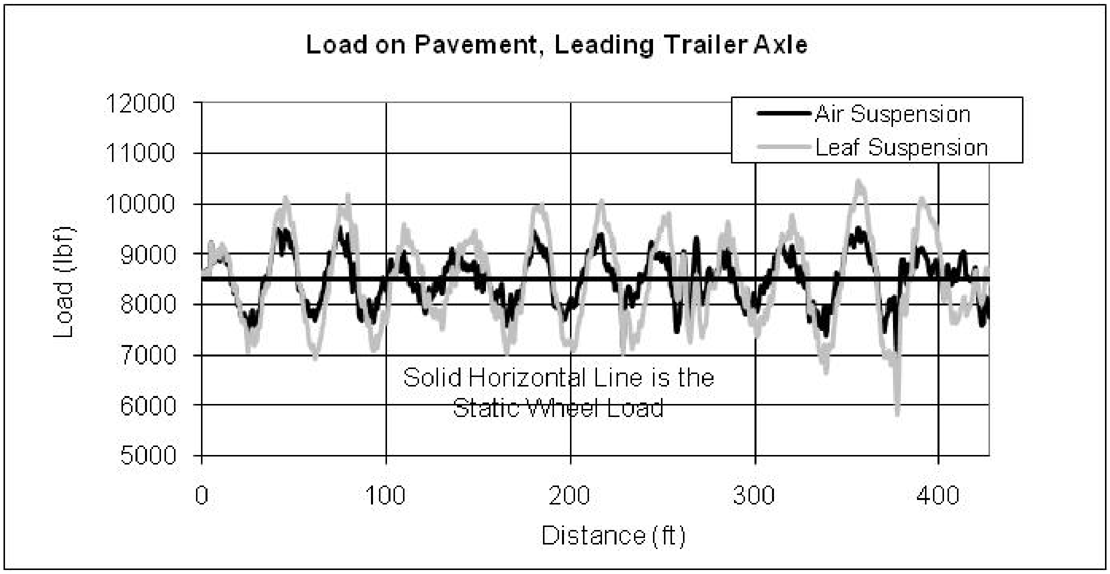

Figure 11. Graph. Dynamic loads applied to road profile.

As previously noted, if a new pavement has dominant wavelengths that will cause resonance body bounce motion that can cause high dynamic loads, pavement distress may result. Such distresses will influence the axle hop motion of the truck, resulting in accelerated distress due to both body bounce and axle hop.

IRI is influenced by wavelengths ranging from 3 to about 100 ft. So, IRI will include the wavelengths that influence dynamic truck loads. The IRI has maximum sensitivity to sinusoids with wavelengths of 7.9 and 50.5 ft. The wavelength of 7.9 ft is close to spatial wavelengths that have a significant impact on axle hop. The wavelength of 50.5 ft is somewhat close to spatial wavelengths that influence body bounce.

From the information presented thus far, it could be argued that the relationship between ride quality and structural adequacy is tenuous at best. However, the discussion has revolved almost entirely around IRI as the surrogate to ride quality, which is not intended to specifically capture pavement profile features known to induce dynamic loading from heavy trucks, which is more likely associated with pavement deterioration. In addition, no clear specific definition of a structural adequacy measure has been provided. Accordingly, a more rational look at ride quality and structural adequacy is needed.

The investigation of the relationship in question must begin with a clear understanding of pavement performance and the factors that affect it. More specifically, the separate and combined effects of the following four factors define the performance of pavements:

- Pavement structure:
    - Pavement type—HMA, new PCC, HMA overlay over existing HMA, HMA overlay over existing PCC, PCC overlay over existing PCC, PCC overlay over existing HMA, and others (paver blocks, white topping overlay, etc.).
    - Pavement layers—Thicknesses, material types, material properties, drainage, shoulders, joints and steel reinforcement in PCC pavements, quality of construction and related issues, ambient conditions at time of construction, and others.
- Subgrade soil—Material types, material properties, stabilization, embankment, cut/fill, depth to bedrock, drainage, and others.
- Traffic—Traffic volumes (design versus actual), traffic loads/load spectra (design versus actual), traffic growth (design versus actual), seasonal trends, load restrictions, and others.
- Environmental conditions—Air and surface temperatures, precipitation, wind, solar radiation, subsurface moisture, subsurface temperature, construction ambient conditions, unusual or catastrophic events, freeze-thaw cycles, freeze days, and others.

Without question, the best source of data to explore the ride quality-structural adequacy relationship is the LTPP program, which was established to provide the data necessary to explain how pavements perform and why they perform as they do. The LTPP database contains the most complete and comprehensive set of pavement performance data and associated factors, including the following:

- Pavement performance information, including roughness/elevation and deflection data.
- Pavement structure and subgrade soil information obtained through one or more of the following methods: test pits and coring/boring, ground penetrating radar, dynamic cone penetrometer, drainage surveys (video), field materials sampling and testing activities, laboratory materials testing, specialized testing, and other destructive and nondestructive testing (NDT) techniques.
- Traffic information obtained through one or more of the following methods: automatic vehicle classifier counts, weigh-in-motion (WIM) measurements, average daily traffic, and estimated equivalent single-axle load (ESAL) estimates.
- Environmental information obtained from one or more weather stations (e.g., National Climatic Data Center, Canadian Climatic Center, and LTPP-installed stations) or through the use of surface or subsurface instrumentation at the SMP test sections.

In particular, the use of data associated with the SPS-1 (new asphalt concrete (AC) pavements), SPS-2 (new PCC pavements), SPS-5 (rehabilitation of existing AC pavements), SPS-6 (rehabilitation of existing PCC pavements), and SPS-8 (study of environmental factors in the absence of heavy loads) project test sections are considered relevant. Unlike most General Pavement Study (GPS) test sections, the SPS data capture pavement performance and the factors that affect it over the entire performance life cycle.

1.3 PROJECT GOAL AND OBJECTIVE

The objective of this project was to identify and verify the relationship, if any, between ride quality and structural support or between ride deterioration and structural adequacy using LTPP and other pavement performance data sources. This was done in an effort to improve the evaluation and use of pavement condition data in pavement rehabilitation and design decisions.

More specifically, this project was intended to develop and document a mechanism to include both ride quality and structural adequacy values within the context of current network-level PMS practices for highway agency implementation. The results of the project are intended for use by pavement management engineers to ensure smooth pavements that are also structurally adequate.

To accomplish the project objective, the following three tasks were initially performed under phase I, "Identification and Demonstration of the Ride-Structure Relationship," which was intended to establish the foundation for actual development of the ride quality-structural adequacy relationship under phase II, "Guidance for Implementing the Ride-Structure Relationship into PMS":

- **Literature search**—Available information relating ride quality and structural adequacy for pavement rehabilitation and design decisions was gathered, reviewed, and synthesized. Pertinent information was gathered through Web-based searches of State highway agencies, university pavement research centers, the Transportation Research Board (TRB), the American Society of Civil Engineers (ASCE), industry, and other national and international (e.g., World Road Association (PIARC) and AustRoads) organizations. The information gathered under this task was synthesized and presented by relevant topics to serve as the foundation for the work to be carried out under tasks 2 and 3. As part of this effort, consideration was given to how the ride quality-structural adequacy relationship and decisionmaking processes contribute to improved resource allocation through the highway agency's network-level PMS.

- **Data review and assessment**—This effort focused on the review and assessment of relevant data from the LTPP SPS-1, SPS-2, and SPS-5 project test sections because of data completeness and because the sections capture pavement performance and the factors that affect it over entire performance life cycles. General ride quality-structural adequacy trend analyses were performed on those data to see if promising relationships could be identified. In the pursuit of relationships, both changes in ride quality or structural capacity over time and changes in ride quality or structural capacity within the test sections were considered.

- **Phase I report**—Under this task, a draft phase I report was prepared to document the findings from the research performed under tasks 1 and 2. The report was to include the proposed work plan for the phase II effort. However, because a promising ride quality-structural adequacy relationship could not be identified, the project team recommended not proceeding with the phase II effort.

This report documents the phase I results and findings, as detailed under the task 3 summary.

1.4 REPORT ORGANIZATION

The information presented in this report is organized into the following sections:

- **Chapter 1. Introduction**—Includes project background information, the project goal and objective, and the report organization.

- **Chapter 2. Literature Search**—Provides the results of the literature search, including the sources of information and a summary of information contained in the more relevant references.

- **Chapter 3. Data Review and Assessment**—Details the results and findings from the review and assessment of relevant data from the LTPP SPS and GPS test sections, including the selection of test sections and the pursuit of promising ride quality-structural adequacy relationships. The primary criteria used in the selection of test sections and subsequent analyses were changes in ride quality or structural capacity over time and changes in ride quality or structural capacity within the test sections.

- **Chapter 4. Other Data Analysis Considerations**—Presents additional data analyses performed as part of the study to validate the findings and conclusions presented in chapter 3.

- **Chapter 5. Summary and Conclusions**—Highlights the major observations, findings, and conclusions from the phase I effort.

- Four appendices contain plots generated during the data review and assessment effort as well as the data analysis validations, which are not included in the main text of the report.

- The references list contains relevant references identified from the literature search or used in the preparation of this report.

- The bibliography contains references identified from the literature search that were not considered of sufficient relevance to include in the project.

CHAPTER 2. LITERATURE SEARCH

The objective of the literature search was to collect, review, and synthesize available information relating ride quality and structural adequacy for pavement rehabilitation and design decisions. Pertinent information was gathered through Web-based searches of State highway agencies, university pavement research centers, TRB, ASCE, industry, and other national and international (e.g., PIARC and AustRoads) organizations. A particularly relevant source of information was the references database prepared under the LTPP program and posted on the program's Web site (http://www.ltpp.org). In addition to looking at previous attempts to establish such a relationship, the following topics were also considered during the literature search:

- Relationships between ride quality and structural adequacy.
- Factors influencing pavement performance.
- Structural- and functional-based approaches for pavement evaluations.
- Relationship between ride and distress.

The key observations, findings, and conclusions from the literature search are detailed in this chapter.

2.1 OVERVIEW

The purpose of the literature review was to identify, review, and synthesize information for eventual use in the planning and execution of an effort to look for the potential relationship between ride quality and structural adequacy of pavement structures. A total of 62 references were identified from various sources and reviewed. Of those, 16 references were considered of particular value to the project. They have been synthesized and included in the references list of this report. The remaining 47 references were not considered sufficiently relevant and have been included in the bibliography section.

Each of the 16 relevant references was reviewed by identifying the reference type, source, objectives and goals, findings and observations, relevance to the project, and other pertinent information. Table 2 shows the distribution of these references by type and source. As shown, the majority (62 percent) of references were from studies related to the LTPP program. Although the LTPP program has been categorized separately, it could be considered together with the transportation departments since all LTPP test sections are on State highways. Table 2 also shows that the bulk of references were articles (69 percent). Five reports (31 percent) relevant to the current study were reviewed in addition to the articles.

Table 2. Distribution of references by type and source.

Type	State Transportation Department/ University	LTPP Program	Total
Report/ guideline	3	2	5 (31 percent)
Article/ presentation	3	8	11 (69 percent)
Total	6 (38 percent)	10 (62 percent)	16 (100 percent)

Table 3 shows the distribution of elements in the references that are relevant to this study on relating ride quality to structural adequacy for rehabilitation and design decisions. The values shown in this table indicate the number of references of the total (16) that contained a topic related to the current study. As expected, many of the references covered more than one topic. The majority of these references relate to factors influencing pavement performance (43 percent). Understanding the factors influencing pavement performance was considered an important first step in the effort to establish a relationship between ride quality and structural adequacy. Only two promising studies were identified in the literature search that directly relate to the research topic at hand. One article on the topic of structural and functional evaluation approaches was reviewed, and six references that looked at relationships between ride and distress were reviewed. Figure 12 shows the distribution of the topics considered essential for evaluating a relationship between ride and structural adequacy.

Table 3. Distribution of references by type and topic.

Type	Relationship Between Ride and Structural Adequacy	Factors Influencing Pavement Performance	Structural- and Functional-Based Approaches for Pavement Evaluations	Relationship Between Ride and Distress	Total
Report/ guideline	2	1	0	2	5 (31 percent)
Article/ presentation	0	6	1	4	11 (69 percent)
Total	2 (13 percent)	7 (43 percent)	1 (6 percent)	6 (38 percent)	16 (100 percent)

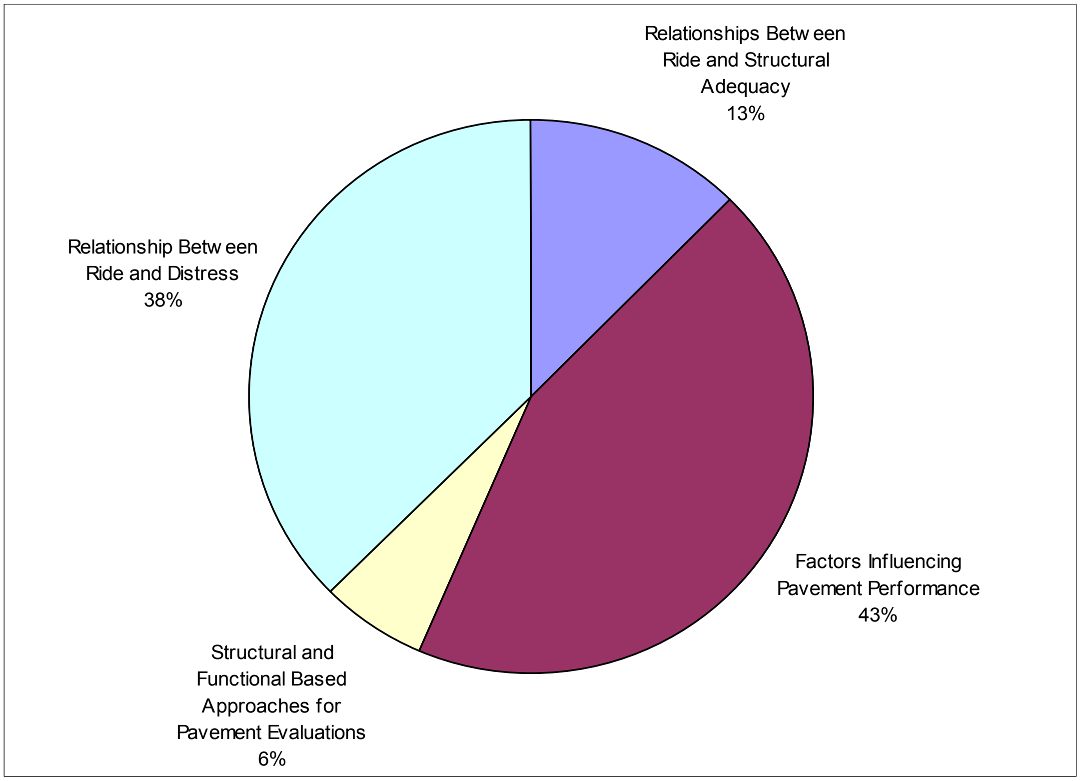

Figure 12. Graph. Distribution of references.

2.2 SPECIFIC FINDINGS

Two studies relate directly to this study—relating ride quality to structural adequacy for rehabilitation and design considerations. The first was an FHWA study conducted by Von Quintus et al. on LTPP data that looked at the dissipated work obtained from deflection time history data and pavement condition data (distresses, IRI, etc.) to see if a relationship exists between the dissipated work and pavement performance.(4) In this study, dissipated work was defined as the area under the loaded and unloaded portion of the stress-strain curve (hysteresis loop) and was used to define the viscoelastic and inelastic properties of pavement material. Several LTPP sites with varying IRI values, distress magnitudes, and traffic levels were analyzed to determine if a relationship existed between the dissipated work and pavement performance. The dissipated work and hysteresis loop were found to vary extensively by structure and pavement type. Based on the sections evaluated in the study, lower amounts of dissipated work were observed on PCC-surfaced pavements than on AC-surfaced pavements. The findings from the study indicate that the greater the dissipated work, the greater the amount of pavement distress observed in terms of magnitude, severity, and type. The conclusions from this study indicate that dissipated work can be used to determine the performance behavior of pavement structures.

The second study was performed by Zhang et al. and looked at the structural adequacy of pavements in implementing pavement management decisions.(5) The study evaluated various methods to look at the structural condition of the roadway prior to applying thin overlays to correct ride. The study indicated that the Texas Department of Transportation (TxDOT) pavement management information system (PMIS) database shows a yearly decrease of

0.3 points in ride score for the highway network in Texas as a result of the increase in pavement roughness attributed to permanent deformation. The permanent deformation was a result of inadequate pavement strength for existing traffic loads. The study was aimed at determining a structural index using the FWD data to evaluate the structural adequacy prior to planning maintenance.

In the process of determining a suitable methodology for characterizing structural estimators, the TxDOT study looked at the deterioration process of the pavement. As the deterioration process represents the behavior of a non-linear system, it can be characterized by different rates of deterioration in different stages of the pavement service life. The true condition of a pavement at any moment can be described more accurately if the deterioration rate is known. Unfortunately, a mathematical solution to this problem is impossible because there are no models that can precisely represent the true deterioration process of a pavement. Even complicated mathematical models such as sigmoid forms cannot be calibrated accurately enough to represent a true deterioration process.

The TxDOT study points out that if the general mathematical formula describing the transition of a system from one state to another is not available, one can use the finite difference between the states. The study presents a unique way of characterizing the condition deterioration (ride and distress). It also proposes a method to characterize deterioration in terms of differences between condition measures over a unit time period, normalized to the initial condition, to give a more accurate picture of pavement deterioration. Furthermore, the study points out the importance of considering the traffic applied when determining the pavement deterioration. An equal yearly drop in the condition score of a pavement subjected to different ESALs represents different structural conditions of the pavement. The normalized drop in condition divided by the ESALs for the year, called the "unit ESAL deterioration" (UED), provides a more accurate condition of the pavement. Structural failure occurs when the roughness starts progressing at a high rate, and the UED concept helps describe the deterioration rate. In the study's analysis the UED is calculated as the normalized yearly drop in the PMIS scores (ride, condition, and distress scores) caused by a single ESAL for a consecutive two-year period, as shown in figure 13 to figure 15.

$$\text{UED (Distress Score)} = (dDS/(DS \times ESAL_y))*10^6$$

Figure 13. Equation. UED distress score.

$$\text{UED (Condition Score)} = (dCS/(CS \times ESAL_y))*10^6$$

Figure 14. Equation. UED condition score.

$$\text{UED (Ride Score)} = (dRS/(RS \times ESAL_y))*10^6$$

Figure 15. Equation. UED ride score.

Where:

DS = Distress score in initial year.
RS = Ride score in initial year.
CS = Condition score in initial year.
dDS = Yearly drop in distress score.
dCS = Yearly drop in condition score.

dRS = Yearly drop in ride score.
$ESAL_y$ = Estimated amount of ESALs in a year.

The results from the TxDOT study indicate that different factors, such as dRS, dCS/CS, and UED(RS), show different levels of sensitivity to the structural estimators, but the outputs from all considered methods indicate some level of sensitivity to the UED values. As deterioration increases, the structural estimators tend to produce smaller values. The factor defined as UED(RS) showed the best trend for all methods (structural estimators considered). The intent of the trend analyses was to visualize whether there was a trend between the deterioration variables (e.g., UED of the PMIS score values) and the pavement structural estimators (e.g., structural number (SN)). However, it was not the intention of the study to quantify the correlation between them through regression analysis or other means. An example of the trend found between SN and UED(RS) is shown in figure 16. The study also puts forth the concept of a structural condition index, a ratio of the effective SN (SN_{eff}) to the required SN (SN_{reqd}), as a measure of structural adequacy.

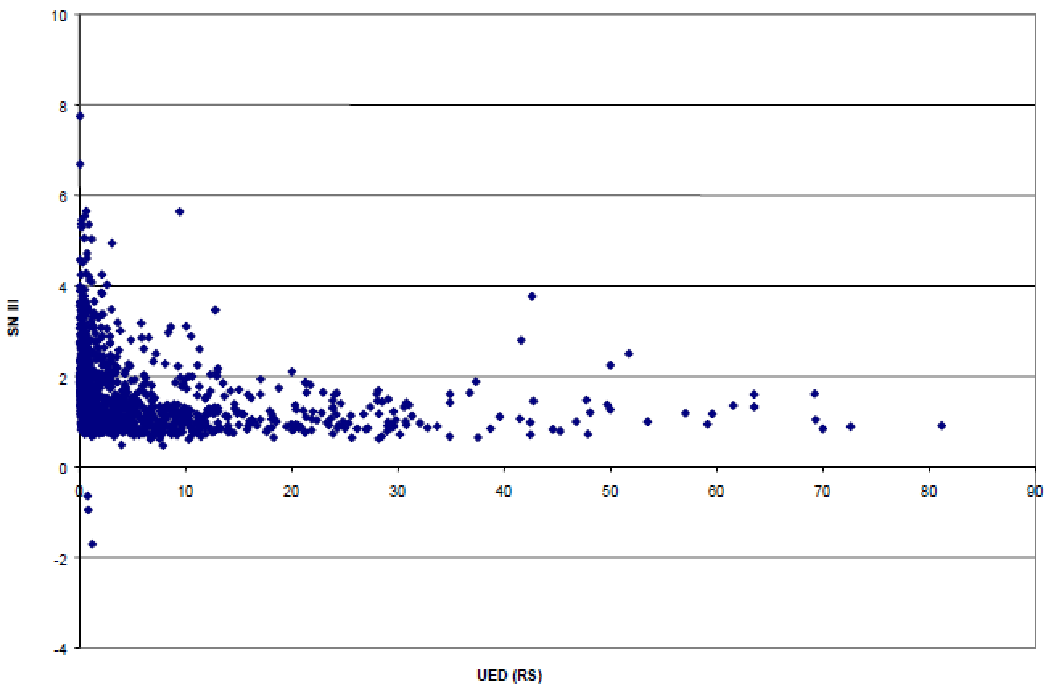

Figure 16. Graph. Sensitivity of SN to UED of ride score.

In order to investigate a potential relationship between ride quality and structural adequacy, it is important to understand the factors that influence pavement performance. Seven of the reviewed references identify factors influencing pavement performance. The findings from these studies are summarized in table 4.

Table 4. Summary of factors influencing pavement performance.

Pavement Surface Type	Performance Indicator	Most Influencing Factors	Least Influencing Factors	Factors Not Influencing	Reference No.
Hot mix AC (HMAC)	Overlay roughness	Overlay thickness, climatic zones	Subgrade type	—	6
HMAC	Overlay roughness	—	—	IRI prior to overlay, overlay thickness, and milling prior to overlay	7
Jointed plain concrete (JPC)	Cracking and roughness	Base type, pavement drainage, and slab thickness	—	—	8
HMAC	Roughness	Base type, drainage, and climatic conditions	Base thickness and subgrade type	—	9
HMAC	Roughness, rutting, fatigue cracking, and transverse cracking	—	—	—	10
HMAC	Roughness and rutting	Construction	—	—	11
JPC	Roughness and faulting	Dowels	—	—	12
Jointed reinforced concrete	Roughness	Moisture in subgrade, joint spacing, thicker slabs, and concrete modulus	—	—	12
Continuously reinforced concrete	Roughness	—	—	—	12

— Indicates that the reference did not apply.

A study by Vepa et al. looked at structural- and functional-based approaches for pavement evaluations.[13] In this study, approaches including the 1993 AASHTO procedure based on NDT data, a pavement condition rating procedure, and a survivor curve method were used to evaluate the remaining life of flexible and rigid pavements. The conclusions from the study indicate that structural failure-based remaining life calculations result in conservative estimates compared to functional failure-based methodologies.

Finally, in an effort to identify an indirect relationship between ride and structural adequacy, studies relating ride and distress were reviewed. Six references were identified. The results from four of these studies are summarized in table 5. The other two references included models to relate IRI and distress and are discussed in detail in the following paragraphs.

Table 5. Relationship between pavement performance measures.

Pavement Type	Performance Measures	Statistically Significant Relationship	Strength of Relationship	Reference No.
HMAC and HMAC over PCC	IRI and distress	Yes	Weak	14
HMAC and HMAC over PCC	IRI and rutting	Yes	Weak	14
HMAC	IRI and Pavement Condition Index	Yes	Weak	15
HMAC	IRI and initial IRI, fatigue, and rutting	Yes	Strong, but mainly influenced by initial IRI	16
HMAC	IRI and distress	Yes	Strong	17

In the *Mechanistic-Empirical Pavement Design Guide* (MEPDG), the functional adequacy for both flexible and rigid pavements is quantified by pavement smoothness.[18] The parameter used to define pavement smoothness in the MEPDG is IRI.

In the MEPDG, models are available to empirically predict the IRI at any point in the life of the pavement by adding the increase in IRI of the pavement due to pavement distress and a site factor to a known initial IRI of the pavement. The site factor accounts for the increase in roughness due to the shrink/swell and frost heave characteristics of the subgrade. Distress prediction models are used to predict the distresses that are used as an input to the roughness models.

The MEPDG presents models for predicting the IRI for the following pavement types:

- New HMA pavements and HMA overlays of flexible pavements (the model form is the same for both, but coefficients in the model are different for the two pavement types).
- HMA overlays of rigid pavements.
- Jointed plain concrete pavements (JPCP).
- Continuously reinforced concrete pavements (CRCP).

The following is a brief description of the distress types and site factors included in the roughness prediction models for each of the pavement types:

- **New HMA pavements and HMA overlays of flexible pavements—**The distress types included in the roughness prediction model are (1) area of fatigue cracking expressed as a percent of total lane area (combined alligator, longitudinal, and reflection cracking in the wheel path, with length of cracks multiplied by 1 ft to convert length to an area basis), (2) length of transverse cracking (includes the reflection of transverse cracks in the existing HMA pavement), and (3) average rut depth. The site factor is a function of the pavement age, plasticity index of the subgrade, average annual freezing index, and average annual precipitation. The model form for roughness prediction is the same for new HMA pavements and HMA overlays of flexible pavements, but the coefficients in the model are different for the two pavement types.

- **HMA overlays of rigid pavements—**The distress types affecting IRI as well as the parameters considered in the site factor are the same as those for new HMA pavements and HMA overlays of flexible pavements. The coefficients in the model for each distress type as well as the site factor are different from those used in the HMA pavement models.

- **JPCP—**The distress types included in the roughness prediction model are (1) percentage of slabs with transverse cracks (all severities), (2) percentage of joints with spalling (medium and high severities), and (3) total cumulative faulting per mile (in inches). The site factor included in the model is a function of the pavement age, freezing index, and percent of subgrade material passing the No. 200 sieve.

- **CRCP—**The only distress type included in the model is the number of medium and high severity punchouts. As in the case of the JPCP model, the site factor included in the model is a function of the pavement age, freezing index, and percentage of subgrade material passing the No. 200 sieve.

As previously described, in all of the models presented in the MEPDG for predicting roughness, age is included in the site factor, which accounts for the increase in roughness that occurs over time due to the frost heave and shrink/swell characteristics of the subgrade.

The three distress types considered in the roughness prediction model for new HMA pavements and flexible overlay of HMA pavements are fatigue cracking, transverse cracking, and rut depth. The amount of fatigue cracking in the pavement should have a strong influence on the structural strength of the pavement as determined from FWD testing conducted along the wheel path. However, transverse cracks are unlikely to impact the structural strength of the pavement as determined from the FWD testing if the FWD test is carried out away from a crack location. Rut depths may or may not affect the structural strength of the pavement as determined from FWD testing. If the rutting is caused by a weak base or subbase layer, the structural strength of the pavement will be affected. However, rutting caused by the distortion of the HMA layer may not result in a loss of structural capacity of the pavement. Rutting caused by weak subgrade, base, or subbase layers can result in early fatigue cracking of the pavement.

The three distress types considered in the roughness prediction model for JPCP pavements are transverse cracks, joint spalling, and faulting. FWD tests to evaluate the structural capacity of JPCP pavements are conducted at the center of the slab. Transverse cracks present on the slab will affect the structural capacity of a JPCP slab as determined from FWD testing. However, joint spalling and faulting are not related to the structural strength of the concrete pavement. Spalling may be caused by concrete durability issues as well as by low load transfer at joints. Faulting is also related to low load transfer at joints and can be exacerbated by the presence of erodible bases.

The only distress type influencing the roughness of CRCP pavements is punchouts, which are load-related distresses.

In the MEPDG roughness models, some of the distresses that result in an increase in IRI will result in a decrease in the structural strength of the pavement. However, some distresses that contribute to the increase in roughness may not necessarily cause a decrease in the structural strength of the pavement. The MEPDG models account for the increase in roughness due to shrink/swell and frost heave characteristics of the subgrade. Changes in the pavement profile caused by shrink/swell and frost heave of the subgrade may not directly impact the structural strength of a pavement. However, these actions could initiate pavement distress, which would have an impact on roughness.

Lastly, the World Bank has developed software called Highway Development and Management (HDM) System to make comparative cost estimates and economic evaluation of different policy options.(19) The HDM-III model was developed using data collected from a multiyear empirical study carried out in Brazil. The statistical relationships in this model were validated and extended using data from several other deterioration studies carried out in various locations such as Kenya, the Caribbean, India, and Texas. The revised and improved models are included in the latest version, HDM-4. HDM-4 includes a model for predicting roughness of roadways. The roughness prediction model predicts the incremental change in roughness during an analysis year based on contributions to roughness from five sources: (1) change in roughness due to structural deterioration, (2) cracking, (3) rutting, (4) potholes, and (5) environmental effects. Models are provided to predict the incremental change in roughness due to each of the factors. The HDM-4 model has been widely used in many countries with calibration to suit local conditions.

2.3 SUMMARY

Although a few studies were identified during the literature search that indicated a potential relationship between structural response and pavement performance, none of these studies established a direct relationship between ride quality and structural adequacy. As discussed in this chapter, several studies have been successful at relating ride quality to pavement condition or distress. In fact, the roughness models in the MEPDG use distress as an input to predict roughness. Similarly, structural response has been used to predict certain distresses. While it is evident that a multitude of factors influence pavement performance in different ways (i.e., ride condition and structural response), a strong correlation between the three different performance measures has yet to be established such that measurement of any one performance indicator is adequate to identify both the structural and functional condition of the pavement.

CHAPTER 3. DATA AVAILABILITY AND DATA ASSESSMENT

3.1 INTRODUCTION

Roughness indices computed from the profile data collected at LTPP sections are stored in the LTPP database. The roughness indices available in the LTPP database are IRI, root-mean-square vertical acceleration (RMSVA) for base lengths of 1, 2, 4, 8, 16, 32, 64, and 128 ft, slope variance, and Mays output. The IRI of the left and right wheel paths and the mean IRI (average of the left and right wheel paths) are available in the LTPP database. Although RMSVA, slope variance, and Mays output have been used in the past as measures of roughness, these indices are not currently used.

An assessment of the availability of IRI values and FWD data for SPS-1, SPS-2, and SPS-5 was performed to obtain a general idea about the length of time over which data have been collected at these projects.

Thereafter, a few sections were selected from each experiment to investigate the change in ride quality and structural strength that had occurred over time and to investigate if there was a relationship between the change in ride quality and change in structural strength. The primary emphasis was placed on analyzing data from SPS-1 projects. Hence, most of the test sections analyzed were SPS-1 sections.

3.2 DATA AVAILABILITY

Table 6 shows the following information for the SPS-1 projects: State where the project is located, construction date of the project, last available profile date in the database, and number of times profile data were collected at the project. Similar information for SPS-2 and SPS-5 is shown in table 7 and table 8, respectively. The information shown in table 6 through table 8 was obtained from work performed for a previous research project, and more recent roughness data are expected to be available in the most recent LTPP data release. There is a possibility that monitoring of one or more sections in a SPS project may have stopped at an earlier date than that listed as the last available profile date in these tables because of rehabilitation being performed on the test sections. It appears that most SPS-1 test sections that had a weak pavement structure (e.g., sections 2 and 13) failed within a very short time period after being opened to traffic.

Based on the information shown in table 6 through table 8, adequate ride quality data are available to evaluate changes in roughness at SPS-1, SPS-2, and SPS-5 sections. A review of the FWD data for these projects also indicated that adequate test data are available in the LTPP database to evaluate changes in structural strength over time.

Table 6. Roughness data availability for SPS-1 projects.

State	Construction Date	Last Available Profile Date	Number of Times Profiled
Alabama	3/1/1993	5/4/2005	9
Arizona	8/1/1993	3/27/2006	13
Arkansas	3/15/1994	5/22/2007	8
Delaware	5/1/1996	6/13/2006	14
Florida	2/1/1995	7/26/2006	8
Iowa	5/19/1992	9/22/2004	11
Kansas	11/1/1993	3/15/2004	9
Louisiana	7/1/1997	8/7/2006	3
Michigan	11/1/1995	6/2/2006	10
Nebraska	1/1/1995	4/24/2002	9
Nevada	9/1/1995	8/27/2006	12
New Mexico	11/1/1995	4/24/2006	7
Ohio	9/1/1995	8/9/2006	12
Oklahoma	6/1/1997	4/11/2007	8
Texas	6/1/1997	3/19/2007	11
Virginia	11/28/1995	12/2/2006	18

Table 7. Roughness data availability for SPS-2 projects.

State	Construction Date	Last Available Profile Date	Number of Times Profiled
Arizona	10/1/1993	08/11/2006	12
Arkansas	12/1/1995	4/2/2005	6
California	2000	11/7/2004	7
Colorado	11/1/1993	06/02/2006	10
Delaware	5/1/1996	06/11/2006	14
Iowa	12/1/1994	10/29/2004	9
Kansas	8/1/1992	06/05/2006	14
Michigan	11/1/1993	08/16/2006	17
Nevada	9/1/1995	12/3/2003	10
North Carolina	1/1/1994	06/14/2006	18
North Dakota	11/1/1994	5/18/2004	6
Ohio	8/14/1996	08/08/2006	12
Washington	11/1/1995	06/07/2006	11
Wisconsin	1/1/1997	9/12/2005	9

Table 8. Roughness data availability for SPS-5 projects.

State/Province	Construction Date	Last Available Profile Date	Number of Times Profiled
Alabama	12/19/1991	8/3/2006	10
Alberta	10/3/1990	6/12/2006	16
Arizona	4/20/1990	3/24/2006	13
California	4/25/1992	3/20/2007	12
Colorado	10/3/1991	4/24/2000	9
Florida	4/5/1995	7/27/2006	8
Georgia	6/7/1993	5/2/2005	8
Maine	6/20/1995	7/29/2004	8
Manitoba	9/1/1989	6/8/2006	15
Maryland	3/31/1992	6/15/2006	15
Minnesota	9/15/1990	6/6/2005	13
Mississippi	9/24/1990	4/13/1999	5
Montana	9/11/1991	6/7/2005	14
New Jersey	8/18/1992	6/10/2006	18
New Mexico	9/11/1996	4/24/2006	7
Oklahoma	7/8/1997	4/11/2007	8
Texas	9/1/1991	4/10/2007	11

3.3 RIDE QUALITY PARAMETER SELECTED FOR STUDY

In selecting an appropriate ride quality parameter to be used in this study, parameters including PSD plots, smoothness indices developed for selecting locations for WIM scales, and IRI were investigated.

A road profile encompasses a spectrum of sinusoidal wavelengths. A PSD function is a statistical representation of the importance of the various wavelengths contained in the profile.(20) A Fourier transform is used to generate a PSD plot from profile data. A PSD plot can assist in data interpretation by detecting cases where a significant portion of roughness is concentrated in a specific waveband and by detecting the type of content (i.e., short or long wavelengths) that dominates the profile.(21) Profile data collected on the same road section at two different times can be used to investigate the changes that have occurred for a specific wavelength. However, a PSD plot will not give any information about the location within a pavement section where changes have occurred. Hence, an investigation to determine whether there is a correlation between locations within a test section where changes in structural strength have taken place and changes in the ride quality of that area cannot be performed using a PSD plot. If changes in a pavement profile have occurred only at a few localized locations, there is a possibility for a PSD plot to give misleading results, as the PSD plot is generated by fitting sine waves to the pavement profile.

Smoothness indices for finding a suitable location to place a WIM scale were developed under a research project sponsored by FHWA.(22) These indices were developed to see if the smoothness of the pavement before the WIM site is suitable such that the axle hop and body bounce motions of a truck will not have an influence on the weights recorded. Two indices were developed, one based on short wavelengths that cause axle hop and the other based on long wavelengths that cause body bounce motion. A location was deemed suitable for establishing a WIM scale if the pavement before the WIM location met smoothness criteria based on the short and long wavelength smoothness indices. These WIM indices and IRI had a high correlation.[22] Hence, using the WIM indices as the smoothness index in this study would not provide additional information that is not already provided by IRI.

IRI is widely used throughout the world as a ride quality indicator. It is a measurement of the roughness in the road that impacts the vehicle response and, thereby, the riding comfort of passengers in the vehicle.[20] IRI correlates well with the vertical passenger acceleration, which is related to the ride quality experienced by a passenger in a vehicle.[20] State highway agencies in the United States use IRI to track the ride quality of their pavement network. The profile data on LTPP sections are collected along the left and right wheel path using an inertial profiler, and these data are used to compute the IRI of the wheel paths. The computed IRI values and the profile data are stored in the LTPP database. Locations of high IRI values within a test section can be determined by using a continuous IRI plot (described later in this report). Because of the wide acceptance of IRI by State highway agencies and the ability of a continuous IRI plot to pinpoint locations within a section where high changes in IRI have occurred, IRI was selected as the ride quality parameter to be used in this study.

3.4 STRUCTURAL STRENGTH PARAMETER SELECTED FOR STUDY

3.4.1 Flexible Pavements

The parameters considered to evaluate the structural strength of the pavements in this study include the SN_{eff} of the pavement and the Structural Adequacy Index (SAI). The SN concept was developed during the AASHO Road Test and is widely used in the United States to design and evaluate the structural strength of flexible pavements. SN_{eff} can be calculated using deflection data collected by an FWD.

Several agencies use SAI as a means to assess the structural ability of the pavement to support the anticipated traffic loads. Typically, the maximum allowable deflection is determined as a function of the anticipated traffic and compared against the measured deflection to determine SAI. To use this method, the anticipated traffic must be known. Although the LTPP database contains observed traffic information, future traffic estimates are not available. Hence, SN_{eff} was selected as the parameter to represent the structural strength of the pavement in this study.

The procedure to determine the SN of a flexible pavement from FWD measurements is described in the AASHTO *Guide for the Design of Pavement Structures*.[23] In this procedure, the deflection data are first used to determine the subgrade modulus. Then, the effective pavement modulus (E_p), which is the effective modulus of all pavement layers above the subgrade, is determined. E_p is calculated as a function of the deflection measured directly beneath the load, the applied pressure, the load plate radius of the FWD, the total thickness of the pavement layers above the subgrade, and the subgrade modulus, as shown in figure 17.

$$d_0 = 1.5pa\left[\left(\frac{1}{M_R\sqrt{1+\left(\frac{D}{a}\sqrt[3]{\frac{E_p}{M_R}}\right)^2}}\right) + \frac{\left(1-\frac{1}{\sqrt{1+\left(\frac{D}{a}\right)^2}}\right)}{E_p}\right]$$

Figure 17. Equation. d_0.

Where:

d_0 = Deflection at center of load corrected to 68 °F in inches.
p = Pressure applied by the FWD load plate in psi.
a = FWD load plate radius in inches.
D = Total thickness of pavement layers above subgrade in inches.
M_R = Subgrade resilient modulus in psi.
E_p = Effective pavement modulus of all layers above subgrade in psi.

SN is estimated from E_p using the equation in figure 18.

$$\mathrm{SN}_{\mathrm{eff}} = 0.0045\mathrm{D}\sqrt[3]{\mathrm{E}_{\mathrm{p}}}$$

Figure 18. Equation. $\mathrm{SN}_{\mathrm{eff}}$.

Where:

$\mathrm{SN}_{\mathrm{eff}}$ = Effective structural number.
E_p = Effective pavement modulus of all pavement layers in psi.
D = Total thickness of all pavement layers above subgrade in inches.

SN can be determined for each FWD test location. Because the deflection measured at the center of the load plate depends on the temperature of the asphalt layer, this deflection is adjusted to a standard temperature of 68 °F before computing SN.

3.4.2 Rigid Pavements

Effective slab thickness was the parameter selected in this study to define the structural strength of rigid pavements. The FWD data were used to compute an effective concrete slab thickness using the computer program ILLI-BACK. This program computes an effective slab thickness using FWD data based on a user input elastic modulus for concrete. A concrete modulus value of 4.5 million psi was used for this analysis. The program can use either an elastic solid or a dense-liquid foundation below the PCC slab. A dense-liquid foundation was used in this study. The program estimates a modulus of subgrade reaction (k-value) and the effective concrete slab thickness for each FWD sensor at a test location and outputs an average *k*-value and effective slab thickness.

3.5 CONTINUOUS ROUGHNESS PLOT

IRI is reported in units of inches per mile. The IRI of a pavement segment can be computed over any desired length (e.g., 500 ft, 0.1 mi, 0.5 mi, 1 mi, etc.). The test sections used in the LTPP program for both GPS and SPS studies are 500 ft long except for two sections in the SPS-6 experiment that are 1,000 ft long. For each LTPP section, the IRI of the left and right wheel path computed from the profile data collected at the section are stored in the LTPP database. This stored IRI value represents the average IRI of the 500-ft section. The average IRI does not provide any information about the variability of IRI within a test section.

Consider a pavement section that is 0.1 mi long with a right wheel path IRI of 96 inches/mi. As previously described, this IRI value represents the average IRI over the 0.1-mi length. This section can be divided into 10 52.8-ft segments. The IRI values of these 10 segments are shown in figure 19. The IRI of the 0.1-mile long segment is the average IRI of these 10 52.8-ft segments. Figure 19 shows that the IRI of segment 6 is significantly higher than the rest of the segments and that segment 9 has the lowest IRI of all segments. As shown in the figure, the IRI is not uniform within this 0.1-mi segment, with a significant localized roughness event occurring in segment 6.

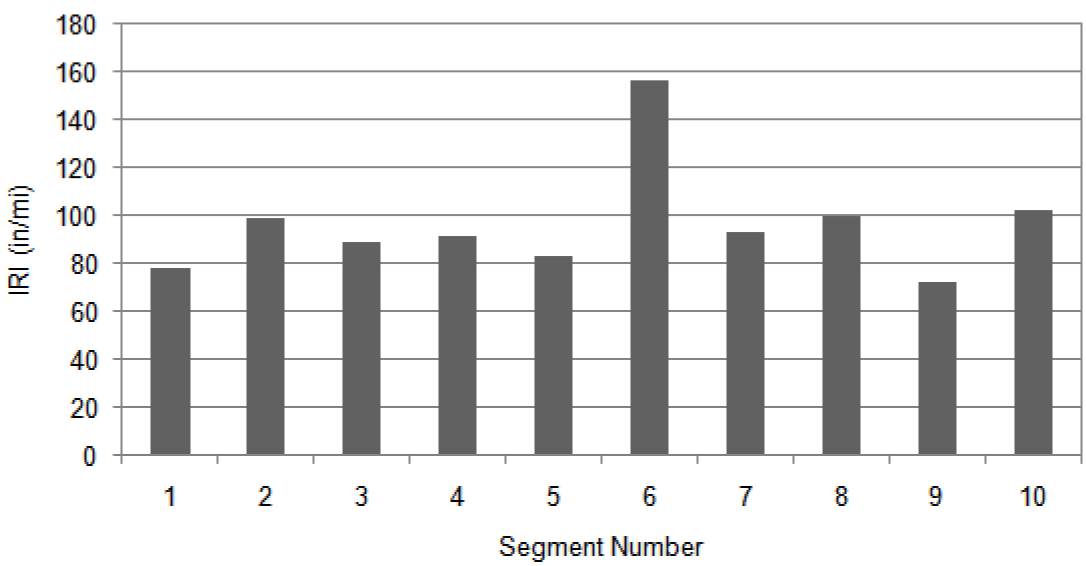

Figure 19. Graph. IRI of 52.8-ft segments in 0.1-mi pavement section.

Instead of using a single value to show the IRI of a road over a fixed distance, a continuous roughness plot can be used to show how IRI varies with distance along a roadway. Figure 20 shows a continuous IRI plot based on a 25-ft base length for the same data that were used to compute the IRI of 52.8-ft segments shown in figure 19. The IRI shown at any location in figure 20 is the average IRI over a 25-ft length (i.e., base length of the continuous roughness plot) that is centered at that location. For example, the IRI shown in this plot at a distance of 100 ft is the average IRI from 87.5 to 112.5 ft. Any base length can be used for generating a continuous IRI plot. Typically, a base length of 25 ft is used for locating areas of localized roughness. A detailed description of continuous roughness plots is presented by Sayers.[(24)]

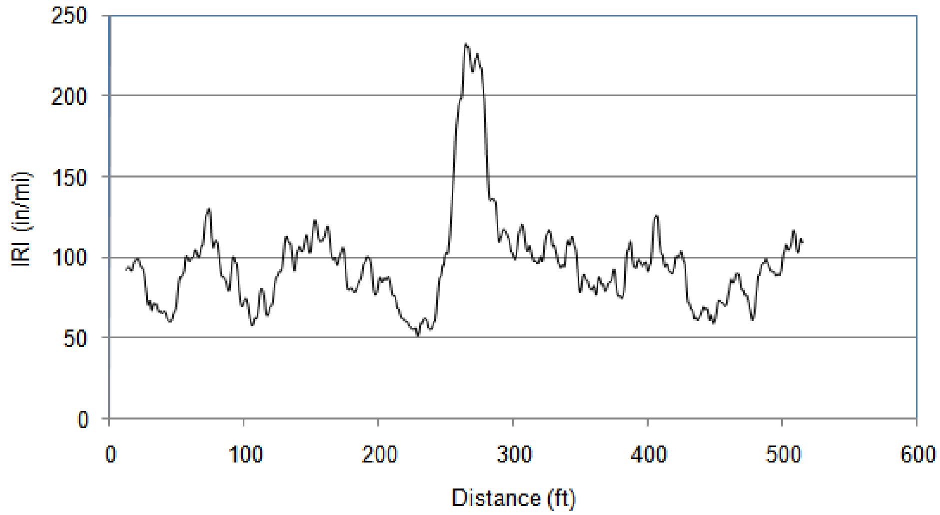

Figure 20. Graph. Continuous roughness plot based on 25-ft base length.

3.6 EVALUATING CHANGES IN RIDE QUALITY AND STRUCTURAL CAPACITY OVER TIME

3.6.1 Changes in IRI

Figure 21 shows the right wheel path continuous IRI plots (based on a 25-ft base length) for SPS-1 section 050119 in Arkansas for profile runs performed on July 6, 1995, and March 18, 2004. In 1995, data on this test section were collected immediately after construction. The IRI values of the right wheel path for the 500-ft LTPP section for July 6, 1995, and March 19, 2004, were 47 and 98 inches/mi, respectively. The continuous IRI plot shows most of the increase in IRI occurred between about 150 and 260 ft. This information would not be known if only the average IRI of the section was evaluated. Hence, as shown in this example, continuous IRI plots provide a method to determine the locations within the section where significant changes in IRI occur over time.

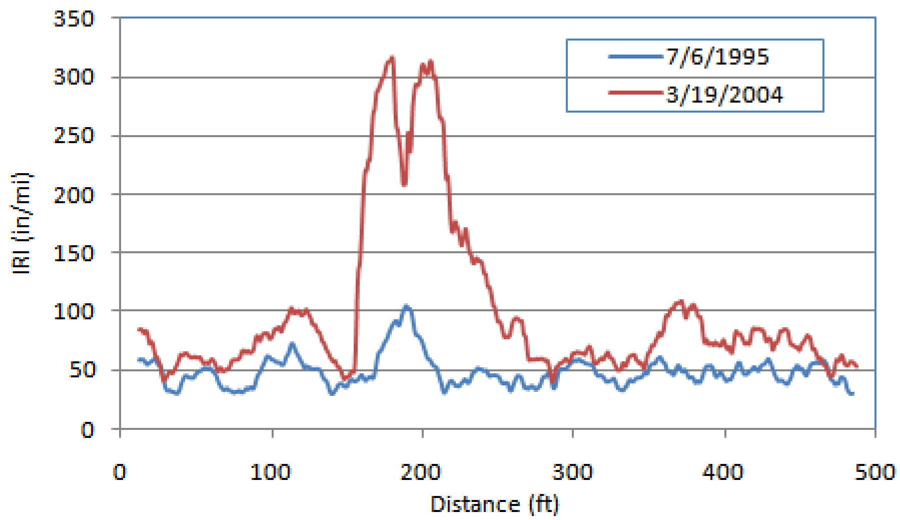

Figure 21. Graph. Continuous IRI plots for two test dates.

3.6.2 Changes in Structural Strength—Flexible Pavements

As described earlier, SN was used to characterize the structural strength of flexible pavements. FWD testing is performed on flexible pavements in the LTPP program at 50-ft intervals. An SN value can be computed at each FWD test location. Figure 22 shows the SN values computed from FWD data collected along the right wheel path of SPS-1 section 050119 in Arkansas for March 15, 1994, and May 24, 2004. Such a plot can be used to evaluate the change in SN that occurred at each FWD test location over time.

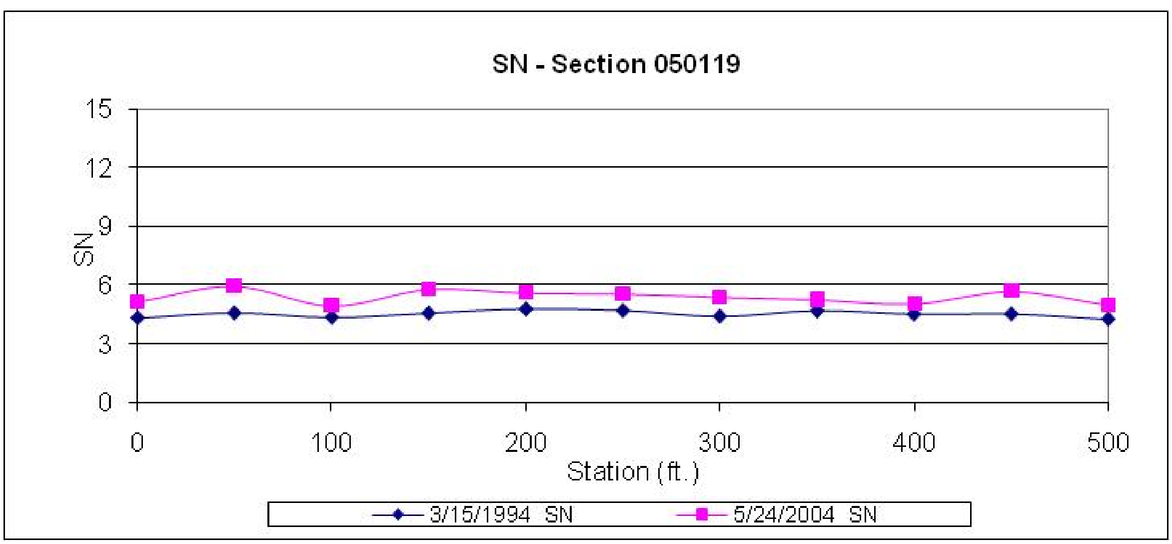

Figure 22. Graph. SN from FWD tests performed at two test dates.

3.6.3 Change in Structural Strength—Rigid Pavements

As previously described, the effective concrete slab thickness was used to characterize the structural strength of rigid pavements. The data from FWD tests performed at the center of the slab were used for this analysis, and the effective slab thickness was computed at each center slab FWD test location. Similar to the SN analysis, the effective slab thickness determined from tests performed at different time periods was used to evaluate the change in this parameter. Distress within a PCC slab is expected to result in an increase in IRI values, while the effective slab thickness is expected to decrease if distress is located within a slab. An important point to remember is that distress frequently occurs at joints in PCC pavements (e.g., faulting and spalling), which causes an increase in IRI. However, such distress will not impact the deflection obtained at the center of the slab, which is used to compute the effective slab thickness.

3.7 METHODOLOGY FOR COMPARING RIDE QUALITY-STRUCTURAL CAPACITY RELATIONSHIP

For each LTPP test section, profile data are available for five repeat runs for each monitoring date. One representative profile run was selected for generating the IRI values for analysis in this study. The structural capacity data used for analysis are described throughout this section according to pavement type.

3.7.1 Flexible Pavements

For flexible pavements, four load levels (6,000, 9,000, 12,000, and 16,000 lb) were used at each FWD test location, with four drops for each load level. This test sequence resulted in 16 deflection basins for each test location. SN values were computed for all 16 drops and then averaged. The average SN at each test location was used for analysis.

FWD testing on LTPP flexible pavements was performed along the center of the lane and the right wheel path at 50-ft intervals. Profile data at LTPP test sections were collected along the left and right wheel path. Hence, for flexible pavements, the SN values computed from FWD data collected along the right wheel path were compared with a continuous IRI plot for the right wheel path to examine if there was a relationship between the change in IRI and change in SN. Profile testing and FWD testing were not performed on the same day at LTPP test sections. Therefore, IRI and FWD data collected on dates close to each other were selected from the LTPP database for analysis.

Figure 21 shows that a large increase in IRI occurred along the right wheel path of the test section between 150 and 260 ft. If this increase in IRI occurred because of pavement distress along the right wheel path, a reduction in the SN within these limits is expected when SN data for the two test dates are compared. Locations with a low subgrade modulus can result in subgrade settlement or movement, causing a dip in the pavement and resulting in an increase in IRI. The subgrade modulus at each FWD test location was computed using the procedure described in the AASHTO *Guide for Design of Pavement Structures* and plotted versus distance to evaluate if locations where high changes in IRI occur can be related to locations with a low subgrade modulus.[23] The deflection below the load of the FWD represents the response due to the pavement structure and the subgrade. The deflections below the load of the FWD were also plotted versus the distance and compared with the continuous IRI plot to see if there was any relationship between high changes in roughness and the deflection below the load.

For all flexible pavements considered in this study, the continuous IRI and SN data were plotted on the same graph to evaluate changes and compare the relationship between the two data parameters. Figure 23 shows an example of such a plot, with SN and IRI data for two test dates.

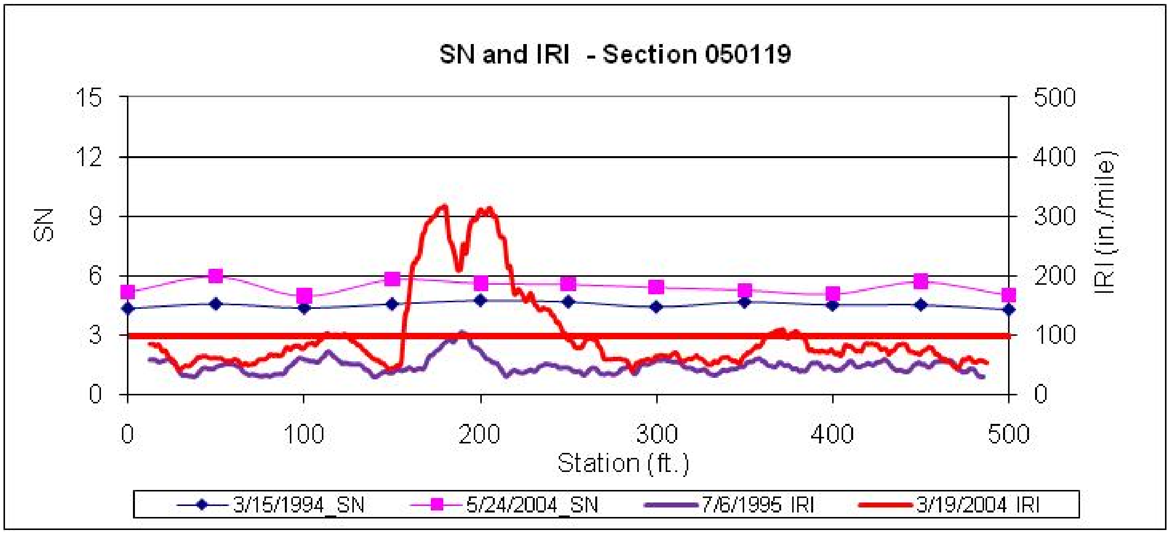

Figure 23. Graph. SN and IRI data on same plot.

Thereafter, normalized plots were created to visualize the percent changes in IRI and SN. Figure 24 shows an example of a normalized plot. The normalized IRI values were computed by dividing the continuous IRI value at each location for the initial and final test dates by the average initial IRI of the test section (i.e., average IRI for the entire section) and then expressing the computed value as a percentage. The normalized SN values were computed by dividing SN at each test location for the initial and final test dates by the average initial SN (i.e., average SN of the section for the initial test date) and then expressing the computed value as a percentage.

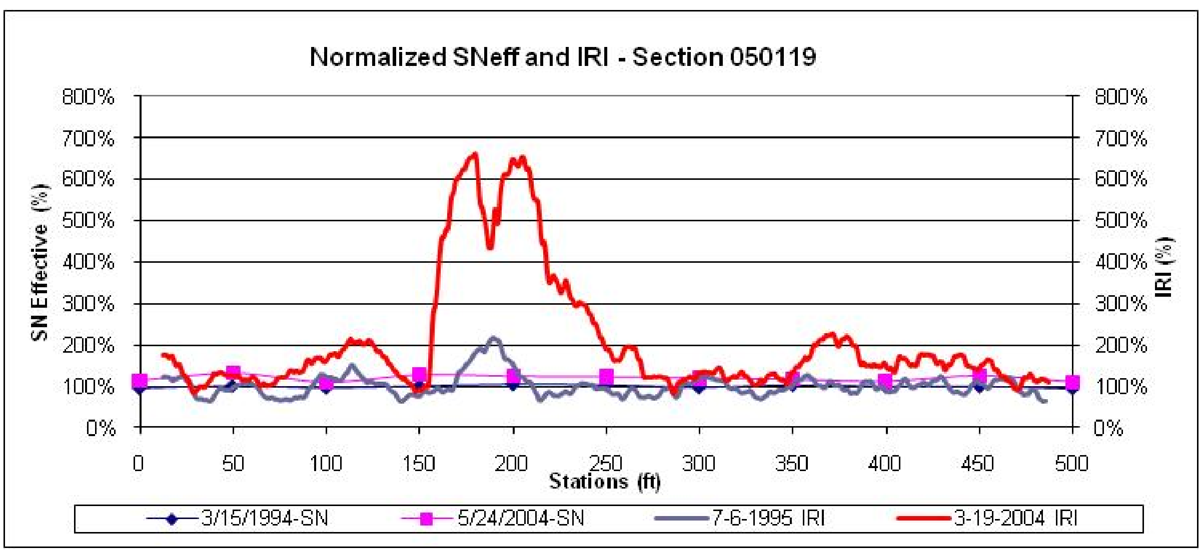

Figure 24. Graph. Normalized SN and IRI data on same plot.

3.7.2 Rigid Pavements

For rigid pavements, three load levels (9,000, 12,000, and 16,000 lb) were used at each FWD test location, with four drops for each load level. This test sequence resulted in 12 deflection basins for each test location. The effective concrete slab thickness (D_{eff}) values were computed for all 12 drops and then averaged. The average D_{eff} at each test location was used for analysis.

FWD tests on rigid pavements were performed at the center of the slab. The center slab deflections were used to compute D_{eff}. The continuous IRI plots for the right wheel path were then compared to D_{eff} to evaluate if a decrease in effective slab thickness was noted at locations that had a high increase in IRI. In addition, the plot showing deflection below the load was compared with the continuous IRI plot to see if any relationship could be detected between changes in IRI and changes in deflection.

Thereafter, normalized plots were created to visualize the percent changes in IRI and D_{eff}. The normalized IRI values were computed by dividing the continuous IRI value at each location for the initial and final test dates by the average initial IRI of the test section (i.e., average IRI for the entire section) and then expressing the computed value as a percentage. The normalized D_{eff} values were computed by dividing the D_{eff} at each test location for the initial and final test dates by the average initial D_{eff} (i.e., average D_{eff} of the section for the initial test date) and then expressing the computed value as a percentage.

3.8 TEST SECTIONS SELECTED FOR ANALYSIS

The pavement sections selected for the study were divided into the following five groups:

- **Group 1**: The sections in this group were selected by evaluating the change in IRI that occurred at SPS-1 sections. The change in IRI since construction was computed for all SPS-1 sections. Thereafter, seven sections were selected for analysis such that the change in IRI for the sections covered a wide range.

- **Group 2**: A previous study evaluated the change in effective pavement thickness at SPS-1 sections over time.[25] The effective pavement thickness in that study was computed from FWD data. Four sections that showed a significant decrease in the effective pavement thickness were selected for analysis.

- **Group 3**: In a previous study, SPS-1 sections with different base types appeared to behave differently from a structural point of view.[25] Based on this observation, a pair of sections with aggregate base and ATB was selected from two SPS-1 projects for analysis.

- **Group 4**: This group consists of flexible pavements that have been subjected to an AC overlay. Three test sections from the SPS-5 experiment were selected for analysis. The selected sections have had a significant increase in IRI since the overlay.

- **Group 5**: The sections in this group were selected by evaluating the change in IRI that occurred at SPS-2 sections. The change in IRI since construction was computed for all

SPS-2 sections. Thereafter, three sections that showed a significant change in IRI since construction were selected for analysis.

3.9 ANALYSIS OF GROUP 1 SECTIONS

Table 9 shows the following parameters for the test sections selected for analysis: LTPP section number, date corresponding to first IRI (first IRI date), date corresponding to last IRI (last IRI date), FWD test date close to the first IRI date (first FWD date), FWD test date close to the last IRI date (last FWD date), and the time difference between the first and last dates for IRI and FWD data collection.

Table 9. Group 1 sections selected for analysis.

LTPP Section	IRI Date		FWD Date		Time Difference Between First and Last Date (years)	
	First Date	Last Date	First Date	Last Date	IRI Data	FWD Data
050119, Arkansas	7/6/1995	3/19/2004	3/15/1994	5/24/2004	8.7	10.2
480114, Texas	9/8/1997	3/19/2007	11/17/1997	6/24/2004	9.5	6.6
310113, Nebraska	11/1/1995	3/20/2000	8/3/1995	10/14/1999	4.4	4.2
010102, Alabama	8/25/1994	5/4/2005	6/21/1995	4/29/2005	10.7	9.9
390112, Ohio	8/14/1996	5/5/2005	11/6/1996	9/1/2004	8.7	7.8
040123, Arizona	1/27/1994	3/27/2006	2/16/1994	4/7/2005	12.2	11.2
190108, Iowa	10/15/1993	9/22/2004	5/19/1993	6/27/2005	10.9	13.9

Table 10 shows the IRI values for the 500-ft-long sections for the first and last profile dates for the selected profile runs as well as the average SN values for the section for the first and last FWD date.

Table 10. IRI and SN for group 1 sections.

LTPP Section	IRI (inches/mi) First Date	IRI (inches/mi) Last Date	SN First Date	SN Last Date	Change Between First and Last* IRI (in/mi)	Change Between First and Last* SN
050119, Arkansas	48	98	4.51	5.40	50	-0.89
480114, Texas	46	65	10.90	10.39	19	0.51
310113, Nebraska	93	126	5.73	5.82	33	-0.09
010102, Alabama	62	204	2.86	2.19	143	0.67
390112, Ohio	57	101	7.83	7.39	44	0.44
040123, Arizona	52	138	7.94	7.26	86	0.68
190108, Iowa	49	141	8.30	9.94	93	-1.64

*A negative change in SN indicates that the SN increased from the first to the last date.

Table 11 shows the average pavement layer thickness of the selected test section computed from the layer thickness data in the LTPP database.

Table 11. Pavement layer thickness for group 1 sections.

LTPP Section	Layer Type	Layer Thickness (inches)	Material Type
050119, Arkansas	AC	6.8	Hot-mixed, dense-graded
	PATB	3.4	Open-graded, hot laid, central plant mix
	Granular base (GB)	4.1	Crushed stone
480114, Texas	AC	6.8	Hot-mixed, dense-graded
	GB	12.1	Crushed stone
	Treated subgrade (TS)	23	Lime-treated soil
310113, Nebraska	AC	5.1	Hot-mixed, dense-graded
	GB	8	Crushed stone
	Granular subbase (GS)	24	Fine-grained soils, lean inorganic clay
010102, Alabama	AC	4.2	Hot-mixed, dense-graded
	GB	12	Crushed stone
390112, Ohio	AC	4	Hot-mixed, dense-graded
	ATB	11.8	HMAC
	PATB	4	Open-graded, hot laid, central plant mix
040123, Arizona	AC	6.8	Hot-mixed, dense-graded
	ATB	7.9	HMAC
	PATB	3.8	Open-graded, hot laid, central plant mix
190108, Iowa	AC	6	Hot-mixed, dense-graded
	PATB	4.5	Open-graded, hot laid, central plant mix
	GB	8	Crushed stone
	GS	24	Fine-grained soils, lean clay with sand

3.9.1 LTPP Section 050119 (Arkansas)

The first and last profile dates for section 050119 (Arkansas) were July 6, 1995, and March 19, 2004, and the IRI of the right wheel path increased by 50 inches/mi (from 48 to 98 inches/mi) during this 9-year period. The first and last FWD dates for this section were March 15, 1994, and May 24, 2004, and the average SN for this section increased by 0.89 (from 4.51 to 5.40) during this 10-year period. Figure 25 shows the continuous IRI plots for this section for the first and last profile dates, and figure 26 shows the SN values for the first and last FWD dates. Figure 27 shows the deflection measured below the load for a 9,000-lb load for the first and last FWD dates. Figure 28 shows the subgrade modulus estimated from the FWD data for the first and last FWD dates. Figure 29 shows the first and last IRI and SN values on a single plot. The straight, solid line in this plot corresponds to the average IRI at the last profile date. This line can be used as a reference to identify areas that have a high IRI value at the last profile date. Figure 30 shows the normalized IRI and SN data for the first and last dates. For all other sections, only the SN and IRI single plot and the normalized plot are shown. Plots for deflection below the load for a normalized load of 9,000 lb and the subgrade modulus for all sections are included in appendix A.

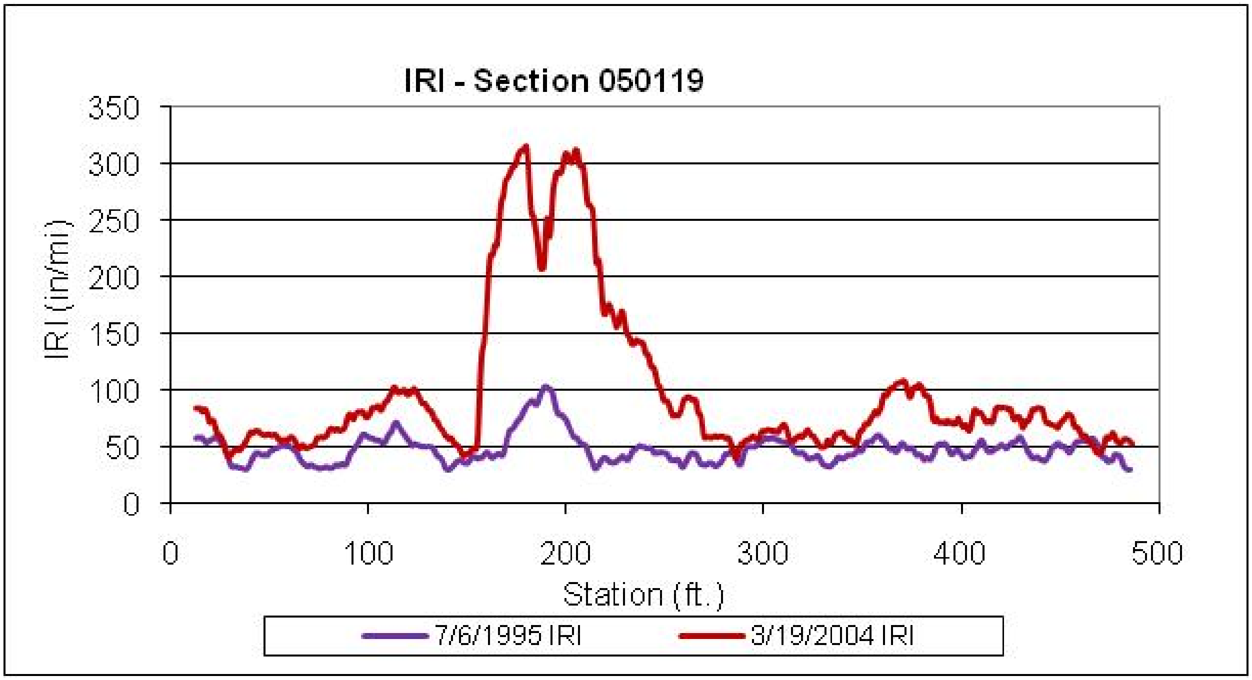

Figure 25. Graph. IRI for two test dates, section 050119 (Arkansas).

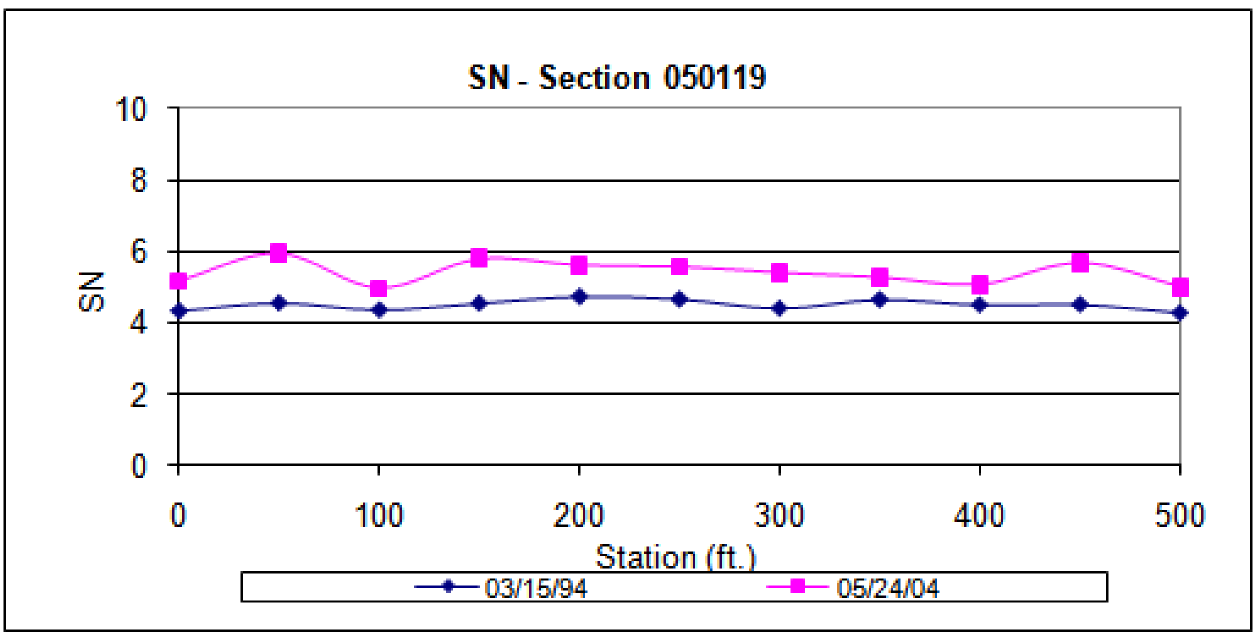

Figure 26. Graph. SN for two test dates, section 050119 (Arkansas).

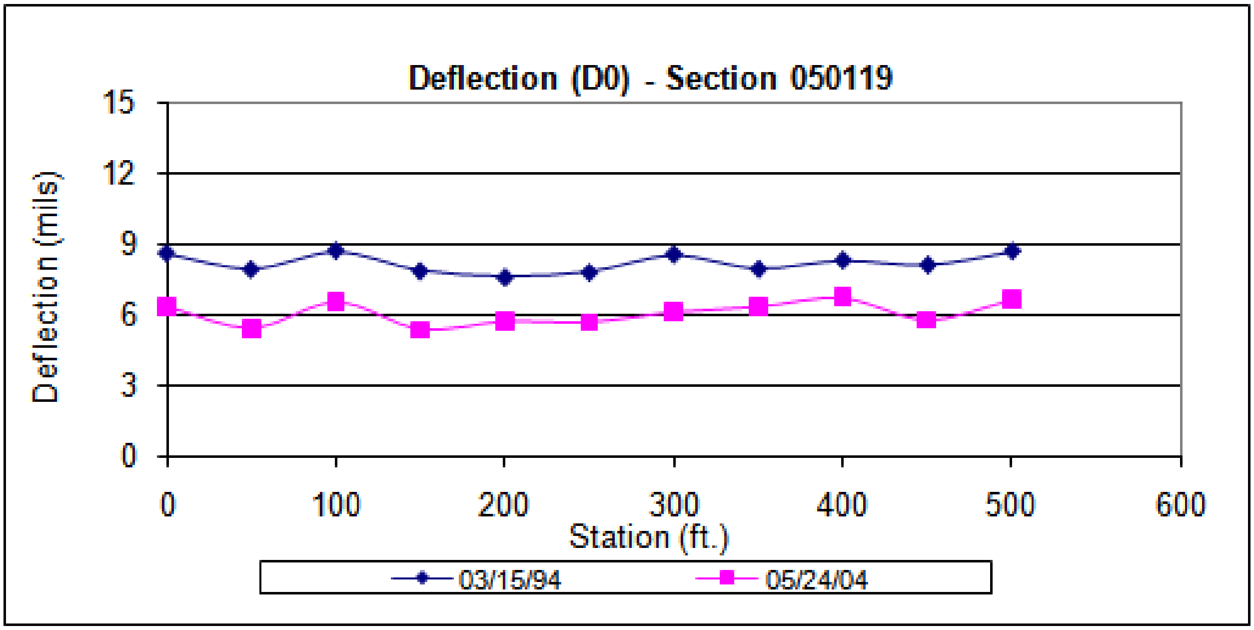

Figure 27. Graph. Deflection below load for 9,000 lb for two test dates, section 050119 (Arkansas).

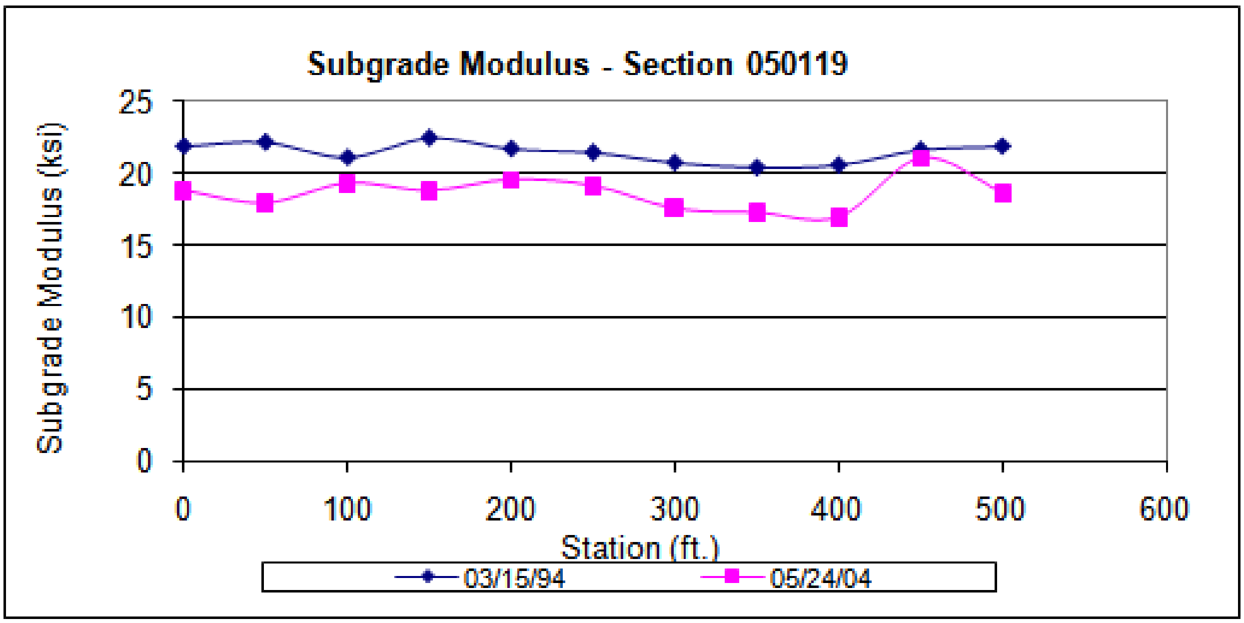

Figure 28. Graph. Subgrade modulus for two test dates, section 050119 (Arkansas).

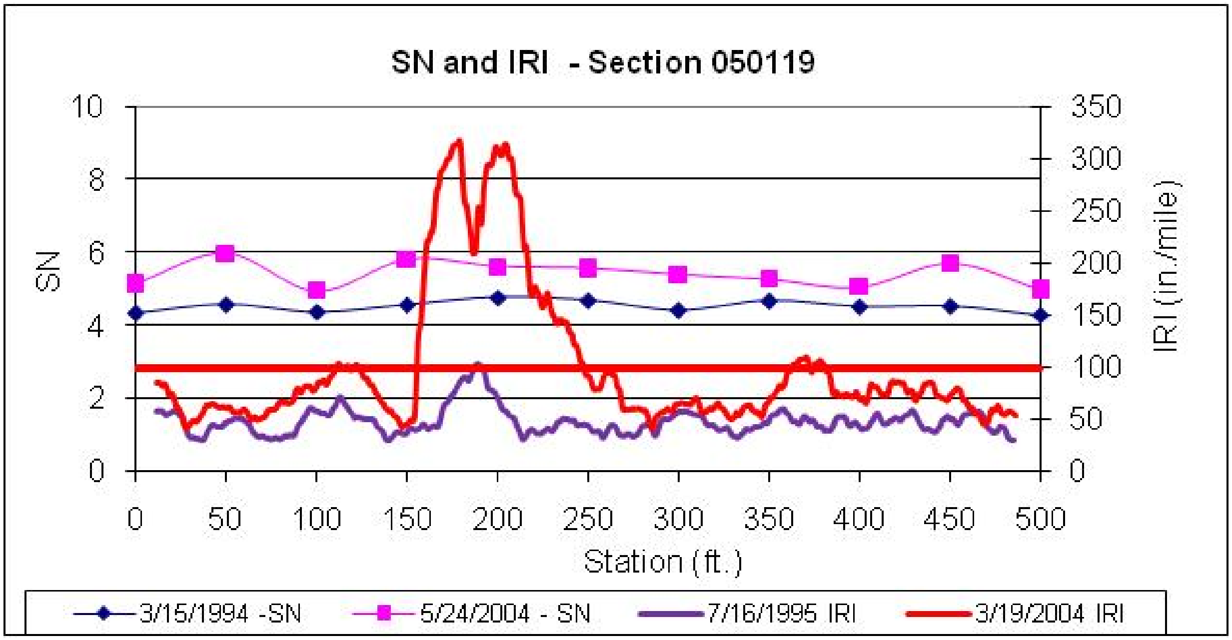

Figure 29. Graph. SN and IRI for two test dates, section 050119 (Arkansas).

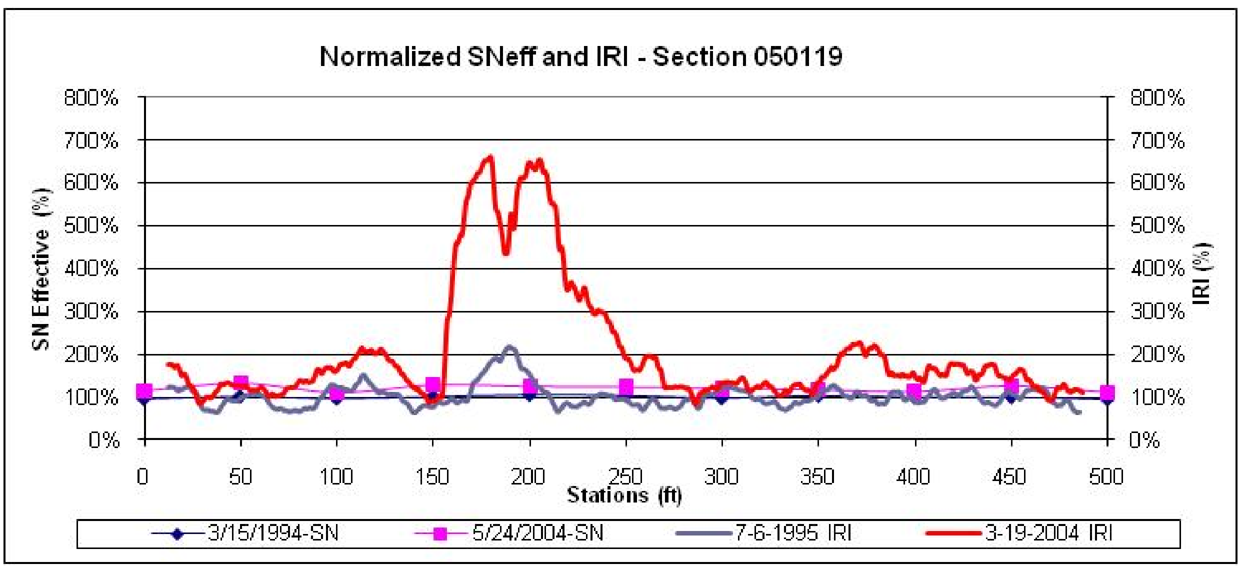

Figure 30. Graph. Normalized SN and IRI for two test dates, section 050119 (Arkansas).

For this test section, SN corresponding to the last test date was higher than SN corresponding to the first test date at all test locations. Figure 29 and figure 30 show that a large increase in IRI occurred in this section between about 160 and 240 ft. Only one FWD test point is located within these limits (at 200 ft), and SN corresponding to that test point does not show any significant difference when compared to SN obtained at the other test locations. The average increase in SN for this section between the two FWD test dates was 0.89, with the SN at 200 ft increasing by 0.85. The deflection below the load as well as the subgrade modulus at 200 ft does not show any trends that suggest a weaker subgrade was present at this location. Figure 27 shows the deflection below the load was lower at the last FWD date compared to the first FWD date at all test locations. Figure 28 shows the subgrade modulus for the last FWD date was lower than that for the first FWD date at all locations.

3.9.2 LTPP Section 480114 (Texas)

The first and last profile dates for section 480114 (Texas) were September 8, 1997, and March 19, 2007, and the IRI of the right wheel path increased by 19 inches/mi (from 46 to 65 inches/mi) during this 10-year period. The first and last FWD dates for this section were November 17, 1997, and June 24, 2004, and the average SN of this section decreased by 0.51 (from 10.90 to 10.39), during this 7-year period.

Figure 31 shows the first and last IRI and SN values, and figure 32 shows the normalized IRI and SN plots. The first 120 ft of the test section had a higher increase in IRI compared to the rest of the section. However, the decrease in SN that occurred at the test locations within these limits does not appear to be significantly different from the decrease in SN that occurred at the other test points. The average decrease in SN for this section was 0.51, and the average decrease in SN at the first three FWD locations was 0.46. No relationship was noted between the increase in IRI and the deflection below the load or the subgrade modulus.

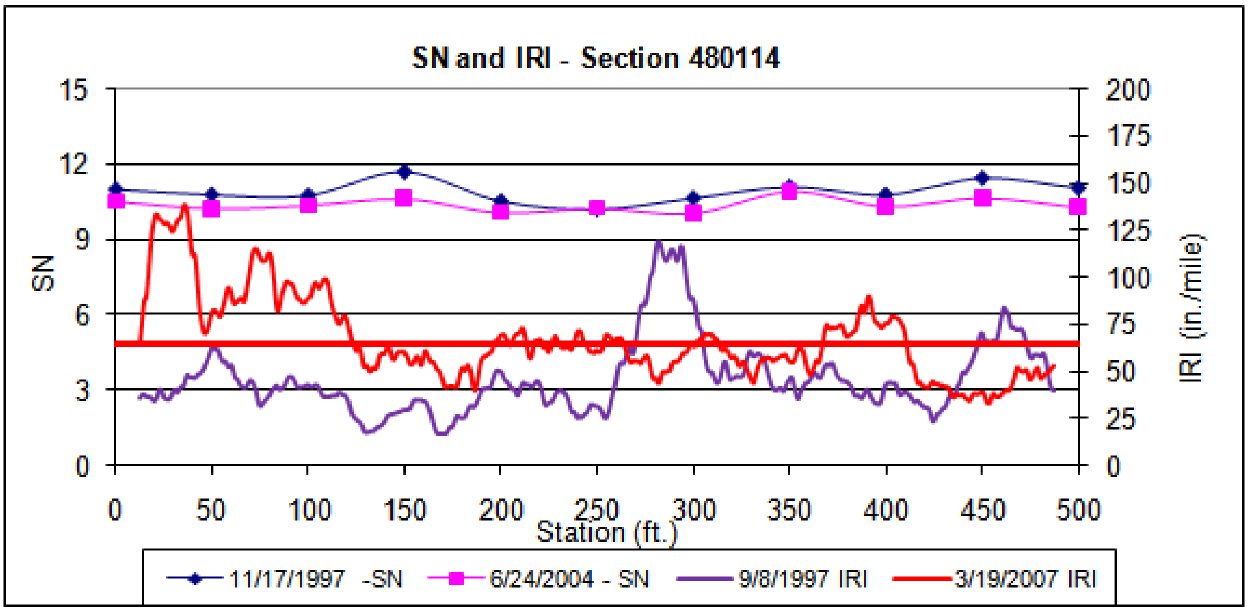

Figure 31. Graph. SN and IRI for two test dates, section 480114 (Texas).

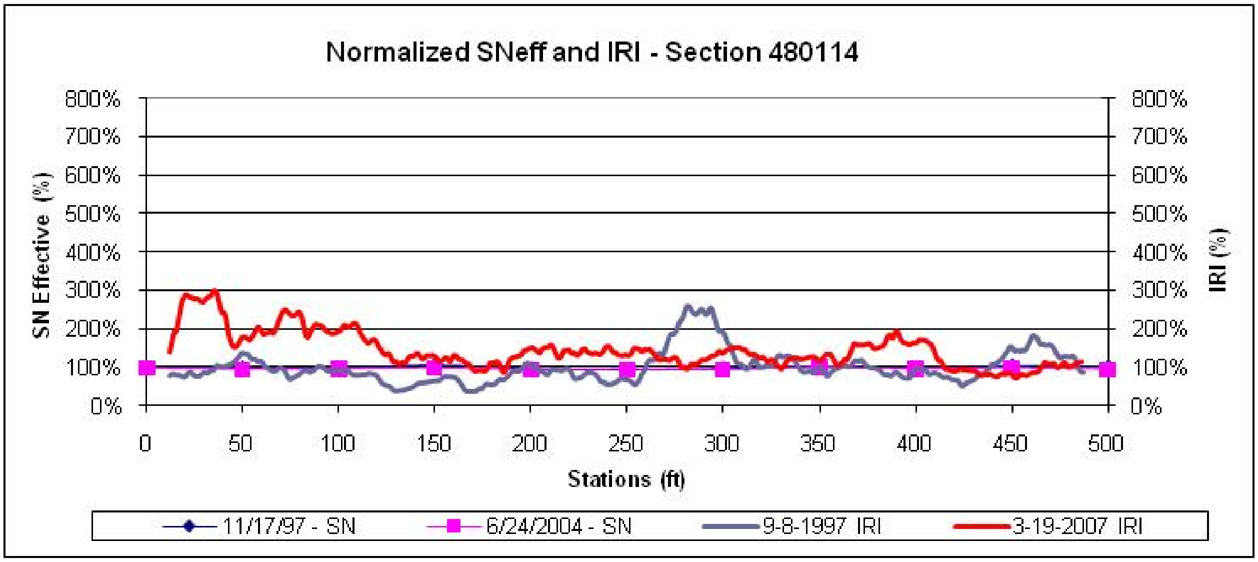

Figure 32. Graph. Normalized SN and IRI for two test dates, section 480114 (Texas).

3.9.3 LTPP Section 310113 (Nebraska)

The first and last profile dates for section 310113 (Nebraska) were November 1, 1995, and March 20, 2000, and the average IRI of the right wheel path increased by 33 inches/mi (from 93 to 126 inches/mi) during this 4-year period. The first and last FWD dates for this section were August 3, 1995, and October 14, 1999, and the average SN of this section increased by 0.09 (from 5.73 to 5.82) during this 4-year period.

Figure 33 shows the first and last IRI and SN values for this section, and figure 34 shows the normalized IRI and SN plots. No major changes in IRI occurred at any localized location within the test section. A slight increase in SN occurred over time at about half of the test locations, and the other half showed a slight decrease in SN. No test location showed a change in SN that was vastly different than the rest of the test locations. No relationship was noted between the increase in IRI and the deflection below the load or the subgrade modulus.

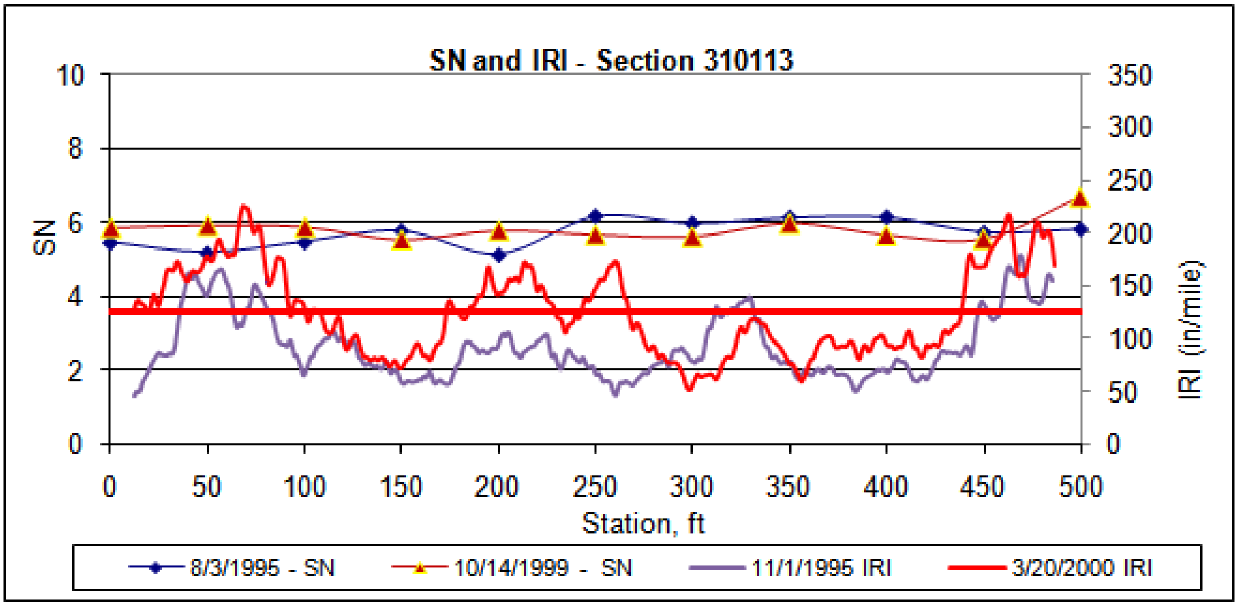

Figure 33. Graph. SN and IRI for two test dates, section 310113 (Nebraska).

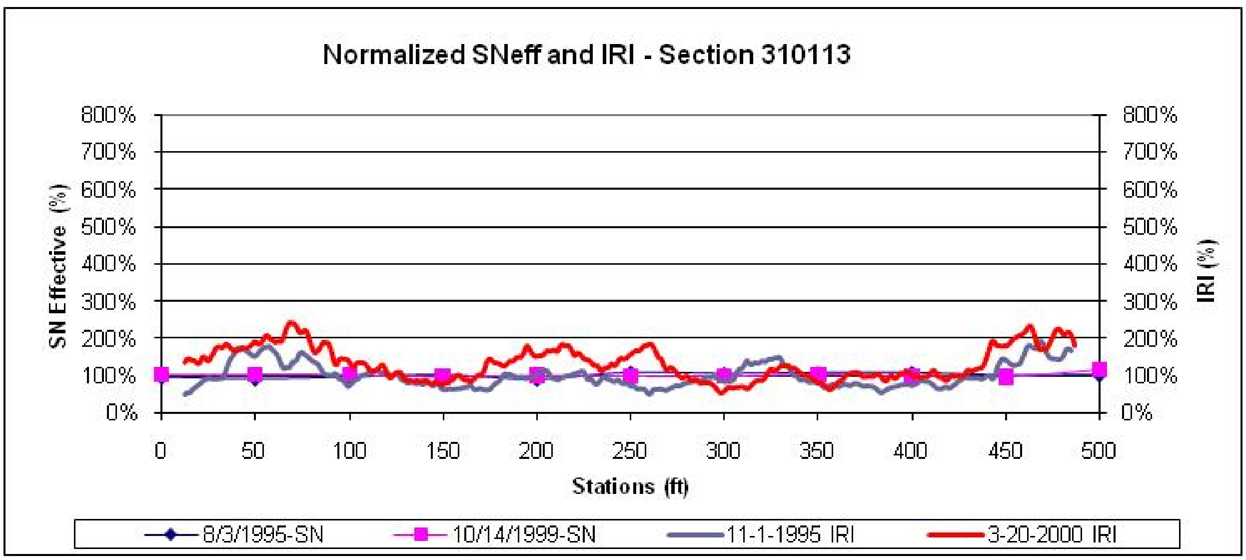

Figure 34. Graph. Normalized SN and IRI for two test dates, section 310113 (Nebraska).

3.9.4 LTPP Section 010102 (Alabama)

The first and last profile dates for section 010102 (Alabama) were August 25, 1994, and May 4, 2005, and the average IRI of the right wheel path increased by 143 inches/mi (from 62 to 204 inches/mi) during this 11-year period. The first and last FWD dates for this section were June 21, 1995, and April 29, 2005, and the average SN of this section decreased by 0.67 (from 2.86 to 2.19) during this 10-year period.

Figure 35 shows the first and last IRI and SN values, and figure 36 shows the normalized IRI and SN plots. The IRI of the last 300 ft of the test section showed a high increase in IRI when compared to the first 200 ft. IRI of the first 200 ft of the section increased from 75 to 114 inches/mi, and IRI of the section from 200 to 500 ft increased from 53 to 271 inches/mi. The highest increase in IRI occurred between about 260 and 380 ft. The average decrease in SN for the first 200 ft was 0.59, and average decrease in SN between 250 and 500 ft was 0.74. Although the last 300 ft of the section had a higher increase in IRI and showed a larger decrease in SN when compared to the first 200 ft, the decrease in SN of the last 300 ft was only slightly higher than that for the first 200 ft. In addition, a small SN decrease of 0.24 was noted at 300 ft, which was within the limits that showed the highest increase in IRI for this section. No relationship was noted between the increase in IRI and the deflection below the load or the subgrade modulus.

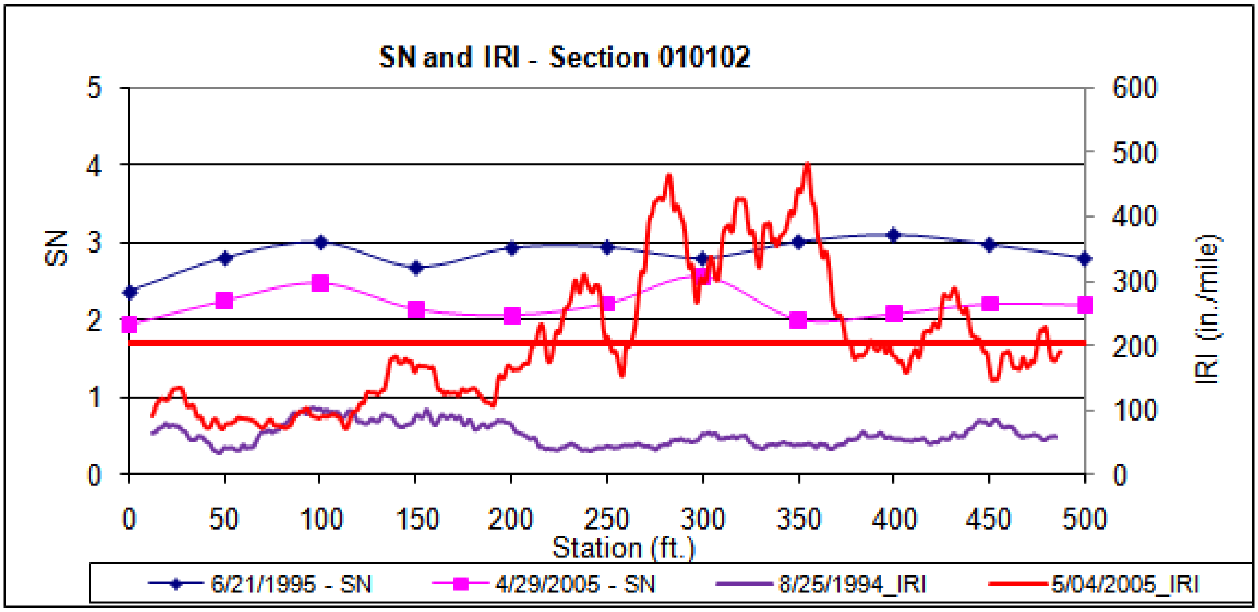

Figure 35. Graph. SN and IRI for two test dates, section 010102 (Alabama).

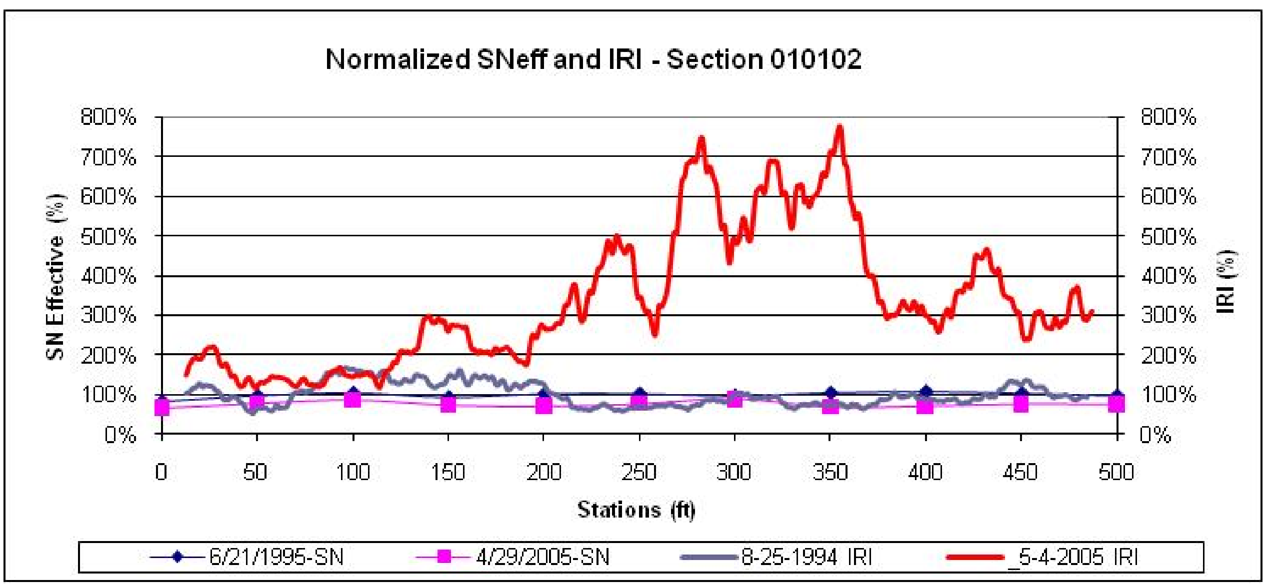

Figure 36. Graph. Normalized SN and IRI for two test dates, section 010102 (Alabama).

3.9.5 LTPP Section 390112 (Ohio)

The first and last profile dates for section 390112 (Ohio) were August 14, 1996, and May 5, 2005, and the IRI of the right wheel path increased by 44 inches/mi (from 57 to 101 inches/mi) during this 9-year period. The first and last FWD dates for this section were November 6, 1996, and September 1, 2004, and the average SN of this section decreased by 0.44 (from 7.83 to 7.39) during this 8-year period.

Figure 37 shows the first and last IRI and SN values, and figure 38 shows the normalized IRI and SN plots. SN corresponding to the last FWD date was slightly higher than SN corresponding to the first FWD date at the first test location. At all other test locations, SN decreased, with the decrease ranging from 0.37 to 0.76 and an average value of 0.51. High IRI values at the last profile date were noted between approximately 180 to 210 ft, 230 to 310 ft, and 390 to 430 ft. The lowest initial and final SN at this section occurred at 200 ft (within 180 to 210 ft), which was the area that had a high increase in IRI. Hence, for this particular area, a high increase in IRI was associated with a low initial SN. However, the decrease in SN at 200 ft was 0.51, which was equal to the average decrease in SN for this section. Two FWD test points are located between 230 and 310 ft, and the average decrease in SN at these two points was 0.49, while the decrease in SN at 400 ft (within 390 to 430 ft) was 0.45. The decrease in SN at these locations was less than the average decrease in SN for this section. No relationship was noted between the increase in IRI and the deflection below the load or the subgrade modulus.

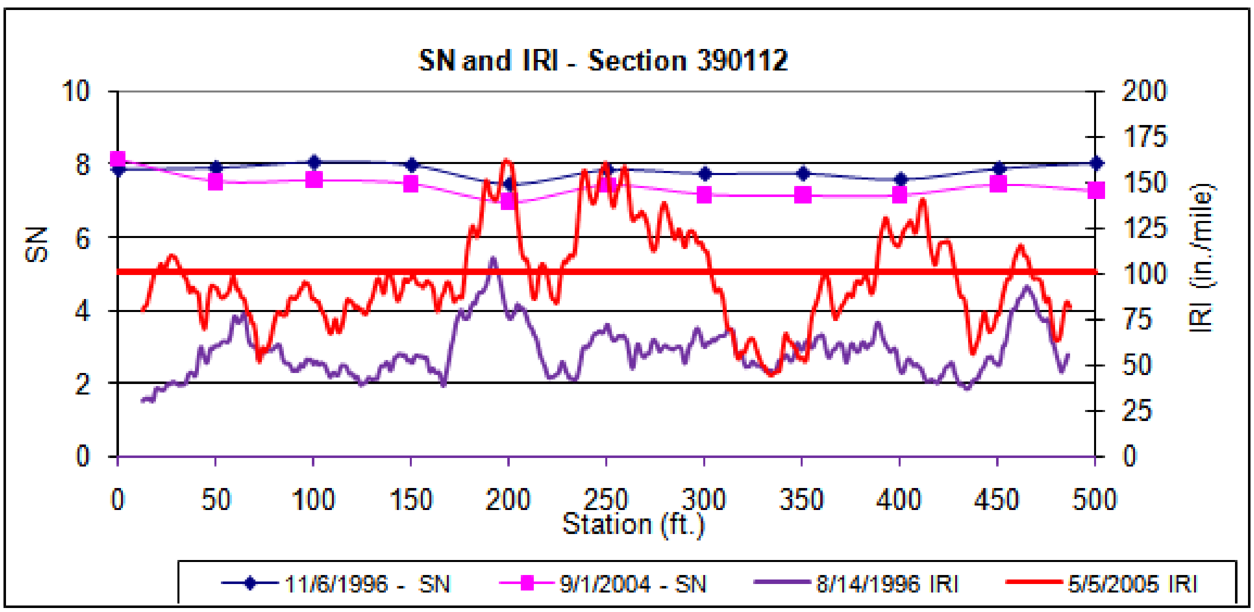

Figure 37. Graph. SN and IRI for two test dates, section 390112 (Ohio).

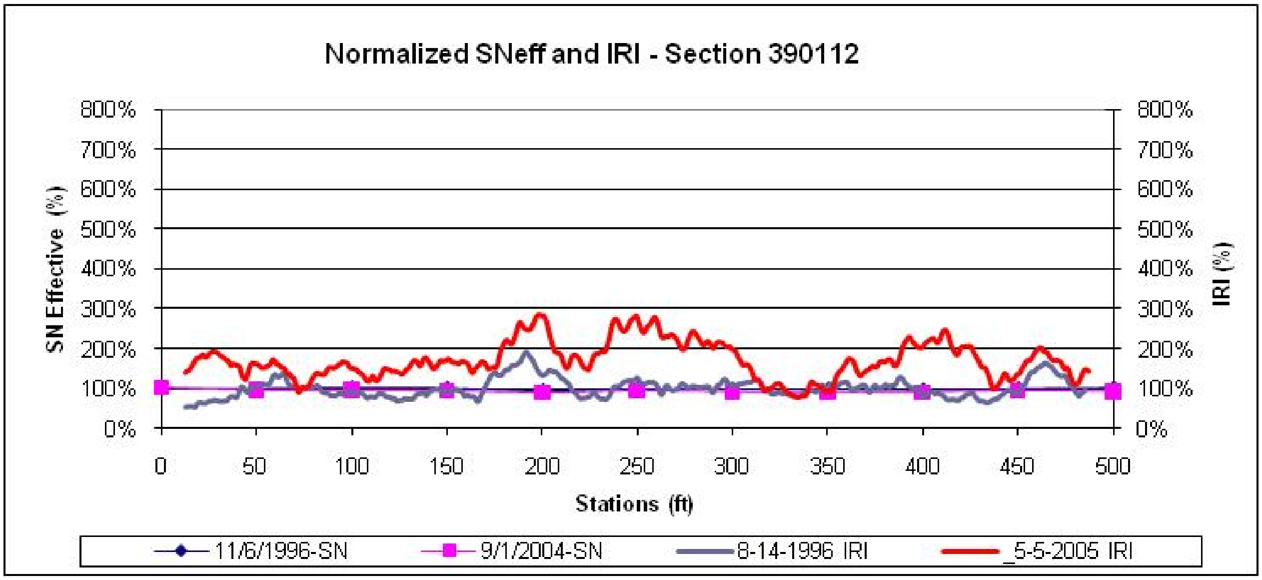

Figure 38. Graph. Normalized SN and IRI for two test dates, section 390112 (Ohio).

3.9.6 LTPP Section 040123 (Arizona)

The first and last profile dates for section 040123 (Arizona) were January 27, 1994, and March 27, 2006, and the average IRI of the right wheel path increased by 86 inches/mi from (52 to 138 inches/mi) during this 12-year period. The first and last FWD dates for this section were February 16, 1994, and April 7, 2005, and the average SN of this section decreased by 0.68 (from 7.94 to 7.26) during this 11-year period.

Figure 39 shows the first and last IRI and SN values, and figure 40 shows the normalized IRI and SN plots. A higher decrease in SN was observed between 0 and 200 ft compared to 250 to 500 ft. All test locations between 0 and 200 ft showed a decrease in SN, with an average decrease of 1.48. Four of the six test locations between 250 and 500 ft showed an increase in SN. For the two points that showed a decrease in SN, the average decrease was 0.40. A significant increase in IRI occurred within the section between the following approximate limits: about 80 to 140 ft, 210 to 260 ft, and 300 to 350 ft. An FWD test point that was close to a peak IRI location occurred only at 100 ft. At this location, a decrease in SN of 1.14 was noted. The average decrease in SN at test locations between 0 and 200 ft was 1.57 and was more than the decrease in IRI noted at 100 ft. However, the change in IRI seen at these test locations was much less when compared to the change in IRI seen at 100 ft. No relationship was noted between the increase in IRI and the deflection below the load or the subgrade modulus.

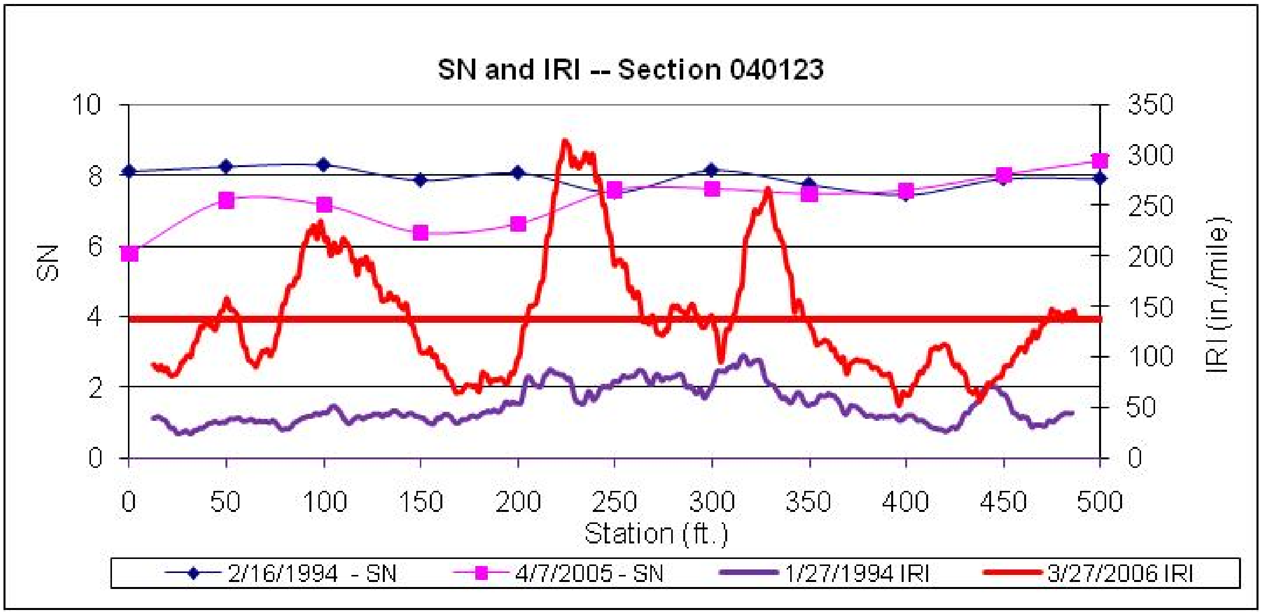

Figure 39. Graph. SN and IRI for two test dates, section 040123 (Arizona).

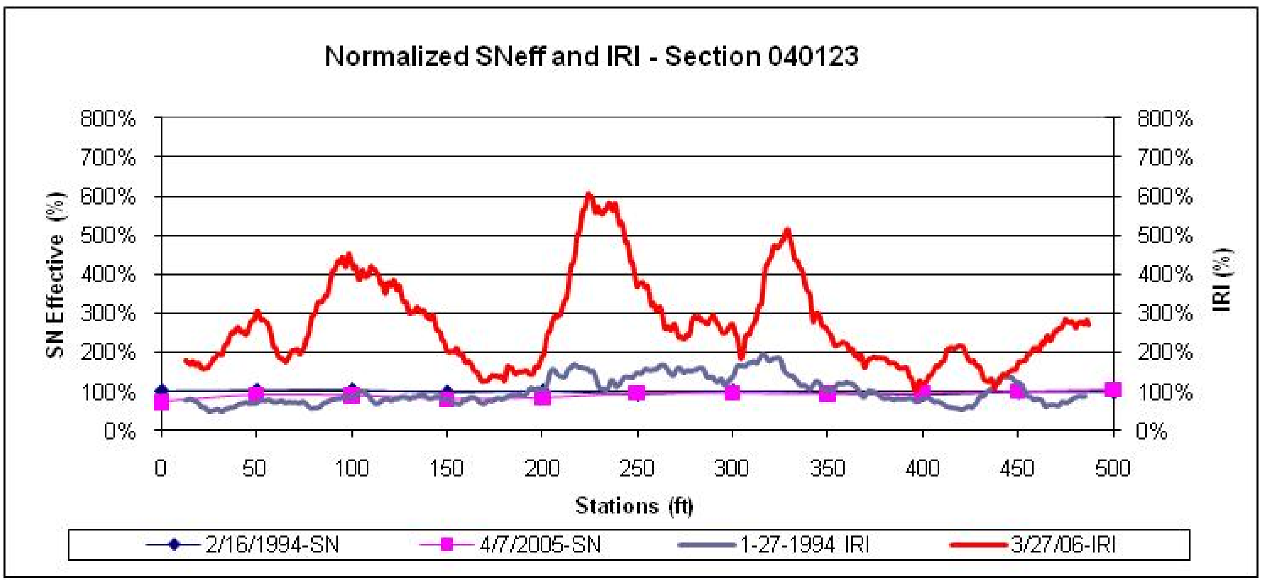

Figure 40. Graph. Normalized SN and IRI for two test dates, section 040123 (Arizona).

3.9.7 LTPP Section 190108 (Iowa)

The first and last profile dates for section 190108 (Iowa) were October 15, 1993, and September 22, 2004, and the IRI of the right wheel path increased by 93 inches/mi (from 49 to 141 inches/mi) during this 11-year period. The first and last FWD dates for this section were May 19, 1993, and April 24, 2007, and the average SN of this section increased by 1.64 (from 8.30 to 9.94) during this 14-year period.

Figure 41 shows the first and last IRI and SN values, and figure 42 shows the normalized IRI and SN plots. SN at the last FWD date was greater than SN at the first FWD date at all test locations. The peaks in the IRI plot for the last IRI date are locations where major increases in IRI had occurred. Except at one location (450 ft), the FWD data points are located outside the peak IRI areas. The average increase in SN between the FWD test dates at this section was 1.65, with SN at 450 ft showing an increase of 2.13 between the two test dates. No relationship was noted between the increase in IRI and the deflection below the load or the subgrade modulus.

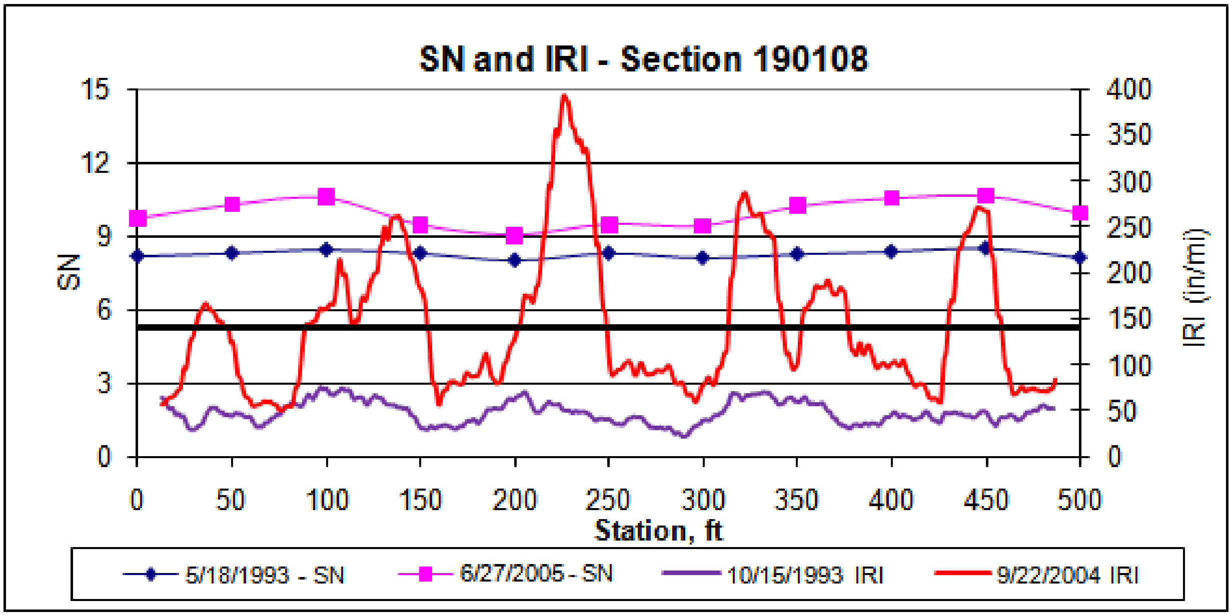

Figure 41. Graph. SN and IRI for two test dates, section 190108 (Iowa).

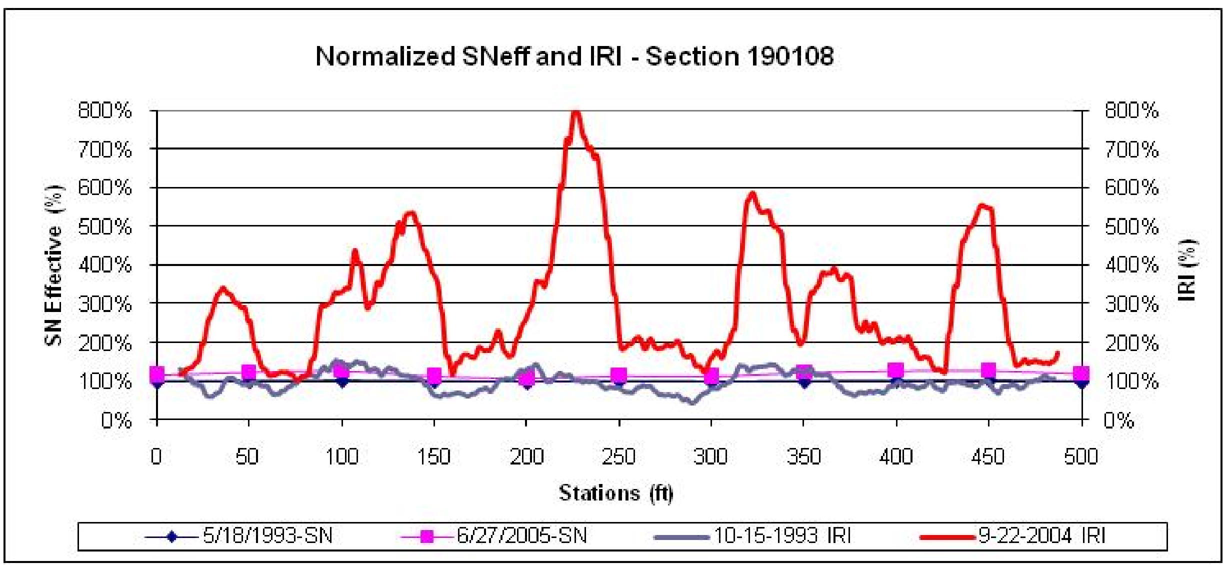

Figure 42. Graph. Normalized SN and IRI for two test dates, section 190108 (Iowa).

3.10 ANALYSIS OF GROUP 2 SECTIONS

Table 12 shows the following parameters for the test sections selected for analysis: LTPP section number, date corresponding to first IRI (first IRI date), date corresponding to last IRI (last IRI date), FWD test date close to the first IRI date (first FWD date), FWD test date close to the last

IRI date (last FWD date), and the time difference between first and last dates for IRI and FWD data collection.

Table 12. Group 2 sections selected for analysis.

LTPP Section	IRI Date		FWD Date		Time Difference Between First and Last Date (years)	
	First Date	Last Date	First Date	Last Date	IRI Data	FWD Data
320101, Nevada	12/3/1996	8/7/2006	3/27/1996	8/28/2006	9.7	10.4
390106, Ohio	8/14/1996	8/9/2006	11/5/1996	7/15/2008	10.0	11.7
310117, Nebraska	11/1/1995	4/24/2002	8/2/1995	7/9/2002	6.5	6.9
310118, Nebraska	11/1/1995	4/24/2002	8/3/1995	7/10/2002	6.5	6.9

Table 13 shows the IRI values for the 500-ft-long sections for the first and last profile dates for the selected profile runs as well as the average SN for the first and last FWD date. Table 14 shows the average pavement layer thickness of the group 2 sections computed from the layer thickness data available in the LTPP database.

Table 13. IRI and SN for group 2 sections.

	IRI (inches/mi)		SN		Change Between First and Last*	
LTPP Section	First Date	Last Date	First Date	Last Date	IRI (inches/mi)	SN
320101, Nevada	57	57	11.91	11.23	0	0.68
390106, Ohio	71	114	6.94	5.04	43	1.90
310117, Nebraska	68	53	8.32	7.30	-15	1.02
310118, Nebraska	74	54	9.21	7.62	-20	1.59

*A negative IRI indicates IRI at the last date was less than the IRI at the first date.

Table 14. Pavement layer thickness, group 2 sections.

LTPP Section	Layer Type	Layer Thickness (inches)	Material Type
320101, Nevada	AC	7.2	Hot-mixed, dense-graded
	GB	8.5	Crushed gravel
	GS	22.8	Soil-aggregate mixture (predominantly coarse-grained)
	TS	12	Lime-treated soil
390106, Ohio	AC	6.7	Hot-mixed, dense-graded
	ATB	7.9	HMAC
	GB	3.8	Crushed stone
310107, Nebraska	AC	7.1	Hot-mixed, dense-graded
	PATB	3.8	Open-graded
	GB	4	Crushed stone
	GS	24	Fine-grained soils, lean inorganic clay
310118, Nebraska	AC	4.3	Hot-mixed, dense-graded
	ATB	8.2	HMAC
	GB	4	Crushed stone
	GS	24	Fine-grained soils, lean inorganic clay

3.10.1 LTPP Section 320101 (Nevada)

The first and last profile dates for section 320101 (Nevada) were December 3, 1996, and August 7, 2006, and the IRI of the right wheel path remained the same at 57 inches/mi over this 10-year period. The first and last FWD dates for this section were March 27, 1996, and August 28, 2006, and the average SN of this section decreased by 0.68 (from 11.91 to 11.23) over this 10-year period.

Figure 43 shows the first and last IRI and SN values, and figure 44 shows the normalized IRI and SN plots. SN decreased from the first to the last FWD date at all test locations, with the decrease in SN ranging from 0.13 to 1.41. However, as seen in figure 43 and figure 44, there is virtually no noticeable change in IRI throughout the section.

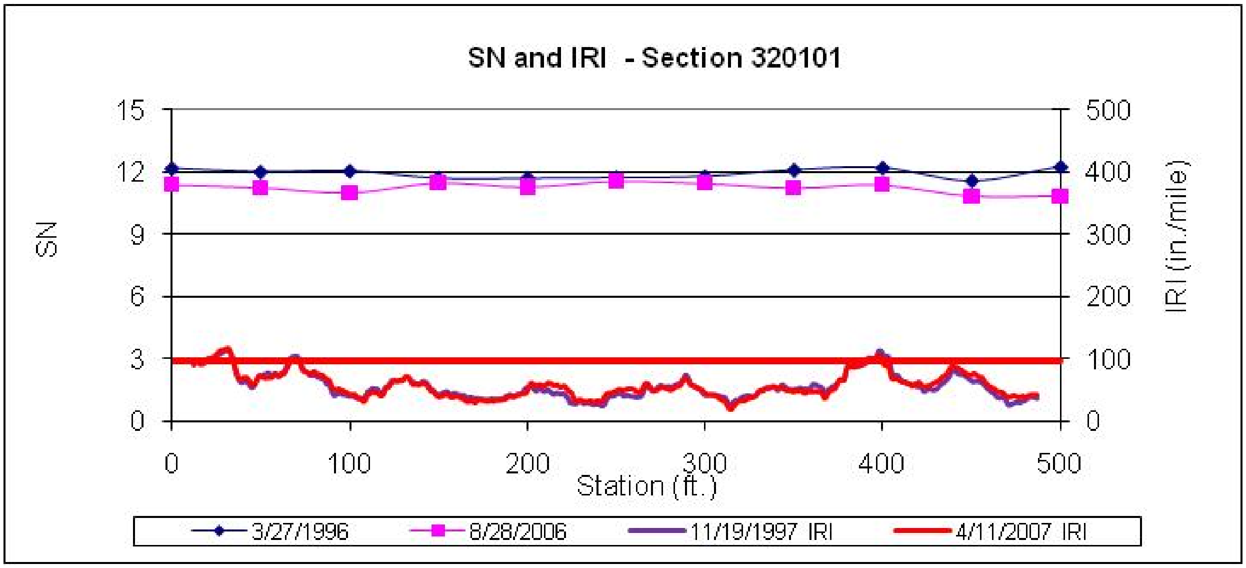

Figure 43. Graph. SN and IRI for two test dates, section 320101 (Nevada).

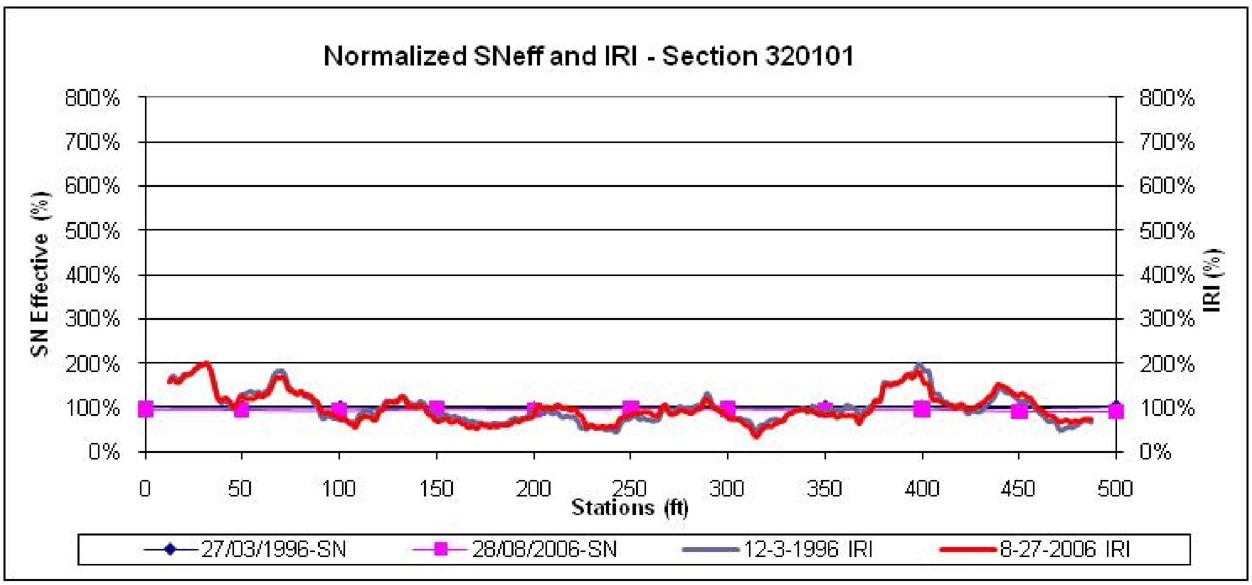

Figure 44. Graph. Normalized SN and IRI for two test dates, section 320101 (Nevada).

3.10.2 LTPP Section 390106 (Ohio)

The first and last profile dates for section 390106 (Ohio) were August 14, 1996, and August 9, 2006, and the IRI of the right wheel path increased by 43 inches/mi (from 71 to 114 inches/mi) during this 10-year period. The first and last FWD dates for this section were November 5, 1996, and July 15, 2008, and the average SN of the section decreased by 1.90 from (6.94 to 5.04) during this 12-year period.

Figure 45 shows the first and last IRI and SN values, and figure 46 shows the normalized IRI and SN plots. An increase in IRI was observed at most locations within the section, with the highest change in IRI occurring between about 140 and 190 ft. The highest increase in IRI occurred close to 150 ft, where an FWD test was performed. SN decreased from the first to the last FWD dates at all test locations. The decrease in SN at 150 ft was 2.06, slightly higher than the average decrease in SN of 1.90 for this section. A decrease in SN greater than the 2.06 decrease that was observed at 150 ft was noted at 50, 100, 200, and 450 ft. The magnitude of the IRI change at these locations was much less than that observed at 150 ft. No relationship was noted between the increase in IRI and the deflection below the load or the subgrade modulus (see appendix A).

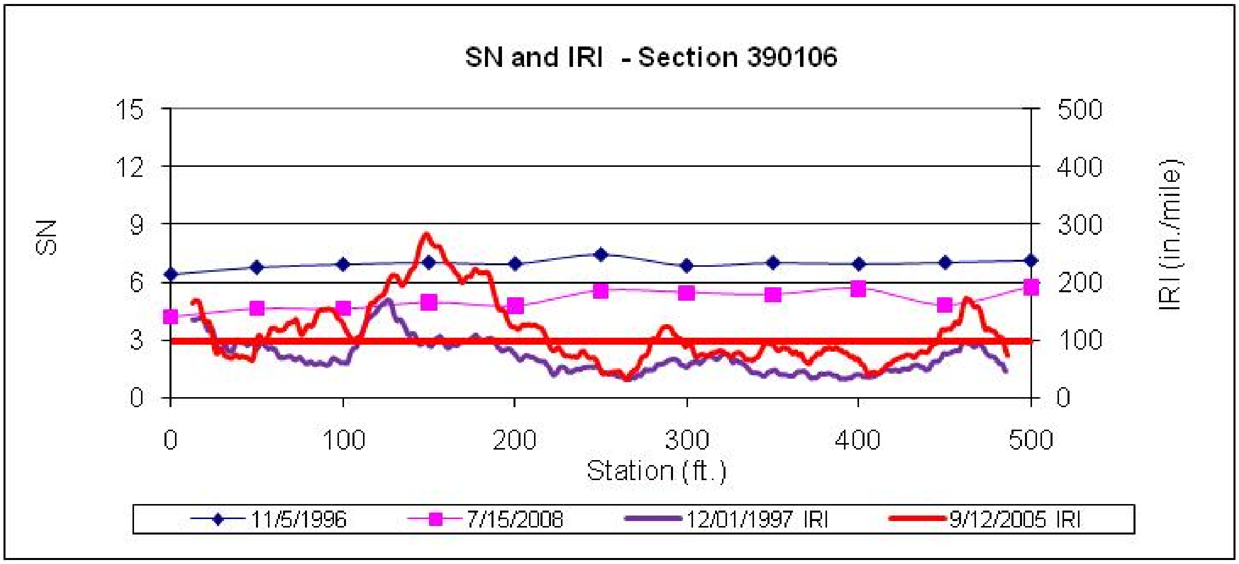

Figure 45. Graph. SN and IRI for two test dates, section 390106 (Ohio).

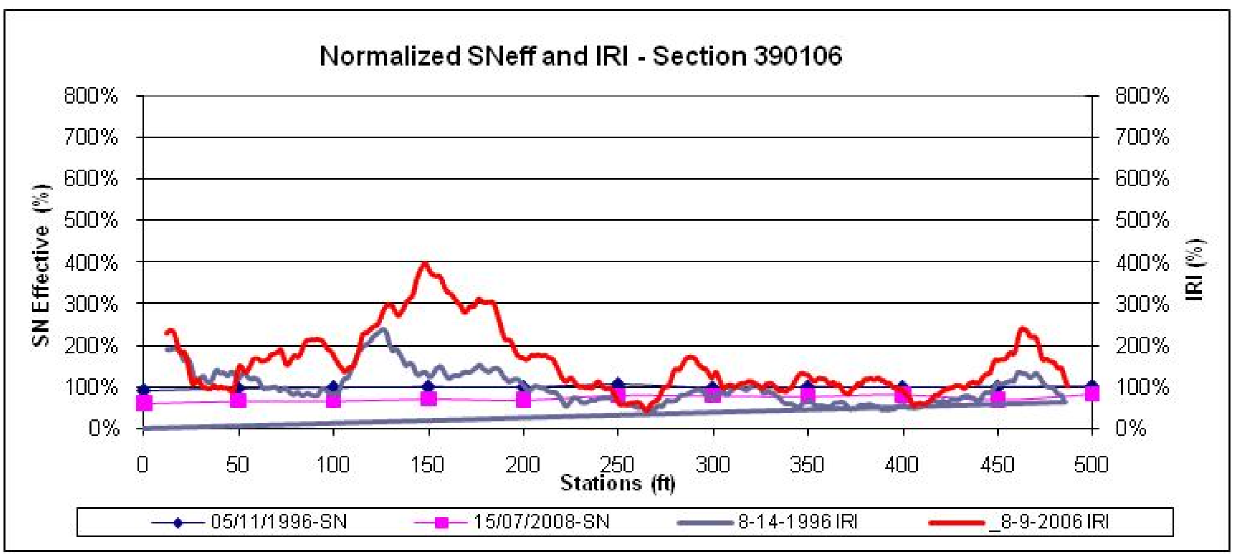

Figure 46. Graph. Normalized SN and IRI for two test dates, section 390106 (Ohio).

3.10.3 LTPP Section 310117 (Nebraska)

The first and last profile dates for section 310117 (Nebraska) were November 1, 1995, and April 24, 2002, and the IRI of the right wheel path decreased by 15 inches/mi (from 68 to 53 inches/mi) during this 7-year period. The LTPP database indicated this section was diamond ground on July 12, 2000. The reduction in IRI is attributed to the diamond grinding. The first and last FWD dates for this section were August 2, 1995, and July 9, 2002, and the average SN of this section decreased by 1.02 (from 8.32 to 7.30) during this 7-year period. IRI and SN plots were not developed for this section because it was subjected to diamond grinding.

3.10.4 LTPP Section 310118 (Nebraska)

The first and last profile dates for section 310118 (Nebraska) were November 1, 1995, and April 24, 2002, and the IRI of the right wheel path decreased by 20 inches/mi (from 74 to 54 inches/mi) during this 7-year period. This section is in the same SPS-1 project as section 310117 (Nebraska). The LTPP database indicated the section was diamond ground on July 12, 2000. The reduction in IRI is attributed to the diamond grinding. The first and last FWD dates for this section were August 3, 1995, and July 10, 2002, and the average SN of this section decreased by 1.59 (from 9.21 to 7.62) during this 7-year period. IRI and SN plots were not developed for this section because it was subjected to diamond grinding.

3.11 ANALYSIS OF GROUP 3 SECTIONS

Table 15 shows the following parameters for the test sections selected for analysis: LTPP section number, date corresponding to first IRI (first IRI date), date corresponding to last IRI (last IRI date), FWD test date close to the first IRI date (first FWD date), FWD test date close to the last IRI date (last FWD date), and the time difference between first and last dates for IRI and FWD data collection.

Table 15. Group 3 sections selected for analysis.

LTPP Section	IRI Date		FWD Date		Time Difference Between First and Last Date (years)	
	First Date	Last Date	First Date	Last Date	IRI Data	FWD Data
190101, Iowa	10/15/1993	9/22/2004	5/19/1993	6/28/2005	10.9	12.1
190103, Iowa	10/15/1993	9/22/2004	5/19/1993	6/29/2005	10.9	12.1
050114, Arkansas	7/7/1995	4/6/2005	3/16/1994	5/12/2005	9.8	11.2
050116, Arkansas	7/7/1995	4/6/2005	3/16/1994	5/11/2005	9.8	11.2

Table 16 shows the IRI values for the 500-ft-long section for the first and last profile dates for the selected profile runs as well as the average SN for the section for the first and last FWD date. Table 17 shows the pavement layer thickness for group 3 sections.

Table 16. IRI and SN for group 3 sections.

LTPP Section	IRI (inches/mi)		SN		Change Between First and Last*	
	First	Last	First	Last	IRI (inches/mi)	SN
190101, Iowa	83	159	7.48	7.62	76	-0.14
190103, Iowa	46	92	9.39	8.68	46	0.71
050114, Arkansas	49	72	4.26	5.13	23	-0.87
050116, Arkansas	68	63	7.81	10.30	-5	-2.49

*A negative change in SN indicates SN at the last date was higher than SN at the first date. A negative change in IRI indicates IRI at the last date was lower than IRI at the first date.

Table 17. Pavement layer thickness, group 3 sections.

LTPP Section	Layer Type	Layer Thickness (inches)	Material Type
190101, Iowa	AC	7.7	Hot-mixed, dense-graded
	GB	8	Crushed stone
	GS	25	Fine-grained soils, clay with gravel
190103, Iowa	AC	3.8	Hot-mixed, dense-graded
	ATB	8.4	HMAC
	GS	24	Fine-grained soils, clay with gravel
050114, Arkansas	AC	6.9	Hot-mixed, dense-graded
	GB	11	Gravel (uncrushed)
050116, Arkansas	AC	4.1	Hot-mixed, dense-graded
	ATB	11.8	HMAC

Sections 190101 and 190103 are both test sections in the Iowa SPS-1 project. Section 190101 has DGAB, and section 190103 has ATB. Section 050114 and 050116 are test sections in the Arkansas SPS-1 project. Section 050114 has DGAB, and section 050116 has ATB. In each project, the test section with the DGAB base showed a higher increase in IRI between the first and the last dates when compared to the test section with ATB.

3.11.1 LTPP Section 190101 (Iowa)

The first and last profile dates for section 190101 (Iowa) were October 15, 1993, and September 22, 2004, and the IRI of the right wheel path increased by 76 inches/mi (from 83 to 159 inches/mi) during this 11-year period. The first and last FWD dates for this section were May 19, 1993, and June 28, 2005, and the average SN of this section increased by 0.14 (from 7.48 to 7.62) during this 12-year period.

Figure 47 shows the first and last IRI and SN values, and figure 48 shows the normalized IRI and SN plots. SN at the last FWD date was greater than SN at the first FWD date at all test locations, except for the last three (400, 450, and 500 ft). There are five peaks in the IRI plot for the last IRI date, and, except for two, the peak IRI locations fall outside locations where FWD testing was conducted. SN values are available between 380 to 410 ft and 440 to 460 ft, where two of the peaks occur. The reductions in SN at 400 and 450 ft were 0.31 and 1.39, respectively. Therefore, a reduction in SN was seen at the locations that had a high increase in IRI. No relationship was noted between the increase in IRI and the deflection below the load or the subgrade modulus (see appendix A).

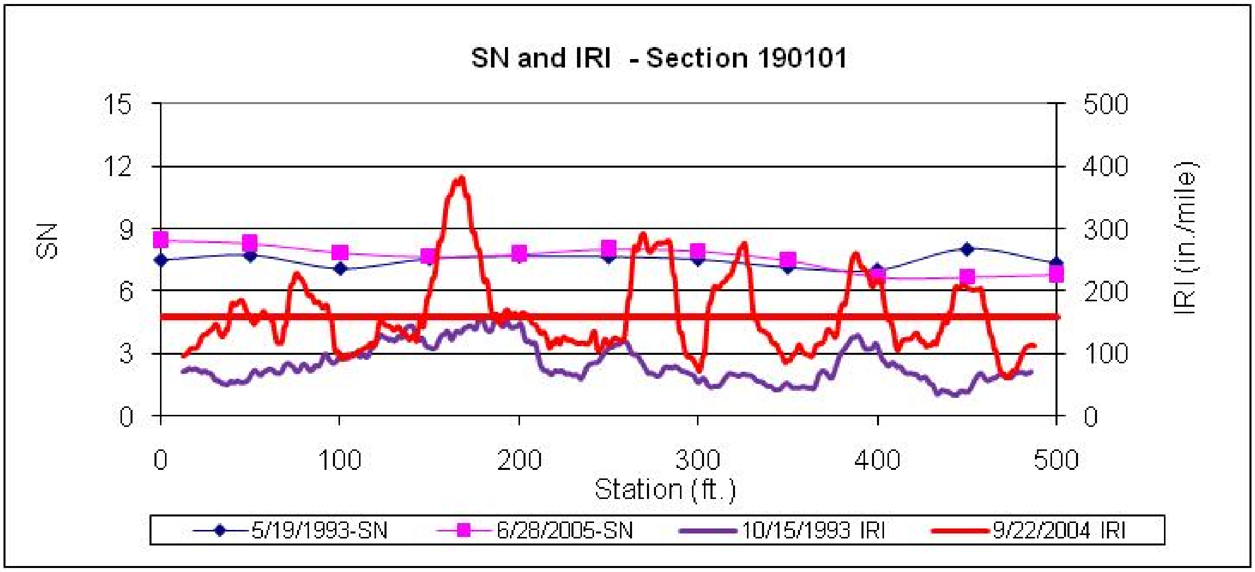

Figure 47. Graph. SN and IRI for two test dates, section 190101 (Iowa).

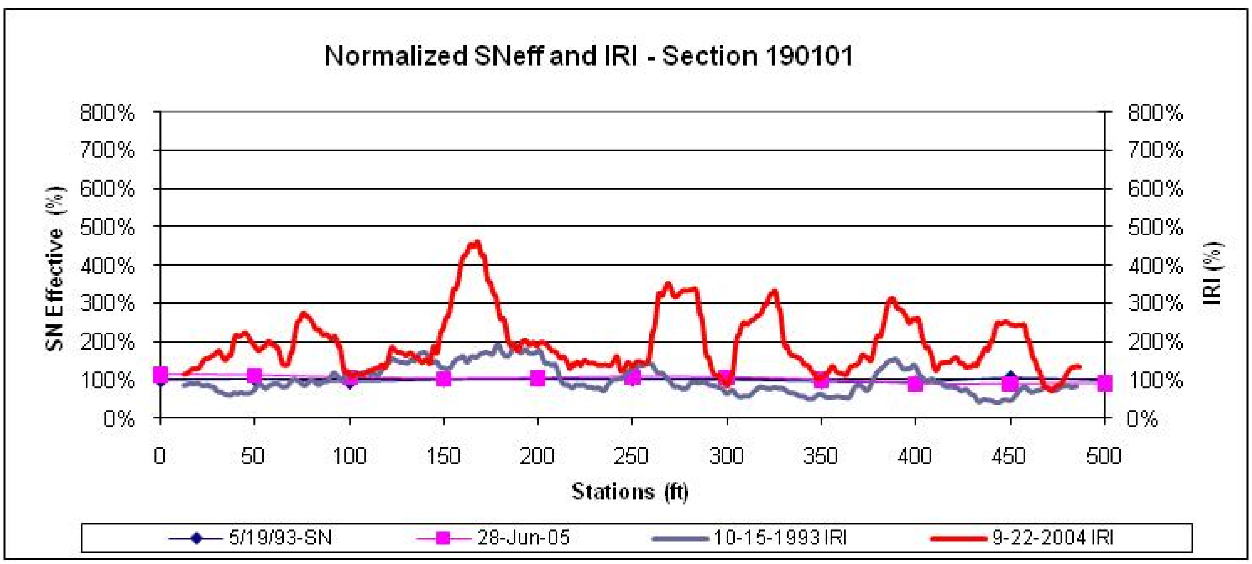

Figure 48. Graph. Normalized SN and IRI for two test dates, section 190101 (Iowa).

3.11.2 LTPP Section 190103 (Iowa)

The first and last profile dates for section 190103 (Iowa) were October 15, 1993, and September 22, 2004, and the IRI of the right wheel path increased by 46 inches/mi (from 46 to 92 inches/mi) during this 11-year period. The first and last FWD dates for this section were May 19, 1993, and June 29, 2005, and the average SN of this section decreased by 0.71 (from 9.39 to 8.68) during this 12-year period.

Figure 49 shows the first and last IRI and SN values, and figure 50 shows the normalized IRI and SN plots. SN at the last FWD date was lower than SN at the first FWD date at all test locations. An increase in IRI is noted throughout the section, with a major increase in IRI close to 250 ft. An FWD test was performed at 250 ft, and the decrease in SN observed at this location was 0.32, which was less than the average decrease in SN at this section. No relationship was noted between the increase in IRI and the deflection below the load or the subgrade modulus (see appendix A).

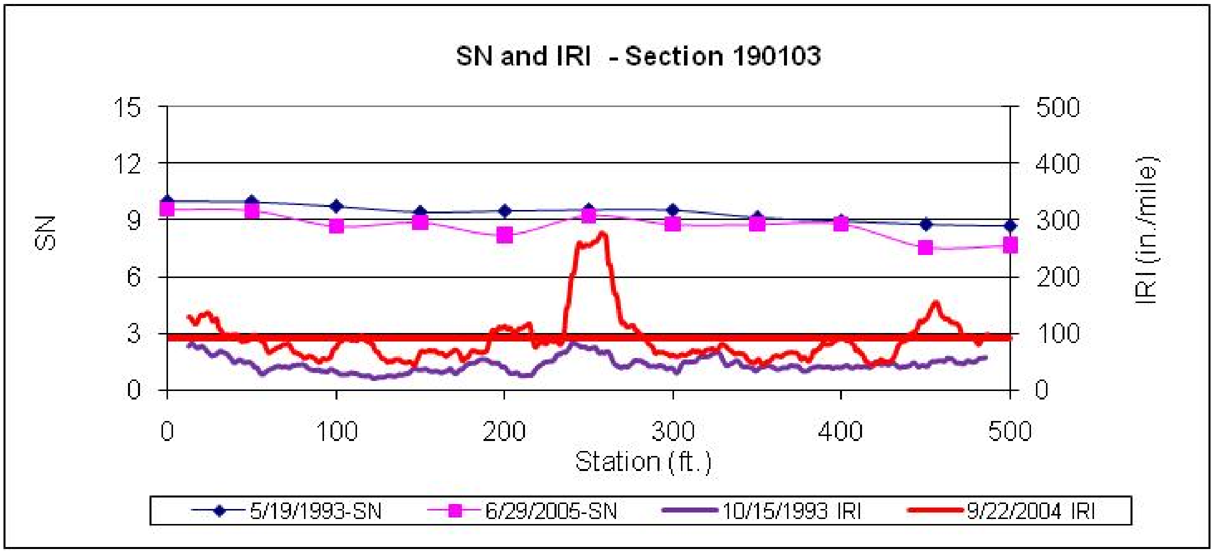

Figure 49. Graph. SN and IRI for two test dates, section 190103 (Iowa).

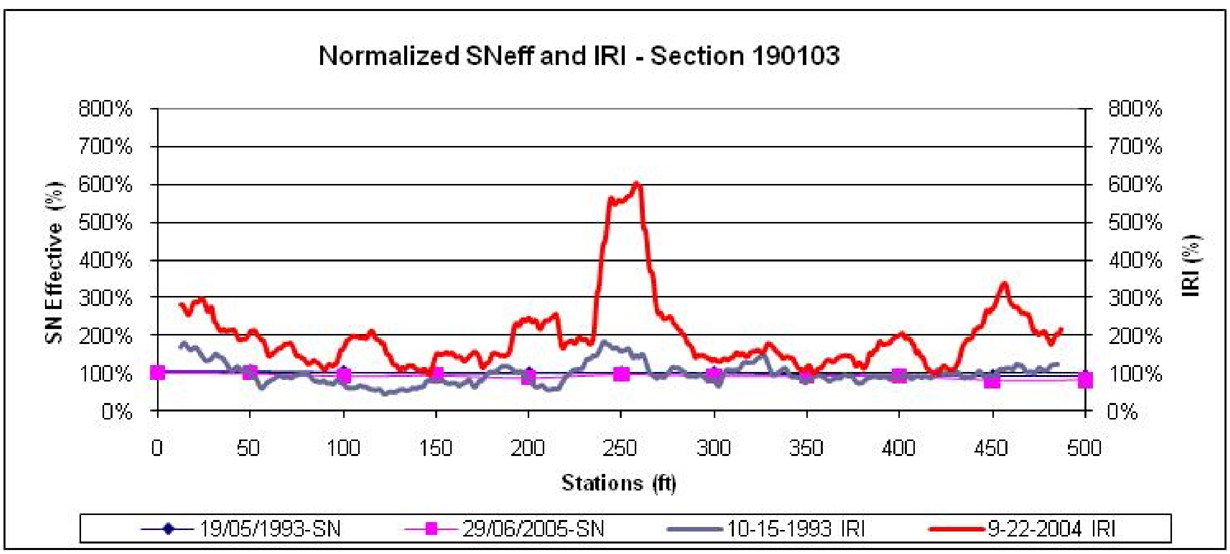

Figure 50. Graph. Normalized SN and IRI for two test dates, section 190103 (Iowa).

3.11.3 LTPP Section 050114 (Arkansas)

The first and last profile dates for section 050114 (Arkansas) were July 7, 1995, and April 6, 2005, and the IRI of the right wheel path increased by 23 inches/mi (from 49 to 72 inches/mi) during this 10-year period. The first and last FWD dates for this section were March 16, 1994, and May 12, 2005, and the average SN of this section increased by 0.87 (from 4.26 to 5.13) during this 11-year period.

Figure 51 shows the first and last IRI and SN values, and figure 52 shows the normalized IRI and SN plots. SN at the last FWD date was greater than SN at the first FWD date at all test locations. The increase in SN at the FWD test locations ranged from 0.55 to 1.25 and averaged 0.87. An increase in IRI between the test dates is noted for the entire section, but there were no major localized roughness increases in this section. The greatest increase in IRI within the section occurred between 350 to 400 ft, which borders the FWD tests that were performed at 350 and 400 ft. However, a FWD test point is not located within these limits. No relationship was noted between the increase in IRI and the deflection below the load or the subgrade modulus (see appendix A).

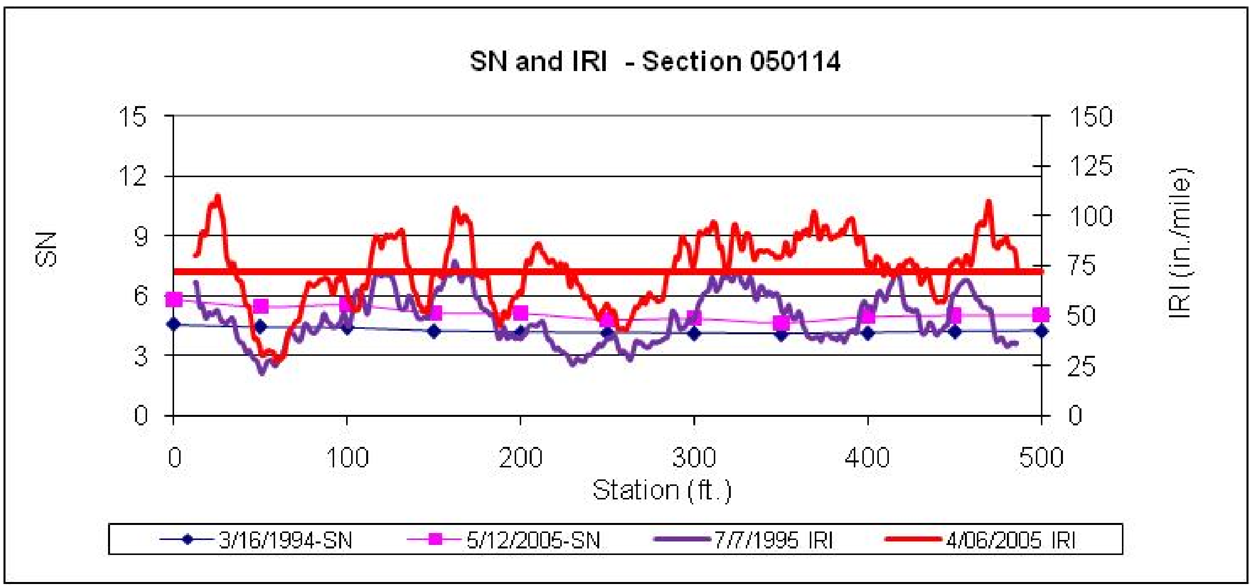

Figure 51. Graph. SN and IRI for two test dates, section 050114 (Arkansas).

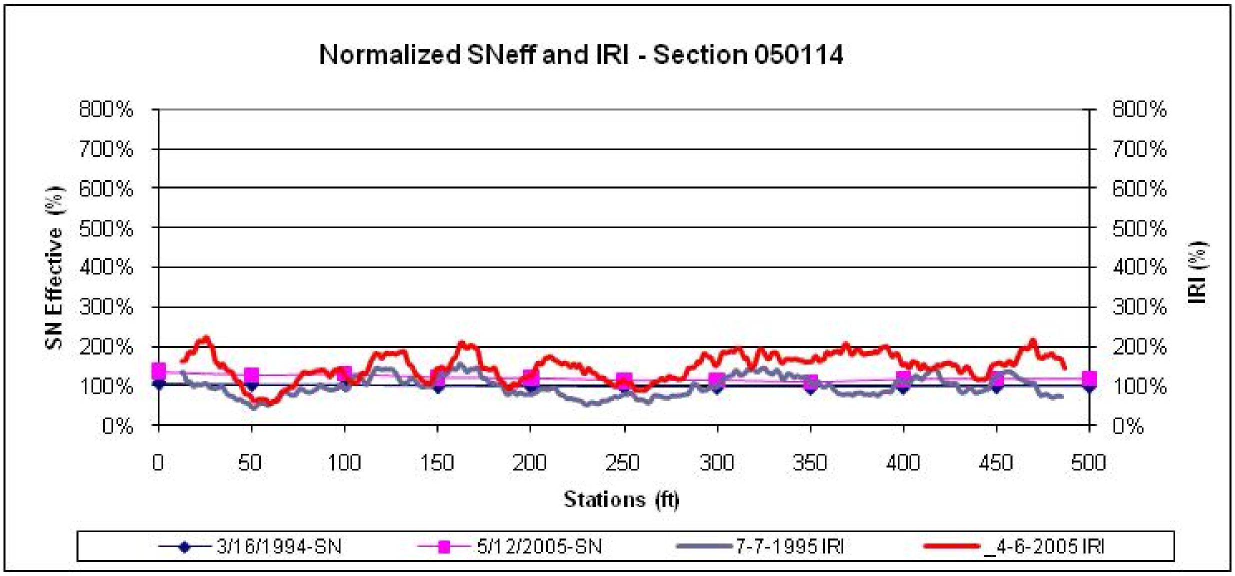

Figure 52. Graph. Normalized SN and IRI for two test dates, section 050114 (Arkansas).

3.11.4 LTPP Section 050116 (Arkansas)

The first and last profile dates for section 050116 (Arkansas) were July 7, 1995, and April 6, 2005, and the IRI of the right wheel path decreased by 5 inches/mi (from 68 to 63 inches/mi) during this 10-year period. The first and last FWD dates for this section were March 16, 1994, and May 11, 2005, and the average SN of this section increased by 2.49 (from 7.81 to 10.30) during this 11-year period.

Figure 53 shows the first and last IRI and SN values, and figure 54 shows the normalized IRI and SN plots. SN at the last FWD date was greater than SN at the first FWD date at all test locations. The increase in SN ranged from 0.92 to 3.13 and averaged 2.49. The overall IRI of this section decreased from 68 to 63 inches/mi. The continuous IRI plots show little change in IRI, with the IRI for the last date showing a slight increase at some locations and a slight decrease at other locations. The highest IRI for the first and last IRI dates occurred around 270 ft. No relationship was noted between the increase in IRI and the deflection below the load or the subgrade modulus (see appendix A).

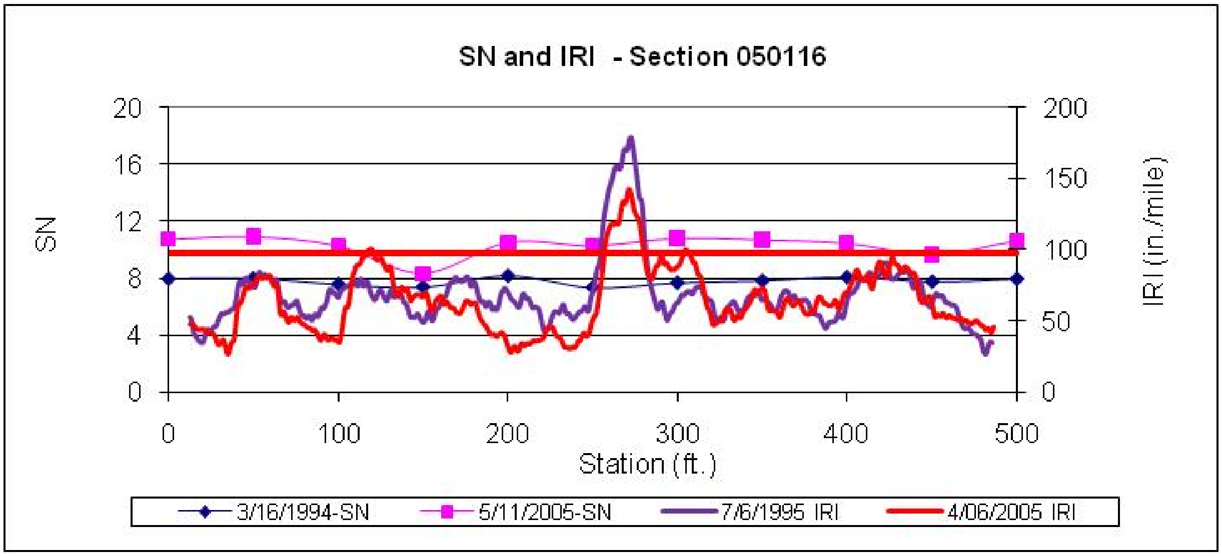

Figure 53. Graph. SN and IRI for two test dates, section 050116 (Arkansas).

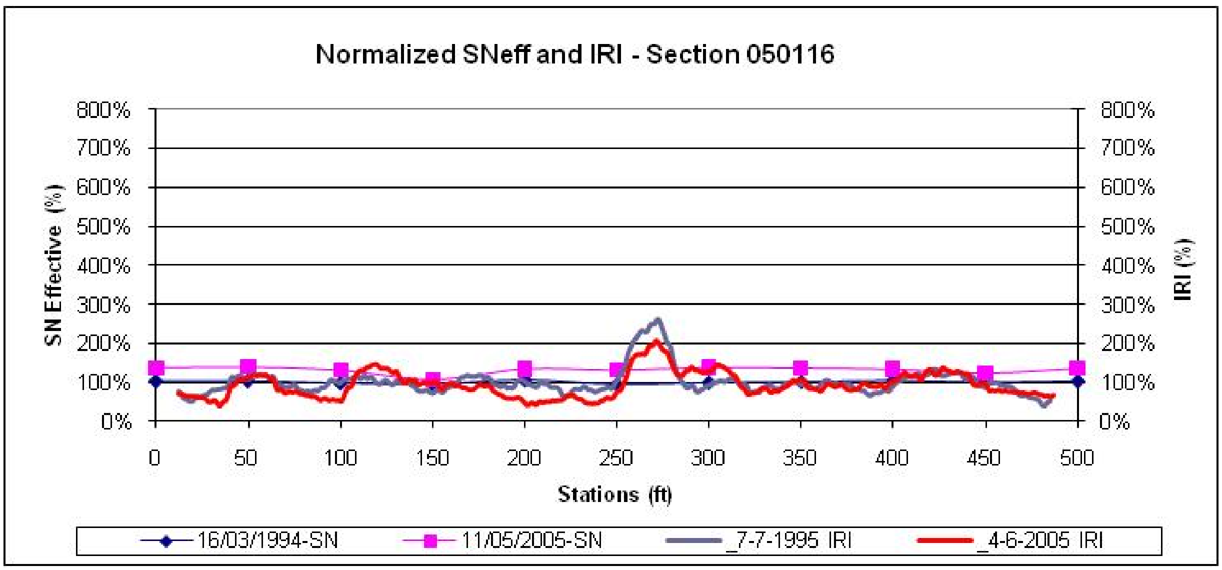

Figure 54. Graph. Normalized SN and IRI for two test dates, section 050116 (Arkansas).

3.12 ANALYSIS OF GROUP 4 SECTIONS

The test sections in group 4 are SPS-5 sections. FWD testing and roughness data collection were performed at these test sections before and immediately after rehabilitation. The date corresponding to the data collection performed immediately after rehabilitation is referred to as the first IRI date or first FWD date. Table 18 shows the following information for the test sections selected for analysis: LTPP section number, date when IRI data were collected before rehabilitation, date corresponding to first IRI (first IRI date), date corresponding to last IRI (last IRI date), date when FWD data were collected before rehabilitation, FWD test date close to the first IRI date (first FWD date), FWD test date close to the last IRI date (last FWD date), and the time difference between first and last dates for IRI and FWD data collection.

Table 18. Group 4 sections selected for analysis.

LTPP Section	IRI Date			FWD Date			Time Difference Between First and Last Date (years)	
	Before Overlay	First Date	Last Date	Before Overlay	First Date	Last Date	IRI Data	FWD Data
040502, Arizona	2/5/1990	9/21/1990	3/24/2006	1/18/1990	10/3/1991	9/15/2008	16.1	18.7
240505, Maryland	1/24/1992	6/11/1992	6/15/2006	2/20/1992	8/25/1992	4/7/2009	14.4	17.1
270509, Minnesota	5/24/1990	7/13/1993	6/6/2005	7/22/1990	11/6/1990	6/7/2005	15.0	14.9

Table 19 shows the IRI values for the 500-ft-long sections for the selected profile runs and the average SN for the section for the three test dates shown in table 18. Table 20 shows the average pavement layer thickness of the three test sections before rehabilitation obtained from the data in the LTPP database. Table 21 shows the milling depths and overlay thickness for the three sections.

Table 19. IRI and SN for group 4 sections.

LTPP Section	IRI (inches/mi)			SN			Change Between First and Last Date	
	Before Overlay	First Date	Last Date	Before Overlay	First Date	Last Date	IRI (inches/mi)	SN
040502, Arizona	139	60	244	3.39	5.91	4.78	184	1.13
240505, Maryland	148	69	228	6.15	8.13	7.40	159	0.73
270509, Minnesota	197	54	117	4.52	5.94	5.78	63	0.16

Table 20. Pavement layer thickness before rehabilitation, group 4 sections.

LTPP Section	Layer Type	Layer Thickness (inches)	Material Type
040502, Arizona	AC	0.9	Hot-mixed, open-graded
	AC	4.2	Hot-mixed, dense-graded
	GB	14.7	Soil-aggregate mixture (predominantly coarse-grained)
240505, Maryland	AC	1.1	Hot-mixed, open-graded
	AC	3.5	Hot-mixed, dense-graded
	TB	3.7	Cement aggregate mixture
	GS	5.9	Crushed stone
	TS	8.9	Cement-treated soil
270509, Minnesota	AC	6.9	Hot-mixed, dense-graded
	GB	4.7	Crushed gravel
	GS	12.6	Gravel (uncrushed)

Table 21. Mill and overlay thickness.

Section	Milled Thickness (inches)	Overlay Thickness (inches)
040502, Arizona	1.4	2.7
240505, Maryland	—	2.1
270509, Minnesota	1.9	3.6

— Indicates milling was not performed.

3.12.1 LTPP Section 040502 (Arizona)

IRI before rehabilitation of section 040503 (Arizona) was 139 inches/mi, and IRI immediately after the overlay was 60 inches/mi. Rehabilitation resulted in IRI decreasing by 79 inches/mi. The first and last profile dates for this section were September 21, 1990, and March 24, 2006, and IRI of the right wheel path increased by 184 inches/mi (from 60 to 244 inches/mi) during this 16-year period.

SN before rehabilitation of this section was 3.39, and it increased to 5.91 after rehabilitation. The first and last FWD dates for this section were October 3, 1991, and September 15, 2008, and the average SN decreased by 1.13 (from 5.91 to 4.78) during this 17-year period.

Figure 55 shows the continuous IRI plots for before the overlay (February 5, 1990), immediately after the overlay (September 21, 1990), and at the last IRI date (March 24, 2006). The continuous IRI plot had higher values at the last date compared to the before overlay plot except at a few locations. Figure 56 shows the SN plots for before the overlay (January 8, 1990), immediately after the overlay (October 3, 1991), and at the last SN date (September 15, 2008). The rehabilitation resulted in an increase in SN at all test locations. SN at all test locations for the last date was lower than SN immediately after rehabilitation (first date) at all test locations.

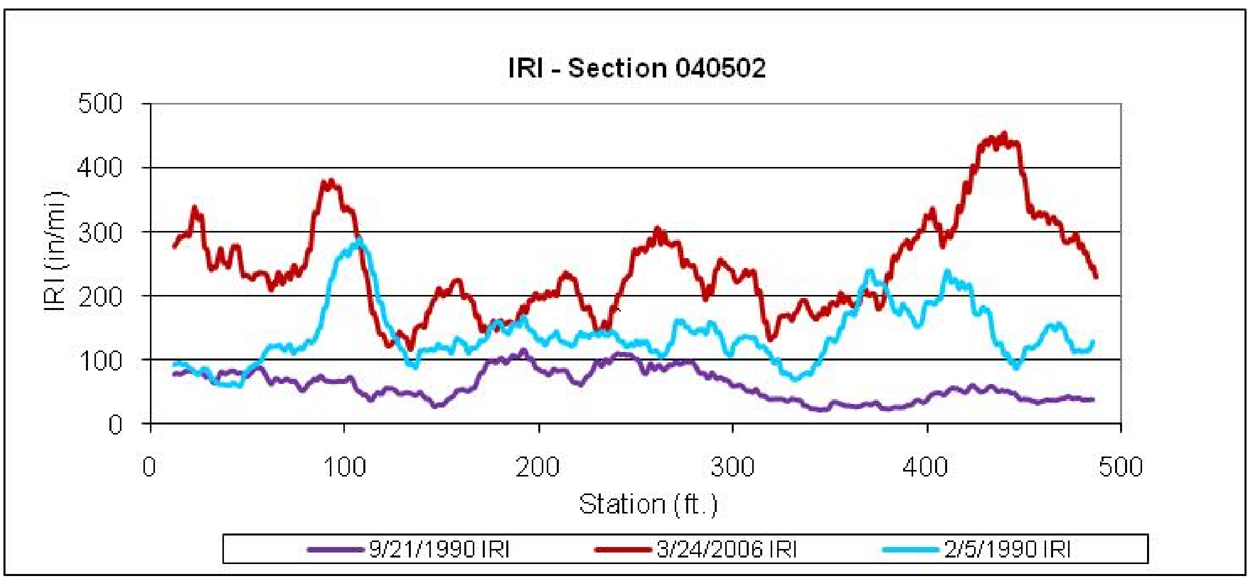

Figure 55. Graph. IRI for before overlay, after overlay, and last test date, section 040502 (Arizona).

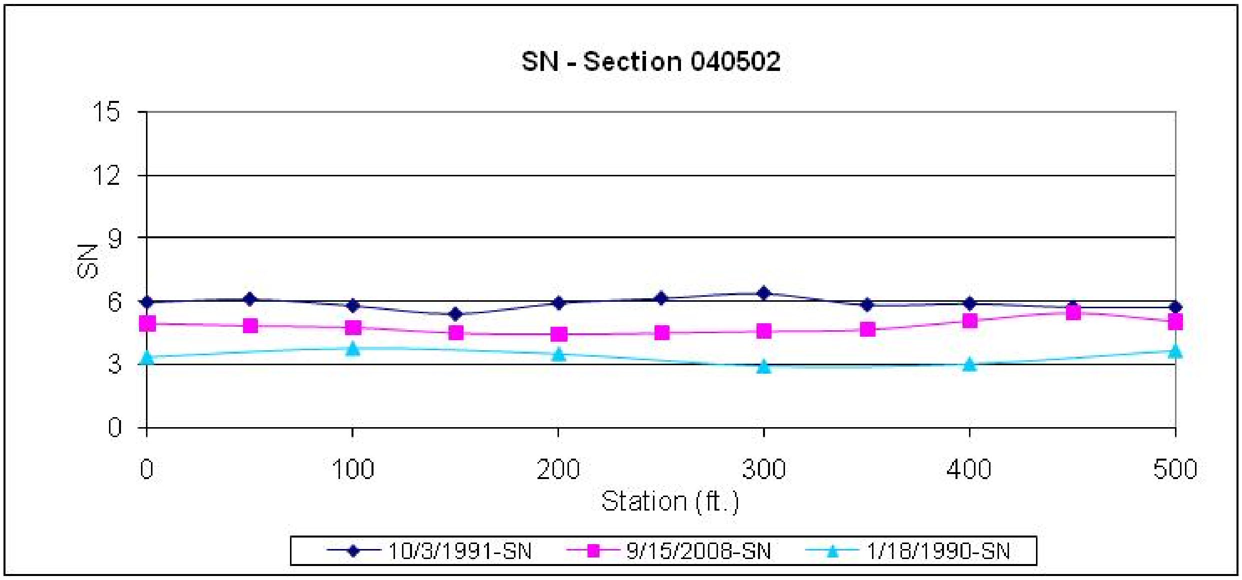

Figure 56. Graph. SN for before overlay, after overlay, and last test date, section 040502 (Arizona).

Figure 57 shows the IRI and SN values after the overlay and at the last test date, and figure 58 shows the normalized IRI and SN plots. IRI increased throughout the section, with the highest increases between 80 and 110 ft and 420 and 460 ft. SN at 100 ft had a decrease of 1.06, which was lower than the average decrease in SN at the section. SN at 450 ft had the lowest decrease for this section, which was 0.31.

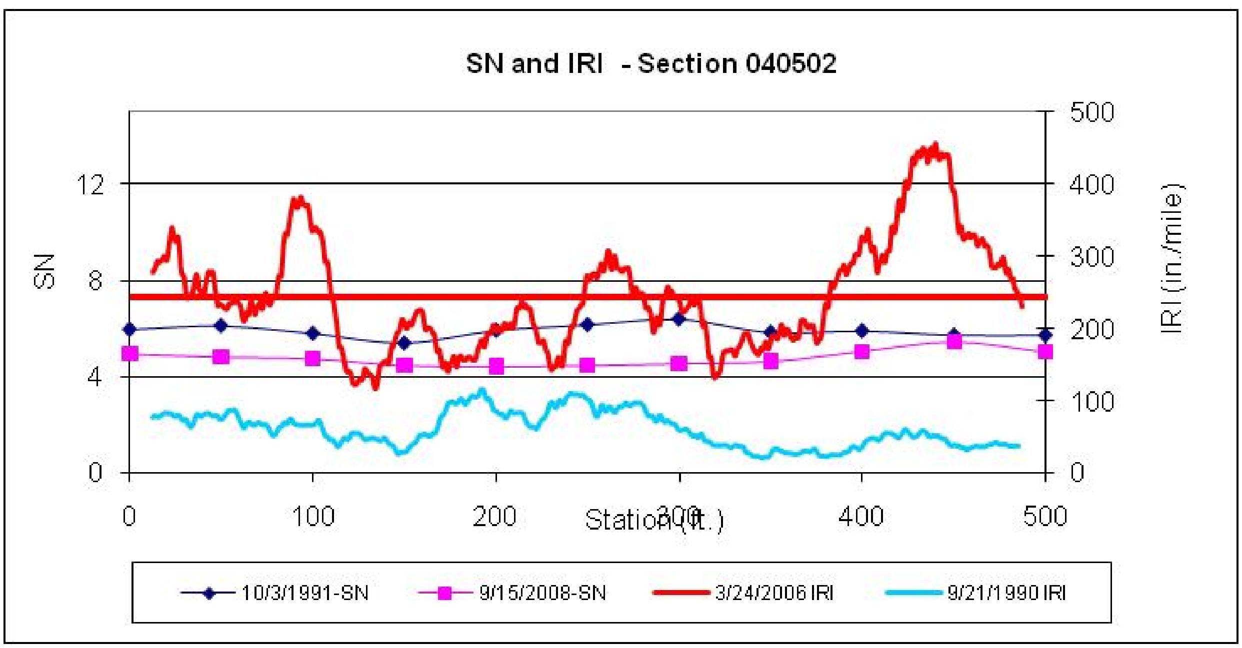

Figure 57. Graph. SN and IRI for two test dates after overlay, section 040502 (Arizona).

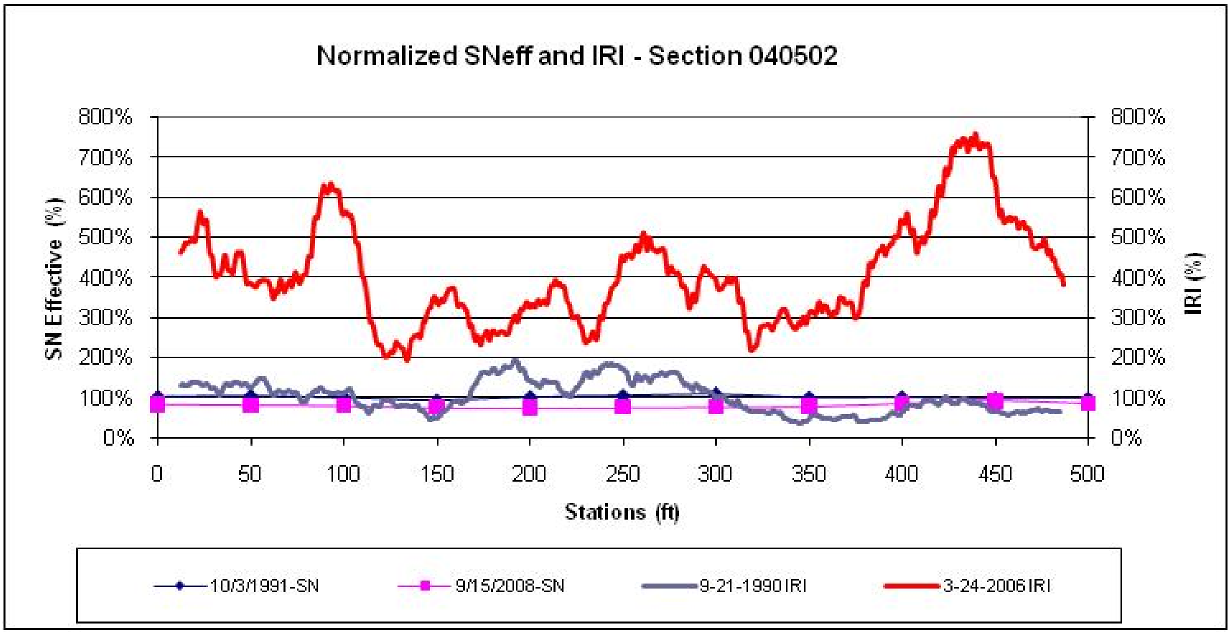

Figure 58. Graph. Normalized SN and IRI for two test dates after overlay, section 040502 (Arizona).

3.12.2 LTPP Section 240505 (Maryland)

IRI before rehabilitation of this section was 148 inches/mi, and IRI immediately after the overlay was 69 inches/mi. The rehabilitation resulted in IRI decreasing by 79 inches/mi. The first (after rehabilitation) and last profile dates were June 11, 1992, and June 15, 2006, and IRI of the right wheel path increased by 159 inches/mi (from 69 to 228 inches/mi) during this 14-year period.

SN before rehabilitation of this section was 6.15, and it increased to 8.13 after rehabilitation. The first (after rehabilitation) and last FWD dates for this section were August 25, 1992, and April 7, 2009, and the average SN decreased by 0.73 (from 8.13 to 7.40) during this 17-year period.

Figure 59 shows the IRI plots for before the overlay (January 24, 1992), immediately after the overlay (June 1, 1992), and at the last IRI date (June 15, 2006). Six distinct peaks are shown in the IRI plot for last IRI date, and, except for one, these peaks generally correspond to the peaks in the before-overlay IRI plot. Figure 60 shows the SN plots for before the overlay (February 20, 1992), immediately after the overlay (August 25, 1992), and at the last FWD date (April 27, 2009). SN at all test locations increased after rehabilitation. SN at the last FWD date was lower than SN immediately after rehabilitation (first FWD date) for all test locations.

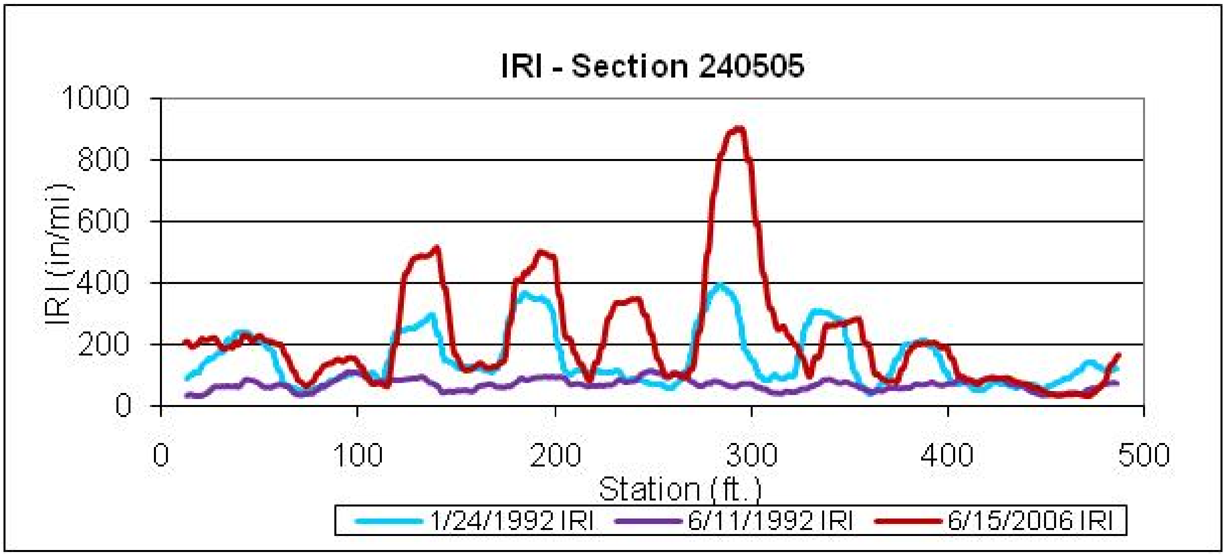

Figure 59. Graph. IRI for before overlay, after overlay, and last test date, section 240505 (Maryland).

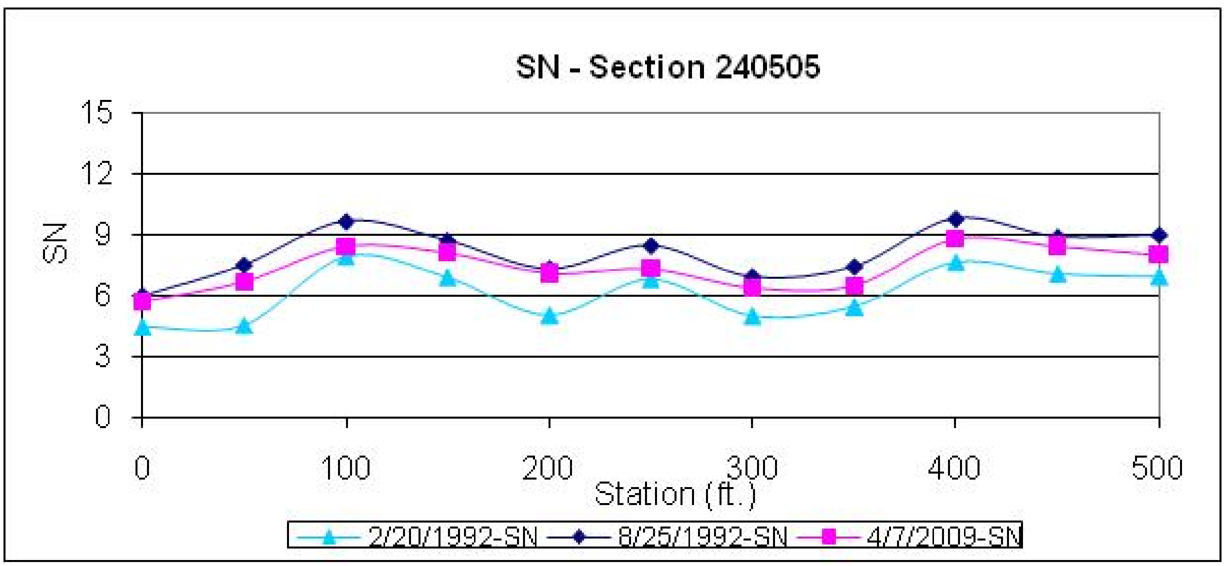

Figure 60. Graph. SN for before overlay, after overlay, and last test date, section 240505 (Maryland).

Figure 61 shows the IRI and SN values for the first (immediately after rehabilitation) and last test dates, and figure 62 shows the normalized IRI and SN plots. High increases in IRI were noted between 120 and 150 ft, 180 and 210 ft, 230 and 250 ft, 270 and 310 ft, and 330 and 360 ft. FWD test locations were present at 200, 300, and 350 ft. The decreases in SN at 200, 300, and 350 ft were 0.19, 0.52, and 0.91 respectively, with the decrease at 200 ft greater than the average decrease in SN for the section (0.73).

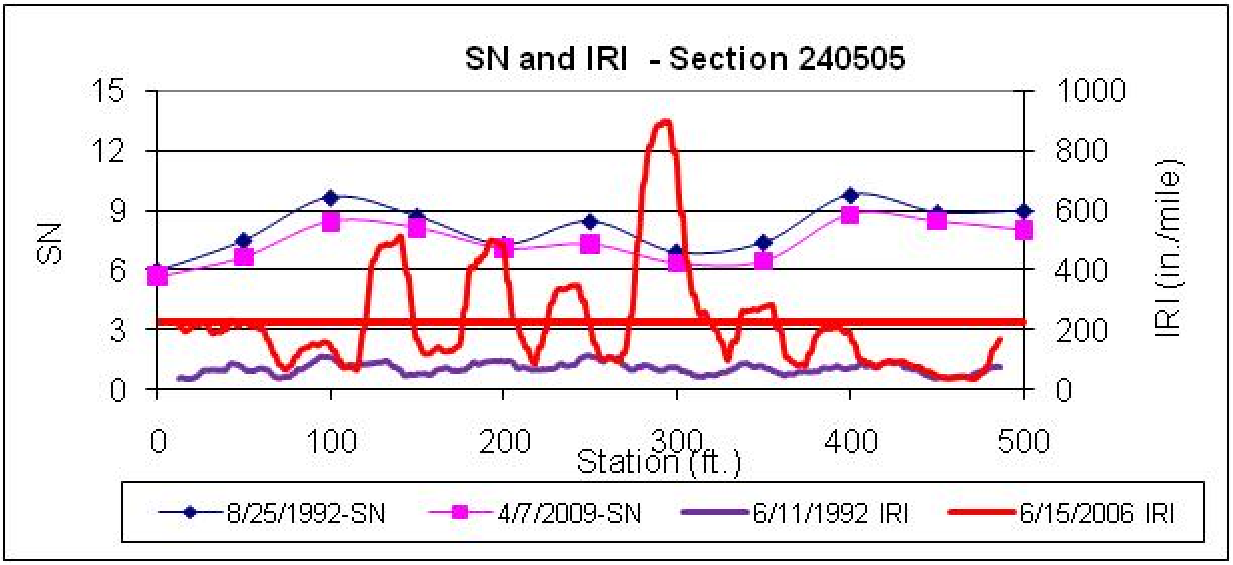

Figure 61. Graph. SN and IRI for two test dates after overlay, section 240505 (Maryland).

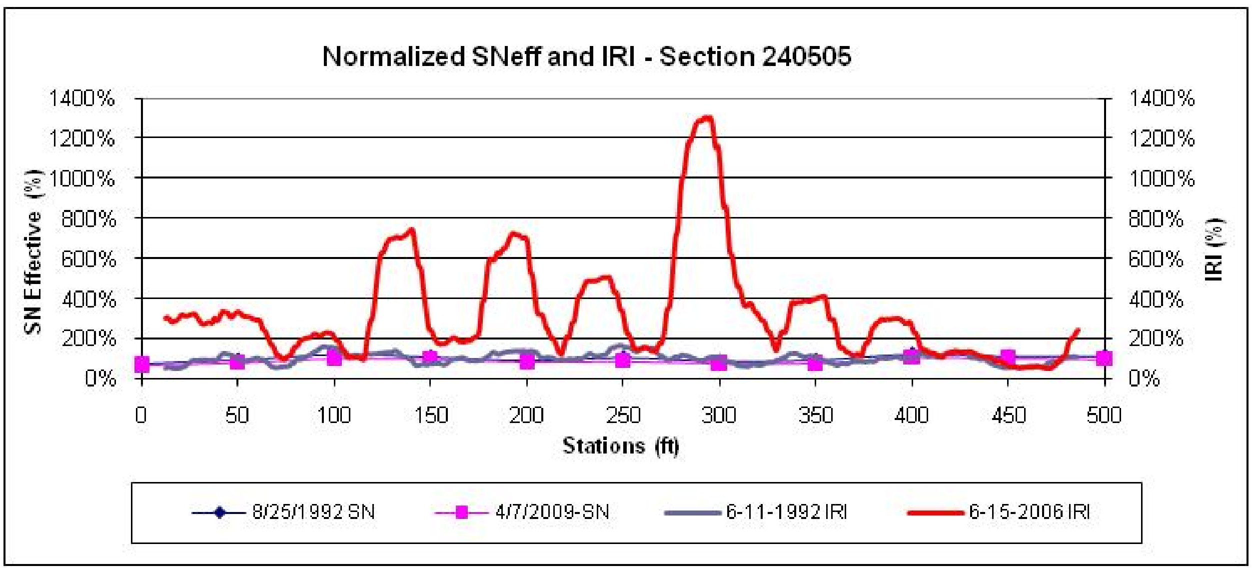

Figure 62. Graph. Normalized SN and IRI for two test dates after overlay, section 240505 (Maryland).

3.12.3 LTPP Section 270509 (Minnesota)

IRI before rehabilitation of section 270509 (Minnesota) was 197 inches/mi, and IRI immediately after the overlay was 54 inches/mi. Rehabilitation resulted in IRI decreasing by 143 inches/mi. The first and last profile dates for this section were July 13, 1993, and June 6, 2005, and IRI of the right wheel path increased by 63 inches/mi (from 54 to 117 inches/mi) during this 12-year period.

SN before rehabilitation of this section was 4.52, and it increased to 5.94 after rehabilitation. The first (after rehabilitation) and last FWD dates for this section were November 6, 1990, and June 27, 2005, and the average SN decreased by 0.16 (from 5.94 to 5.78) during this 15-year period.

Figure 63 shows the IRI plots for before the overlay (May 24, 1990), immediately after the overlay (July 13, 1993), and at the last IRI date (June 6, 2005). A significant reduction in IRI occurred due to the overlay. Figure 64 shows the SN plots for before the overlay (July 22, 1990), immediately after the overlay (November 6, 1990), and at the last SN date (June 7, 2005). The overlay resulted in an increase in SN at all test locations.

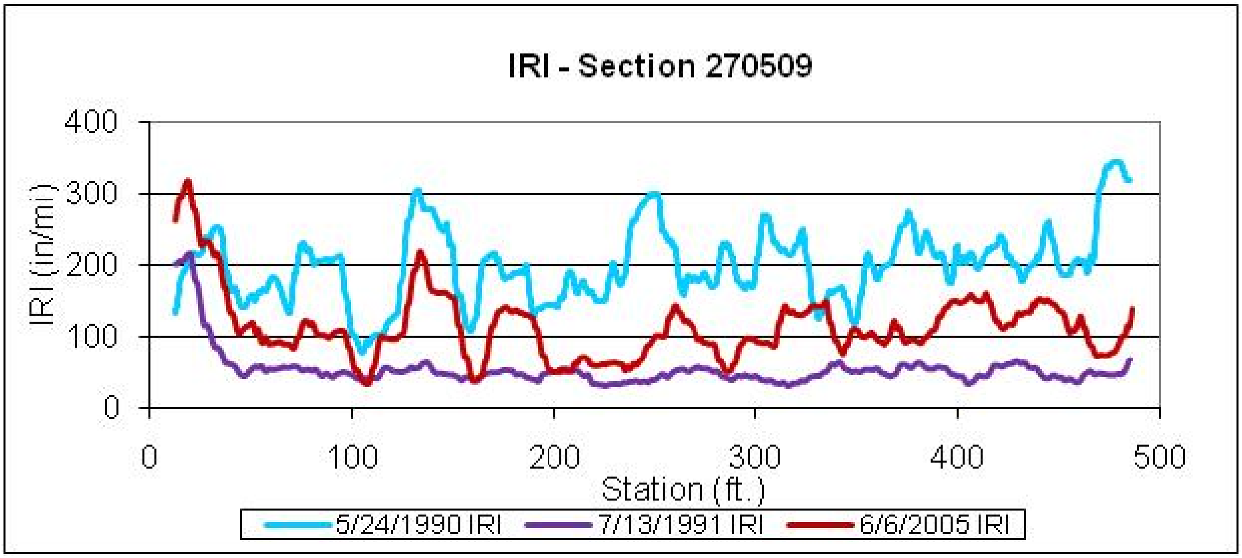

Figure 63. Graph. IRI for before overlay, after overlay, and last test date, section 270509 (Minnesota).

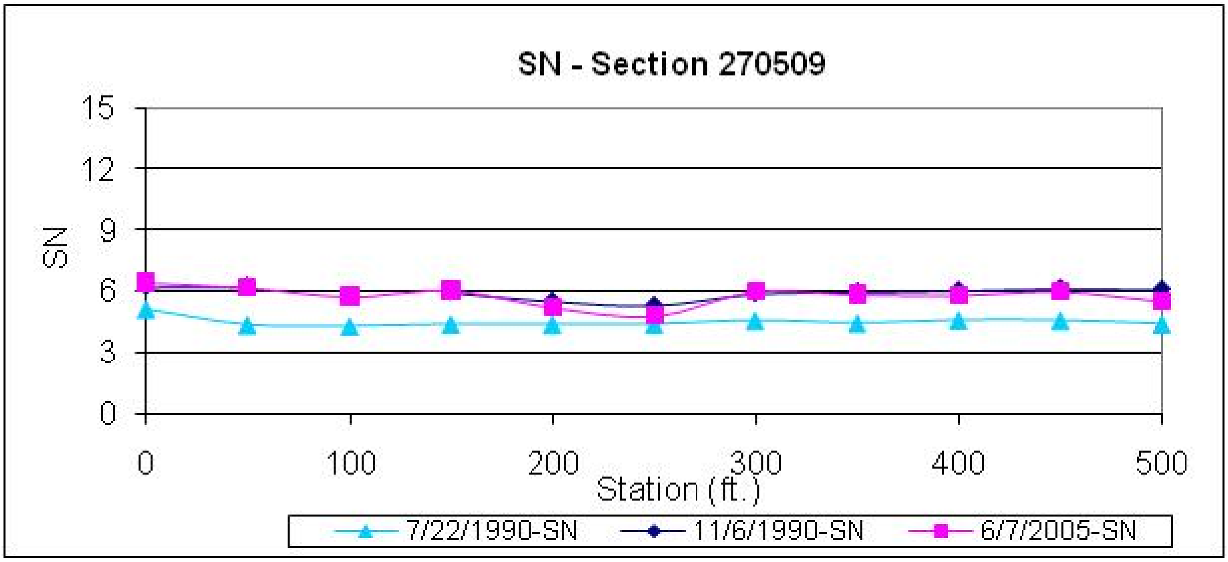

Figure 64. Graph. SN for before overlay, after overlay, and last test date, section 270509 (Minnesota).

Figure 65 shows the IRI and SN at the first test date (after overlay) and the last test date, and figure 66 shows the normalized IRI and SN plots. An increase in IRI is noted throughout the section, but no localized areas showed a very high increase in IRI. Some test locations showed an increase in SN, while others showed a decrease, ranging from 0.06 to 0.57.

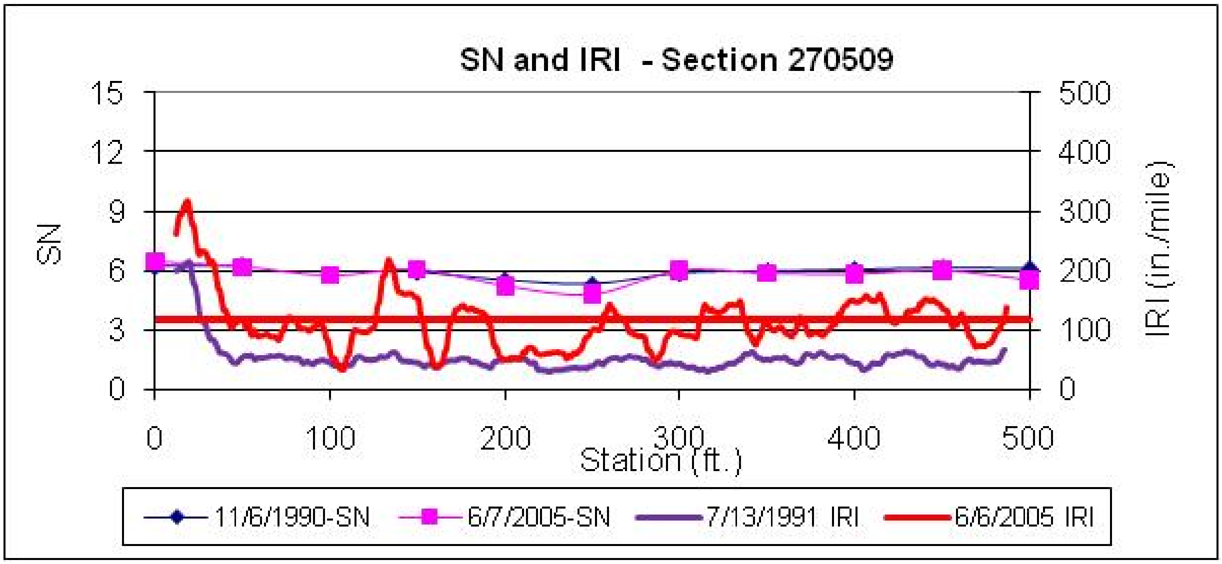

Figure 65. Graph. SN and IRI for two test dates after overlay, section 270509 (Minnesota).

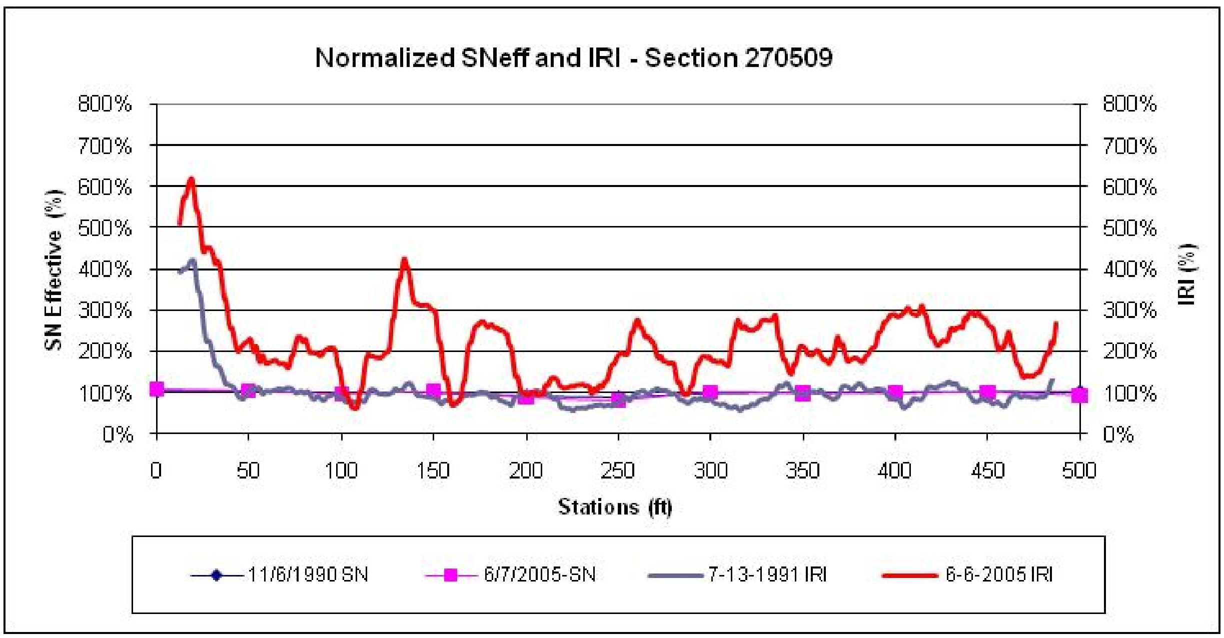

Figure 66. Graph. Normalized SN and IRI for two test dates after overlay, section 270509 (Minnesota).

3.13 ANALYSIS OF GROUP 5 SECTIONS

The test sections in group 5 are SPS-2 test sections. Table 22 shows the following information for the test sections selected for analysis: LTPP section number, date corresponding to first IRI (first IRI date), date corresponding to last IRI (last IRI date), FWD test date close to the first IRI date (first FWD date), FWD test date close to the last IRI date (last FWD date), and the time difference between first and last dates for IRI and FWD data collection.

Table 22. Group 5 sections selected for analysis.

LTPP Section	IRI Date		FWD Date		Time Difference Between First and Last Date (years)	
	First Date	Last Date	First Date	Last Date	IRI Data	FWD Data
040213, Arizona	1/25/1994	8/11/2006	2/8/1994	12/15/2004	12.6	10.9
050217, Arkansas	2/6/1997	4/2/2005	11/14/1996	9/20/2004	8.2	7.9
390205, Ohio	8/14/1996	8/8/2006	12/30/1996	9/9/2004	10.0	7.7

Table 23 shows the IRI values for the 500-ft-long sections and the average effective slab thicknesses for the test dates shown in table 22. Table 24 shows the average pavement layer thickness for the test sections determined from the data in the LTPP database.

Table 23. IRI and effective slab thickness for group 5 sections.

LTPP Section	IRI (inches/mi)		Effective Slab Thickness (inches)		Change Between First and Last Date*	
	First Date	Last Date	First Date	Last Date	IRI (inches/mi)	Effective Slab Thickness (inches)
040213, Arizona	95	165	9.45	9.00	70	0.45
050217, Arkansas	86	160	13.80	16.80	74	-3.00
390205, Ohio	89	161	9.81	10.20	72	-0.39

*A negative effective slab thickness indicates the effective slab thickness at the last date was higher than that for the first date.

Table 24. Pavement layer thickness for group 5 sections.

LTPP Section	Layer Type	Layer Thickness (inches)
040213, Arizona	PCC	7.9
	Aggregate base	5.8
050217, Arkansas	PCC	8.3
	Lean concrete base (LCB)	6.3
390205, Ohio	PCC	8.0
	LCB	6.2

Plots of deflection measured below the load and at a distance of 60 inches from the center of the load plate for the first and last FWD date for all sections are included in appendix B. For the September 20, 2004, FWD test for test section 050217, non-decreasing deflections were encountered at several test locations. The ILLI-BACK program computed high and unreasonable effective slab thickness at these locations. Some of the extremely high effective slab thicknesses were not considered in computing the average, yet the average was higher than the initial effective slab thickness. Sections 050217 and 390205 both had a LCB.

The ILLI-BACK program appears to have combined the PCC and LCB thicknesses when determining the effective slab thickness for these two sections. The computed effective slab thickness for section 040213 was also higher than the actual slab thickness.

3.13.1 LTPP Section 040213 (Arizona)

The first and last profile dates for section 040213 (Arizona) were January 25, 1994, and August 11, 2006, and the IRI of the right wheel path increased by 70 inches/mi (from 95 to 165 inches/mi) during this 13-year period. The first and last FWD test dates for this section were February 8, 1994, and December 15, 2004, and the average effective slab thickness of this section showed a decrease of 0.45 inches (from 9.45 to 9.00 inches) during this period.

Figure 67 shows the first and last IRI and effective slab thickness, and figure 68 shows the normalized IRI and D_{eff} plots. An increase in IRI is seen across the entire section. The effective slab thickness at the last FWD date shows an increase for the first three data points and a decrease for the rest of the points. There are three locations within the section where large changes in IRI occurred, but these locations fall between FWD test locations. No relationship between change in IRI and deflections (below the load and 60 inches from the load) was observed.

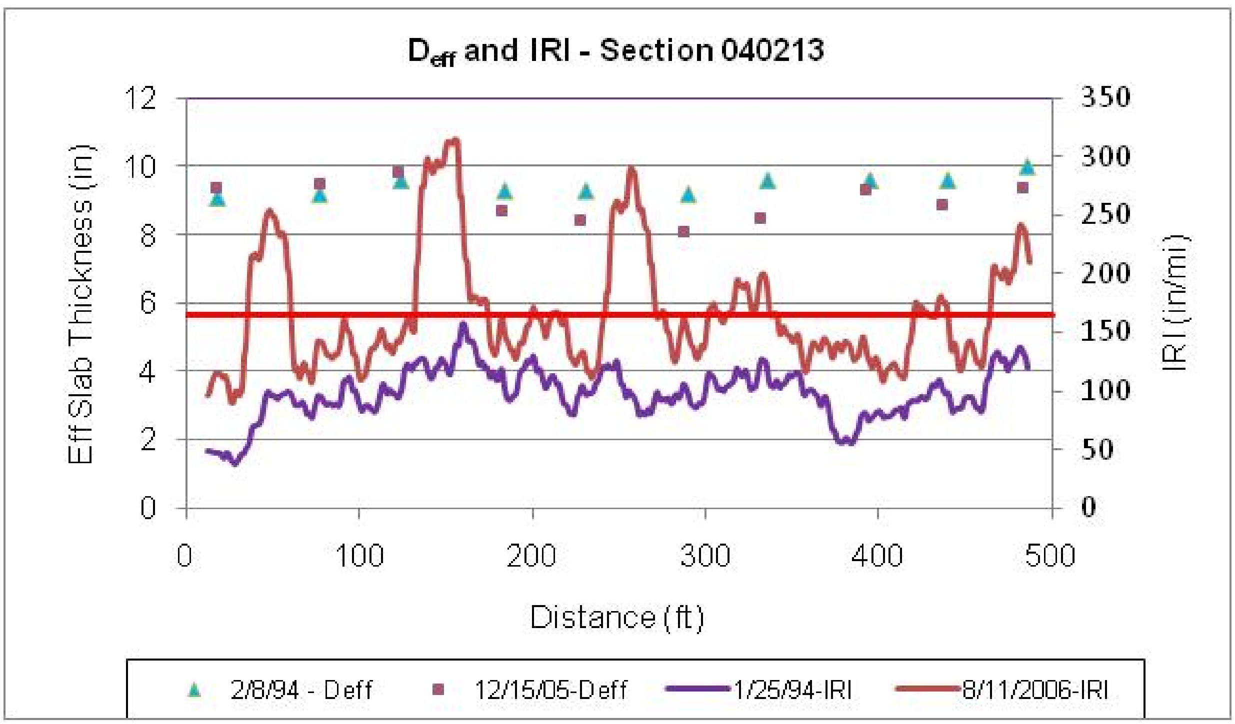

Figure 67. Graph. D_{eff} and IRI for two test dates, section 040213 (Arizona).

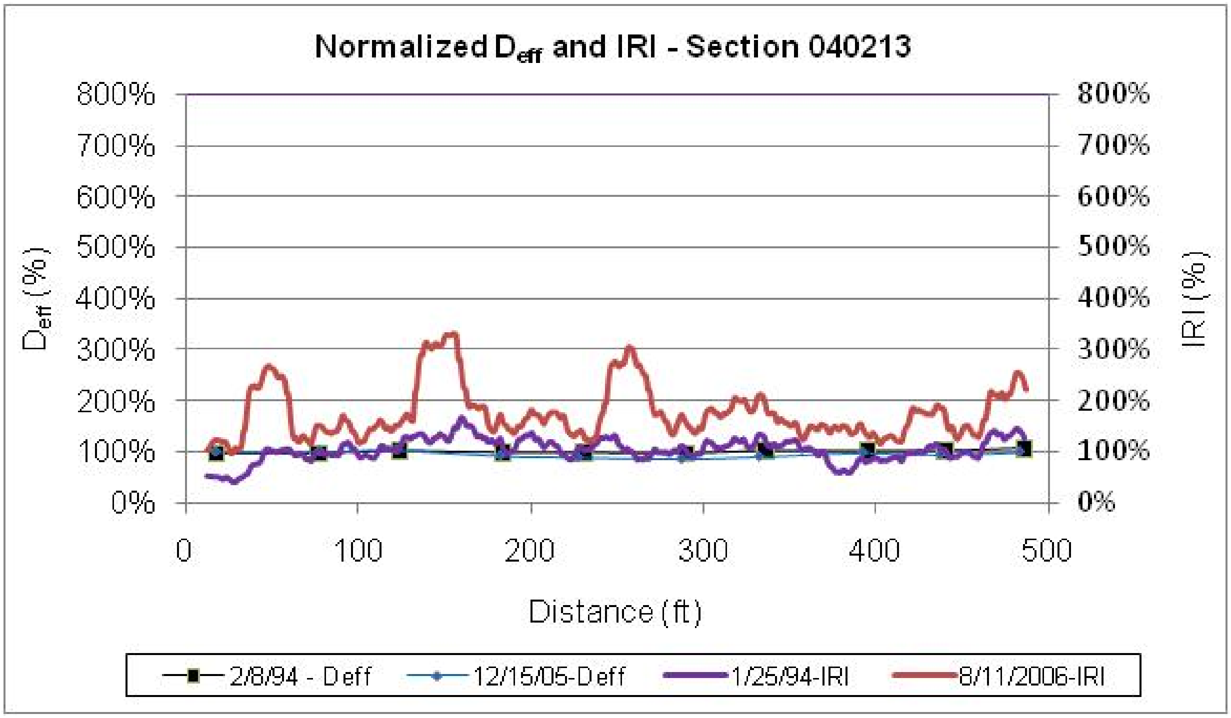

Figure 68. Graph. Normalized D_{eff} and IRI for two test dates, section 040213 (Arizona).

3.13.2 LTPP Section 050217 (Arkansas)

The first and last profile dates for section 050217 (Arkansas) were February 16, 1997, and April 2, 2005, and the IRI of the right wheel path increased by 74 inches/mi (from 86 to 160 inches/mi) during this 8-year period. The first and last FWD dates for this section were November 14, 1996, and September 20, 2004, and the average effective slab thickness of this section increased by 3 inches (from 13.80 to 16.80 inches). As previously described, non-decreasing deflections were noted at many test locations for the September 20, 2004, test, and these deflections caused high effective slab thickness values to be computed at such locations. This resulted in a much higher effective slab thickness for the last test date than for the first test date.

Figure 69 shows the first and last IRI and effective slab thickness, and figure 70 shows the normalized IRI and D_{eff} plots. Some of the high D_{eff} values computed for the second test date are not shown in these plots, and no FWD data were available after 382 ft for the first FWD date. Most of the increase in IRI at this section occurred between 130 and 330 ft. The effective slab thickness at the last FWD date was higher than that for the first date for all test locations. No relationship between the increase in IRI and the effective slab thickness can be seen in the plot. No relationship between change in IRI and deflections (below the load and at 60 inches from the load) could be observed.

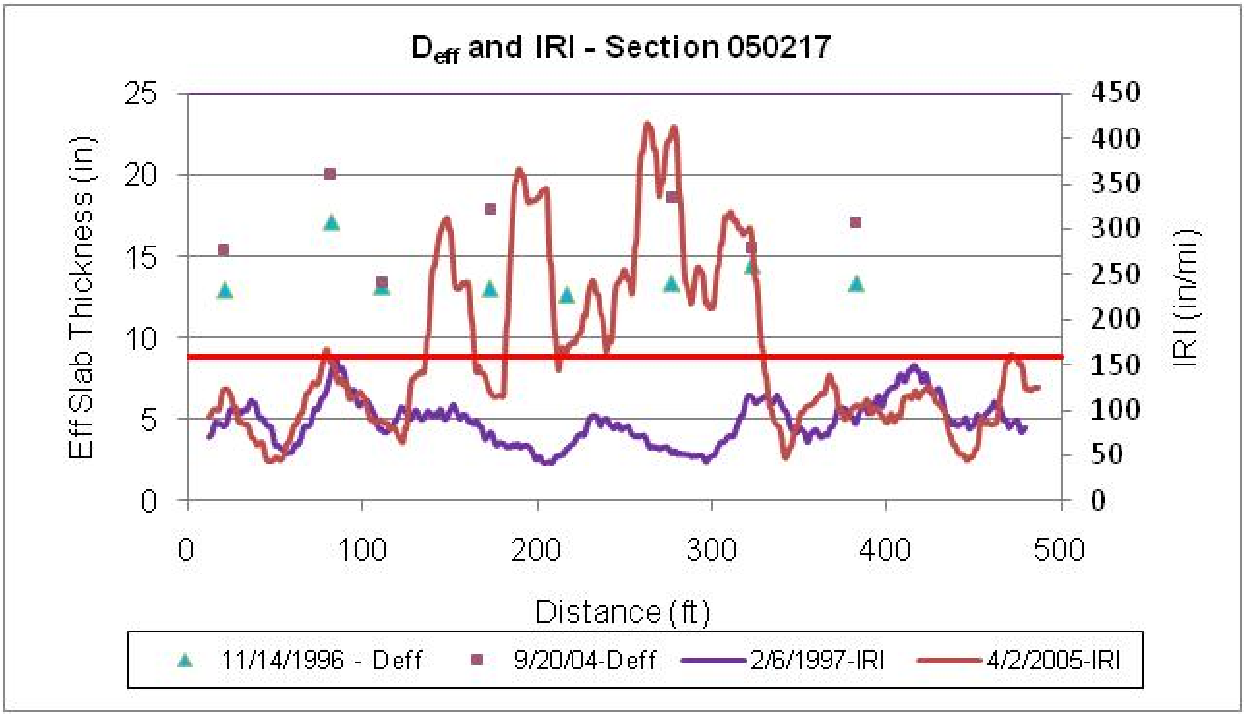

Figure 69. Graph. ***D_{eff}*** **and IRI for two test dates, section 050217 (Arkansas).**

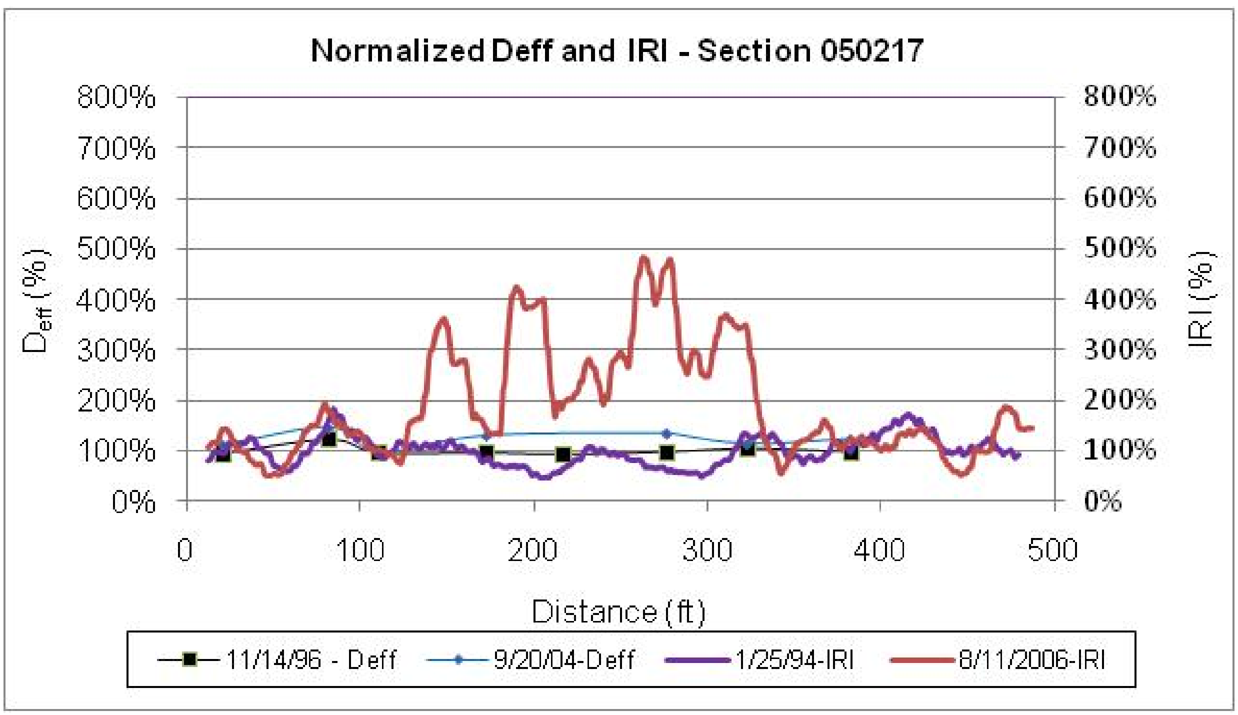

Figure 70. Graph. Normalized ***D_{eff}*** **and IRI for two test dates, section 050217 (Arkansas).**

3.13.3 LTPP Section 390205 (Ohio)

The first and last profile dates for section 390205 (Ohio) were August 14, 1996, and August 8, 2006, and the IRI of the right wheel path increased by 72 inches/mi (from 89 to 161 inches/mi) during this 10-year period. The first and last FWD dates for this section were December 30, 1996, and September 9, 2004, and the average effective slab thickness of this section showed an increase of 0.39 inches (from 9.81 to 10.20 inches) during this 8-year period.

Figure 71 shows the first and last IRI and effective slab thickness, and figure 72 shows the normalized IRI and D_{eff} plots. Most of the increase in IRI at this section occurred between the start of the section and about 200 ft. Within the first 200 ft, the effective slab thickness at the last FWD date was lower than that for the first date at three locations and the same at one location. Among the rest of the FWD test locations within this section, half showed a decrease in effective slab thickness, and the other half showed an increase between the first and last FWD dates. No relationship between change in IRI and deflections (below the load and at 60 inches from the load) could be observed.

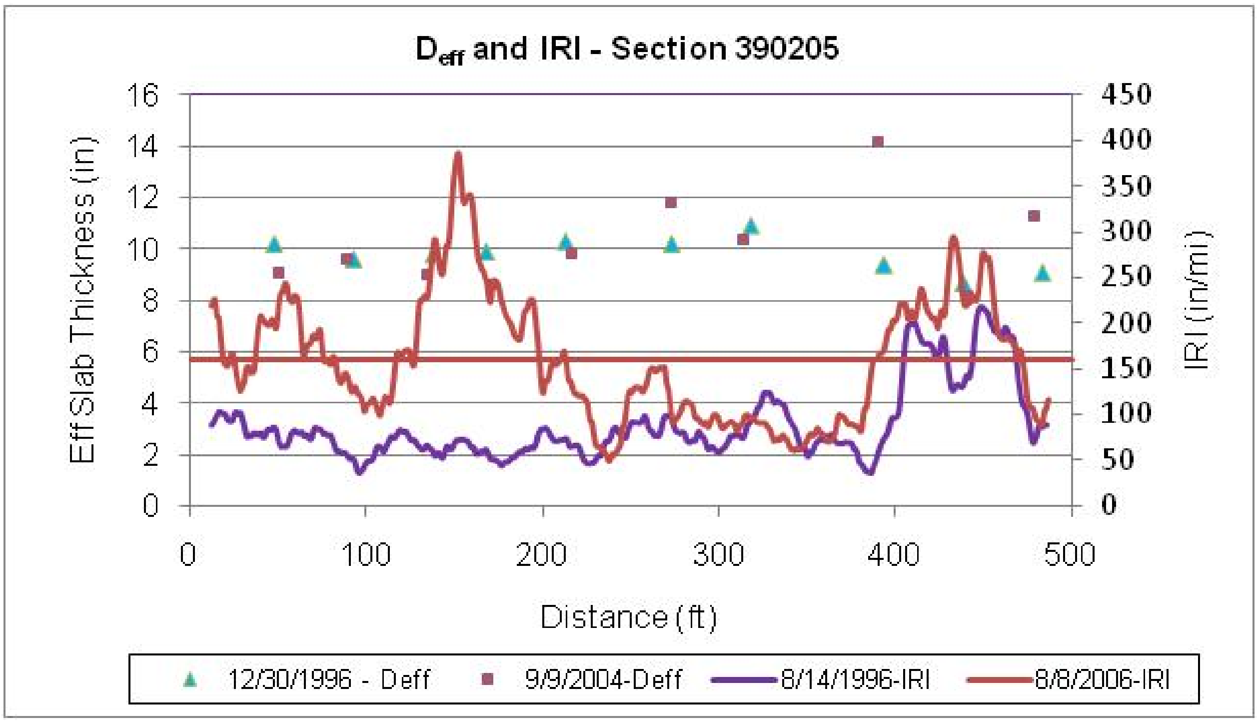

Figure 71. Graph. D_{eff} and IRI for two test dates, section 390205 (Ohio).

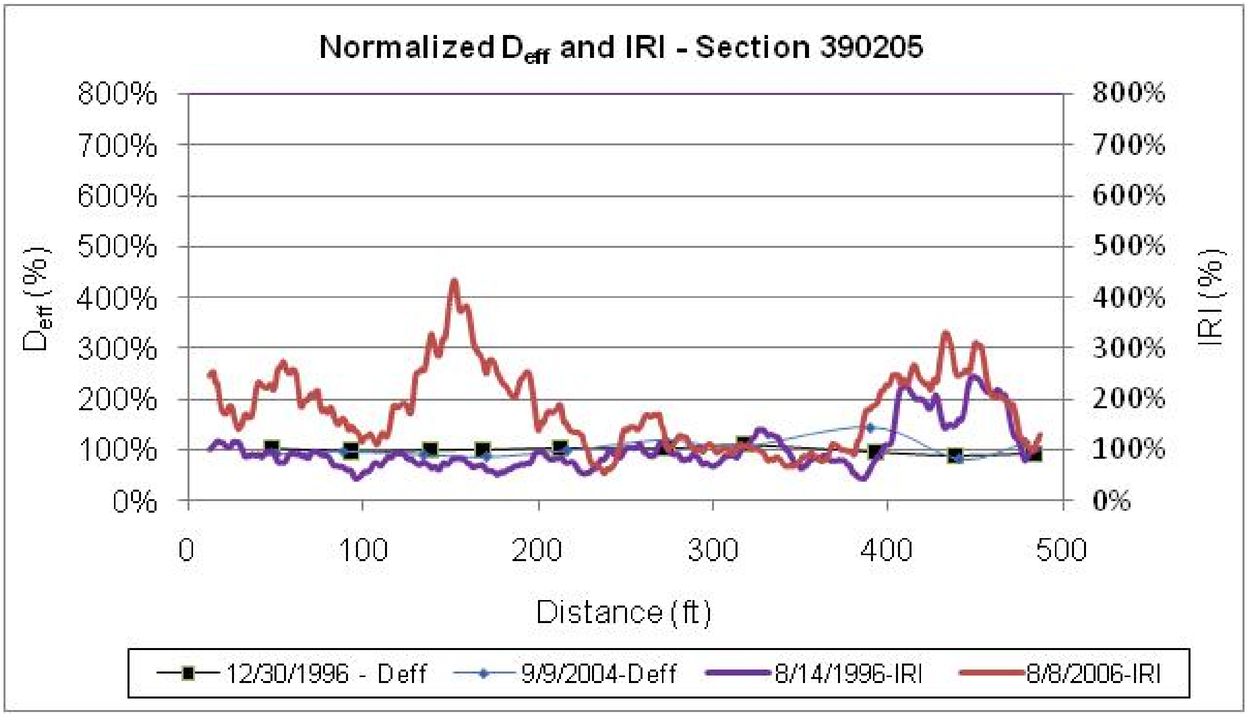

Figure 72. Graph. Normalized D_{eff} and IRI for two test dates, section 390205 (Ohio).

3.14 SUMMARY

Table 25 shows all flexible pavement sections used in the analysis. As previously described, the IRI and FWD data collections were not performed at the same time at LTPP sections. The first IRI and FWD dates correspond to the first time IRI and FWD data were collected at a test section, and the last dates were selected such that the last IRI and FWD dates were close to each other. Overall, the time period used to evaluate IRI and SN changes at a section were reasonably close to each other.

Table 25. Flexible pavement sections used in study.

Group	LTPP Section	IRI Date		FWD Date		Time Difference Between First and Last Date (years)	
		First Date	Last Date	First Date	Last Date	IRI Data	FWD Data
1	050119	7/6/1995	3/19/2004	3/15/1994	5/24/2004	8.7	10.2
	480114	9/8/1997	3/19/2007	11/17/1997	6/24/2004	9.5	6.6
	310113	11/1/1995	3/20/2000	8/3/1995	10/14/1999	4.4	4.2
	010102	8/25/1994	5/4/2005	6/21/1995	4/29/2005	10.7	9.9
	390112	8/14/1996	5/5/2005	11/6/1996	9/1/2004	8.7	7.8
	040123	1/27/1994	3/27/2006	2/16/1994	4/7/2005	12.2	11.1
	190108	10/15/1993	9/22/2004	5/18/1993	6/27/2005	10.9	12.1
2	320101	12/3/1996	8/7/2006	3/27/1996	8/28/2006	9.7	10.4
	390106	8/14/1996	8/9/2006	11/5/1996	7/15/2008	10.0	11.7
	310117	11/1/1995	4/24/2002	8/2/1995	7/9/2002	6.5	6.9
	310118	11/1/1995	4/24/2002	8/3/1995	7/10/2002	6.5	6.9
3	190101	10/15/1993	9/22/2004	5/19/1993	6/28/2005	10.9	12.1
	190103	10/15/1993	9/22/2004	5/19/1993	6/29/2005	10.9	12.1
	050114	7/7/1995	4/6/2005	3/16/1994	5/12/2005	9.8	11.2
	050114	7/7/1995	4/6/2005	3/16/1994	5/11/2005	9.8	11.2
4	040502	9/21/1990	3/24/2006	10/3/1991	9/15/2008	15.5	17.0
	240505	6/11/1992	6/15/2006	8/25/1992	4/7/2009	14.0	16.6
	270509	7/13/1993	6/6/2005	11/6/1990	6/7/2005	11.9	14.6

Table 26 shows the changes in IRI and SN that had occurred at the sections between the first and last dates expressed as magnitude of the change as well as the percent change. Only three sections showed a decrease in IRI between the first and last dates (310117 (Nebraska), 310118 (Nebraska), and 050116 (Arkansas)). The decrease in IRI at sections 310117 and 310118 in Nebraska occurred because of a treatment that was applied on the pavement. Of the 18 sections evaluated in this study, 12 sections showed a decrease in SN between the first and last dates, and 6 sections showed an increase in SN.

Table 26. Change in IRI and SN at evaluated sections.

Group	LTPP Section	IRI (inches/mi) First Date	IRI (inches/mi) Last Date	SN First Date	SN Last Date	Change Between First and Last Date* IRI (inches/mi)	Change Between First and Last Date* SN	Increase in IRI (percent)**	Decrease in SN (percent)**
1	050119	48	98	4.51	5.40	50	-0.89	105	-20
	480114	46	65	10.90	10.39	19	0.51	42	5
	310113	93	126	5.73	5.82	33	-0.09	35	-2
	010102	62	204	2.86	2.19	143	0.67	232	23
	390112	57	101	7.83	7.39	44	0.44	77	6
	040123	52	138	7.94	7.26	86	0.68	163	9
	190108	49	141	8.30	9.94	93	-1.64	191	-20
2	320101	57	57	11.91	11.23	0	0.68	0	6
	390106	71	114	6.94	5.04	43	1.90	61	27
	310117	68	53	8.32	7.30	-15	1.02	-22	12
	310118	74	54	9.21	7.62	-20	1.59	-27	17
3	190101	83	159	7.48	7.62	76	-0.14	92	-2
	190103	46	92	9.39	8.68	46	0.71	100	8
	050114	49	72	4.26	5.13	23	-0.87	47	-20
	050116	68	63	7.81	10.30	-5	-2.49	-7	-32
4	040502	60	244	5.91	4.78	184	1.13	307	19
	240505	69	228	8.13	7.40	159	0.73	230	9
	270509	54	117	5.94	5.78	63	0.16	117	3

*A positive change in IRI indicates that IRI of the section increased. A positive change in SN indicates that SN of the section decreased.
**Percent changes between first and last dates.

Some sections showed an increase in SN between the first and last dates. Some of the factors that may have contributed to the increase include hardening of the AC layer with age resulting in an increase in the structural layer coefficient for the asphalt layer, changes in moisture conditions in the GB/SB layers that resulted in an increase in the structural layer coefficient for these layers, or the effect of the temperature adjustment factor. The deflection below the load was adjusted to a standard temperature of 68 °F before computing the SN values using the temperature adjustment factors shown in the 1993 AASHTO *Guide for Design of Pavement Structures*.[23] However, each AC mix is expected to have unique adjustment factors, and the difference in the adjustment factors presented in the AASHTO *Guide for Design of Pavement Structures* with the actual behavior of the mix may result in errors when the deflections are adjusted to 68 °F.[23]

Figure 73 shows the relationship between changes in IRI and SN observed at the sections, and figure 74 shows this relationship for percent changes. Data for sections 310117 and 310118 in Nebraska, which had a treatment that caused a decrease in SN, are not shown in these plots.

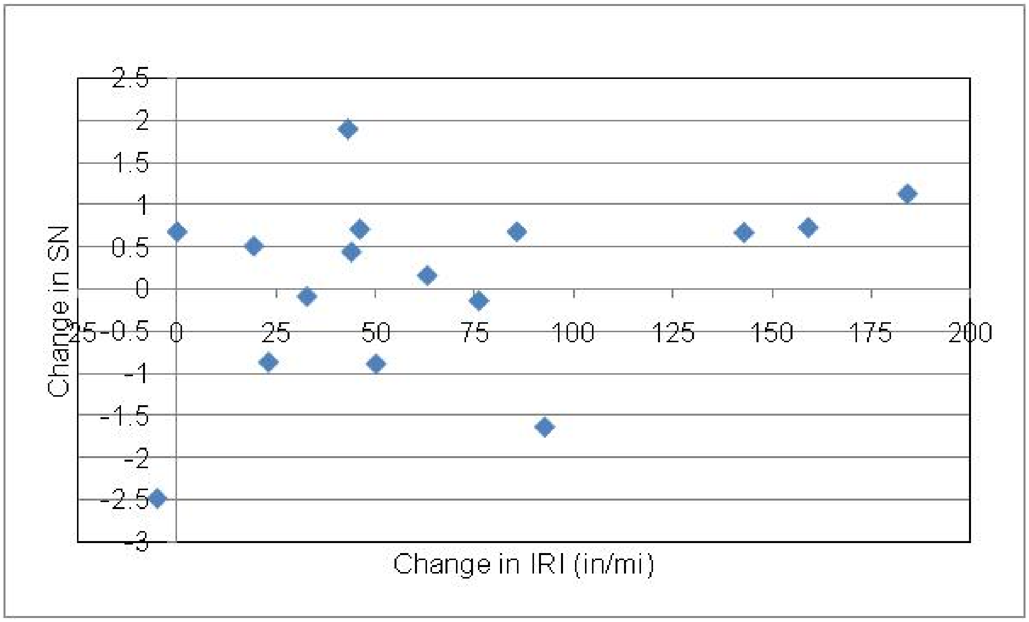

Figure 73. Graph. Relationship between changes in IRI and SN.

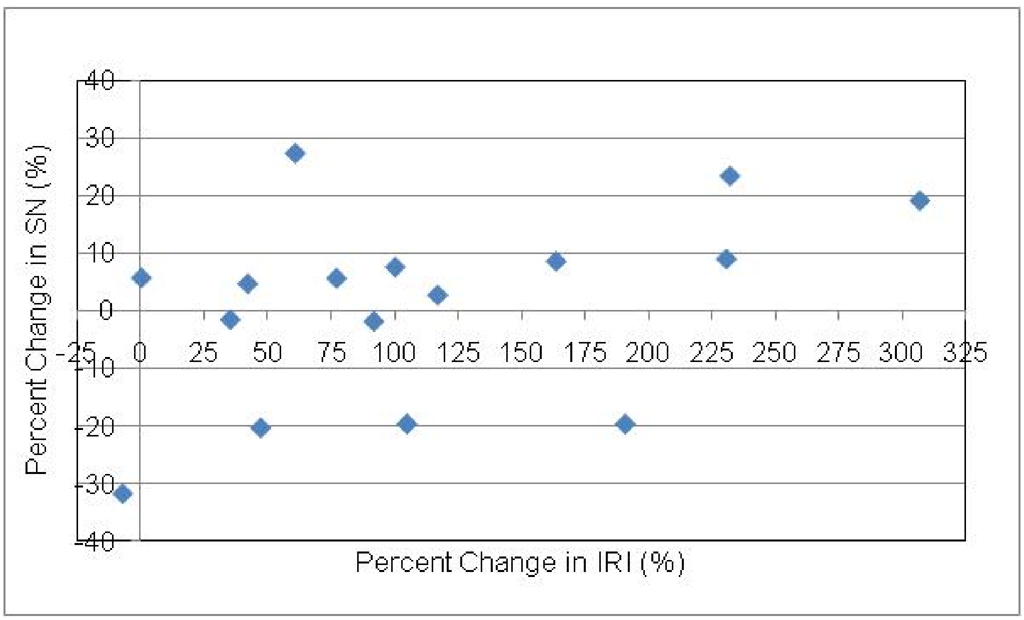

Figure 74. Graph. Relationship between percent changes in IRI and SN.

As shown in these figures, there is no relationship between change or percent change in IRI and the change or percent change in SN. Because only three rigid pavements were evaluated, sufficient data were not available to conduct a similar comparison as presented for flexible pavements.

At all of the analyzed flexible pavement sections, continuous IRI plots for first and last dates were compared with SN values estimated from FWD measurements at the first and last dates. If there was a relationship between IRI and SN, it was hypothesized that areas where large changes in IRI had occurred should show large decreases in SN. However, such a relationship was not seen in the analyzed sections. Generally, no major changes in SN associated with localized areas were seen at the evaluated sections. However, in most sections, major IRI changes were noticed at localized areas within the section. At these areas, the changes in SN were not significantly different from changes in SN that had occurred at areas where major changes in IRI had not occurred. Comparison of continuous IRI plots with deflection below the FWD load and estimated subgrade modulus plots also did not show any relationship between changes in IRI and deflection or subgrade modulus or between changes in IRI and changes in deflection or subgrade modulus.

For the rigid pavements, the effective slab thickness instead of SN was used as the structural strength parameter in this study. Similar to flexible pavements, no relationship was seen between changes in IRI and changes in effective slab thickness.

CHAPTER 4. OTHER DATA ANALYSIS CONSIDERATIONS

4.1 INTRODUCTION

To validate the findings and conclusions presented in chapter 3, the following additional analyses were performed:

- Evaluation of maintenance and repair impacts, intended to demonstrate that maintenance and repair activities on the selected test sections had little, if any, impact on the study findings and conclusions.
- Review of IRI time-history data, intended to confirm that the change between the first and last IRI survey dates used in the analyses was reasonable and not due to outliers in the first or last dates.
- Review of deflection time-history data, intended to confirm that the change between the first and last FWD (SN or D_{eff}) test dates used in the analyses was reasonable and not due to outliers on the first or last dates.
- Assessment of PCC warping and curling, intended to address the effects of warping and curling on the study findings and conclusions for the PCC pavement test sections.

Each of these analyses is explained in this chapter. The first three are based on data specific to the study, while the fourth is based on the findings and conclusions from other literature and another FHWA study carried out at approximately the same time as this one.

4.2 EVALUATION OF MAINTENANCE AND REPAIR IMPACTS

Information on maintenance and repair activities for each of the test sections during the time periods in the study was obtained from the LTPP database to assess the potential impact of these activities on ride quality and structural adequacy. The following discussion addresses each of the maintenance activities reported along with the extent of the section affected (length or percent area of the test section). The main types of maintenance activities identified included crack sealing, seal coats, joint sealing, patching (partial-depth, full-depth, skin, and strip patching), and grinding.

Crack sealing is intended to help reduce moisture infiltration through surface cracks into the layers below, which could accelerate pavement deterioration. This maintenance activity is not expected to improve the ride quality or structural adequacy of the pavement. Table 27 summarizes test sections where crack sealing was reported. As shown in the table, for sections where the quantity of crack sealing was reported, the quantity of treatment applied was small compared to the total length of the section.

Table 27. Test sections with crack sealing application.

LTPP Section	Date	Quantity
040502, Arizona	5/1/2002	Information not available in the LTPP database
050217, Arkansas	12/3/2002	Information not available in the LTPP database
270509, Minnesota	6/15/1991	10 ft
320101, Nevada	5/1/2002	98 ft
040123, Arizona	5/1/2001	248 ft
040123, Arizona	4/2/2002	Information not available in the LTPP database

The application of a fog seal coat was reported for LTPP section 040502 in Arizona, where it was applied three times: May 1998, August 2001, and April 2003. However, no information was provided about the area over which the treatment was applied. Similar to crack sealing, this maintenance activity is not expected to impact the ride quality or structural adequacy of the pavement. As noted in the next section, IRI over time data for the section do not indicate a reduction in IRI as a result of the fog seal coats.

Section 050217 in Arkansas is reported to have received joint sealing in February 1997. This maintenance activity helps reduce pumping, faulting, joint spalling, and blowups. Joint sealing will not improve the structural adequacy of a section. However, deflection values are consistent for this section through October 2003, which could be attributed, at least partially, to the application of the joint sealing in 1997.

Another maintenance activity reported for the sections in question is patching, which includes partial-depth patching (for PCC pavements), full-depth patching, skin patching, and strip patching. Patching helps temporarily or permanently address localized pavement distresses, which could improve structural adequacy and affect ride quality, depending on the type of patching. Table 28 summarizes the sections that received patching. As shown in the table, for those sections where the quantity of patching has been reported, the area of patching was relatively small compared to the total section. It is anticipated that only those sections that received full-depth patches may have affected ride quality and structural adequacy; however, no information on the patching extent is available to confirm this.

Table 28. Test sections with patching application.

LTPP Section	Maintenance Activity Date	Maintenance Activity Description	Quantity
050217	12/3/2002	Partial-depth patching of PCC pavements at joints	2 ft^2
240505	4/1/2009	Machine premix patch (placing premix with paver roller)	Information not available in LTPP database
270509	8/1/2001	Skin patching*	76 ft^2
190101	6/1/2001	Strip patching**	2,800 ft^2
190103	7/1/2001	Strip patching	2,480 ft^2
010102	4/17/2003	Strip patching	Information not available in LTPP database
010102	4/17/2003	Full-depth patching*** of AC pavement	Information not available in LTPP IMS database
050119	5/15/1999	Full-depth patching of AC pavement	560 ft^2
190108	7/1/2001	Strip patching	3,120 ft^2

*Skin patching is using hand tools or hot pot to apply liquid asphalt and aggregate.
**Strip patching is using a spreader and distributor to apply hot liquid asphalt and aggregate.
***Full-depth patching includes removing damaged material and repairing the supporting layer.

Another maintenance activity reported for the sections in question was grinding performed at two AC sections. Grinding, which can improve skid resistance and ride quality, is reported to have been applied over the entire area for sections 310117 and 310118 in Nebraska on July 12, 2000. The grinding had a reported average depth of 0.5 inches, which could have slightly reduced structural adequacy. Both of these sections are in group 2 and were not considered in the analysis because of grinding that was carried out at the sections (see sections 3.10.3 and 3.10.4).

In summary, limited maintenance and repair activities were applied to some of the test sections during the time periods considered in the analysis. Those activities included crack sealing, PCC joint sealing, patching (skin, strip, and full-depth patching at AC sections and partial-depth patching at a section), and grinding. Of these, only full-depth patching and grinding may have affected ride quality, structural adequacy, or both. However, the impact depends on the extent of the patching. Further information on whether patching affected ride quality is provided in section 4.3. The effect of patching on the observed deflections is discussed in section 4.4.

4.3 REVIEW OF IRI TIME HISTORY DATA

In chapter 3, the change in IRI over time that occurred at a test section was evaluated by considering IRI at the first profile date and at the last profile date (i.e., the last date available in the database). The time-sequence IRI values at the test sections that were used in this study were evaluated to investigate if any sudden drops in IRI could be noticed, which would indicate that maintenance or a rehabilitation activity had occurred at that site.

The changes in IRI that occurred at the test sections were evaluated by preparing a table and then using the data from this table to prepare plots, with time = 0 being assigned to the construction date of the test section. The construction date was assumed to be the date the section was opened to traffic except for a few sections. For LTPP sections 050119 (Arkansas), 190108 (Iowa), 190101 (Iowa), 190103 (Iowa), 050114 (Arkansas), and 050116 (Arkansas), the first FWD date was before the traffic open date. The first FWD date for these sections was assigned as the construction date. For LTPP section 390205 (Ohio), the first profile date was before the traffic open date, and the first profile date was assigned as the construction date for this section. Table 29 shows the construction dates assigned to the sections as well as the first profile and first FWD dates.

Table 29. Construction date of test sections.

Group	LTPP Section	State	Construction Date	First IRI Date	First FWD Date
1	050119	Arkansas	3/15/1994	7/6/1995	3/15/1994
	480114	Texas	6/1/1997	9/8/1997	11/17/1997
	310113	Nebraska	8/1/1995	11/1/1995	8/3/1995
	010102	Alabama	3/1/1993	8/25/1994	6/21/1995
	390112	Ohio	9/1/1995	8/14/1996	11/6/1996
	040123	Arizona	8/1/1993	1/27/1994	2/16/1994
	190108	Iowa	5/18/1993	10/15/1993	5/18/1993
2	320101	Nevada	9/1/1995	12/3/1996	3/27/1996
	390106	Ohio	9/1/1995	8/14/1996	11/5/1996
	310117	Nebraska	1/1/1995	11/1/1995	8/2/1995
	310118	Nebraska	1/1/1995	11/1/1995	8/3/1995
3	190101	Iowa	5/19/1993	10/15/1993	5/19/1993
	190103	Iowa	5/19/1993	10/15/1993	5/19/1993
	050114	Arkansas	3/16/1994	7/7/1995	3/16/1994
	050116	Arkansas	3/16/1994	7/7/1995	3/16/1994
4	040502	Arizona	4/20/1990	9/21/1990	10/3/1991
	240505	Maryland	3/31/1992	6/11/1992	8/25/1992
	270509	Minnesota	9/15/1990	7/13/1993	11/6/1990
5	040213	Arizona	10/1/1993	1/25/1994	2/8/1994
	050217	Arkansas	12/1/1995	2/6/1997	11/14/1996
	390205	Ohio	8/14/1996	8/14/1996	12/30/1996

Table 30 shows the time-sequence right wheel path IRI values of the test sections. The IRI values shown are the average IRI obtained from the five profiler runs performed at the test section on each test date. The time shown in the table is the time from the construction date, with time being zero at the construction date. Appendix C includes plots of the time-sequence IRI values.

Table 30. Time-sequence IRI values at test sections.

Group	Section	Profile Date	Time (years)	Right Wheel Path IRI (inches/mi)
1	050119, Arkansas	7/6/1995	1.3	48
		7/1/1997	3.3	49
		1/22/2001	6.9	82
		4/1/2002	8.1	79
		4/23/2003	9.1	81
		3/19/2004	10.0	98
	480114, Texas	9/8/1997	0.3	46
		4/2/1998	0.8	54
		12/10/1999	2.5	47
		5/9/2000	2.9	44
		4/24/2001	3.9	47
		10/17/2001	4.4	53
		5/21/2003	6.0	61
		5/22/2003	6.0	62
		1/21/2005	7.6	62
		12/2/2005	8.5	63
		3/19/2007	9.8	66
	310113, Nebraska	11/1/1995	0.2	94
		4/17/1996	0.7	114
		2/18/1997	1.5	114
		5/16/1998	2.8	125
		5/7/1999	3.8	121
		10/13/1999	4.2	115
		3/20/2000	4.6	125
	010102, Alabama	8/25/1994	1.5	61
		1/10/1996	2.9	56
		7/3/1997	4.3	57
		1/27/1998	4.9	66
		9/28/1999	6.6	79
		3/14/2001	8.0	91
		3/10/2002	9.0	56
		1/29/2003	9.9	140
		4/27/2004	11.2	209
		5/4/2005	12.2	205

Table 30. Time-sequence IRI values at test sections—continued.

Group	Section	Profile Date	Time (years)	Right Wheel Path IRI (inches/mi)
1	390112, Ohio	8/14/1996	1.0	58
		12/27/1996	1.3	58
		12/8/1997	2.3	70
		11/12/1998	3.2	86
		10/20/1999	4.1	91
		8/16/2000	5.0	92
		11/4/2001	6.2	97
		12/6/2002	7.3	92
		2/4/2004	8.4	101
		5/5/2005	9.7	98
	040123, Arizona	1/27/1994	0.5	53
		2/27/1995	1.6	47
		1/23/1997	3.5	56
		4/8/1998	4.7	54
		12/4/1998	5.3	54
		11/17/1999	6.3	58
		12/19/2000	7.4	59
		11/6/2001	8.3	70
		2/20/2002	8.6	59
		3/2/2003	9.6	56
		3/10/2004	10.6	93
		3/15/2005	11.6	69
		3/27/2006	12.7	113
	190108, Iowa	10/15/1993	0.4	53
		2/15/1995	1.7	51
		4/16/1996	2.9	60
		9/25/1997	4.4	83
		10/13/1998	5.4	104
		7/19/1999	6.2	114
		5/22/2000	7.0	120
		5/29/2001	8.0	134
		8/6/2001	8.2	119
		11/22/2002	9.5	123
		9/22/2004	11.4	139

Table 30. Time-sequence IRI values at test sections—continued.

Group	Section	Profile Date	Time (years)	Right Wheel Path IRI (inches/mi)
2	320101, Nevada	12/3/1996	1.3	58
		4/22/1997	1.6	57
		11/18/1997	2.2	59
		8/28/1998	3.0	58
		10/16/1999	4.1	57
		6/14/2000	4.8	56
		6/19/2001	5.8	56
		6/10/2002	6.8	56
		7/31/2002	6.9	56
		10/13/2003	8.1	57
		8/4/2004	8.9	57
		8/27/2006	11.0	56
	390106, Ohio	8/14/1996	1.0	71
		12/27/1996	1.3	74
		12/8/1997	2.3	96
		11/12/1998	3.2	105
		10/20/1999	4.1	107
		8/16/2000	5.0	108
		11/4/2001	6.2	109
		12/6/2002	7.3	109
		4/29/2003	7.7	111
		2/4/2004	8.4	126
		5/5/2005	9.7	119
		8/9/2006	10.9	118
	310117, Nebraska	11/1/1995	0.8	68
		4/17/1996	1.3	81
		2/18/1997	2.1	63
		5/16/1998	3.4	67
		5/7/1999	4.3	66
		10/13/1999	4.8	63
		3/20/2000	5.2	67
		5/16/2001	6.4	75
		4/24/2002	7.3	54

Table 30. Time-sequence IRI values at test sections—continued.

Group	Section	Profile Date	Time (years)	Right Wheel Path IRI (inches/mi)
2	310118, Nebraska	11/1/1995	0.8	74
		4/17/1996	1.3	82
		2/18/1997	2.1	81
		5/16/1998	3.4	82
		5/7/1999	4.3	82
		10/13/1999	4.8	76
		3/20/2000	5.2	82
		5/16/2001	6.4	63
		4/24/2002	7.3	54
3	190101, Iowa	10/15/1993	0.4	85
		2/15/1995	1.7	91
		4/16/1996	2.9	94
		9/25/1997	4.4	100
		10/13/1998	5.4	111
		7/19/1999	6.2	119
		5/22/2000	7.0	122
		5/29/2001	8.0	121
		8/6/2001	8.2	115
		11/22/2002	9.5	121
		9/22/2004	11.4	158
	190103, Iowa	10/15/1993	0.4	46
		2/15/1995	1.7	52
		4/16/1996	2.9	61
		9/25/1997	4.4	66
		10/13/1998	5.4	72
		7/19/1999	6.2	73
		5/22/2000	7.0	77
		5/29/2001	8.0	87
		8/6/2001	8.2	89
		11/22/2002	9.5	85
		9/22/2004	11.4	92
	050114, Arkansas	7/7/1995	1.3	50
		7/1/1997	3.3	53
		1/22/2001	6.9	57
		4/1/2002	8.0	62
		4/23/2003	9.1	62
		3/19/2004	10.0	61
		4/6/2005	11.1	72

Table 30. Time-sequence IRI values at test sections—continued.

Group	Section	Profile Date	Time (years)	Right Wheel Path IRI (inches/mi)
3	050116, Arkansas	7/7/1995	1.3	67
		7/1/1997	3.3	59
		1/22/2001	6.9	61
		4/1/2002	8.0	66
		4/23/2003	9.1	62
		3/19/2004	10.0	62
		4/6/2005	11.1	63
4	040502, Arizona	9/21/1990	0.4	60
		1/15/1992	1.7	70
		2/22/1993	2.8	66
		2/3/1997	6.8	81
		12/9/1997	7.6	88
		12/11/1998	8.6	112
		11/11/1999	9.6	129
		12/6/2000	10.6	139
		11/15/2001	11.6	169
		11/4/2002	12.6	162
		2/6/2004	13.8	192
		12/14/2004	14.7	191
		3/24/2006	15.9	241
	240505, Maryland	6/11/1992	0.2	66
		6/25/1993	1.2	71
		12/6/1995	3.7	75
		12/10/1996	4.7	84
		12/18/1997	5.7	88
		8/19/1998	6.4	96
		10/20/1999	7.6	118
		12/5/2000	8.7	95
		10/8/2002	10.5	98
		11/14/2003	11.6	100
		6/30/2004	12.3	116
		4/26/2005	13.1	134
		9/22/2005	13.5	115
		6/15/2006	14.2	207

Table 30. Time-sequence IRI values at test sections—continued.

Group	Section	Profile Date	Time (years)	Right Wheel Path IRI (inches/mi)
4	270509, Minnesota	7/13/1991	0.8	55
		10/31/1992	2.1	66
		11/16/1993	3.2	70
		7/17/1994	3.8	76
		7/16/1997	6.8	102
		9/30/1998	8.0	114
		6/10/1999	8.7	117
		9/20/2000	10.0	124
		8/19/2001	10.9	100
		12/10/2002	12.2	100
		2/25/2004	13.5	106
		10/9/2004	14.1	113
		6/6/2005	14.7	115
5	040213, Arizona	1/25/1994	0.3	94
		3/5/1995	1.4	82
		1/27/1997	3.3	108
		12/4/1997	4.2	114
		12/8/1998	5.2	115
		11/15/1999	6.1	127
		12/5/2000	7.2	116
		11/8/2001	8.1	129
		10/30/2002	9.1	116
		2/4/2004	10.4	101
		12/12/2004	11.2	114
		8/11/2006	12.9	165
	050217, Arkansas	2/6/1997	1.2	85
		11/16/2000	5.0	91
		4/3/2002	6.3	127
		4/9/2003	7.4	89
		3/12/2004	8.3	135
		4/2/2005	9.3	135

Table 30. Time-sequence IRI values at test sections—continued.

Group	Section	Profile Date	Time (years)	Right Wheel Path IRI (inches/mi)
5	390205, Ohio	8/14/1996	0.0	87
		12/27/1996	0.4	82
		12/8/1997	1.3	90
		11/12/1998	2.2	91
		10/20/1999	3.2	91
		8/16/2000	4.0	92
		11/4/2001	5.2	100
		12/6/2002	6.3	90
		4/29/2003	6.7	98
		2/4/2004	7.5	101
		5/5/2005	8.7	130
		8/8/2006	10.0	163

Lateral variations in the profiled paths can affect the IRI value.(26) Hence, some variability in the time-sequence IRI values is expected. Maintenance activities, such as patching and spall repairs (PCC pavements) that repair pavement distress, can cause a reduction in IRI. Placement of an AC overlay will cause a significant reduction in IRI. After maintenance or rehabilitation, the IRI values will show a gradual increase with time. An IRI value that is greater than the previous and subsequent values is likely the result of lateral variability in the profiled path. Such a phenomenon can occur in PCC pavements due to curling and warping effects.

The time-sequence IRI values were evaluated to determine if evidence of maintenance or rehabilitation could be detected. A reduction in IRI greater than 10 inches/mi between two adjacent profile dates was noted in the time-sequence IRI values at the following sections:

- **Group 1, section 010102 (Alabama):** IRI for March 14, 2001, March 10, 2002, and January 29, 2003, were 91, 56, and 140 inches/mi, respectively. The cause of the sudden drop in IRI for March 10, 2002, is not clear. The tables do not indicate maintenance was carried out on this section between March 14, 2001, and March 10, 2002.

- **Group 1, section 040123 (Arizona):** IRI ranged between 56 and 59 inches/mi from January 23, 1997, (3d profile date) to March 2, 2003, (10th profile date), except for November 6, 2001, (8th profile date), when the IRI value was 70 inches/mi. The reason for a high IRI value on November 6, 2001, is not clear. The IRI on March 2, 2003, (10th profile date) was 56 inches/mi. The IRI values for the profile dates subsequent to March 2, 2003 (March 10, 2004, March 15, 2005, and March 27, 2006) were 93, 69, and 113 inches/mi, respectively. These values show a drop in IRI of 24 inches/mi between March 10, 2004, and March 15, 2006, and an increase in IRI of 44 inches/mi between March 15, 2005, and March 27, 2006. IRI values for the five runs on each of these dates showed significant variations, and the operator comments indicated there was cracking and raveling along the wheel-paths. The maintenance tables do not indicate repairs were carried out on this section during this time frame. Accordingly, the variations in IRI noted at this section seem to be caused by lateral variations in the profiled path.

- **Group 1, section 190108 (Iowa):** The last four IRI values at this section (May 29, 2001, August 6, 2001, November 22, 2002, and September 22, 2004) were 134, 119, 123, and 139 inches/mi, respectively. These values show a drop in IRI of 15 inches/mi between May 29, 2001, and August 6, 2001. The maintenance tables indicate that strip patching was performed on this section on July 1, 2001. The reduction in IRI seen between May 29, 2001, and August 6, 2001, may be due to this patching.

- **Group 2, section 310117 (Nebraska):** IRI ranged between 63 and 68 inches/mi for the seven profile dates between November 1, 1995, and March 20, 2000. However, IRI at the second profile date on April 17, 1996, was 81 inches/mi. The reason for the high IRI value is not clear. IRI on May 16, 2001 (eighth profile date) and April 24, 2002 (ninth and last profile date) were 75 and 54 inches/mi, with a reduction in IRI of 21 inches/mi occurring between the two test dates. The maintenance tables indicate grinding was performed on this section around this time period, and the reduction in IRI is attributed to this grinding. IRI at the first profile date for this section was 68 inches/mi, and IRI at the last profile date was 54 inches/mi, which was less than the IRI at the first profile date.

- **Group 2, section 310118 (Nebraska):** IRI for March 20, 2000 (seventh profile date), May 16, 2001 (eighth profile date), and April 24, 2002 (ninth and last profile date) were 82, 63, and 54 inches/mi, respectively, with a reduction in IRI of 19 inches/mi occurring between March 20, 2000, and May 16, 2001. IRI reduced further by 9 inches/mi between May 16, 2001, and April 24, 2002. The maintenance tables indicate grinding was performed on this section around this time period, and the reduction in IRI probably occurred because of the grinding. The IRI at the first profile date for this section was 74 inches/mi, and IRI at the last profile date was 54 inches/mi, which was less than the IRI at the first profile date.

- **Group 4, section 240505 (Maryland):** IRI from June 11, 1992 (1st profile date) to June 30, 2004 (11th profile date) gradually increased from 66 to 116 inches/mi. However on October 20, 1999 (seventh profile date), IRI was 118 inches/mi, with the IRI previous to this date being 96 inches/mi and the IRI subsequent to this date being 95 inches/mi. The maintenance tables do not indicate any activity performed between October 20, 1999, and December 5, 2000, on this section. Hence, the cause for the high IRI on October 29, 1999, is not clear. The IRI for the last three profile dates (April 26, 2005, September 22, 2005, and June 15, 2006) were 134, 115, and 207 inches/mi, respectively. The maintenance tables do not indicate any maintenance activities occurred within this section between April 26, 2005, and September 22, 2005. The profile operator comments indicated that cracking was present in the section, and a reduction in IRI was noted between April 26, 2005, and September 22, 2005. The increase in IRI from September 22, 2005, to June 15, 2006, may have occurred because of lateral variability in the profiled path.

- **Group 4, section 270509 (Minnesota)**: IRI on September 20, 2000 (eighth profile date) and August 19, 2001 (ninth profile date) were 124 and 100 inches/mi, respectively.

Thereafter, from December 2, 2002 (10th profile date) to June 6, 2005 (13th and last profile date), IRI showed a gradual increase from 100 to 115 inches/mi. These IRI trends indicate some type of maintenance activity was performed on this section between September 20, 2000, and August 19, 2001. The maintenance tables indicate skin patching was performed on August 1, 2001, which probably caused the reduction in roughness.

- **Group 5, section 040213 (Arizona):** IRI increased from 94 to 114 inches/mi from January 25, 1994, to December 12, 2004, with this section being profiled 11 times during this period. The time-sequence IRI values were variable, with four reductions in IRI greater than 10 inches/mi between subsequent profile dates during this period. The cause for this reduction in IRI as well as the variability in the IRI values is not clear and may be due to curling and warping effects of the PCC pavement.

- **Group 5, section 050217 (Arkansas):** IRI was 89 inches/mi on April 9, 2003, 127 inches/mi on April 3, 2002, and 135 inches/mi on March 12, 2004. The cause for the low IRI value on April 9, 2003, is not clear and may be due to curling or warping effects of the PCC slab.

- **Group 5, section 390205 (Ohio):** IRI was 100 inches/mi on November 4, 2001, 92 inches/mi on August 16, 2000, and 90 inches/mi on December 6, 2002. The cause for the high IRI value on August 16, 2000, is not clear and may be due to curling or warping effects of the concrete slab.

As described, there were several cases where an IRI value for a particular date was higher than the preceding and subsequent IRI values. Also, variable IRI values over time were noted at one PCC section. An evaluation of the profile data to investigate the cause for the high IRI or variable IRI was not performed because it was outside the scope of this study.

For sections 310117 and 310118 in Nebraska, the IRI on the last profile date was less than the IRI at the first profile date because of grinding. These two sections were not used in the analysis to determine the relationship between ride quality and structural strength.

For the remaining sections, a reduction in ride quality between subsequent profile dates could be attributed to maintenance activities for only two test sections: sections 190108 (Iowa) and 270509 (Minnesota). In the case of the former, strip patching is believed to have caused IRI to decrease by 15 inches/mi (from 134 to 119 inches/mi), but IRI increased to 139 inches/mi in 3 years. For the latter, skin patching is believed to have caused an IRI reduction of 24 inches/mi (from 124 to 100 inches/mi). Subsequently, IRI increased to 115 inches/mi in 4 years. Neither maintenance activity is expected to have a significant effect on the structural adequacy of the pavement.

Based on the review of the time-sequence IRI data, using the IRI at the first and last profile dates to determine the change in IRI that occurred at the test section appears reasonable. The selected data values do not appear to be influenced by errors in data collection that would have influenced the IRI value.

4.4 REVIEW OF DEFLECTION TIME HISTORY DATA

In chapter 3, the change in SN that occurred over time at a test section was evaluated by considering SN determined from the first and last FWD dates (i.e., last FWD date available in the database). The time-sequence average deflection values obtained below the center of the load plate for a 9,000-lb load at the test sections were studied to evaluate the changes in deflection over time. Such a plot shows if the deflections were affected by patching that was performed at the test sections and also verifies that that the first and last SN values used in the analysis were not outliers.

The modulus of the AC layer changes with temperature, and deflections obtained on AC-surfaced pavements depend on the temperature. The deflection below the load was adjusted to a standard temperature of 68 °F before evaluating the deflections. The deflection adjustment was performed using the procedure outlined in the 1993 AASHTO *Guide for Design of Pavement Structures*.[23] The AC modulus versus temperature relationship depends on the properties of the AC mix. However, only one set of adjustment factors are provided in the guide and applied to all AC surfaces irrespective of mix properties. The guide presents adjustment factors for AC temperatures between 30 and 120 °F. The validity of these adjustment factors when correcting the deflection from a temperature close to the limits (i.e., 30 and 120 °F) could be questionable. Seasonal effects that cause changes in moisture conditions in the base/subbase and subgrade also can have a significant effect on the deflection measured below the load.

Table 31 shows the time-sequence average deflection below the load for a 9,000-lb load corrected to a temperature of 68 °F for each section. The temperature at the mid-depth of the surface layer (i.e., AC for AC-surfaced pavements and PCC for PCC-surfaced pavements) at the time of testing is also shown in this table. For AC-surfaced pavements, the deflections shown are those obtained along the right wheel path, and the value shown is the average of all deflections obtained within the section. For PCC sections, the average deflections obtained at the center of the slab are shown. The time-sequence deflection plots are included in appendix D. For each section, a plot showing the time-sequence temperature values at the mid-depth of the surface layer is shown below the deflection plot.

Table 31. Time-sequence deflection values at test sections.

Group	Section	FWD Test Date	Time (years)	Avg. Deflection Below Load for 9,000 lb Corrected for Temperature (mil)	Temperature of AC (°F)	Deflections Avg. (mil)	Deflections Std Dev (mil)	Deflections COV (Percent)
1	050119	3/15/1994	0.0	7.40	65	5.97	0.73	12
		2/5/1996	1.9	4.92	27			
		3/12/1999	5.0	6.07	56			
		4/5/2001	7.1	6.17	72			
		4/29/2003	9.1	5.45	78			
		3/4/2004	10.0	6.21	61			
		5/24/2004	10.2	5.54	82			

Table 31. Time-sequence deflection values at test sections—continued.

Group	Section	FWD Test Date	Time (years)	Avg. Deflection Below Load for 9,000 lb Corrected for Temperature (mil)	Temperature of AC (°F)	Deflections		
						Avg. (mil)	Std Dev (mil)	COV (Percent)
1	480114	11/17/1997	0.5	5.99	54	5.20	0.40	8
		8/19/1999	2.2	4.82	130			
		5/10/2000	2.9	4.95	86			
		2/13/2002	4.7	4.88	70			
		11/12/2003	6.5	5.22	85			
		6/24/2004	7.1	5.34	87			
	310113	8/3/1995	0.0	27.43	103	26.76	2.17	8
		6/11/1997	1.9	29.01	84			
		10/14/1999	4.2	23.84	59			
	010102	3/10/1993	0.0	5.27	84	4.50	1.01	23
		6/20/1995	2.3	5.93	104			
		4/18/1996	3.1	4.60	88			
		7/22/1998	5.4	5.62	98			
		5/18/2000	7.2	4.54	100			
		5/23/2002	9.2	3.85	87			
		2/20/2004	11.0	2.94	64			
		4/28/2005	12.2	3.28	73			
	390112	11/6/1996	1.2	3.98	61	5.21	0.78	15
		9/16/1999	4.0	5.23	63			
		4/12/2001	5.6	5.50	83			
		9/1/2004	9.0	6.13	93			
	0401223	2/16/1994	0.5	3.06	71	2.98	0.28	9
		2/17/1995	1.5	2.87	74			
		1/7/1998	4.4	2.63	65			
		2/11/1999	5.5	2.60	59			
		5/2/2001	7.8	3.45	79			
		4/14/2003	9.7	3.20	94			
		4/7/2005	11.7	3.03	78			
	190108	5/18/1993	0.0	11.91	70	9.31	1.23	13
		9/11/1995	2.3	8.94	66			
		5/12/1997	4.0	8.92	63			
		10/5/1999	6.4	8.64	54			
		2/13/2001	7.7	9.42	44			
		6/27/2005	12.1	8.05	114			

Table 31. Time-sequence deflection values at test sections—continued.

Group	Section	FWD Test Date	Time (years)	Avg. Deflection Below Load for 9,000 lb Corrected for Temperature (mil)	Temperature of AC (°F)	Deflections Avg. (mil)	Deflections Std Dev (mil)	Deflections COV (Percent)
2	320101	3/27/1996	0.6	7.02	71	7.32	0.70	10
		3/13/1997	1.5	6.02	67			
		8/19/1999	4.0	8.10	112			
		3/24/2000	4.6	6.89	70			
		3/6/2001	5.5	6.90	61			
		3/19/2003	7.6	8.05	63			
		3/29/2004	8.6	7.00	68			
		3/22/2005	9.6	7.58	52			
		8/28/2006	11.0	8.04	79			
	390106	11/5/1996	1.2	4.69	57	6.71	1.78	27
		12/19/1997	2.3	4.86	48			
		9/15/1999	4.0	6.45	97			
		4/12/2001	5.6	6.89	72			
		10/8/2004	9.1	7.34	62			
		7/15/2008	12.9	10.04	89			
	310117	8/2/1995	0.6	10.82	103	12.10	2.17	18
		6/9/1997	2.4	10.64	92			
		10/12/1999	4.8	11.09	84			
		7/9/2002	7.5	15.84	112			
	310118	8/3/1995	0.6	9.82	82	11.00	3.60	33
		6/10/1997	2.4	9.72	99			
		10/13/1999	4.8	7.45	81			
		7/10/2002	7.5	17.03	90			
3	190101	5/19/1993	0.0	14.69	74	13.71	0.90	7
		4/25/1995	1.9	12.02	83			
		9/12/1995	2.3	13.53	68			
		10/8/1999	6.4	13.43	64			
		2/16/2001	7.8	13.90	34			
		6/28/2005	12.1	14.68	113			
	190103	5/19/1993	0.0	7.27	94	6.41	1.12	18
		9/23/1993	0.3	5.64	69			
		9/13/1995	2.3	5.78	79			
		5/14/1997	4.0	6.06	73			
		10/8/1999	6.4	5.64	73			
		2/20/2001	7.8	5.64	42			
		6/29/2005	12.1	8.81	88			

Table 31. Time-sequence deflection values at test sections—continued.

Group	Section	FWD Test Date	Time (years)	Avg. Deflection Below Load for 9,000 lb Corrected for Temperature (mil)	Temperature of AC (°F)	Deflections Avg. (mil)	Deflections Std Dev (mil)	Deflections COV (Percent)
3	050114	3/16/1994	0.0	11.05	86	6.35	1.41	22
		2/7/1996	1.9	7.90	47			
		3/16/1999	5.0	6.99	85			
		4/9/2001	7.1	7.06	107			
		5/1/2003	9.1	7.17	81			
		5/26/2004	10.2	6.49	99			
		5/12/2005	11.2	7.65	91			
	050116	3/16/1994	0.0	3.56	86	3.25	0.43	13
		2/6/1996	1.9	2.95	47			
		3/15/1999	5.0	2.75	85			
		4/9/2001	7.1	2.80	107			
		4/30/2003	9.1	3.87	81			
		5/25/2004	10.2	3.76	99			
		5/11/2005	11.2	3.04	91			
4	040502	1/16/1991	0.7	6.88	57	9.47	3.46	36
		10/3/1991	1.5	4.05	90			
		10/19/1994	4.5	8.25	99			
		9/12/1996	6.4	7.25	111			
		11/13/1997	7.6	10.15	73			
		12/10/1998	8.6	13.88	55			
		12/14/1999	9.7	15.96	54			
		10/17/2000	10.5	8.33	98			
		12/11/2002	12.7	10.73	77			
		12/11/2003	13.7	12.78	73			
		9/15/2008	18.4	5.87	126			
	240505	8/25/1992	0.4	6.58	94	6.45	0.81	13
		8/8/1994	2.4	6.30	107			
		10/16/1995	3.5	6.46	68			
		5/7/1997	5.1	6.30	93			
		7/7/1999	7.3	5.02	118			
		8/28/2001	9.4	6.27	92			
		6/25/2003	11.2	5.87	111			
		6/8/2004	12.2	6.33	109			
		5/25/2005	13.2	8.42	63			
		4/7/2009	17.0	6.98	60			

Table 31. Time-sequence deflection values at test sections—continued.

Group	Section	FWD Test Date	Time (years)	Avg. Deflection Below Load for 9,000 lb Corrected for Temperature (mil)	Temperature of AC (°F)	Deflections Avg. (mil)	Deflections Std Dev (mil)	Deflections COV (Percent)
4	270509	6/18/1991	0.8	13.89	101	11.88	2.35	20
		6/17/1992	1.8	10.78	80			
		9/29/1993	3.0	7.95	52			
		8/23/1995	4.9	16.20	108			
		6/7/1999	8.7	12.45	83			
		8/21/2001	10.9	10.03	82			
		8/20/2003	12.9	12.61	99			
		6/7/2005	14.7	11.15	99			
5	040213	2/8/1994	0.4	4.41	60	6.62	2.52	38
		3/6/1995	1.4	12.58	80			
		11/6/1997	4.1	6.08	85			
		1/11/1999	5.3	4.95	63			
		12/7/2001	8.2	5.81	65			
		12/18/2003	10.2	6.45	68			
		12/15/2004	11.2	6.09	72			
	050217	11/14/1996	1.0	3.48	49	3.27	0.25	8
		4/21/1999	3.4	3.46	81			
		7/30/2001	5.7	3.46	100			
		10/9/2003	7.9	3.10	69			
		9/20/2004	8.8	2.85	77			
	390205	12/30/1996	0.4	4.68	48	6.05	1.06	17
		7/22/1997	0.9	5.10	78			
		9/10/1999	3.1	5.51	84			
		4/4/2001	4.6	6.83	79			
		4/15/2003	6.7	7.73	90			
		9/9/2004	8.1	6.47	67			

COV = Coefficient of variation.

Evaluation of the time-sequence data showed that major changes in deflections had not occurred at most sites. At 15 of the 21 sections evaluated in this study, the coefficient of variation (COV) of the time-sequence deflection values was 20 percent or less. COV values greater than 20 percent were obtained at the following sites: 010102 in Alabama (23 percent), 390106 in Ohio (27 percent), 310118 in Nebraska (33 percent), 050114 in Arkansas (22 percent), 040502 in Arizona (36 percent), and 040213 in Arizona (38 percent). Section 310118 in Nebraska was not used in the analysis.

The following observations were made at the other sections that had COV values greater than 20 percent:

- **010102 (Alabama):** Overall, the time-sequence deflection data showed a decrease with time with some scatter, which caused the high COV value.

- **390106 (Ohio):** The time-sequence deflection data showed an increase over time, which caused the high COV value.

- **050114 (Arkansas):** The average deflection for the first FWD date was much higher than the average deflection at the other test dates and is attributed as the cause for the high COV. The cause for the high deflections at the first FWD date is not clear.

- **040502 (Arizona):** The time-sequence deflections showed large variability. The temperature at time of testing at this section for the different test dates ranged from 54 to 126 °F. The variability in the deflections may be related to the effects of the temperature adjustment factor.

- **040213 (Arizona):** This is a PCC section, and the deflection in March 1996 was more than double the deflections obtained at the other test section, which resulted in a high COV value. The high deflection may be due to excessive downward curing at the time of testing.

Table 28 shows the patching activities performed on the test sections. There are two cases where full-depth patching was performed. If this patching was along the right wheel path where FWD deflections were performed, the SN value of the pavement may show an increase over the SN obtained for the previous FWD date. However, the increase in SN depends on the quantity of patching that was performed. Section 050119 had 560 ft^2 of full-depth patching, and the average deflection after the patching was only 2 percent less than that before patching. Hence, no increase in SN was expected at this section due to patching. The amount of full-depth patching performed on section 190108 is unknown. Skin patching and strip patching are expected to have little, if any, any impact on the structural strength of the pavement. The reason strip patching was performed is not known; filling of ruts is a possible reason.

Based on the review of the time-sequence deflection values, the use of the first and last FWD deflections at a site to characterize the change in SN appears to be reasonable.

4.5 ASSESSMENT OF PCC WARPING AND CURLING

4.5.1 Curling and Warping of Slabs

The shape of PCC slabs in a pavement can vary depending on the temperature and moisture gradient within the slab. A concrete slab can take the following shapes: (1) curled up, when the joints are at a higher elevation than the center of the slab, (2) curled down, when the center of the slab is at a higher elevation than the joints, or (3) flat. Changes in the slab shape caused by temperature effects are referred to as curling, while changes in the slab shape due to moisture effects are referred to as warping.

When the temperature of the pavement surface is lower than the temperature at the bottom of the slab in the night and early morning hours, the edges of the slab tend to curl upward. When the surface of the slab heats up during the day and is at a higher temperature than the bottom of the slab, the edges of the slab tends to curl downward. These changes in slab shape due to temperature are superimposed on the original shape of the slab. Usually, a pavement can either be curled upward or downward, and the temperature gradient influences the severity of the curvature.(26) A PCC slab can change shape from a curled up position during the early morning hours to a curled down position in the afternoon as the surface of the pavements heats up. The curvature that is built into the slab depends on factors such as mix properties, base support, slab length, slab thickness, and temperature and moisture conditions during curing.(26) Changes in the moisture within a slab can also cause a slab to change shape, and these changes occur over time. For example, if the moisture content in the top portion of the slab reduces over time and is less than at the bottom of the slab, the edges of the slab will curl upward.

Curvature in a slab (either upward or downward) contributes to roughness. Byrum et al. developed an equation to predict the IRI due to slab curvature.(27) From an analysis of GPS-3 data in the LTPP database, Byrum et al. noted undoweled slabs have a higher level of curvature compared to doweled slabs.

4.5.2 Diurnal Changes in IRI

As discussed in the previous section, the shape of a PCC slab can change during the day due to temperature variations, which causes changes in roughness. Karamihas et al. presented IRI changes that occurred because of temperature-related slab curling at 11 test sections in the Michigan SPS-2 project.(28) Profile measurements were obtained on March 28, 1997, at this SPS-2 project starting at 5:07 a.m. and ending at 3:42 p.m., with measurements obtained over approximately 10 h. The air temperature during this period increased from 51 to 74 °F. Three of the pavement sections in this project showed no change in IRI over the period. The mean IRI (average of left and right wheel paths) of six sections decreased continuously during testing, with the reduction in IRI ranging from 10 to 25 inches/mi. All of these sections were curled up, and the degree of the upward curling reduced as the air temperature increased, resulting in a decrease in IRI. Two sections showed increases in IRI ranging from 6 to 12 inches/mi. Both of these sections were curled downwards, and the degree of downward curling increased with the increase in air temperature, causing IRI to increase.

4.5.3 Changes in IRI Over Time

Karamihas and Senn studied the progression of IRI at 21 test sections (12 LTPP sections and 9 State supplemental sections) at the LTPP SPS-2 project in Arizona over 16 years after construction.(29) Two of the supplemental sections were surfaced with AC, and the other seven sections were surfaced with PCC. Four of the PCC sections were non-doweled, and the other three were doweled and had designs that were of interest to the Arizona Department of Transportation. The results obtained by Karamihas and Senn at the 12 LTPP SPS-2 sections are presented in this section.(29)

Investigation of the profiles obtained at the SPS-2 sections indicated roughness in some test sections was caused by longitudinal and transverse cracking and some built-in localized defects.

However, slab curvature had a significant contribution to roughness in some sections and, in some cases, was the dominant contributor to roughness. Evaluation of the time-sequence roughness values at the test sections showed significant variability in roughness from year to year at many sections because of changes in slab curvature due to diurnal and seasonal effects. In this study, objective profile analysis methods were used to quantify the level of slab curvature in each section. A procedure for estimating the gross strain gradient needed to deform the slab to the shape noted in the profile was developed to produce a pseudo strain gradient (PSG) value. The level of slab curvature in the section was then summarized by the average PSG value.

Variations in the average PSG over time were able to explain the changes in roughness over time at the sections that had a PCC design flexural strength of 550 psi. A good correlation existed at these sections between the change in IRI and the change in PSG. Table 32 shows the change in IRI that occurred at the test sections that were designed for a flexural strength of 550 psi over a 16-year period, with a positive change indicating an increase in IRI. This table also shows the IRI when the IRI contribution caused by slab curvature was removed. All of these sections were curled up, and the degree of upward curling increased with time. The increase in upward curling of the slabs was the major contributor to the increase in IRI at these test sections. Although not stated by Karamihas and Senn, the increase in upward curling with time was likely related to slab warping.

Table 32. Results for sections designed for flexural strength of 550 psi.

	Section					
Factor	**040213**	**040217**	**040221**	**040215**	**040219**	**040223**
PCC flexural strength (psi)	550	550	550	550	550	550
PCC thickness (inches)	8	8	8	11	11	11
Base type	DGAB	LCB	PATB	DGAB	LCB	PATB
Direction of curl	Up	Up	Up	Up	Up	Up
IRI change (inches/mi), left	20	-12	9	34	20	28
IRI change (inches/mi), right	101	-7	11	38	24	22
IRI change curl removed (inches/mi), left	-3	12	2	-6	6	-6
IRI change curl removed (inches/mi), right	72	9	2	-5	12	-5

Table 33 shows the changes in IRI that occurred at the test sections that were designed for a PCC flexural strength of 900 psi. Little change in IRI was noticed at most of the sections, and a good relationship between the change in PSG and change in IRI could not be established for these sections. Hence, the IRI values with the curling effects removed are not shown in this table.

Table 33. Results for sections designed for flexural strength of 900 psi.

Factor	Section					
	040214	040218	040222	040216	040220	040224
PCC flexural strength (psi)	900	900	900	900	900	900
PCC thickness (inches)	8	8	8	11	11	11
Base type	DGAB	LCB	PATB	DGAB	LCB	PATB
Direction of curl, initial (0.32 years)	Up	Up	Up	Up	Up	Up
Direction of curl, initial (16.32 years)	Down	Up	Up	Down	Up	Up
IRI change (inches/mi), left	15	-14	4	3	3	20
IRI change (inches/mi), right	19	-15	-1	18	3	16

4.5.4 Effect of Curling and Warping on FWD Testing

Upward curling of the pavement at the edges of the slab does not have an effect on FWD tests conducted at the center of the slab, as the center of the slab will be in contact with the base. However, downward curling of the slab where the mid-slab is at a higher elevation when compared to edges will have a significant impact on mid-slab FWD testing. This occurs because the center of the slab will not be in contact with the base when the slab is curled downward, and the degree of downward curling is expected to have a significant impact on the deflections obtained at the center of the slab.

4.5.5 Effect of Roughness on Structural Capacity

The information presented in the previous section shows that diurnal variations in the shape of a PCC slab can have a significant effect on the IRI value. Additionally, changes in slab curvature can occur over time that can cause an increase in roughness. These changes in roughness have no relationship to the structural capacity of the pavement. However, it should be noted that an increase in downward curling over time can result in premature mid-panel cracking initiating at the bottom of the slab, while an increase in upward curling over time can result in top-down cracking adjacent to the joints.

4.6 SUMMARY

Information on the maintenance and repair activities applied to each of the test sections during the time periods considered in the study was obtained from the LTPP database to assess the potential impact of these activities on ride quality and structural adequacy. Only a limited amount of maintenance was performed. The maintenance activities carried out at the test sections were crack sealing, fog sealing, joint sealing, partial-depth patching (at a PCC section), grinding, and patching at AC sections (full-depth, skin, and strip). Only grinding and full-depth patching may have an impact on ride quality, structural adequacy, or both.

Based on the review of the time-sequence IRI data, using IRI at the first and last profile dates to determine the change in IRI that occurred at a test section appears reasonable. The selected data values do not appear to be influenced by errors in data collection.

Little change in deflections occurred over time at many sections. The COV of the deflections values was less than 20 percent at 15 of the 21 sections evaluated in this study. At the sections that had a COV greater than 20 percent, the high COV values were attributed to: (1) deflections showing an increase with time, (2) deflections showing a decrease with time, (3) possible influence of the temperature adjustment factor on the adjusted deflections, and (4) one deflection in the time-sequence deflections being much higher than the other values.

The two AC sections where grinding was performed were not considered in this study. The limited maintenance activities that were performed on other sections appeared to have little or no influence on either the time-sequence IRI or deflection values. Based on the review of the time-sequence IRI and time-sequence deflection values, the use of the first and last profile and FWD dates to characterize changes in IRI and SN appears to be reasonable.

A past study has shown that significant diurnal variations in IRI can occur. A recently concluded FHWA study showed that the degree of curvature in a slab can increase over time, and curvature of the slab can have a significant effect on the IRI. Changes in IRI that occur due to changes in slab shapes have no relationship with the structural adequacy of the pavement.

CHAPTER 5. SUMMARY AND CONCLUSIONS

Ride quality and structural adequacy are key pavement performance indicators. The relationship between these two indicators has been a topic of frequent and continuing discussion in the pavement community, but an accepted and widely used relationship has not been identified to date. To address this issue, FHWA sponsored a study to identify and verify the relationship, if any, between ride quality and structural support or ride deterioration and structural adequacy using the LTPP pavement performance data.

The FHWA study was undertaken in an effort to improve the evaluation and use of pavement condition data in pavement rehabilitation and design decisions. More specifically, this project was intended to develop and document a mechanism to include both ride and structural adequacy values within the context of current network-level PMS practices for highway agency implementation. The results of the project were intended for use by PMS engineers to ensure smooth pavements that are also structurally adequate.

A literature search was undertaken to collect, review, and synthesize available information on relating ride quality and structural adequacy for pavement rehabilitation and design decisions. Pertinent information was sought through Web-based searches of State highway agencies, university pavement research centers, TRB, ASCE, industry, and other national and international organizations. A total of 62 references were identified, but only 16 were considered relevant to the study. Moreover, while these 16 references contained valuable information, they did not contribute to the direct or indirect identification of a potential ride quality-structural capacity relationship.

Following completion of the literature search, a review and assessment of selected LTPP pavement performance data were undertaken to see if a ride quality-structural capacity relationship could be identified through the analysis of these data.

A total of 21 LTPP sections were identified and broken down into 5 groups according to pavement type (new AC, AC overlay over AC, and PCC), base type (granular or asphalt treated), changes in IRI over time, and changes in structural capacity over time. Historical pavement smoothness (profile) and structural capacity (FWD deflection) data were extracted from the LTPP database for the 21 sections, and the resulting data were analyzed. IRI was used to characterize ride quality, while SN and D_{eff} were used to characterize the structural capacity of flexible and rigid pavements, respectively.

Continuous IRI and SN or D_{eff} plots were generated to see if a viable ride quality-structural capacity relationship could be identified. It was hypothesized that areas where large changes in IRI had occurred should show large decreases in SN or D_{eff}. However, such relationship could not be observed for the sections and data investigated. In general, no major changes in SN or D_{eff} associated with localized areas of roughness were observed. In most sections, significant IRI changes were noticed at localized areas. Comparisons of continuous IRI and maximum deflection (i.e., below the FWD load center) or estimated subgrade modulus plots were also performed, but again, a relationship could not be identified.

A number of additional analyses were conducted to validate the study findings and conclusions. The evaluation of maintenance and repair activities showed that only a limited amount of maintenance had been performed on the study sections; with few exceptions, they did not affect the study findings. The review of IRI and FWD time history data confirmed that the use of the first and last test dates at a site to characterize the change in IRI and SN appears reasonable. Finally, the assessment of PCC warping and curling concluded that changes in IRI that occur due to changes in slab shapes have no relationship with the structural adequacy of the pavement.

In view of the findings, actual development of a ride quality-structural adequacy relationship and guidance for implementing the relationship into PMS was not pursued, as it could not be justified on the basis of the approach taken in this study. The lack of correlation found in the study, however, is considered of value to PMS practitioners, as it indicates that good ride quality does not mean good structural support or lower funding requirements to maintain the pavements. This becomes an important consideration for those wishing to base performance measures on ride quality indicators.

It is also important to recognize that these findings are based on the approach taken in the study. It is possible that other researchers will pursue alternate approaches that will yield a reliable relationship. However, while a relationship would be expedient for PMS applications, a fundamental understanding of the differences in factors causing structural deterioration and roughness (as well as the variable cause-effect relationship) makes it unlikely to find a simple relationship, particularly one excluding most other factors.

It is hypothesized that a strong relationship between the two performance indicators in question would require the inclusion of many other variables, potentially undoing its usefulness for the intended purpose in PMS. Clearly, pavement structural and functional performances are not independent of each other, even though they are not related in a one-to-one manner that can provide a PMS shortcut. However, this does not mean that structural parameters are not important for consideration in roughness prediction models, that roughness could not be one factor in the rate of structural deterioration, or that many common factors do not affect both roughness and structural capacity.

APPENDIX A. DEFLECTION BELOW CENTER OF 9,000-LB LOAD AND SUBGRADE MODULUS PLOTS

A.1 GROUP 1 SECTIONS

A.1.1 Section 050119 (Arkansas)

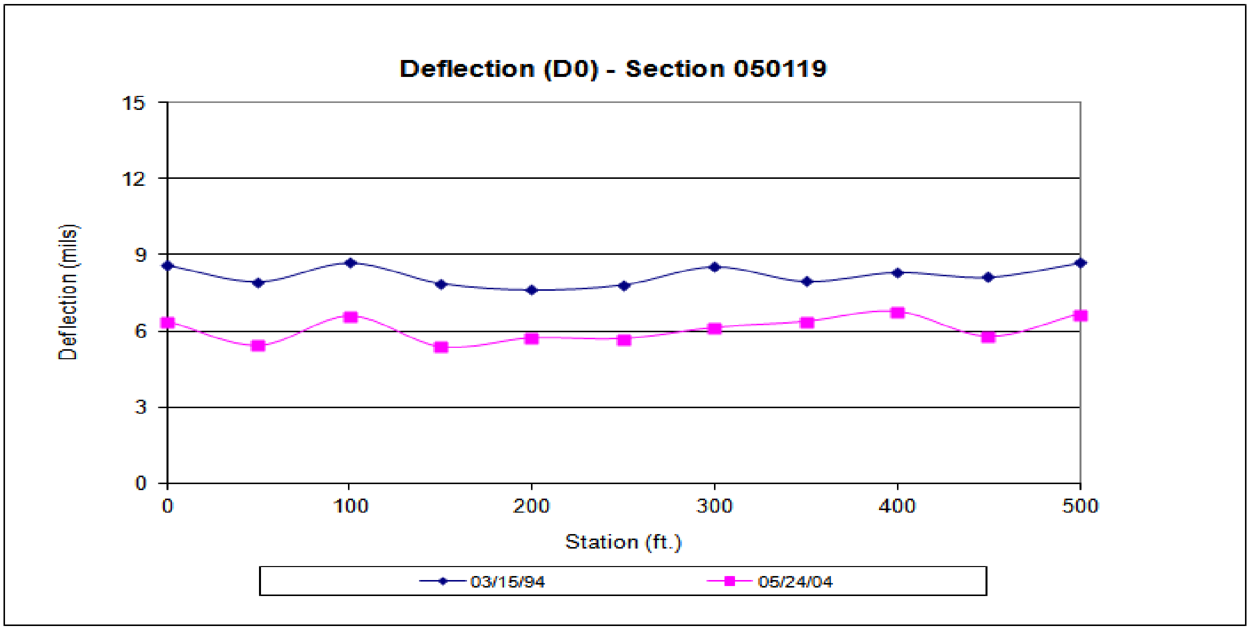

Figure 75. Graph. Deflection plot for section 050119 (Arkansas).

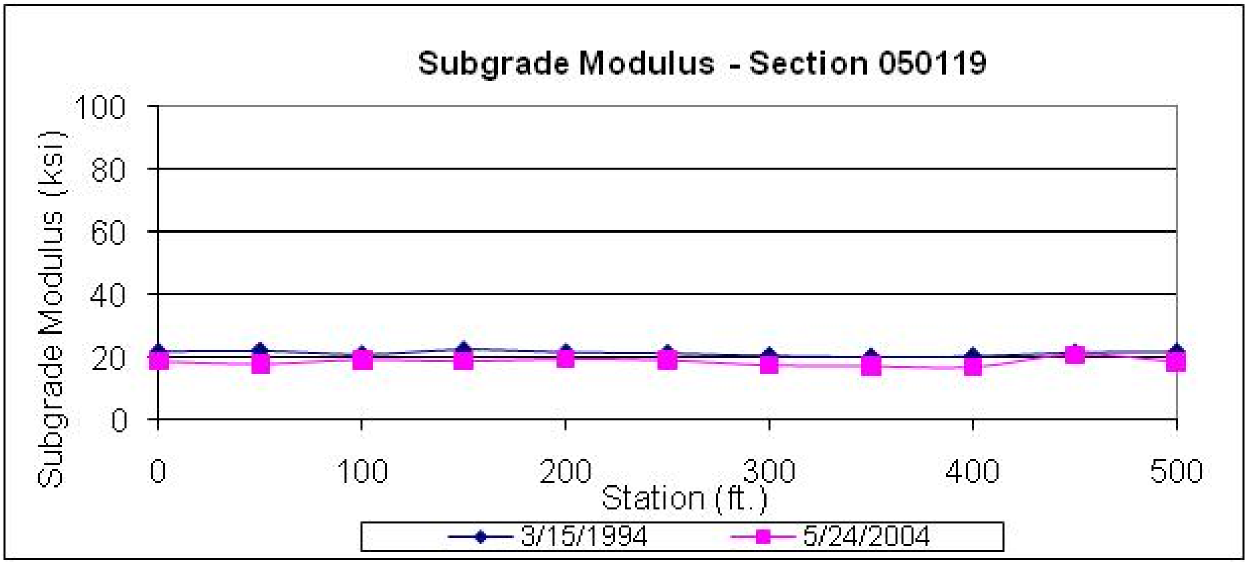

Figure 76. Graph. Subgrade modulus plot for section 050119 (Arkansas).

A.1.2 Section 480114 (Texas)

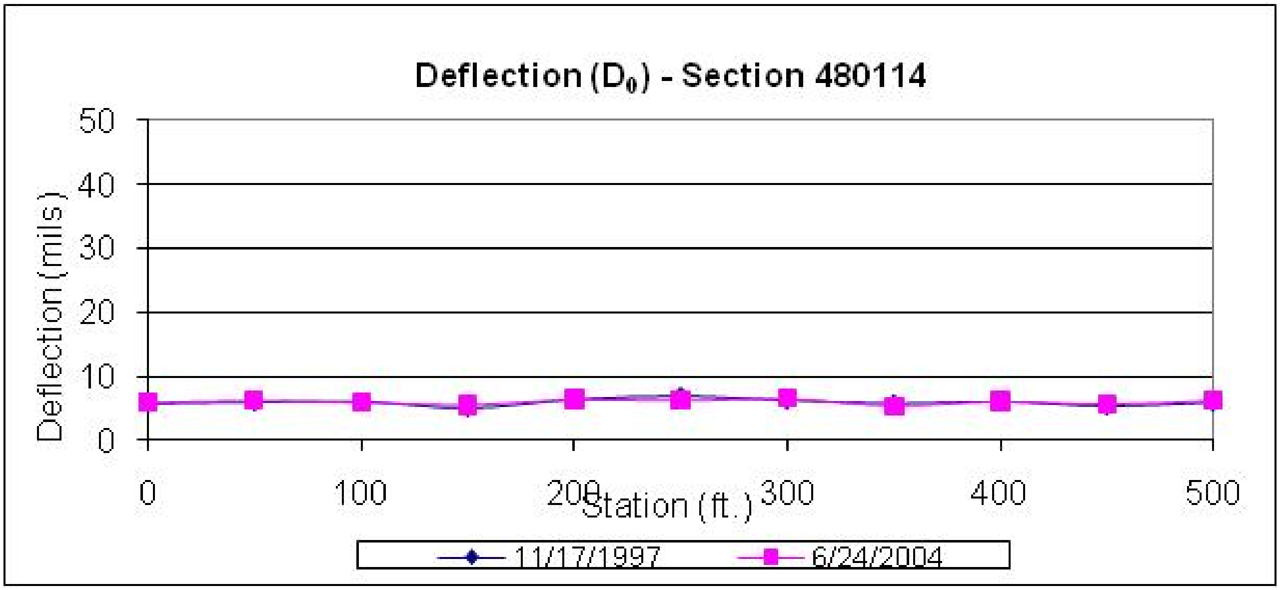

Figure 77. Graph. Deflection plot for section 480114 (Texas).

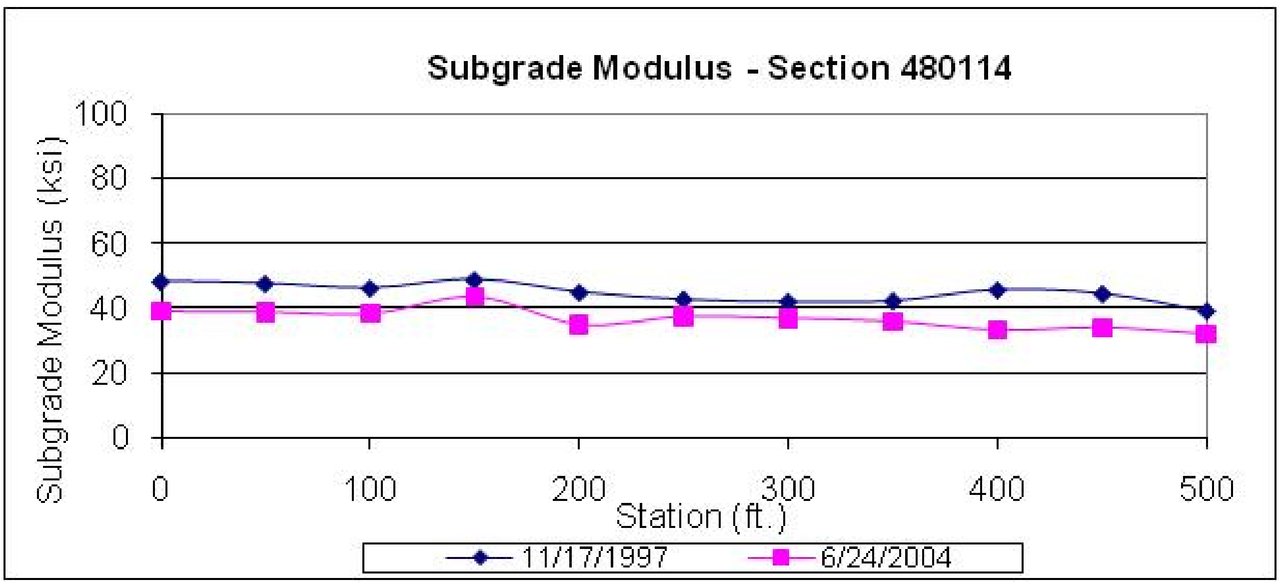

Figure 78. Graph. Subgrade modulus plot for section 480114 (Texas).

A.1.3 Section 310113 (Nebraska)

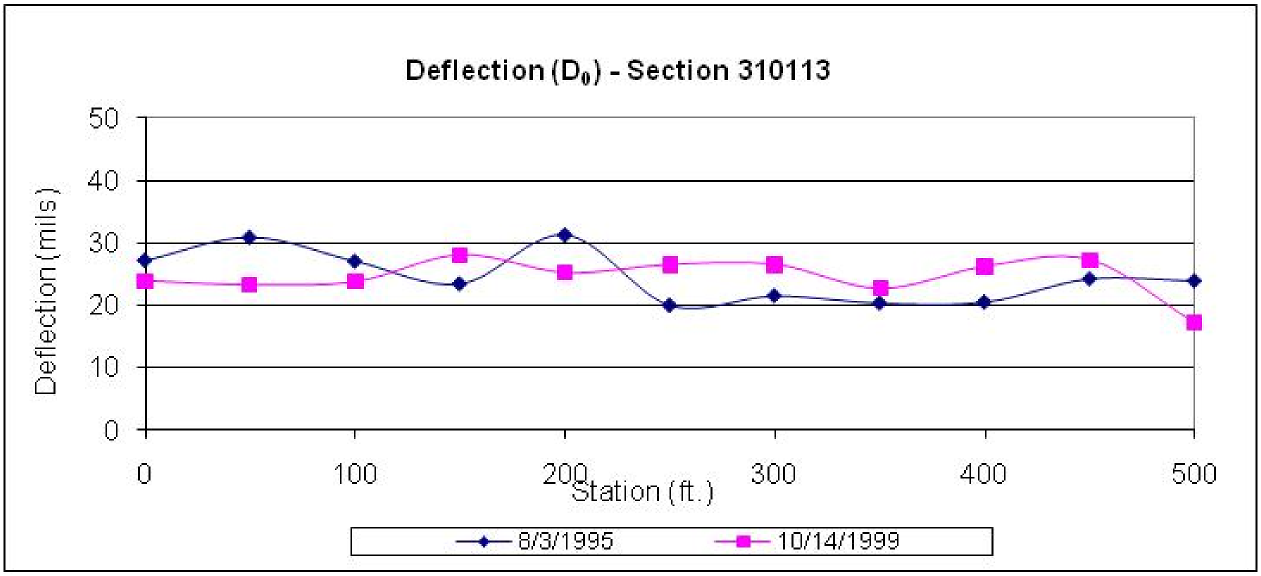

Figure 79. Graph. Deflection plot for section 310113 (Nebraska).

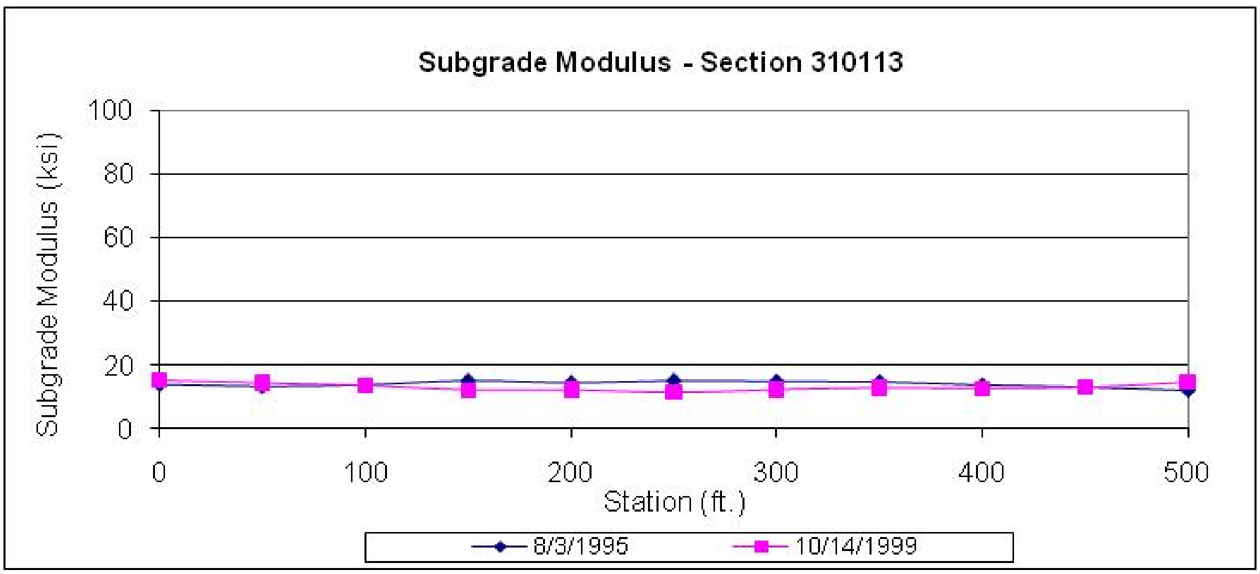

Figure 80. Graph. Subgrade modulus plot for section 310113 (Nebraska).

A.1.4 Section 010102 (Alabama)

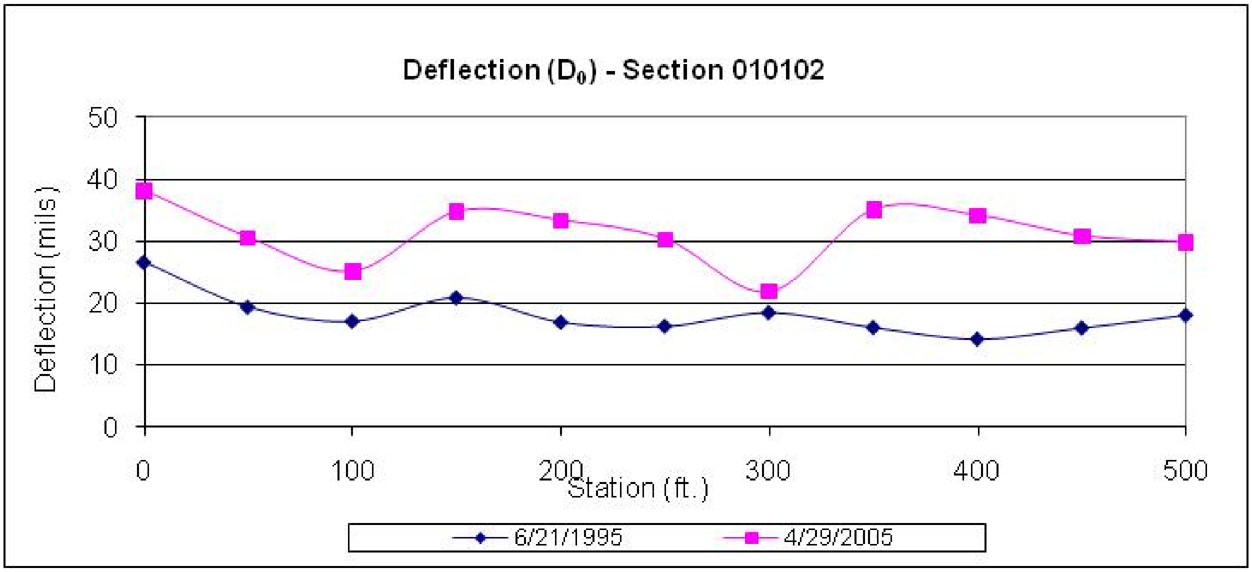

Figure 81. Graph. Deflection plot for section 010102 (Alabama).

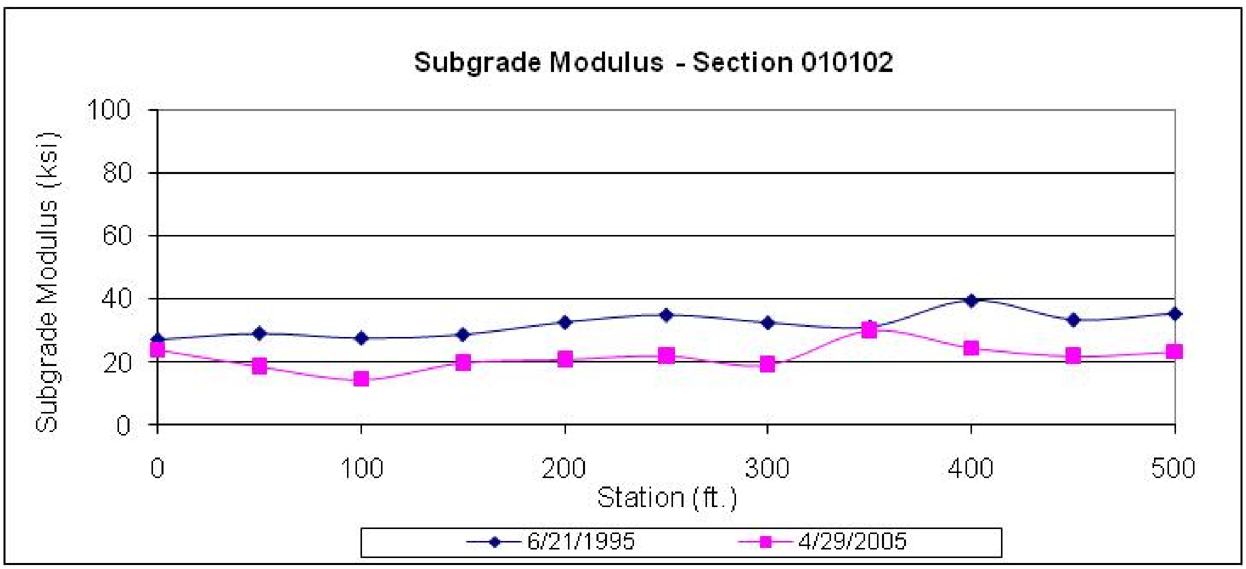

Figure 82. Graph. Subgrade modulus plot for section 010102 (Alabama).

A.1.5 Section 390112 (Ohio)

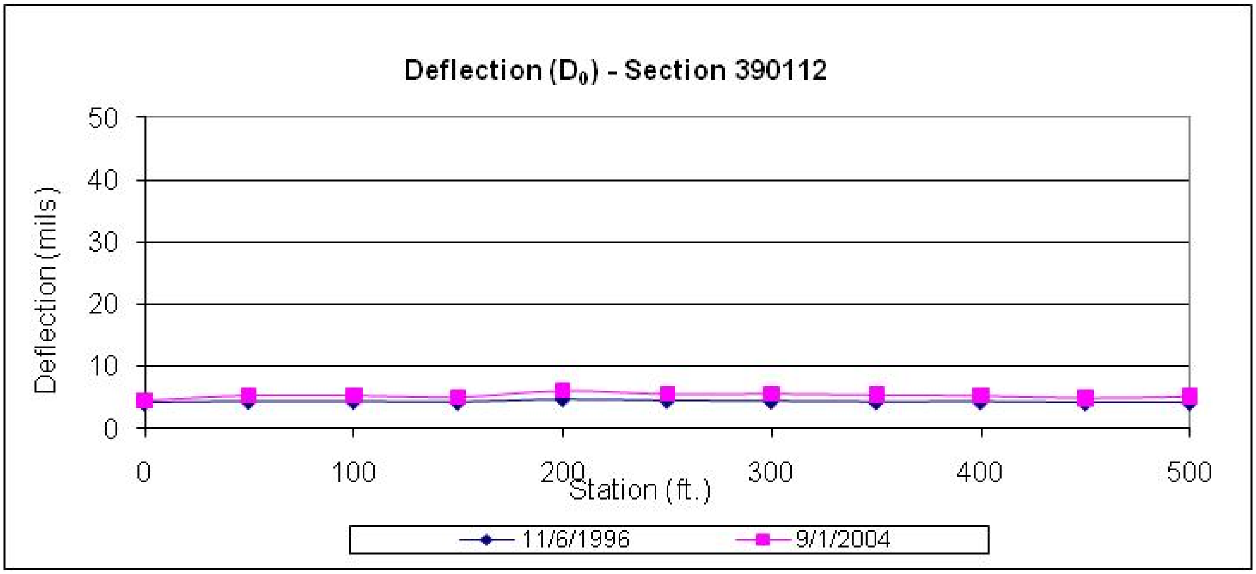

Figure 83. Graph. Deflection plot for section 390112 (Ohio).

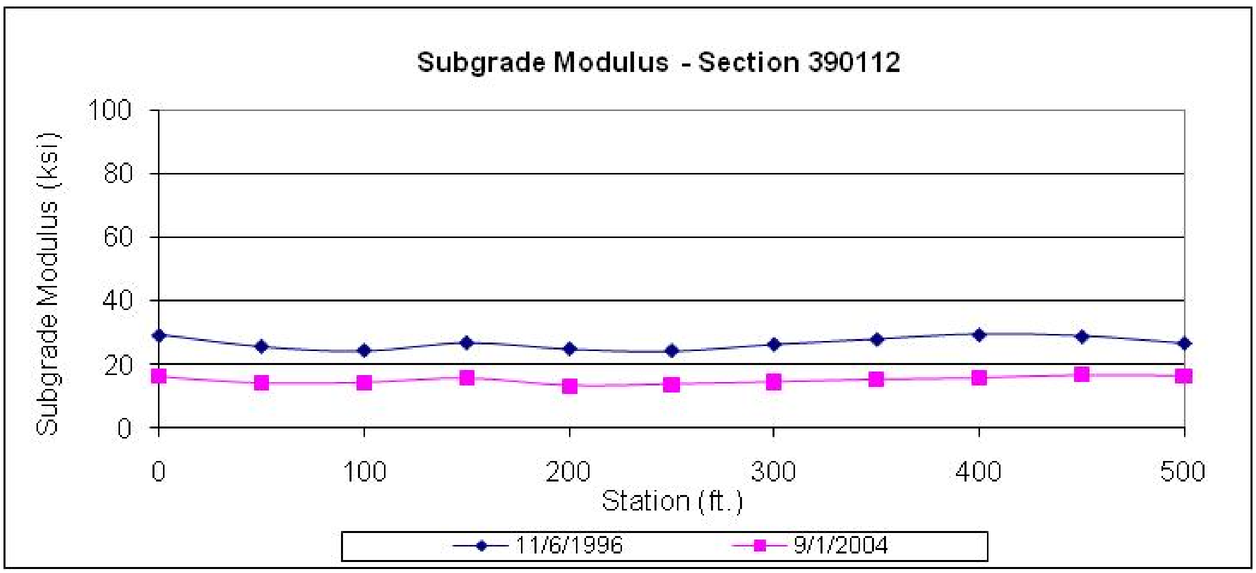

Figure 84. Graph. Subgrade modulus plot for section 390112 (Ohio).

A.1.6 Section 040123 (Arizona)

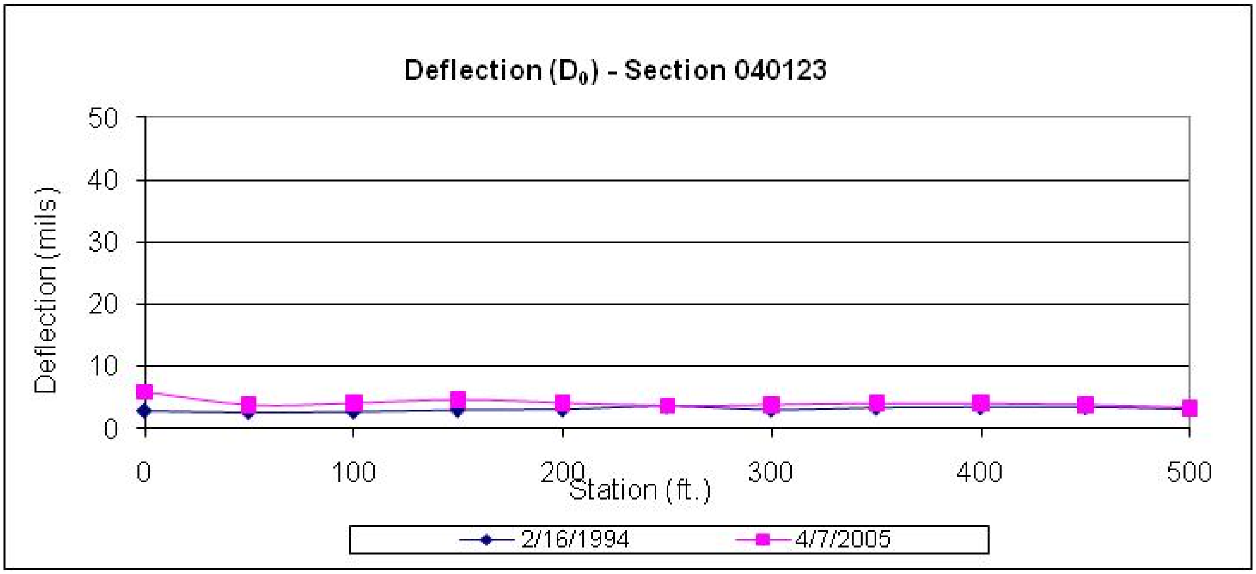

Figure 85. Graph. Deflection plot for section 040123 (Arizona).

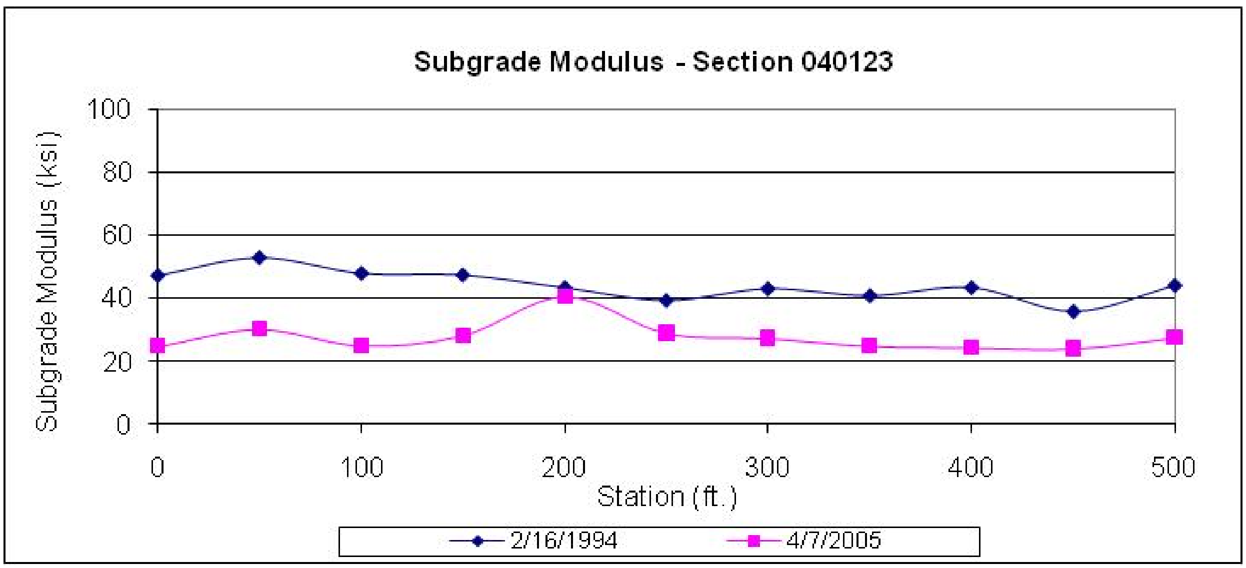

Figure 86. Graph. Subgrade modulus plot for section 040123 (Arizona).

A.1.7 Section 190108 (Iowa)

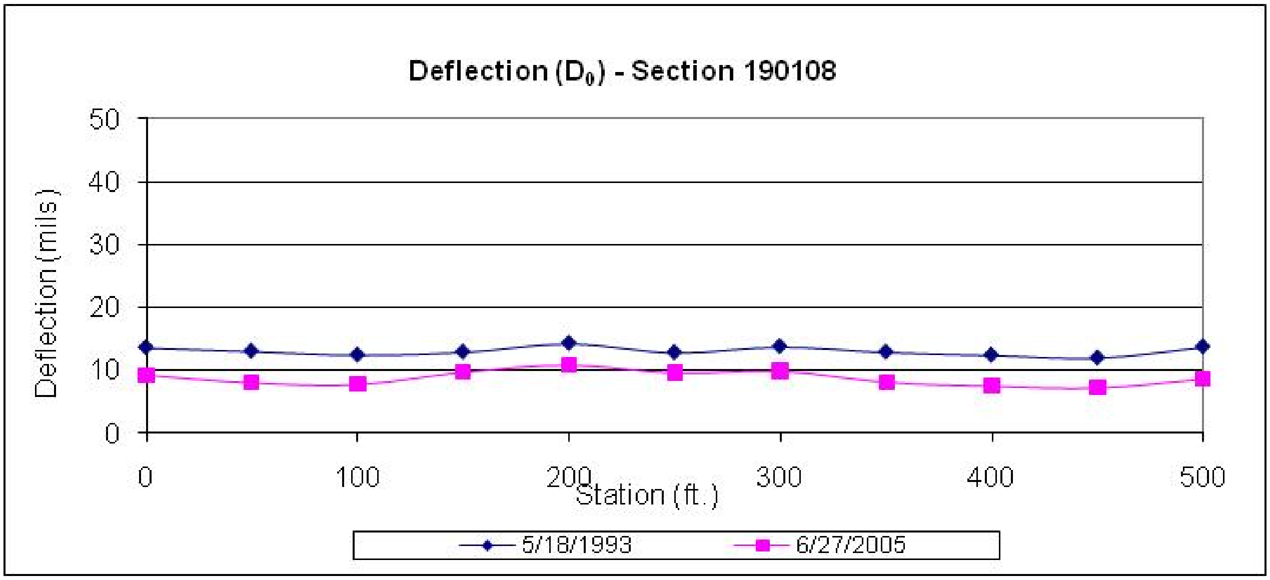

Figure 87. Graph. Deflection plot for section 190108 (Iowa).

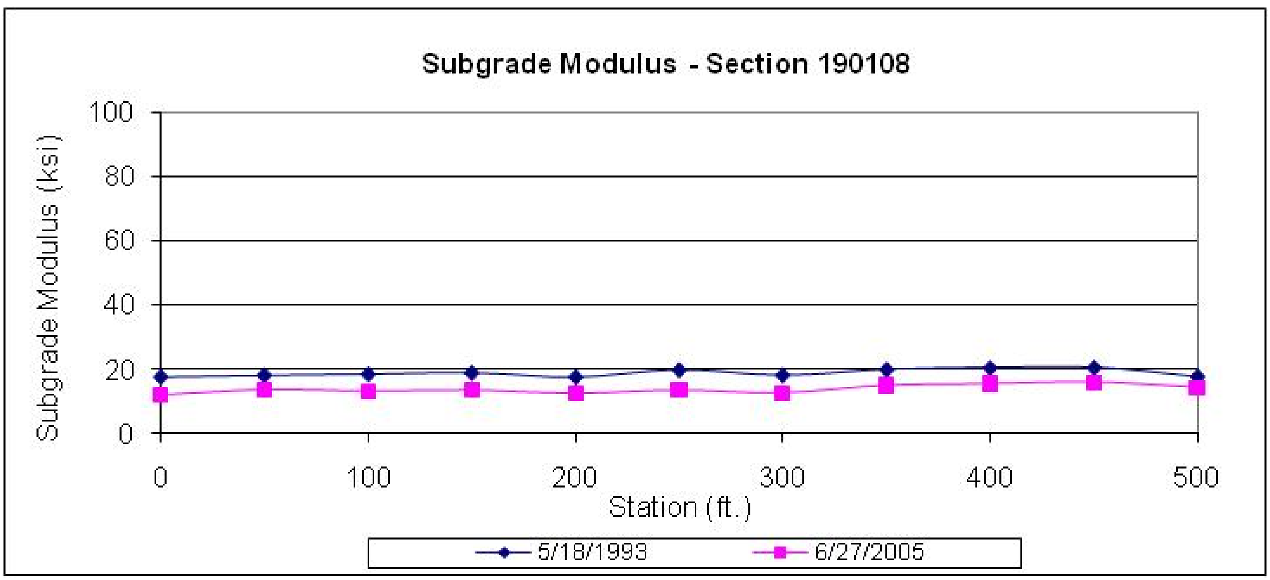

Figure 88. Graph. Subgrade modulus plot for section 190108 (Iowa).

A.2 GROUP 2 SECTIONS

A.2.1 Section 320101 (Nevada)

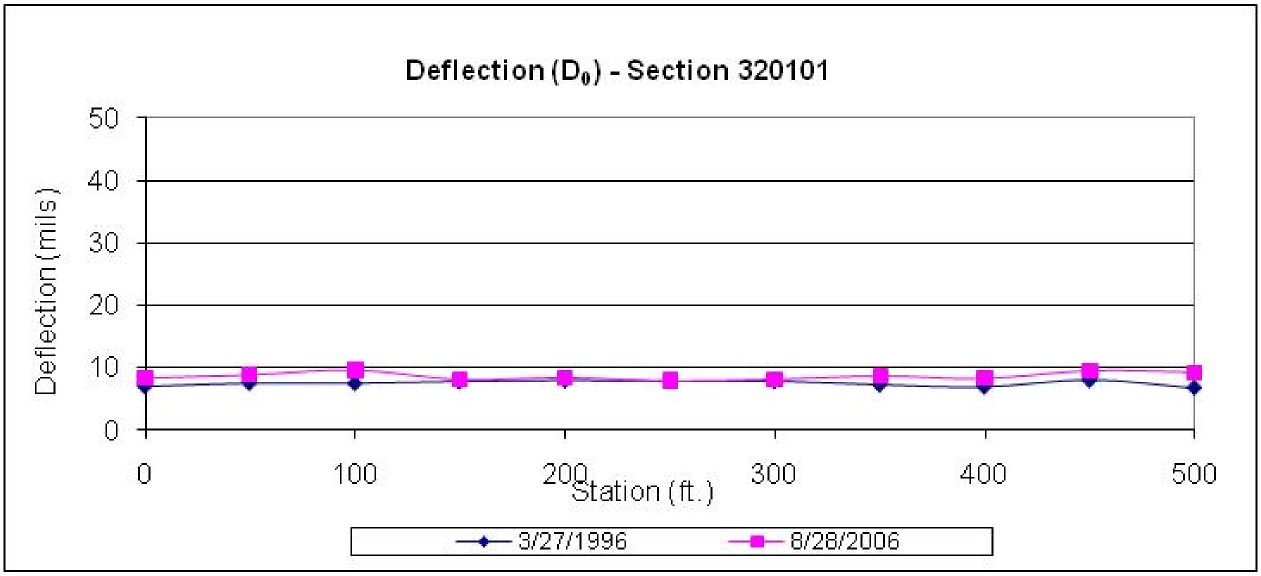

Figure 89. Graph. Deflection plot for section 320101 (Nevada).

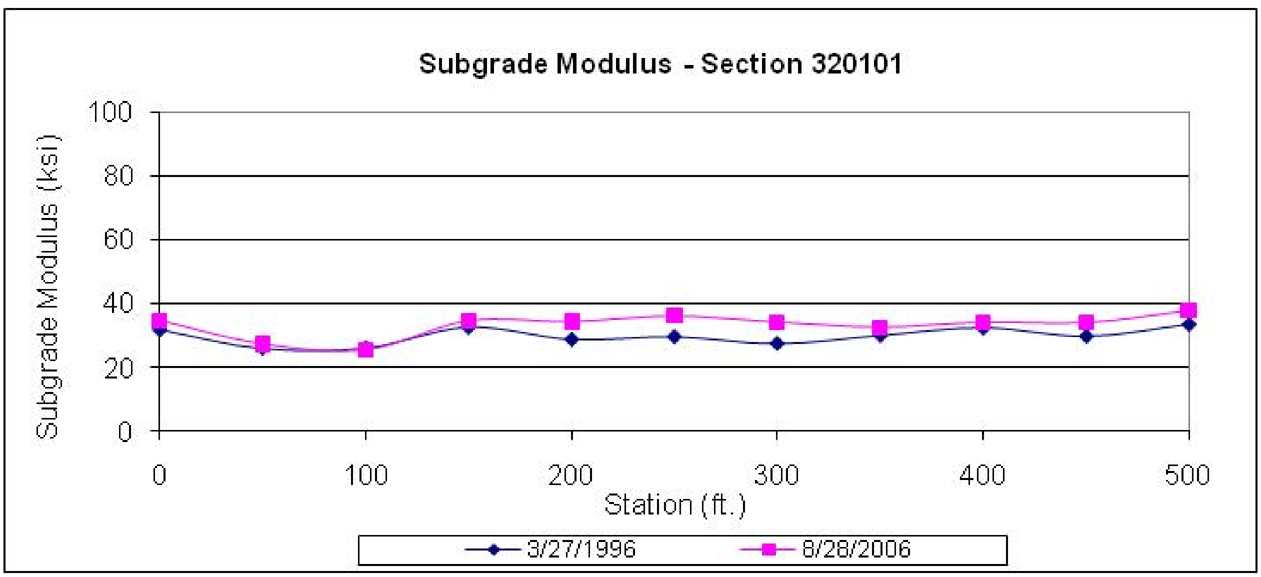

Figure 90. Graph. Subgrade modulus plot for section 320101 (Nevada).

A.2.2 Section 390106 (Nevada)

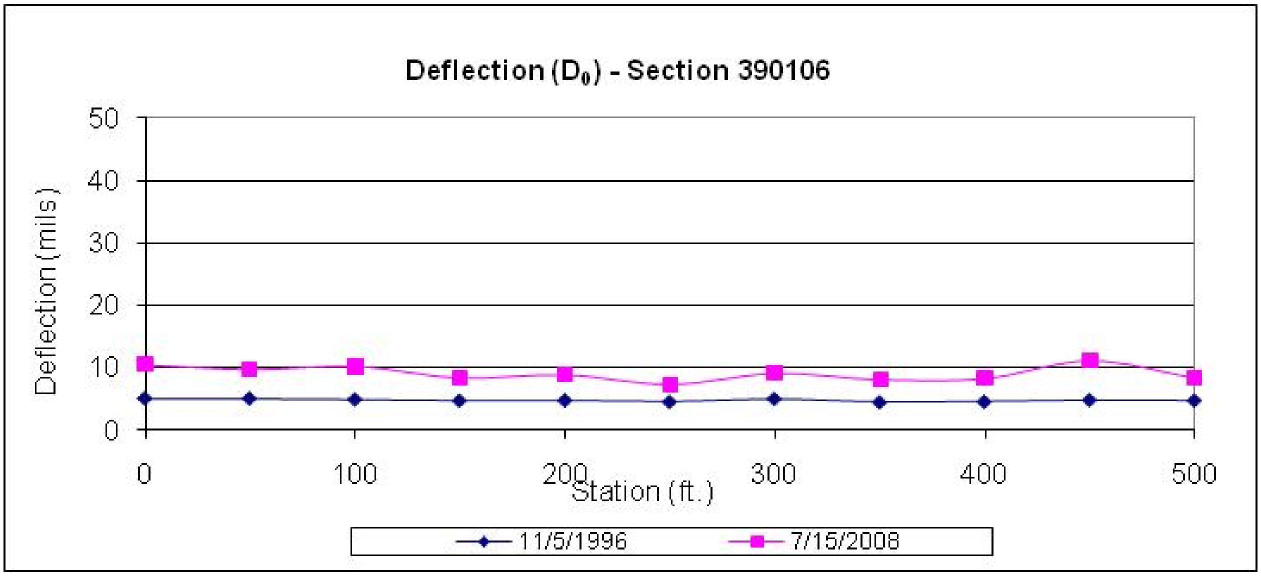

Figure 91. Graph. Deflection plot for section 390106 (Nevada).

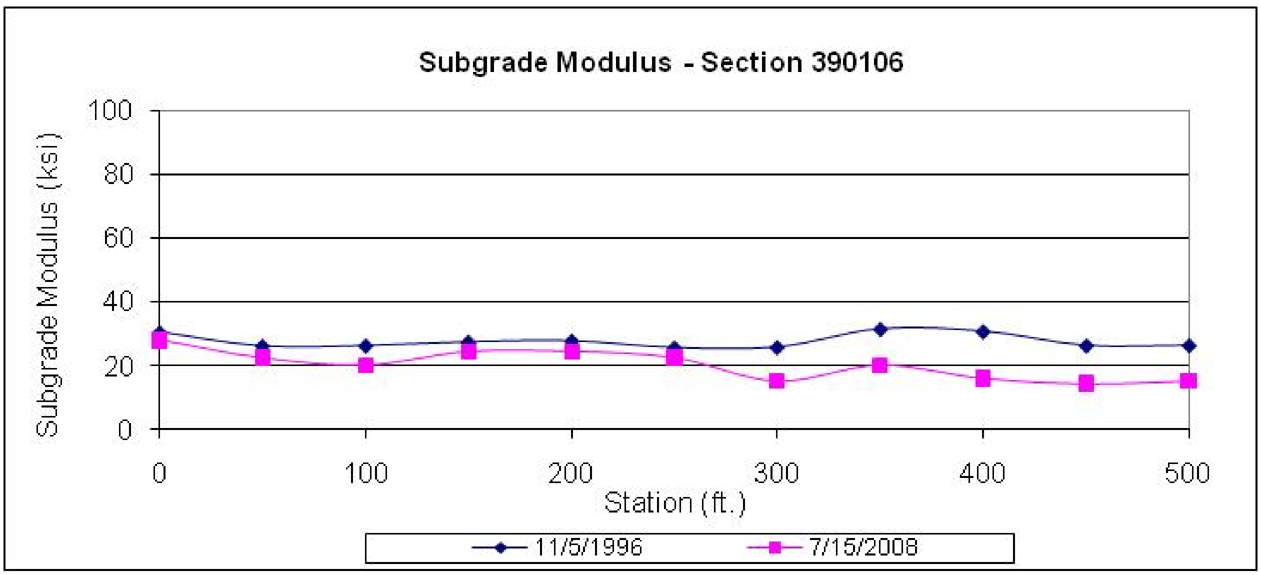

Figure 92. Graph. Subgrade modulus plot for section 390106 (Nevada).

A.3 GROUP 3 SECTIONS

A.3.1 Section 190101 (Iowa)

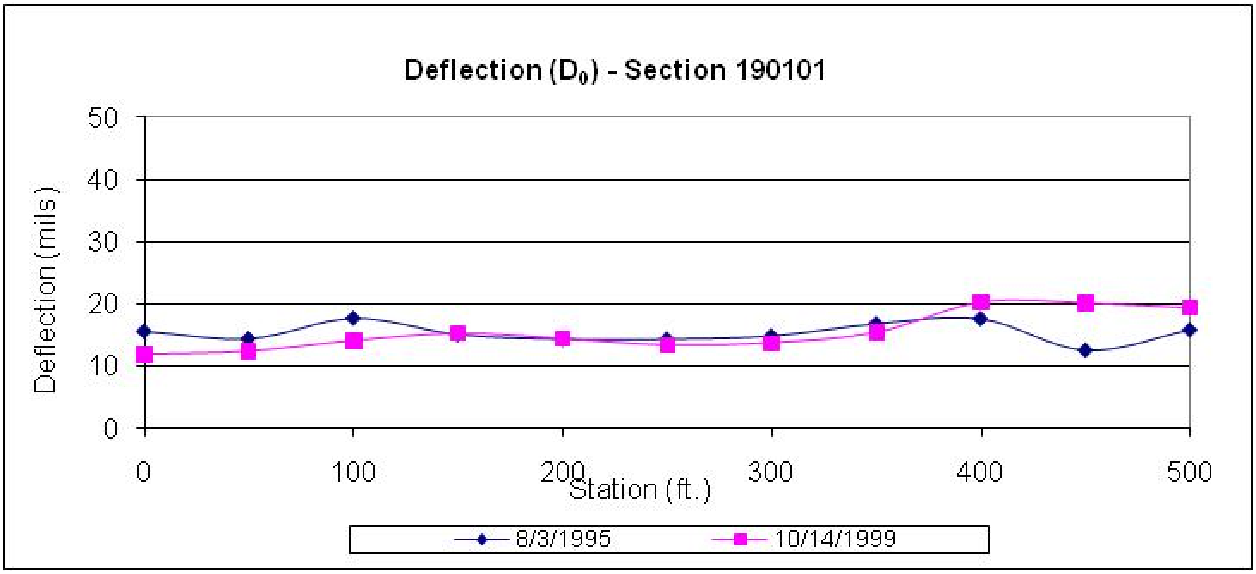

Figure 93. Graph. Deflection plot for section 190101 (Iowa).

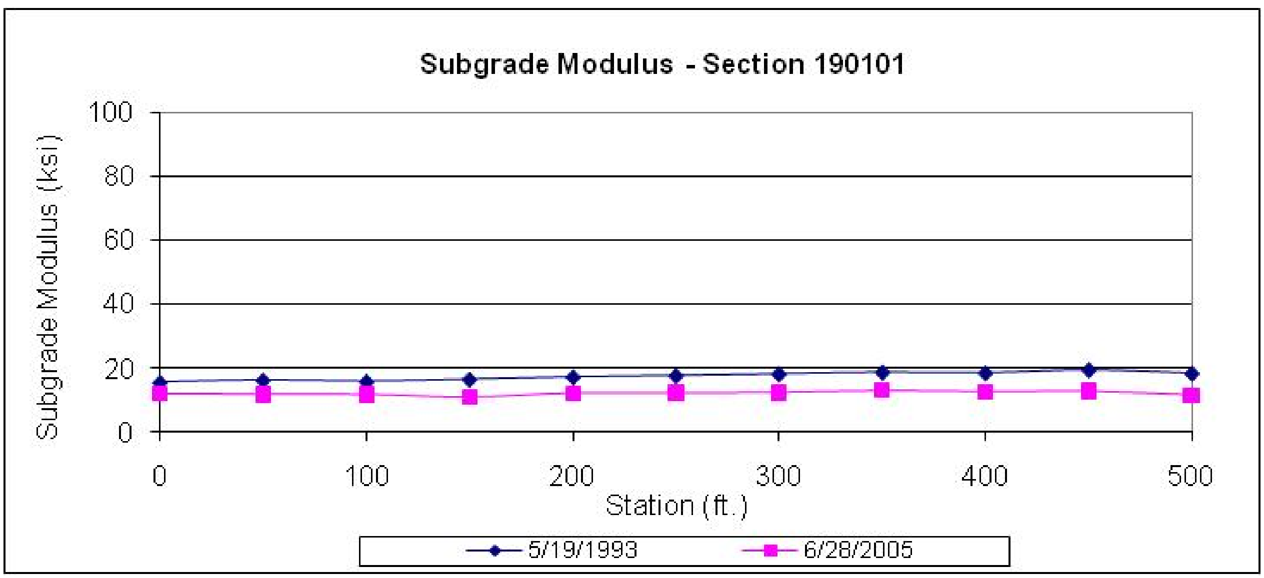

Figure 94. Graph. Subgrade modulus plot for section 190101 (Iowa).

A.3.2 Section 190103 (Iowa)

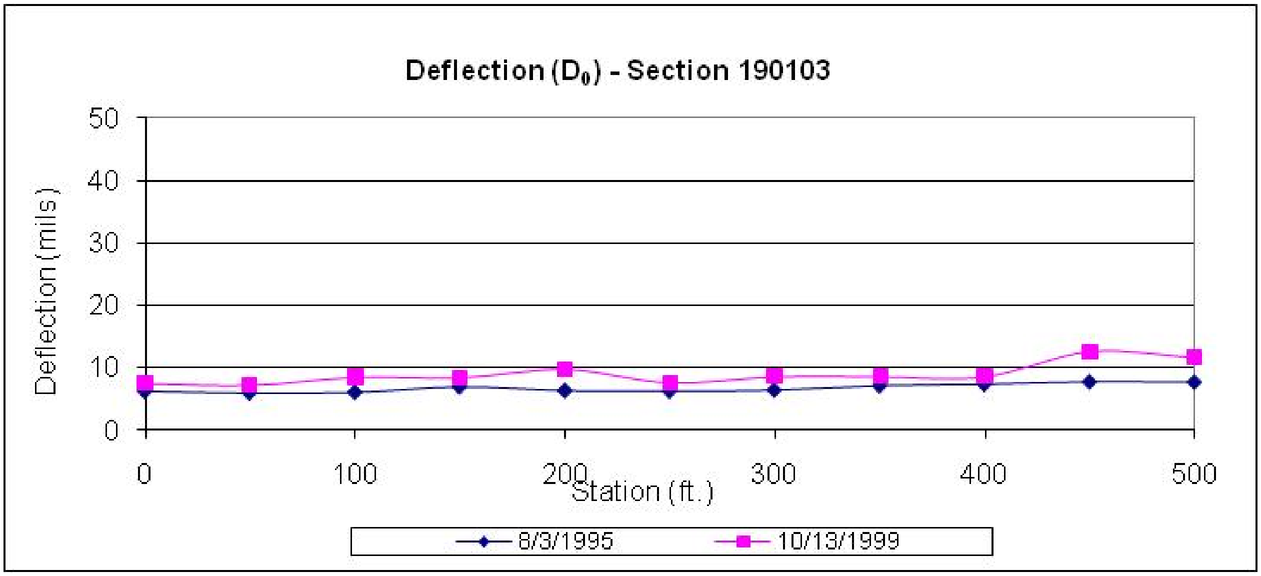

Figure 95. Graph. Deflection plot for section 190103 (Iowa).

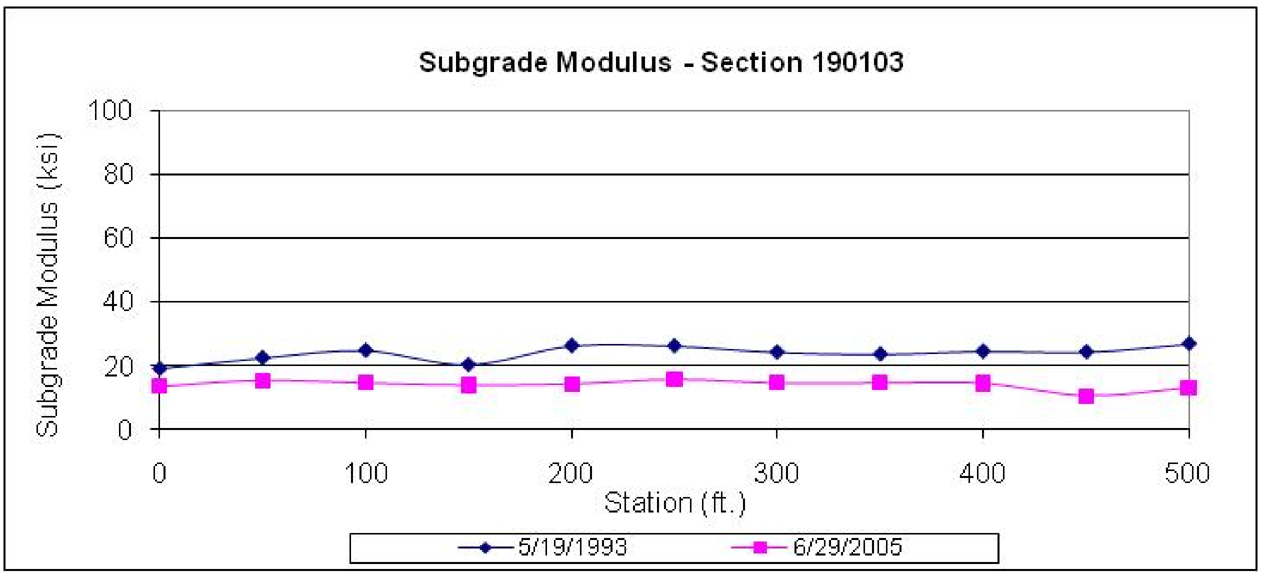

Figure 96. Graph. Subgrade modulus plot for section 190103 (Iowa).

A.3.3 Section 050114 (Arkansas)

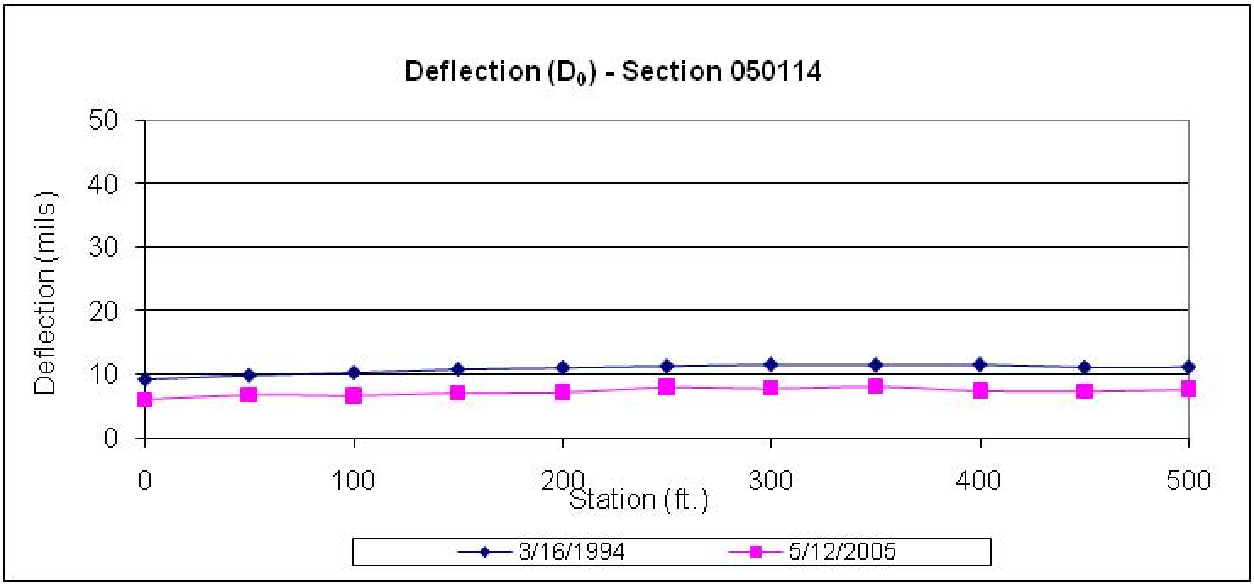

Figure 97. Graph. Deflection plot for section 050114 (Arkansas).

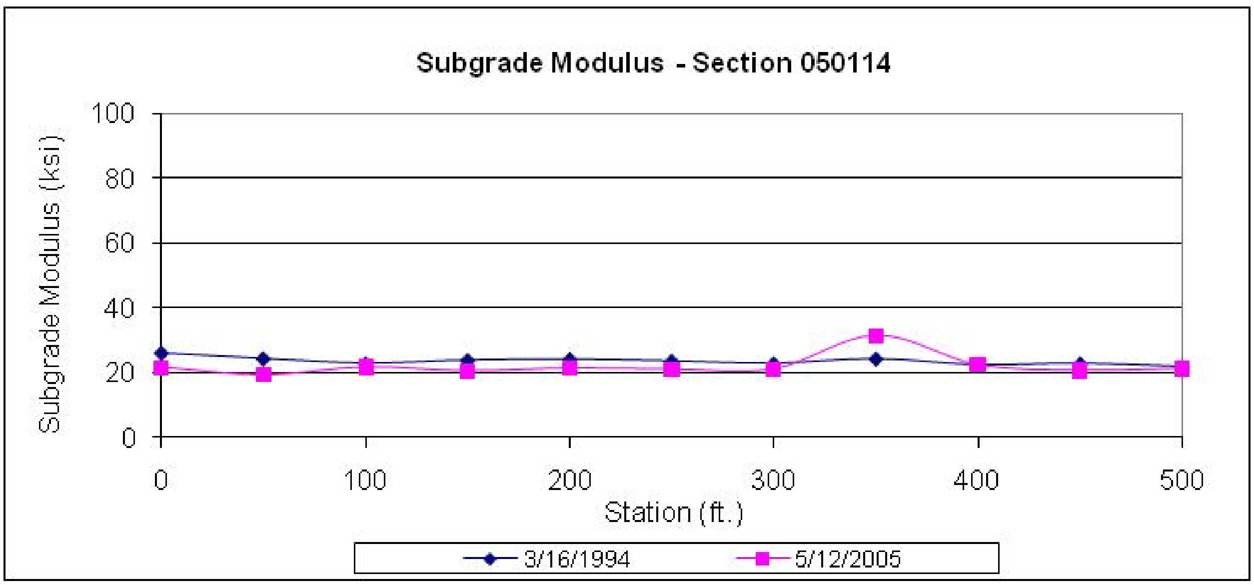

Figure 98. Graph. Subgrade modulus plot for section 050114 (Arkansas).

A.3.4 Section 050116 (Arkansas)

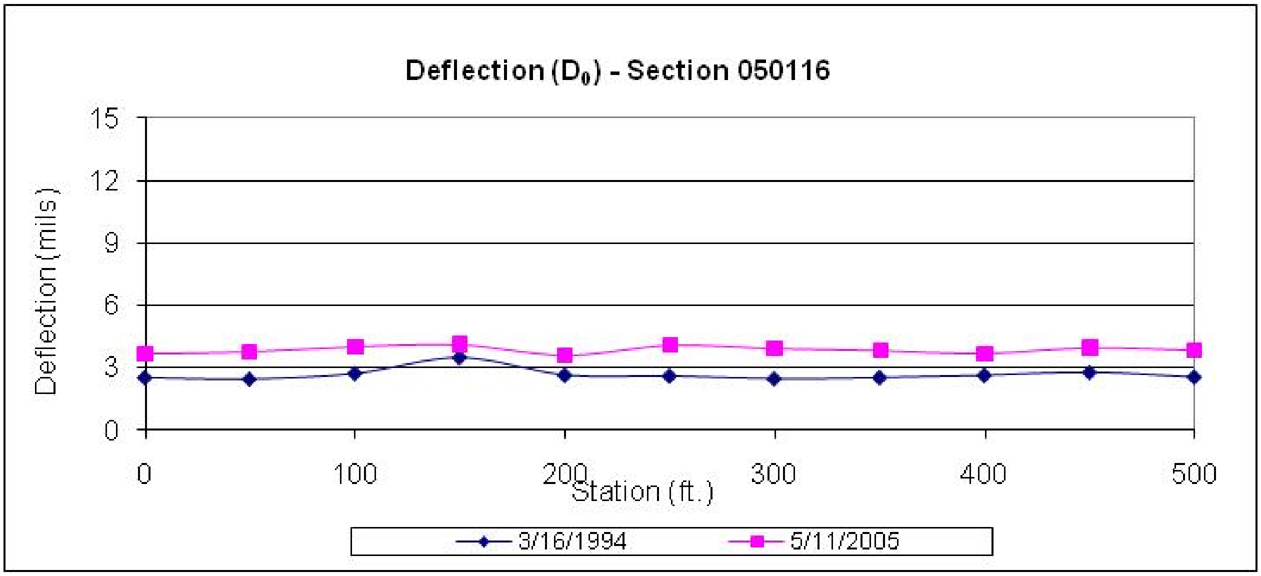

Figure 99. Graph. Deflection plot for section 050116 (Arkansas).

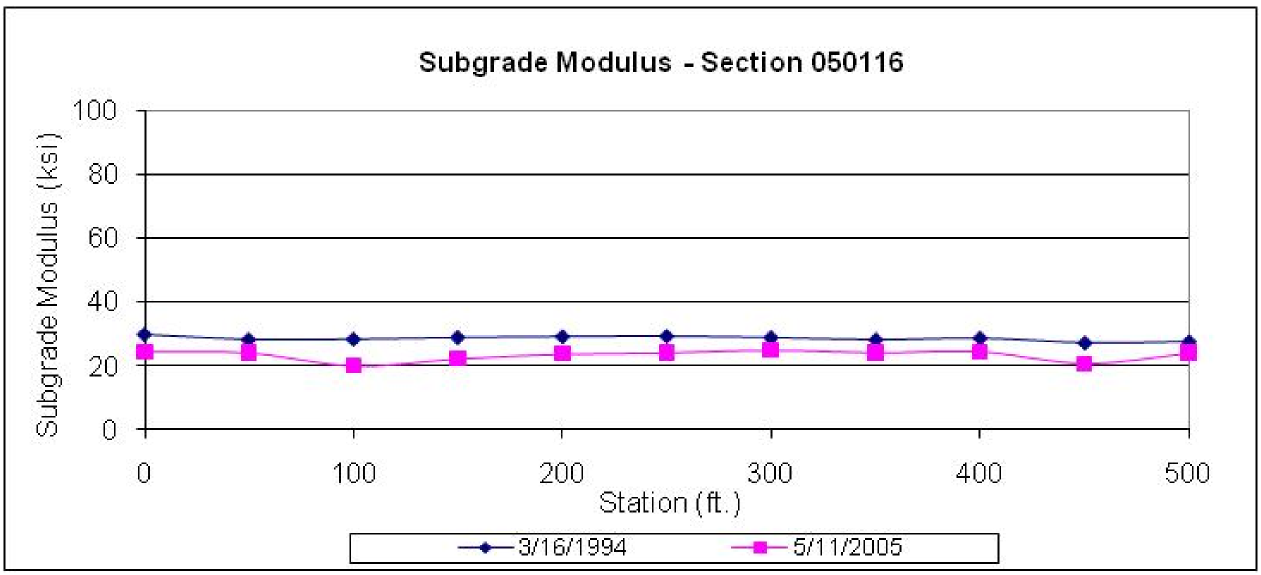

Figure 100. Graph. Subgrade modulus plot for section 050116 (Arkansas).

A.4 GROUP 4 SECTIONS

A.4.1 Section 040502 (Arizona)

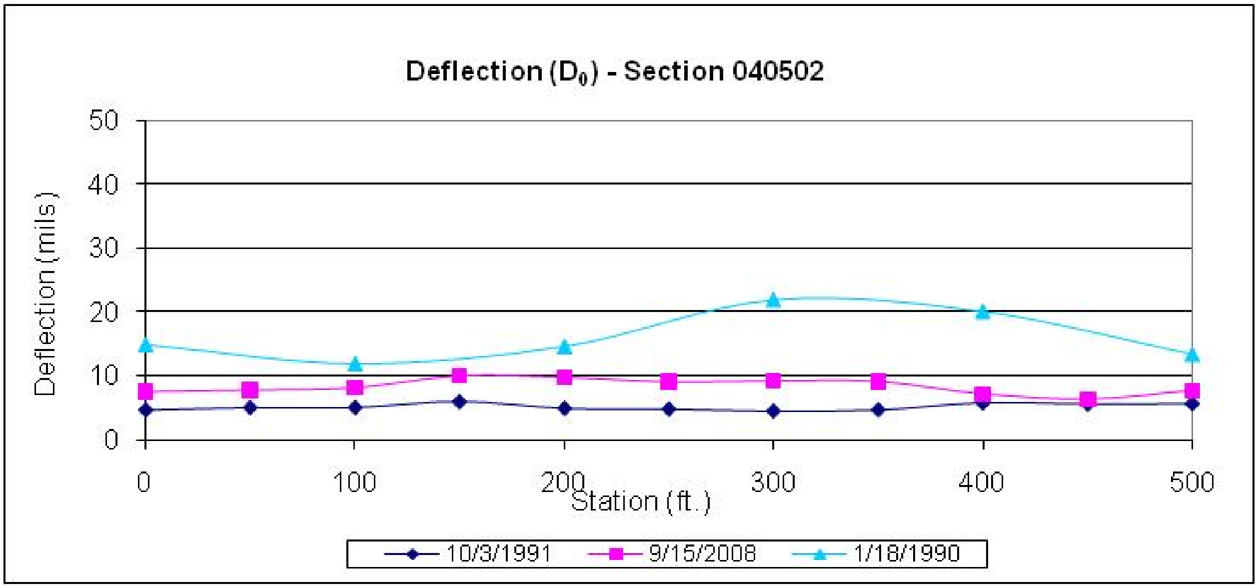

Figure 101. Graph. Deflection plot for section 040502 (Arizona).

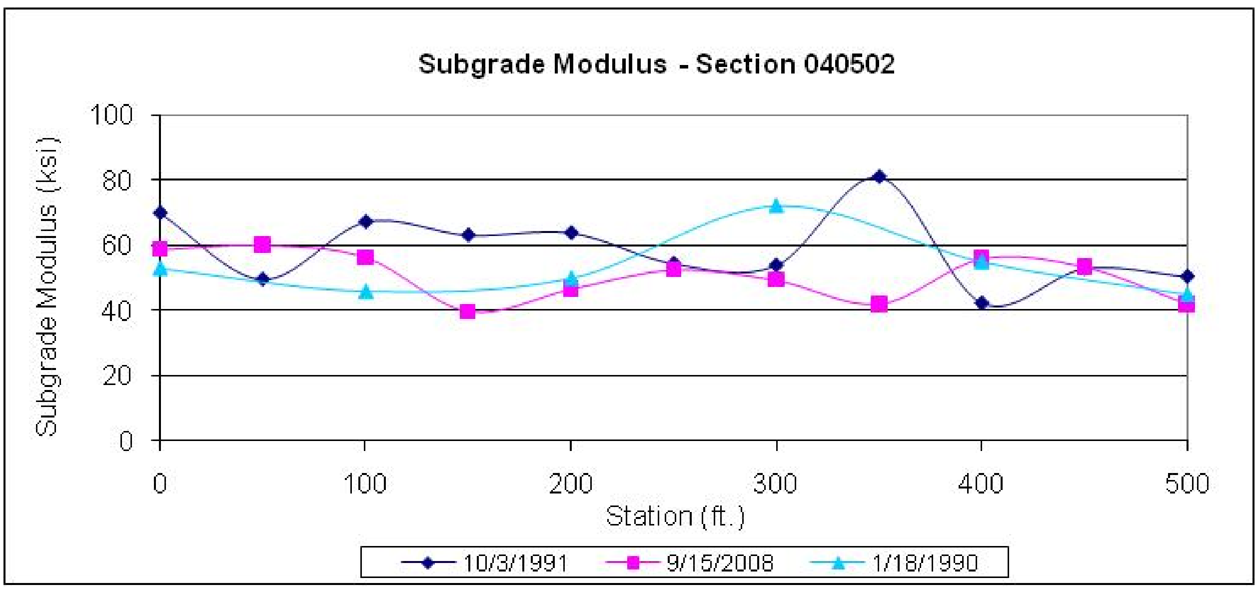

Figure 102. Graph. Subgrade modulus plot for section 040502 (Arizona).

A.4.2 Section 240505 (Maryland)

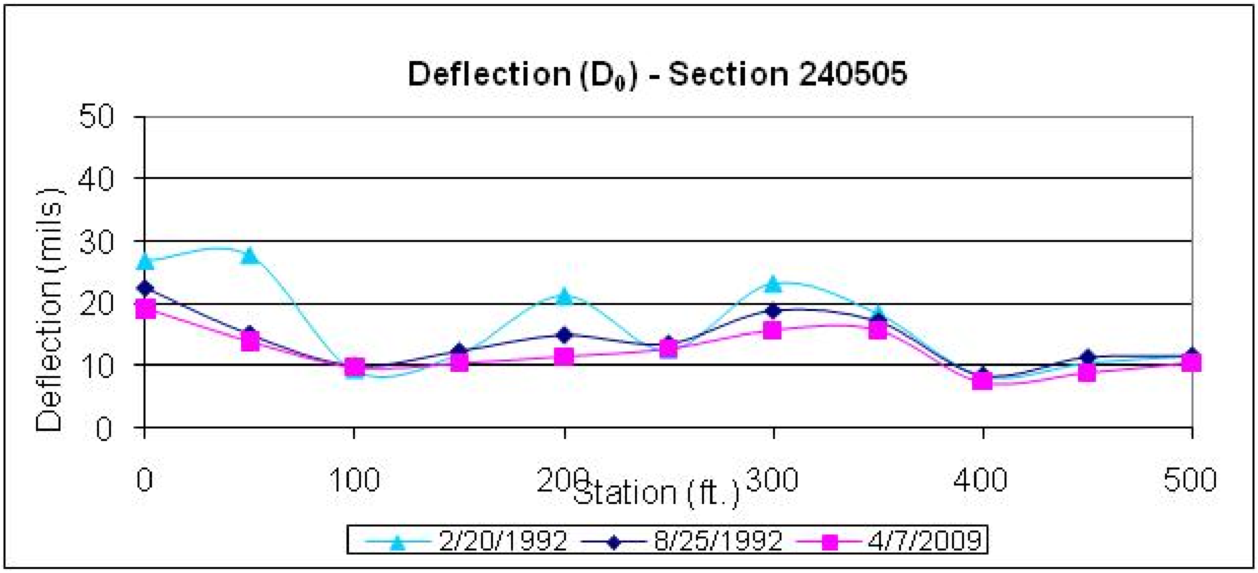

Figure 103. Graph. Deflection plot for section 240505 (Maryland).

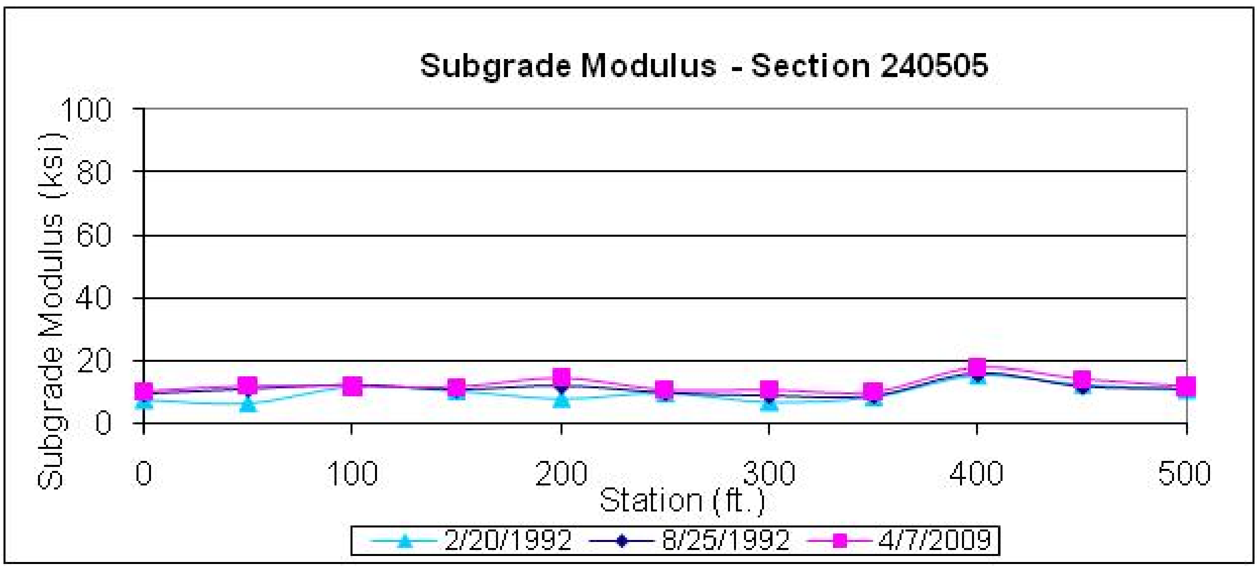

Figure 104. Graph. Subgrade modulus plot for section 240505 (Maryland).

A.4.3 Section 270509 (Minnesota)

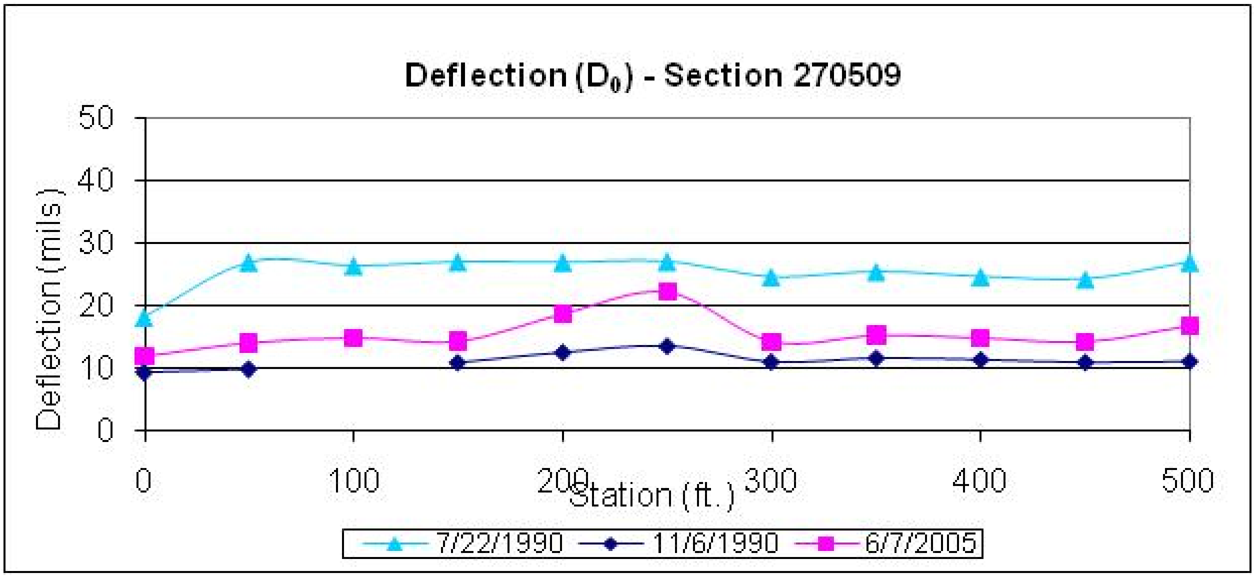

Figure 105. Graph. Deflection plot for section 270509 (Minnesota).

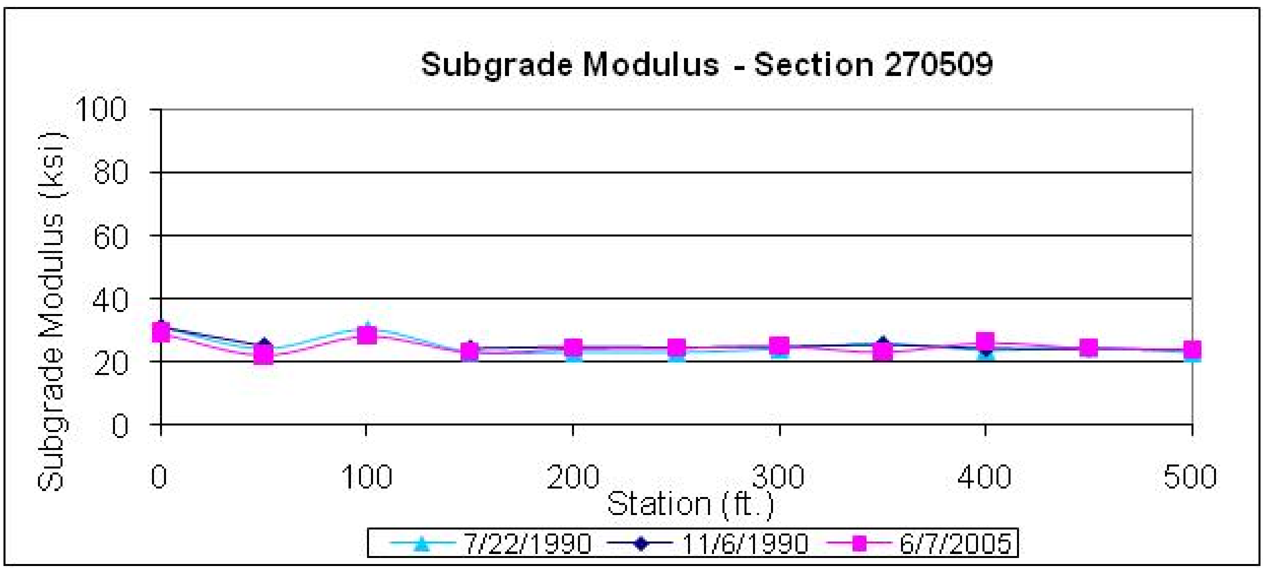

Figure 106. Graph. Subgrade modulus plot for section 270509 (Minnesota).

APPENDIX B. DEFLECTION BELOW LOAD AND AT 60 INCHES FOR A 9,000-LB LOAD

B.1 GROUP 5 SECTIONS

B.1.1 Section 040213 (Arizona)

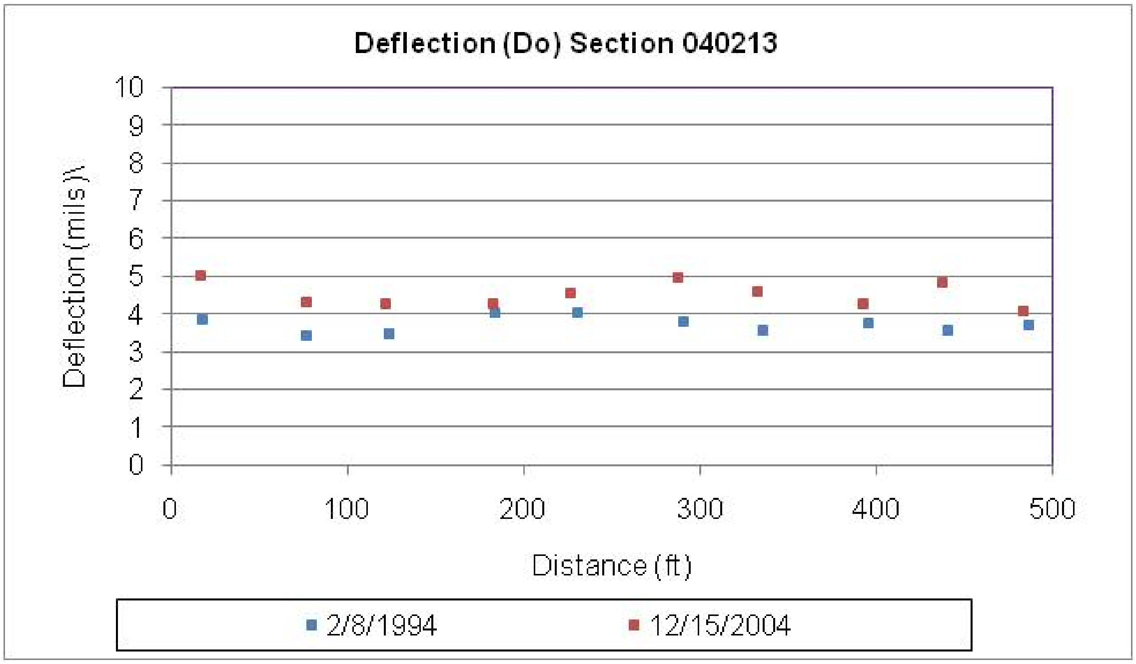

Figure 107. Graph. Deflection at 0 inches for a 9,000-lb load, section 040213 (Arizona).

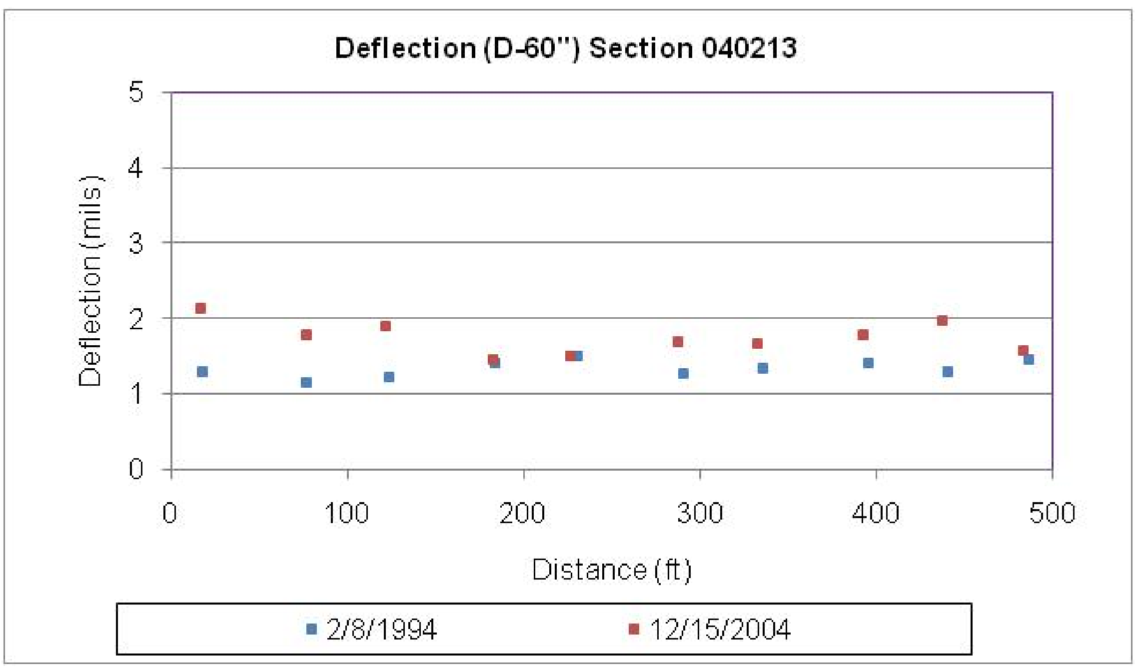

Figure 108. Graph. Deflection at 60 inches for a 9,000-lb load, section 040213 (Arizona).

B.1.2 Section 050217 (Arkansas)

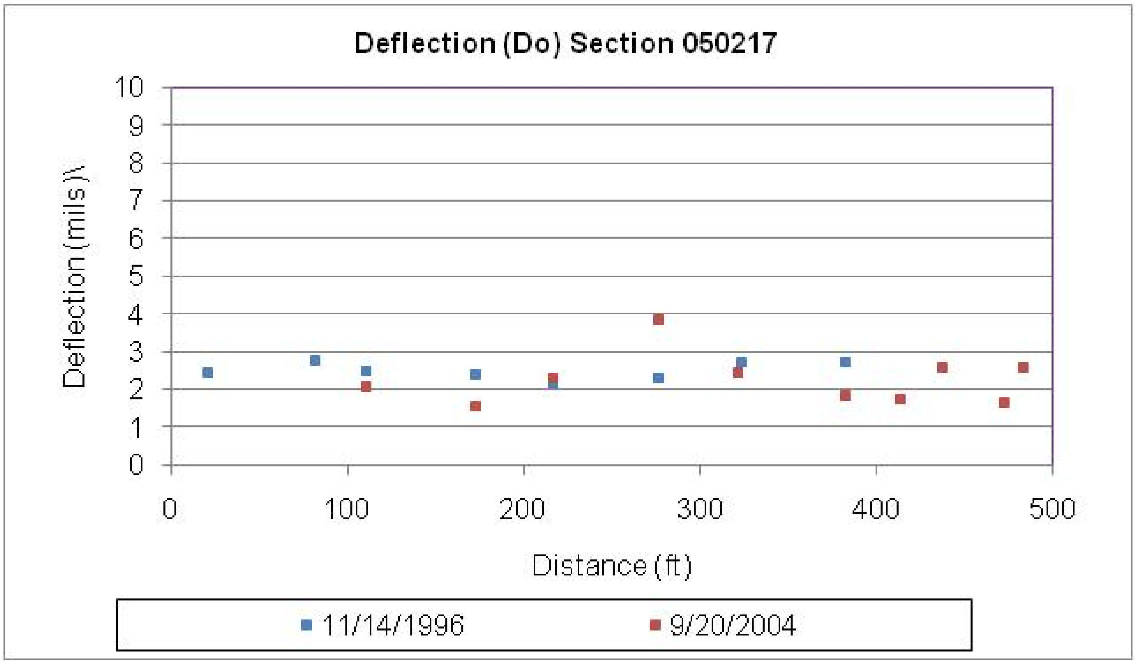

Figure 109. Graph. Deflection at 0 inches for a 9,000-lb load, section 050217 (Arkansas).

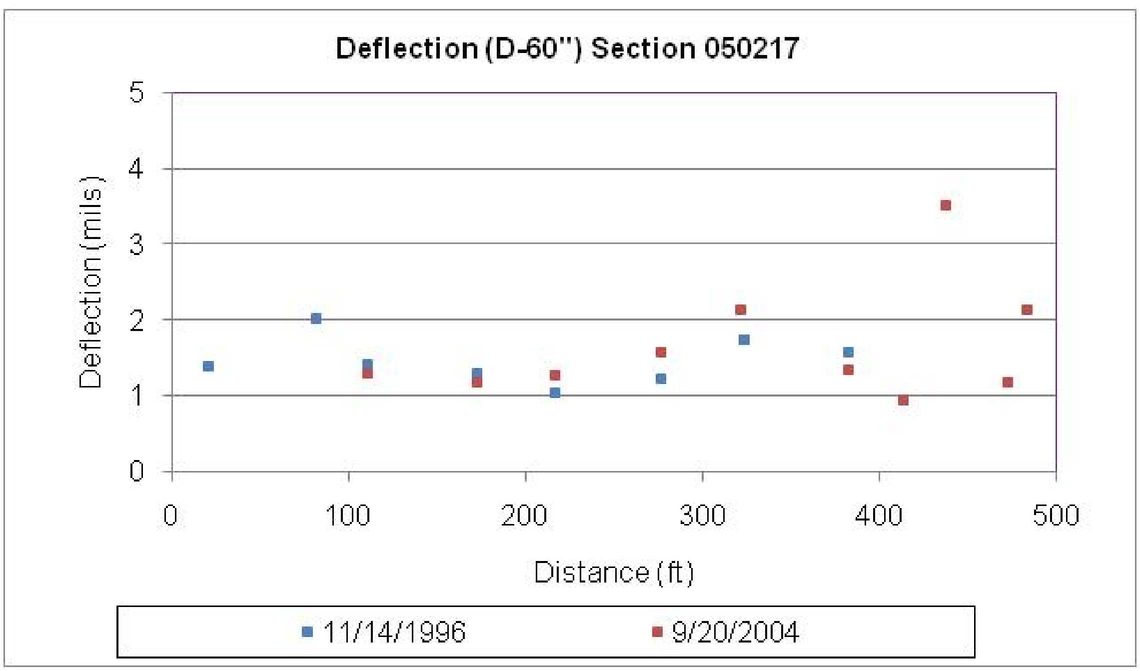

Figure 110. Graph. Deflection at 60 inches for a 9,000-lb load, section 050217 (Arkansas).

B.1.3 Section 390205 (Ohio)

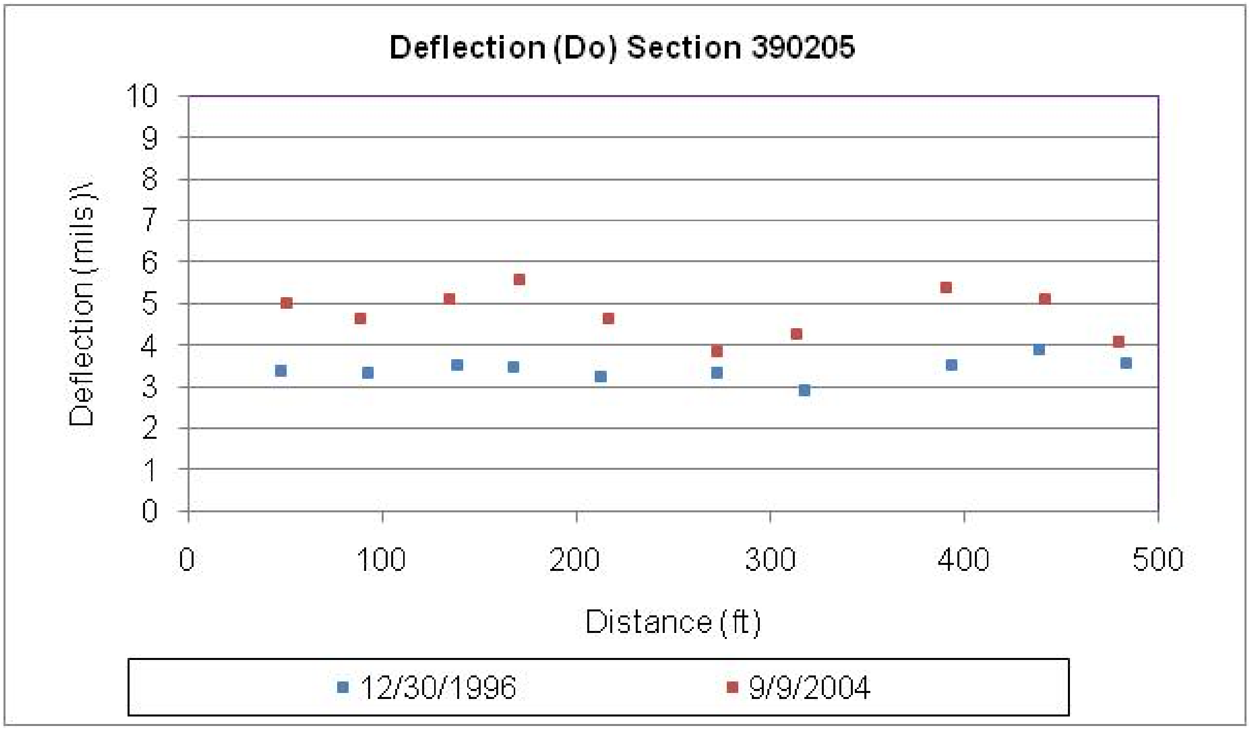

Figure 111. Graph. Deflection at 0 inches for a 9,000-lb load, section 390205 (Ohio).

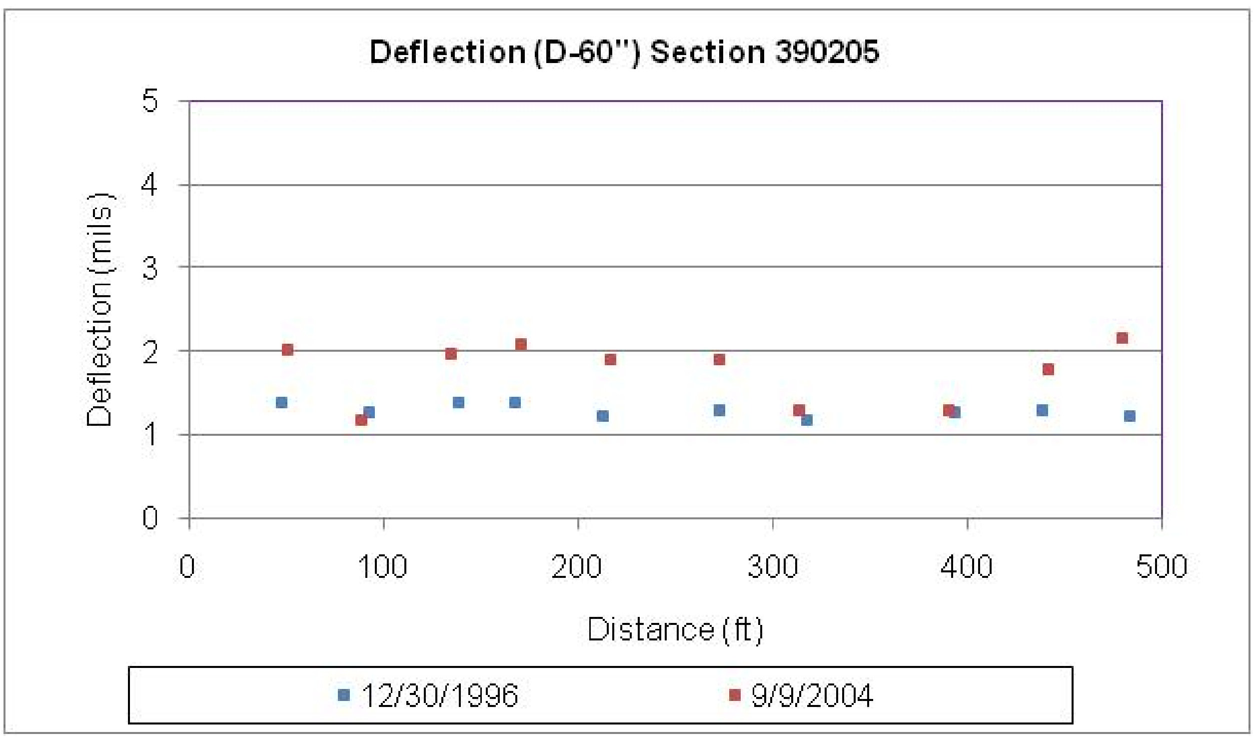

Figure 112. Graph. Deflection at 60 inches for a 9,000-lb load, section 390205 (Ohio).

APPENDIX C. TIME SEQUENCE IRI PLOTS

C.1 GROUP 1 SECTIONS

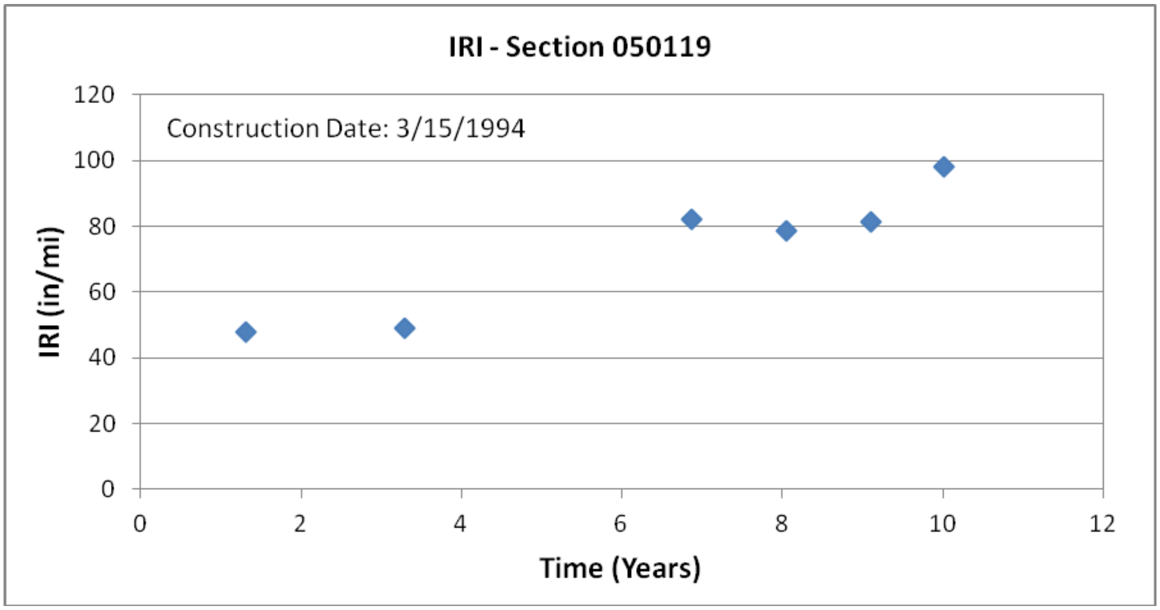

Figure 113. Graph. Time sequence IRI values, section 050119 (Arkansas).

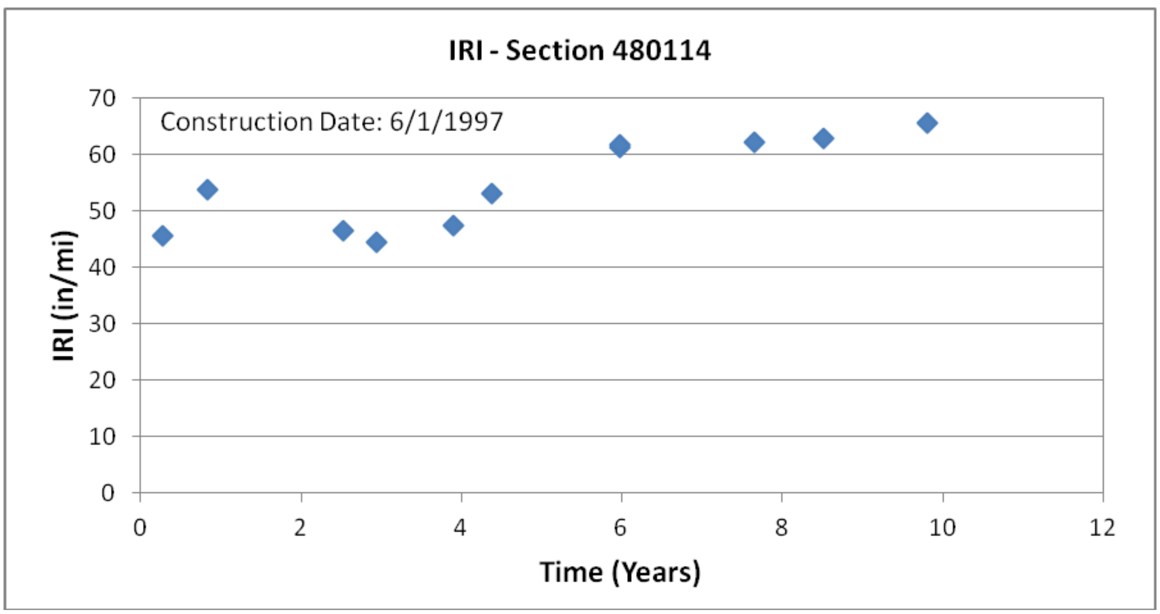

Figure 114. Graph. Time sequence IRI values, section 480114 (Texas).

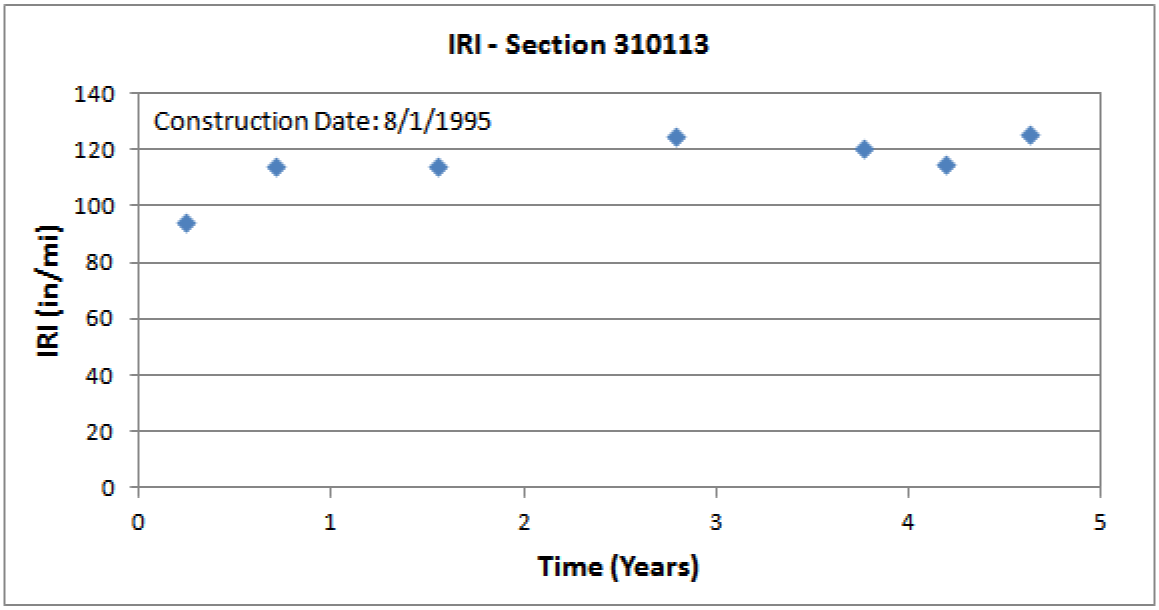

Figure 115. Graph. Time sequence IRI values, section 310113 (Nebraska).

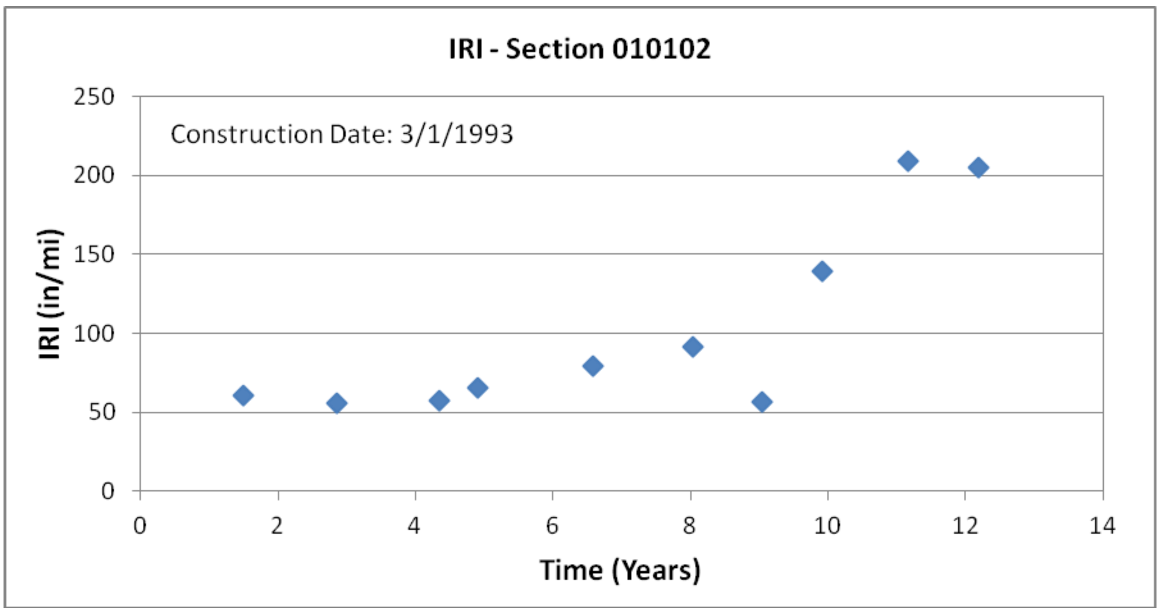

Figure 116. Graph. Time sequence IRI values, section 010102 (Alabama).

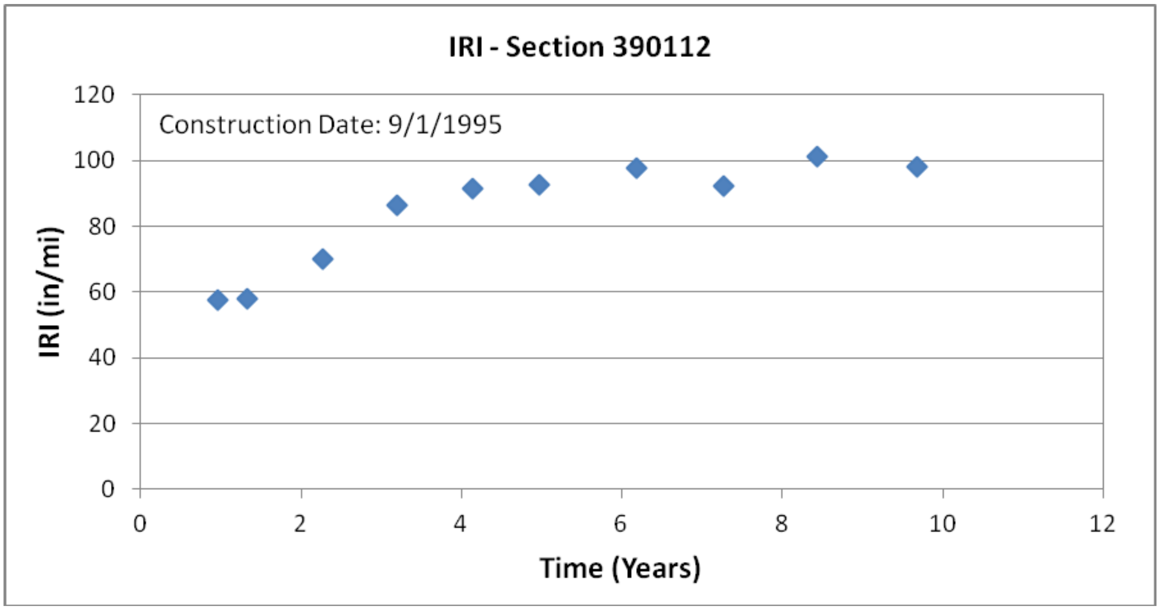

Figure 117. Graph. Time sequence IRI values, section 390112 (Ohio).

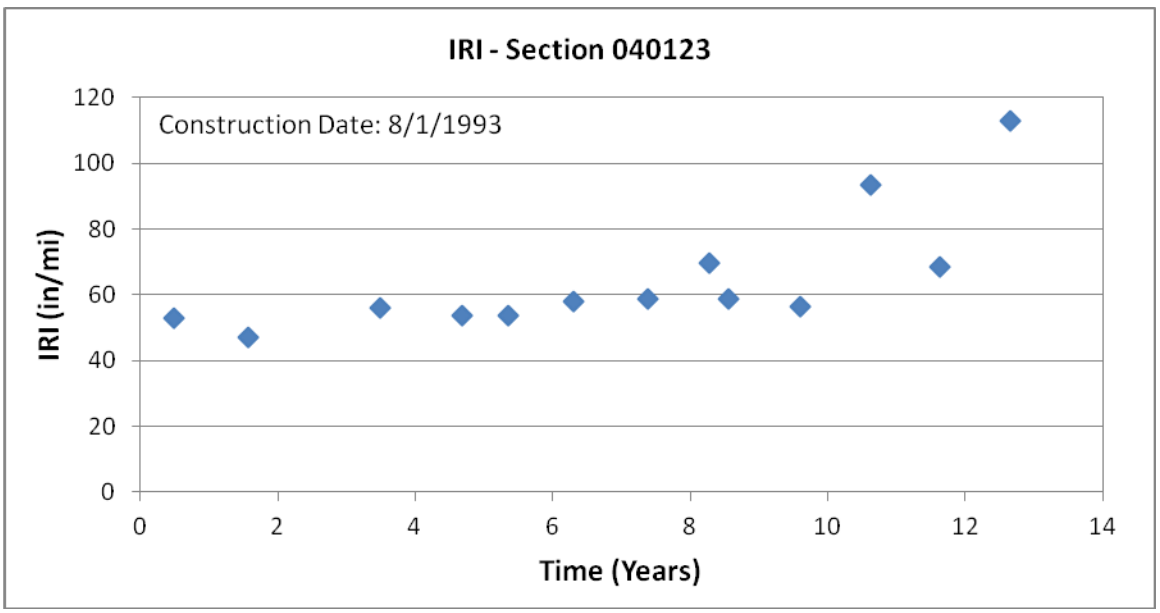

Figure 118. Graph. Time sequence IRI values, section 040123 (Arizona).

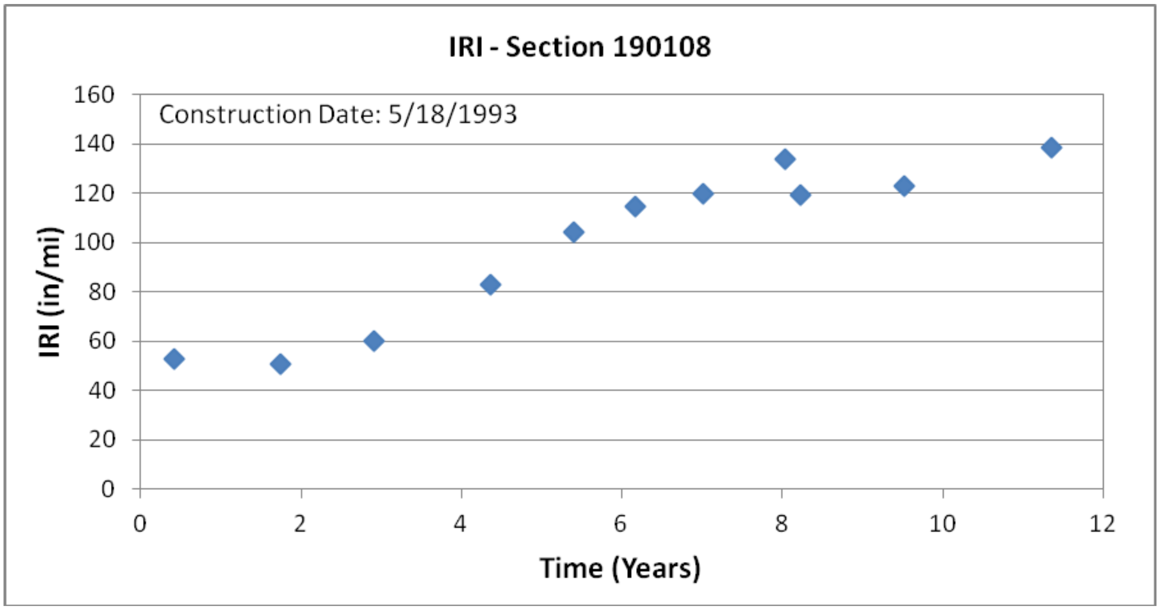

Figure 119. Graph. Time sequence IRI values, section 190108 (Iowa).

C.2 GROUP 2 SECTIONS

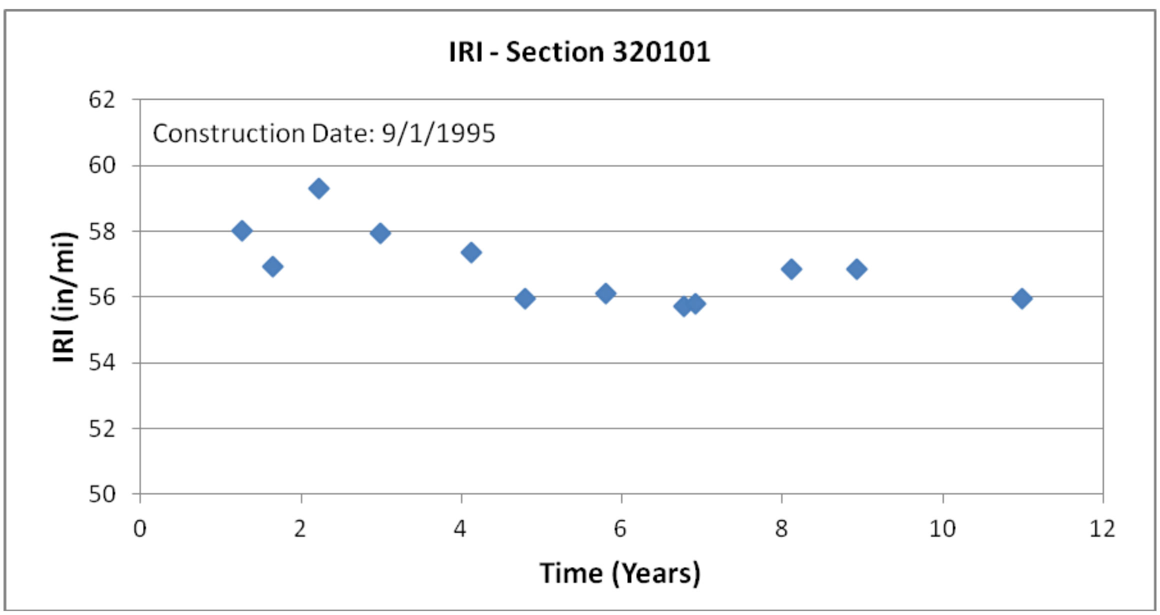

Figure 120. Graph. Time sequence IRI values, section 320101 (Nevada).

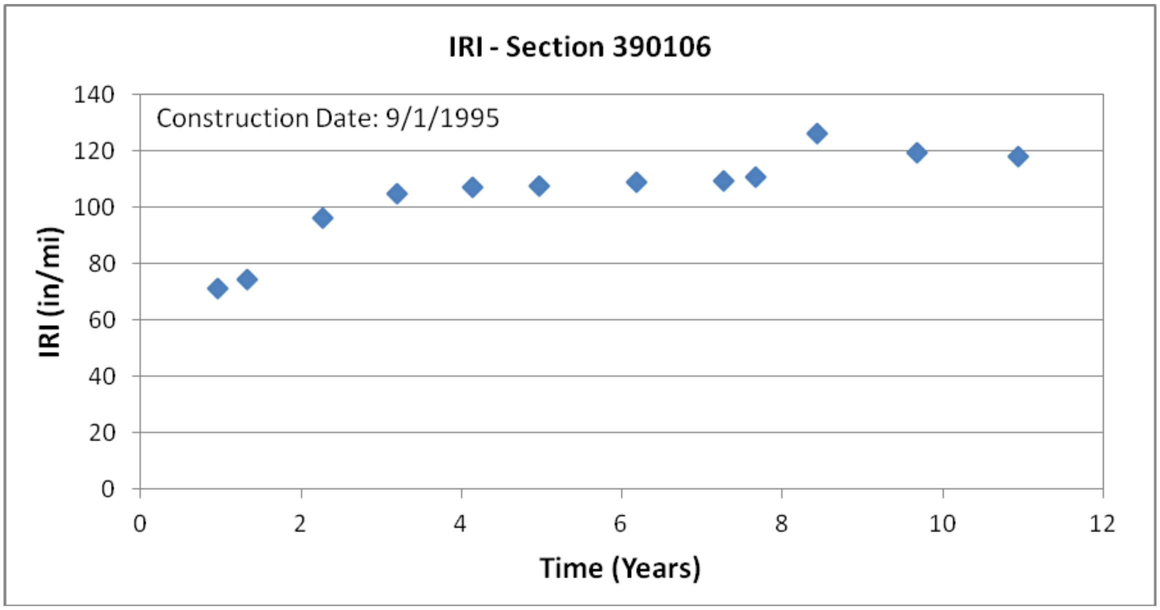

Figure 121. Graph. Time sequence IRI values, section 390106 (Ohio).

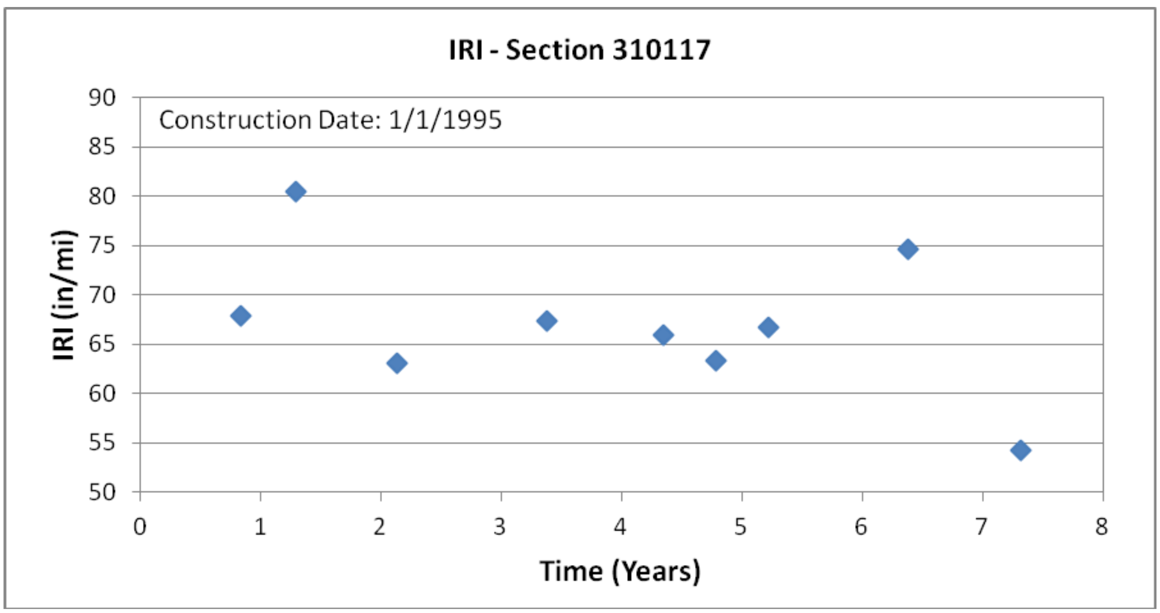

Figure 122. Graph. Time sequence IRI values, section 310117 (Nebraska).

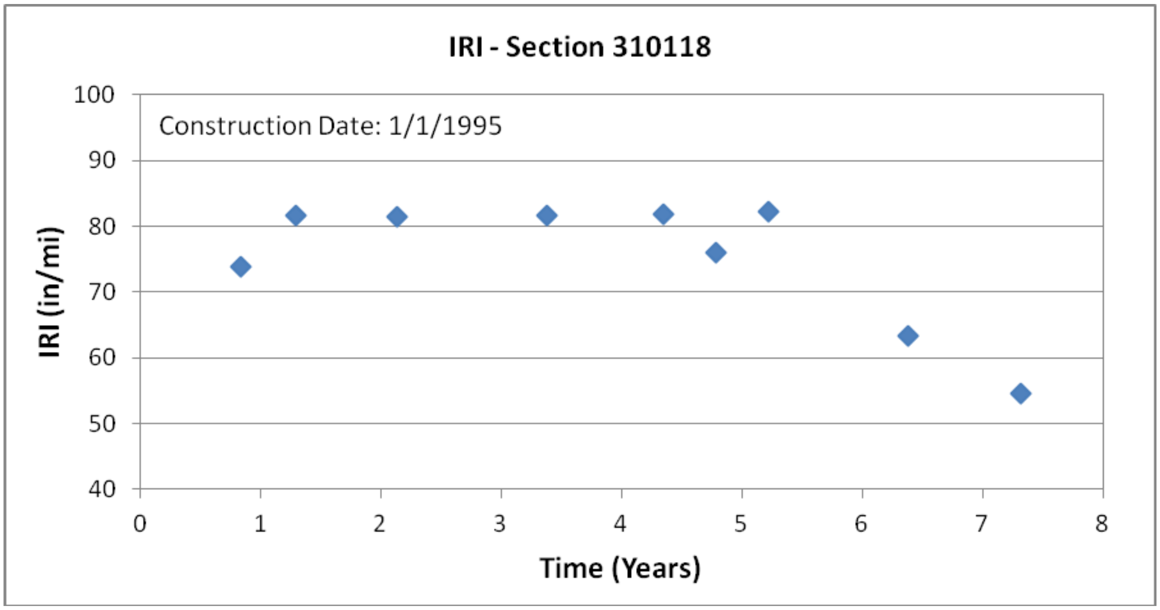

Figure 123. Graph. Time sequence IRI values, section 310118 (Nebraska).

C.3 GROUP 3 SECTIONS

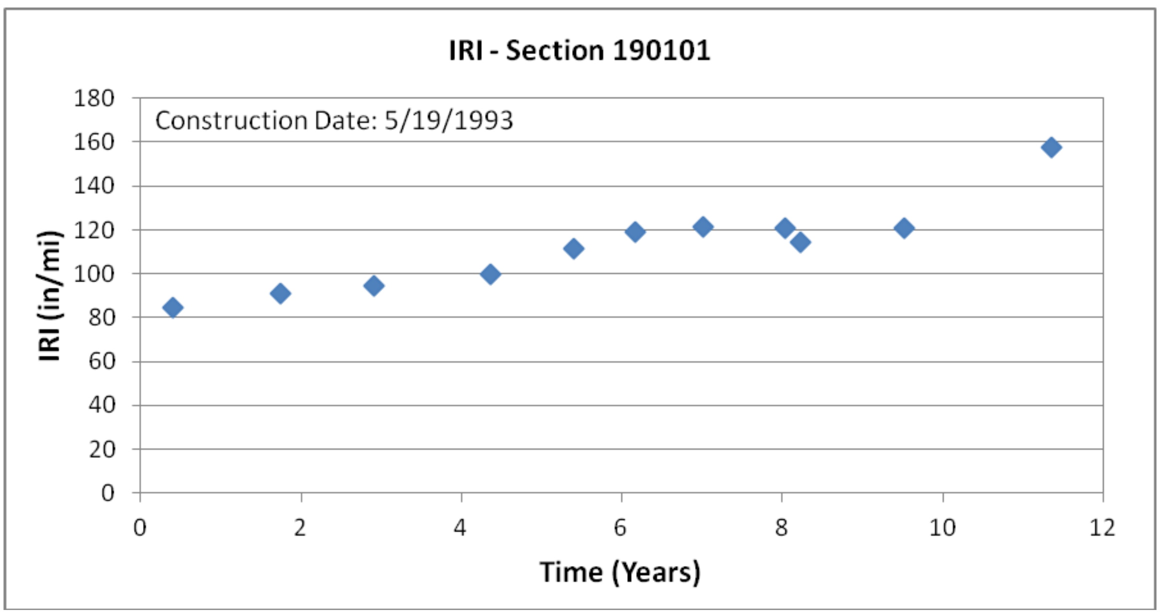

Figure 124. Graph. Time sequence IRI values, section 190101 (Iowa).

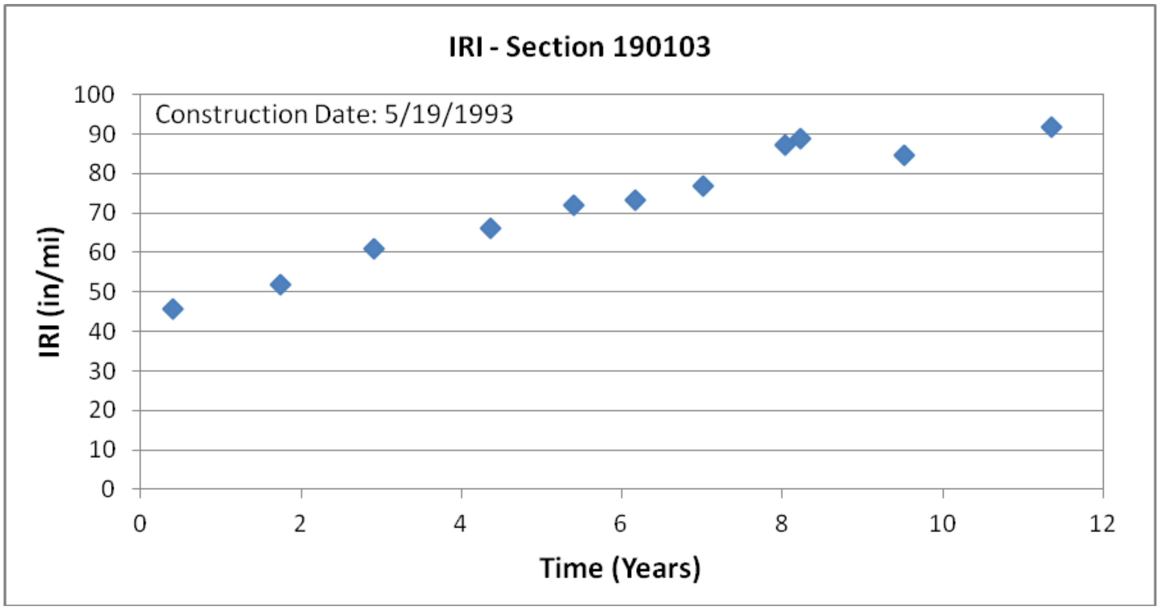

Figure 125. Graph. Time sequence IRI values, section 190103 (Iowa).

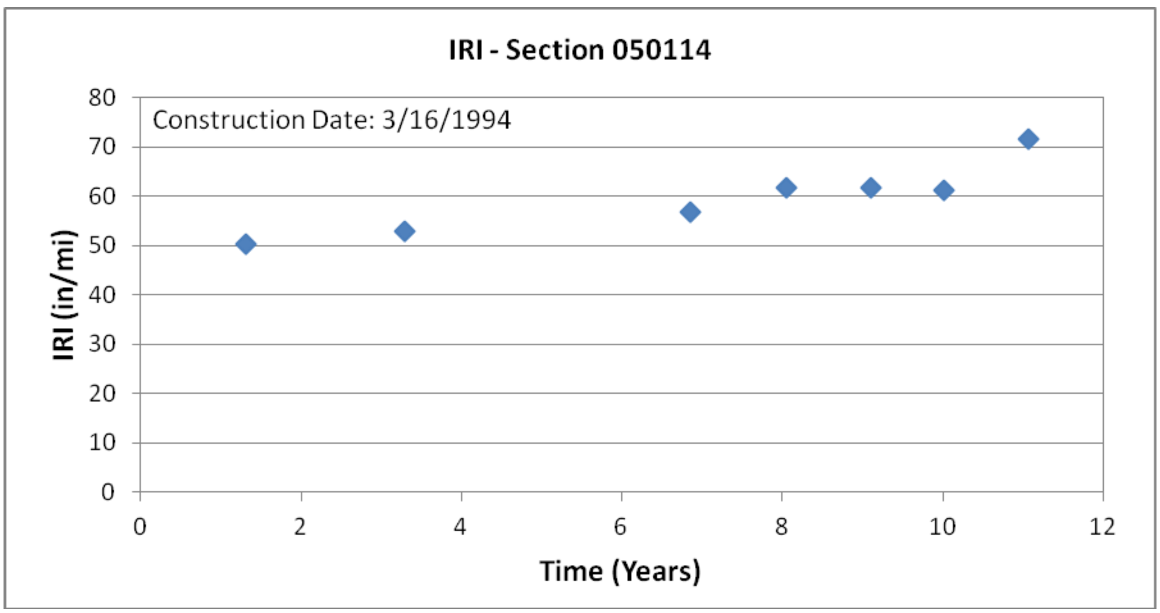

Figure 126. Graph. Time sequence IRI values, section 050114 (Arkansas).

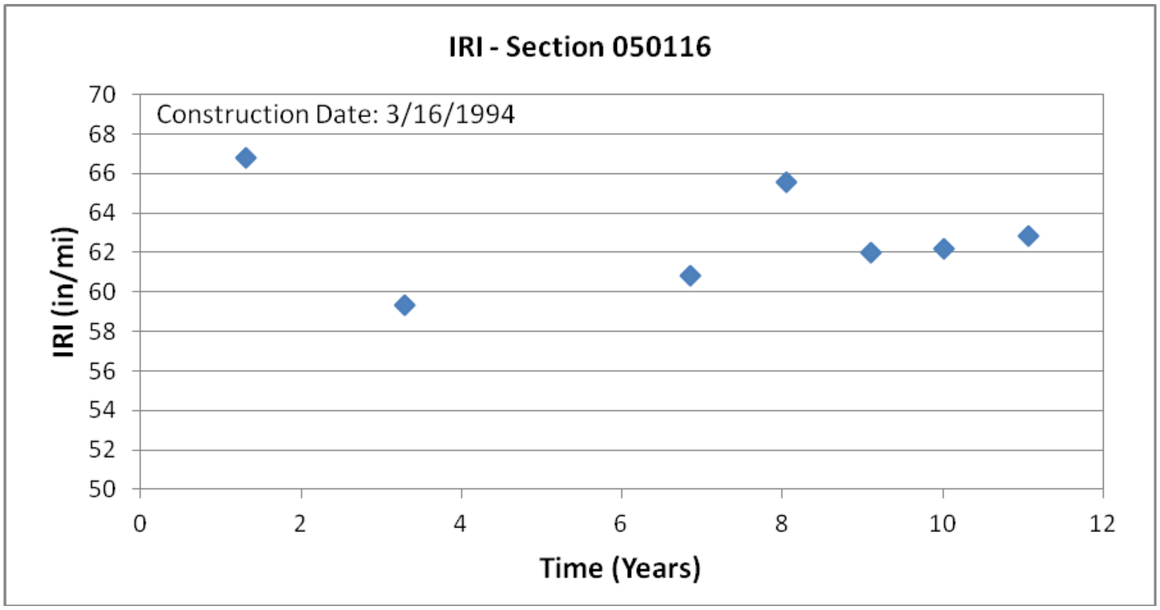

Figure 127. Graph. Time sequence IRI values, section 050116 (Arkansas).

C.4 GROUP 4 SECTIONS

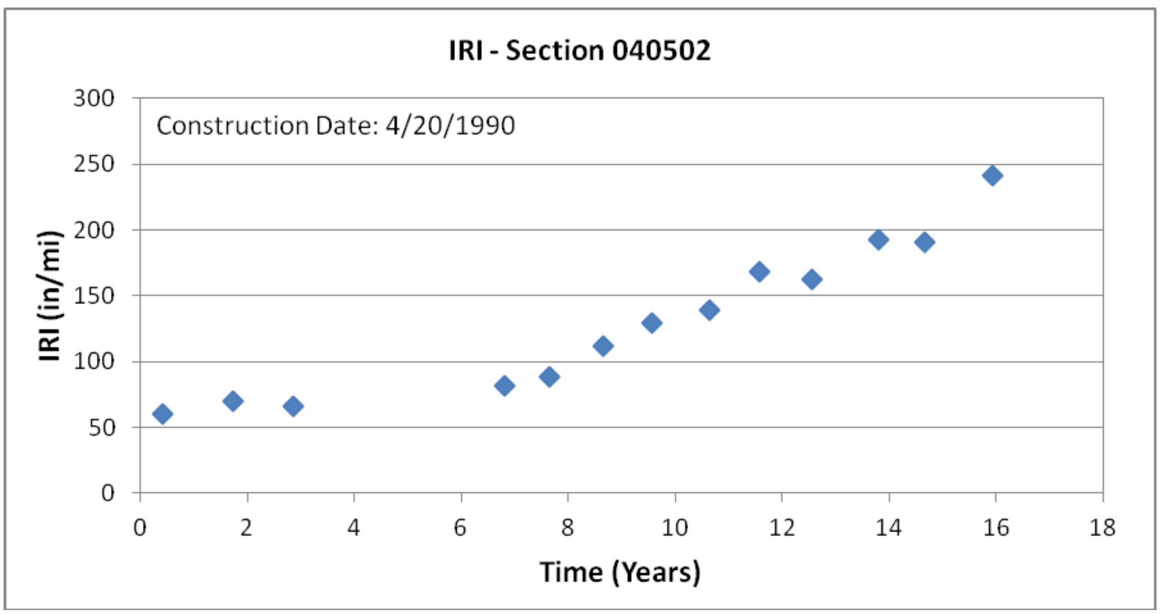

Figure 128. Graph. Time sequence IRI values, section 040502 (Arizona).

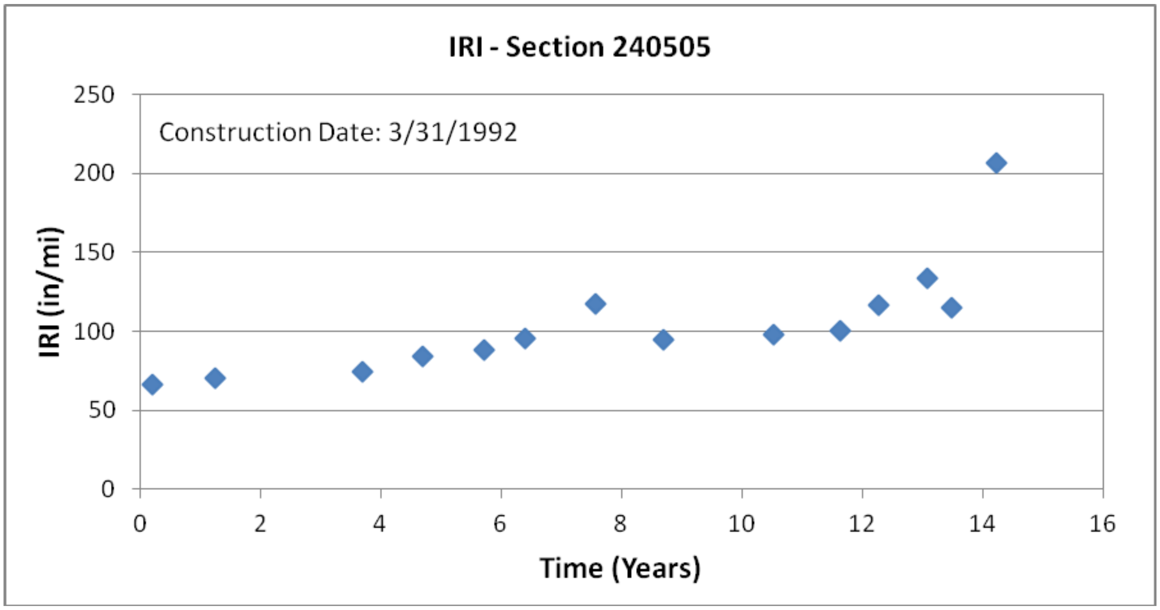

Figure 129. Graph. Time sequence IRI values, section 240505 (Maryland).

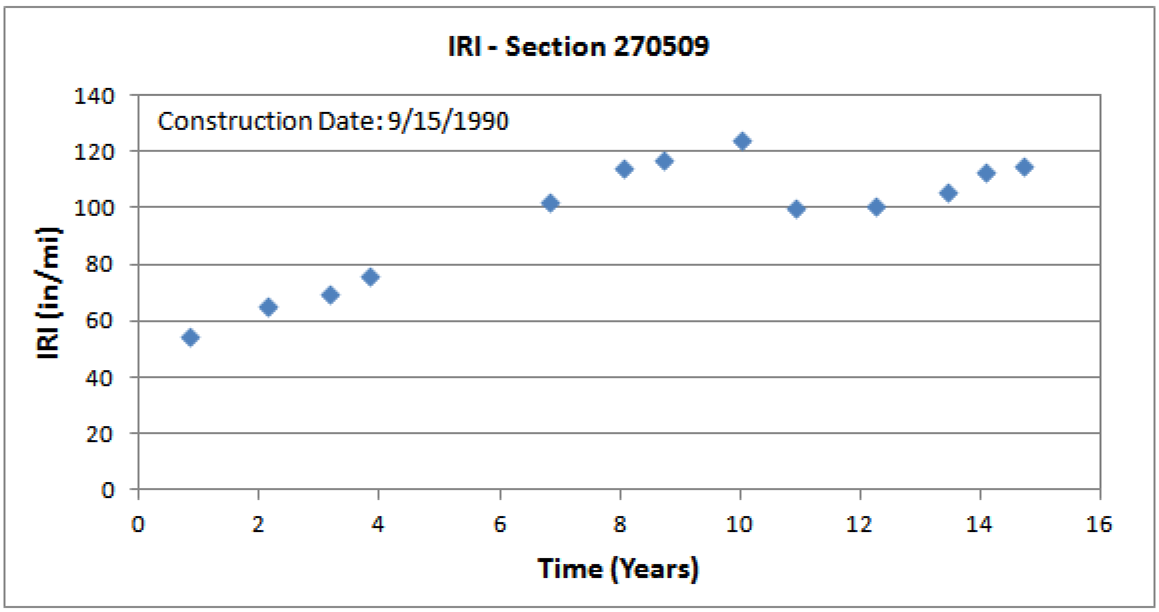

Figure 130. Graph. Time sequence IRI values, section 270509 (Minnesota).

C.5 GROUP 5 SECTIONS

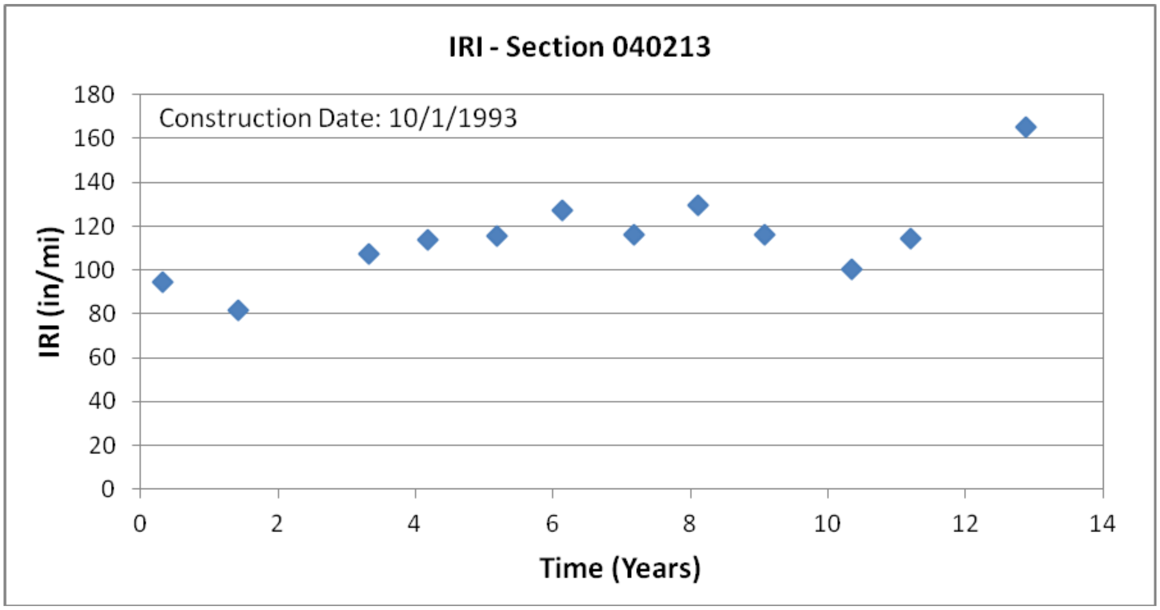

Figure 131. Graph. Time sequence IRI values, section 040213 (Arizona).

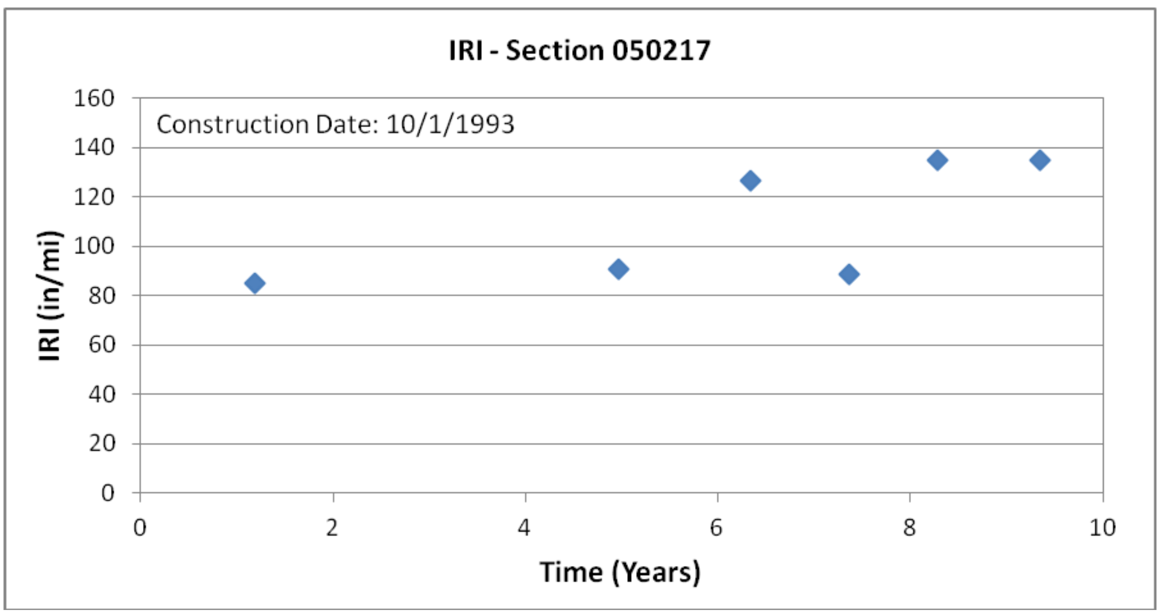

Figure 132. Graph. Time sequence IRI values, section 050217 (Arkansas).

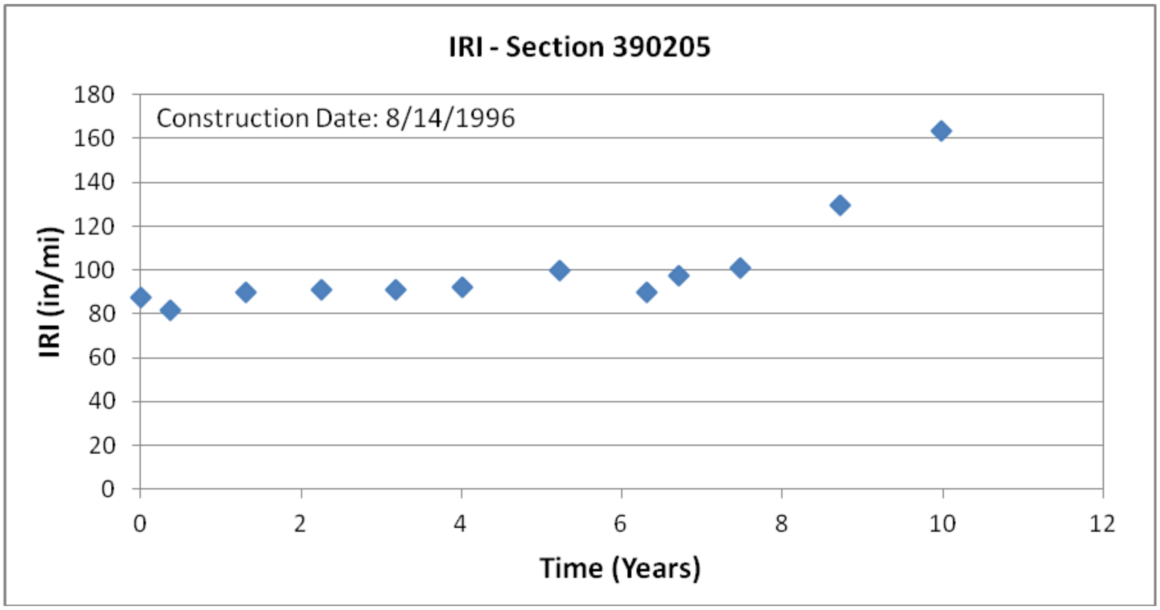

Figure 133. Graph. Time sequence IRI values, section 390205 (Ohio).

APPENDIX D. AVERAGE NORMALIZED DEFLECTION AND MID-DEPTH SURFACE LAYER TEMPERATURE PLOTS

D.1 GROUP 1 SECTIONS

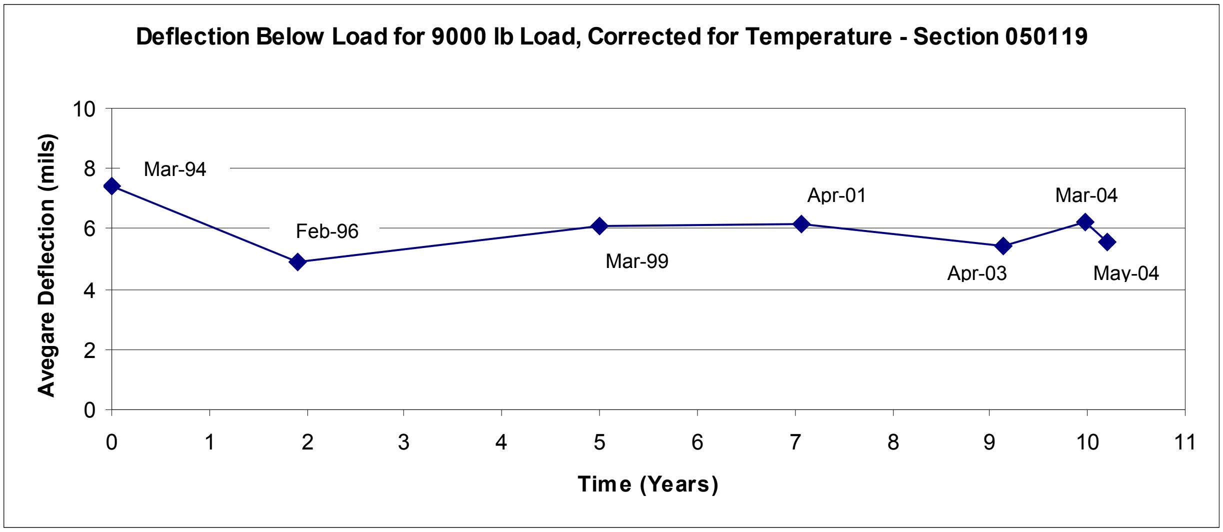

Figure 134. Graph. Average normalized deflection below 9,000-lb load, section 050119 (Arkansas).

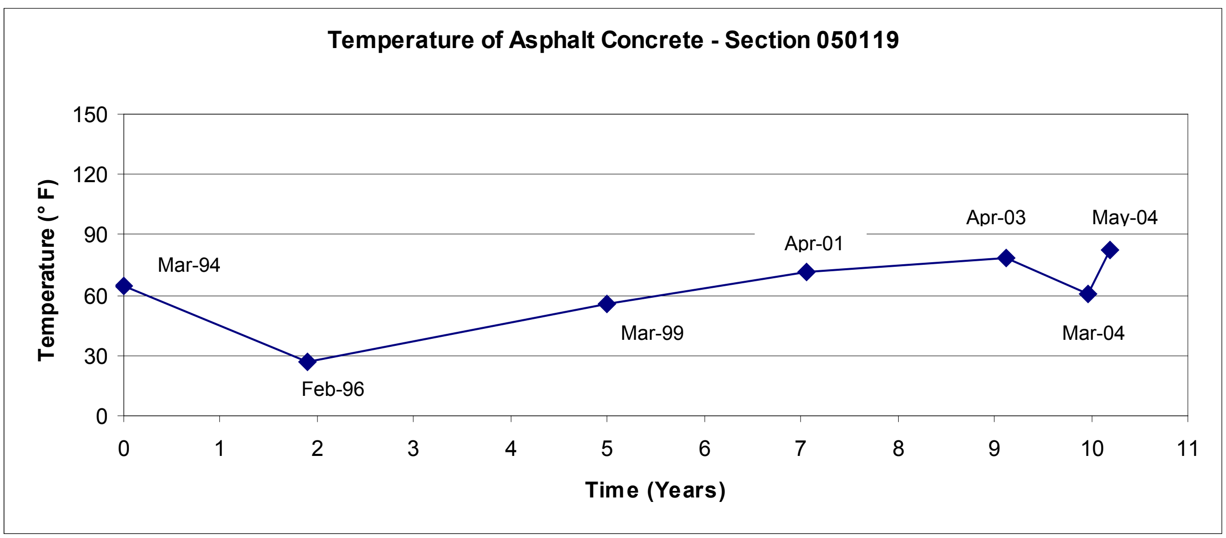

Figure 135. Graph. Mid-depth temperature of AC layer, section 050119 (Arkansas).

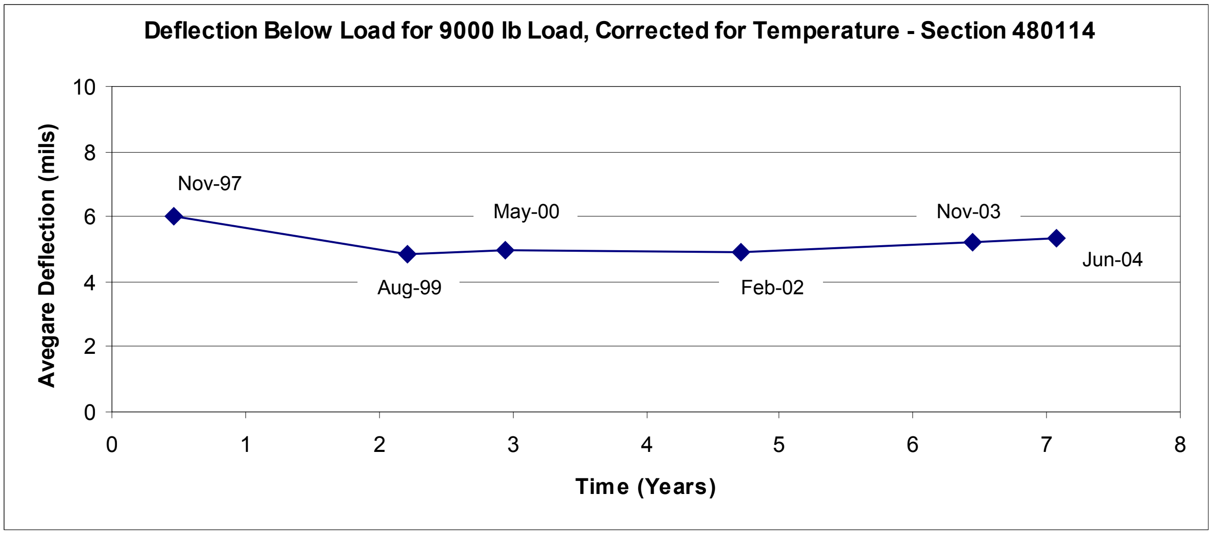

Figure 136. Graph. Average normalized deflection below 9,000-lb load, section 480114 (Texas).

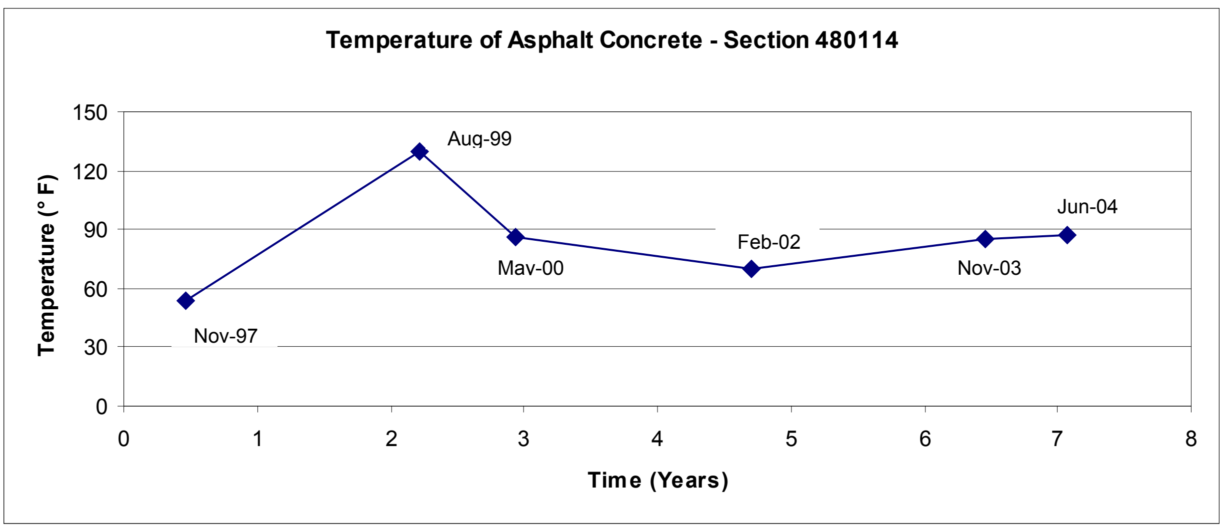

Figure 137. Graph. Mid-depth temperature of AC layer, section 480114 (Texas).

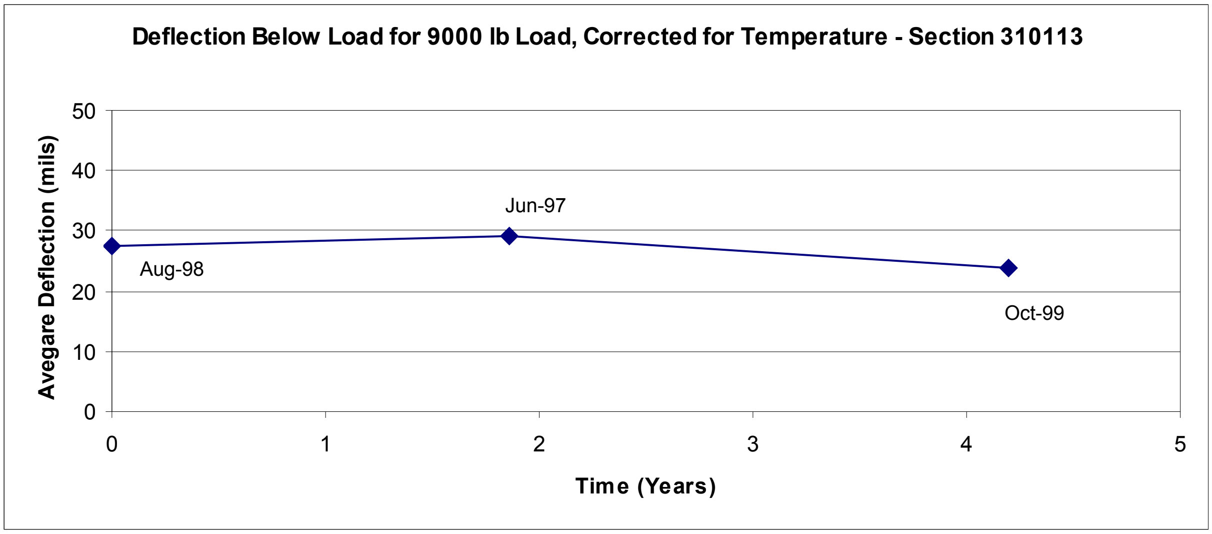

Figure 138. Graph. Average normalized deflection below 9,000-lb load, section 310113 (Nebraska).

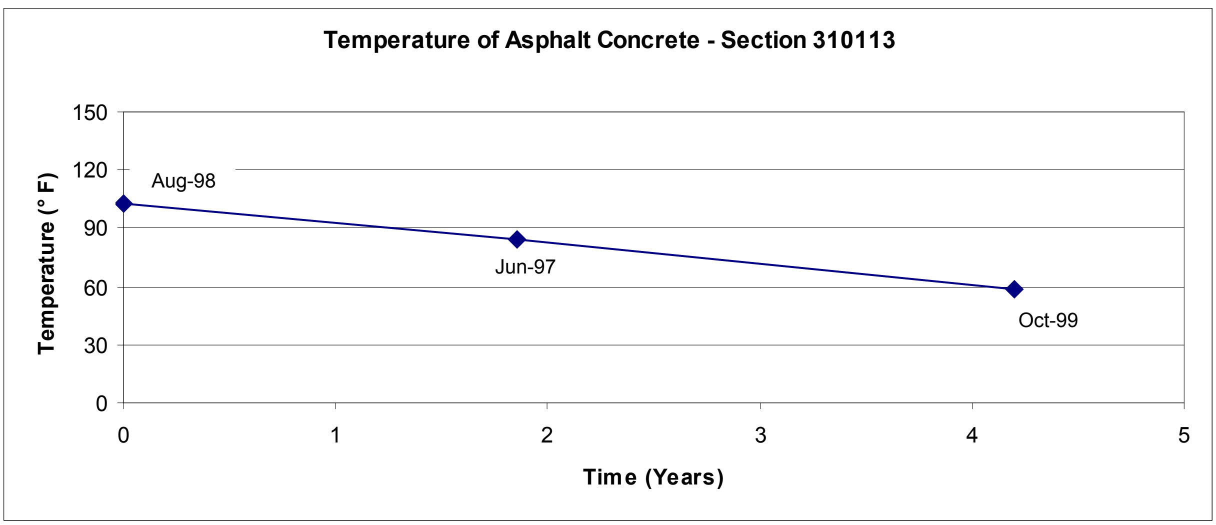

Figure 139. Graph. Mid-depth temperature of AC layer, section 310113 (Nebraska).

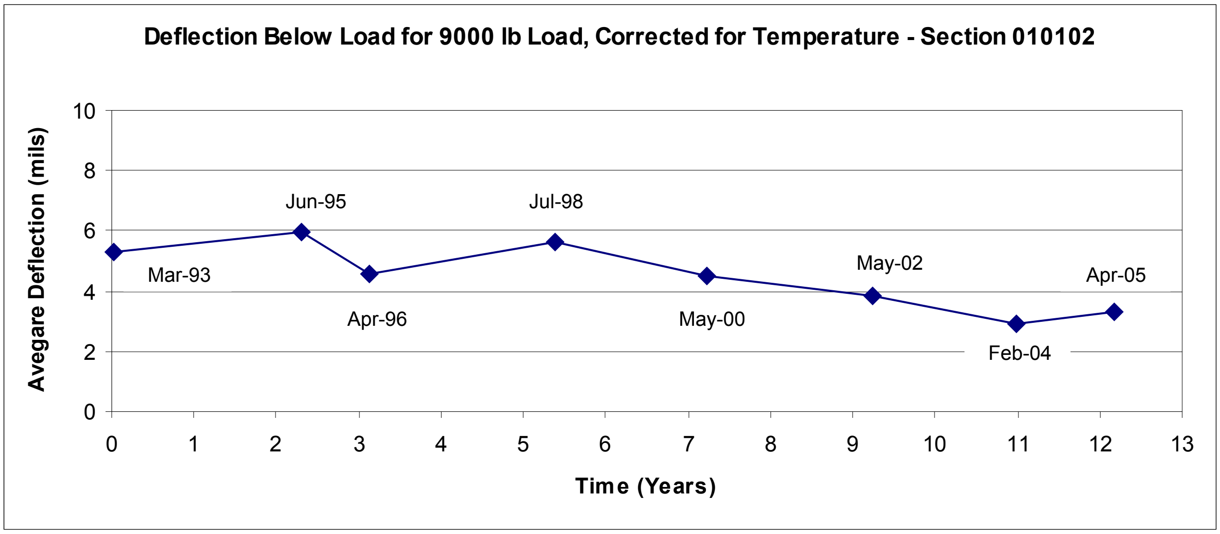

Figure 140. Graph. Average normalized deflection below 9,000-lb load, section 010102 (Alabama).

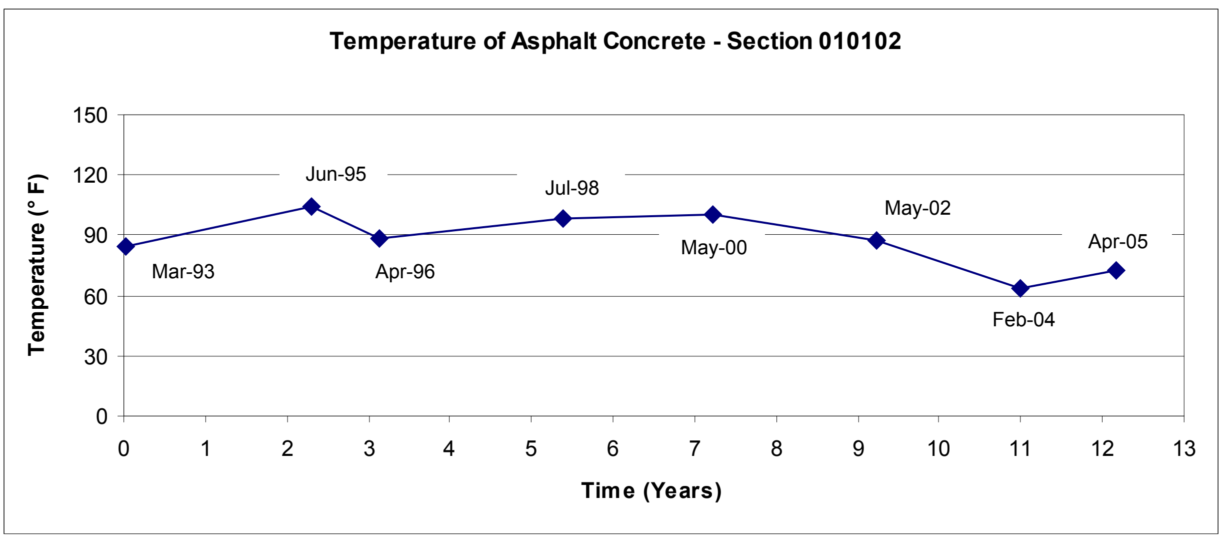

Figure 141. Graph. Mid-depth temperature of AC layer, section 010102 (Alabama).

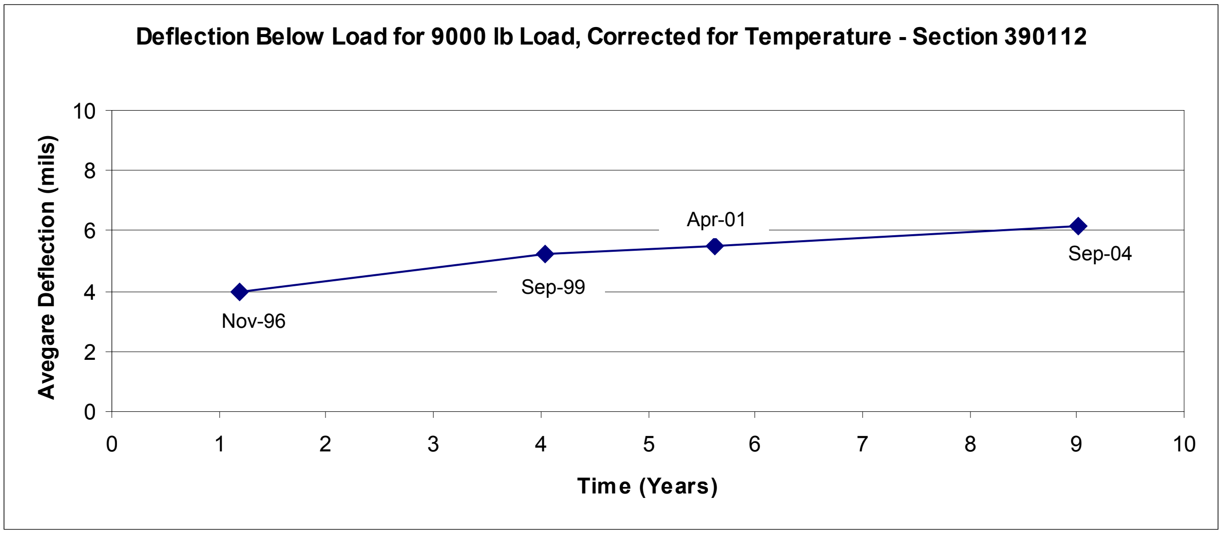

Figure 142. Graph. Average normalized deflection below 9,000-lb load, section 390112 (Ohio).

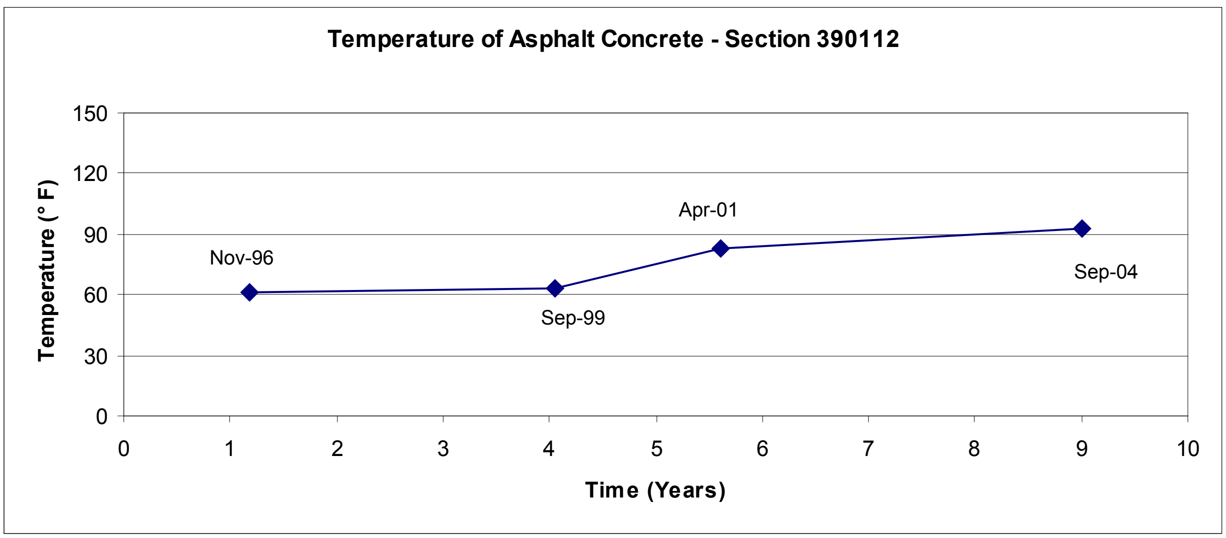

Figure 143. Graph. Mid-depth temperature of AC layer, section 390112 (Ohio).

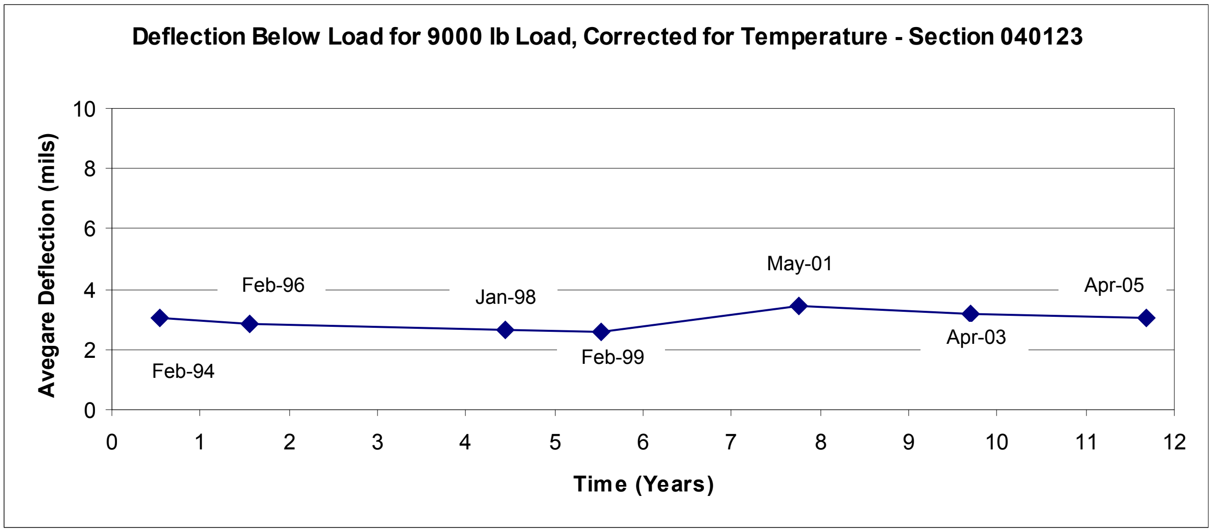

Figure 144. Graph. Average normalized deflection below 9,000-lb load, section 040123 (Arizona).

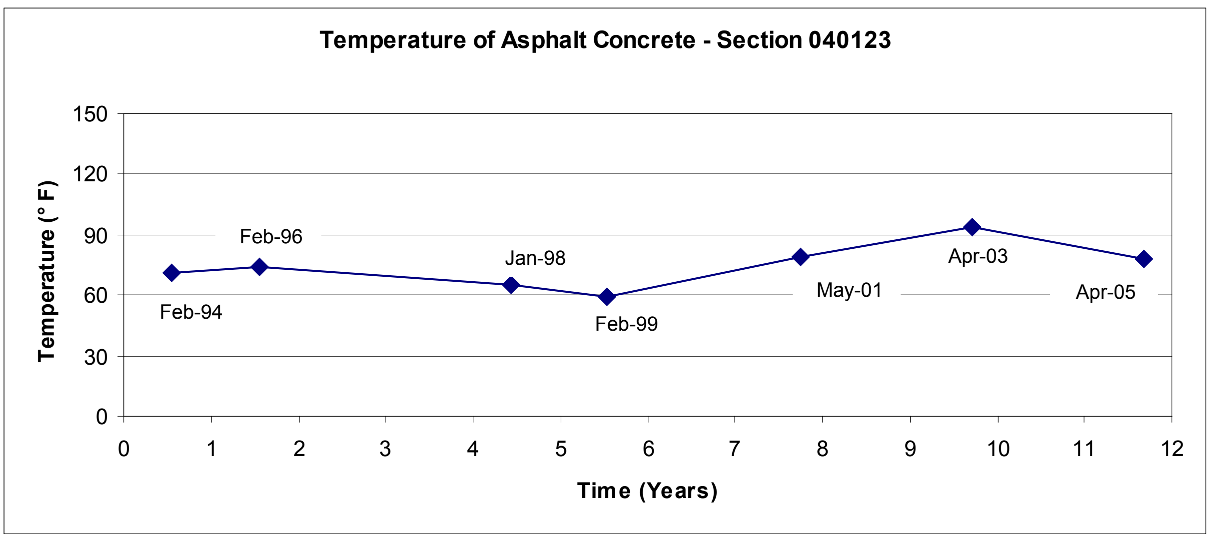

Figure 145. Graph. Mid-depth temperature of AC layer, section 040123 (Arizona).

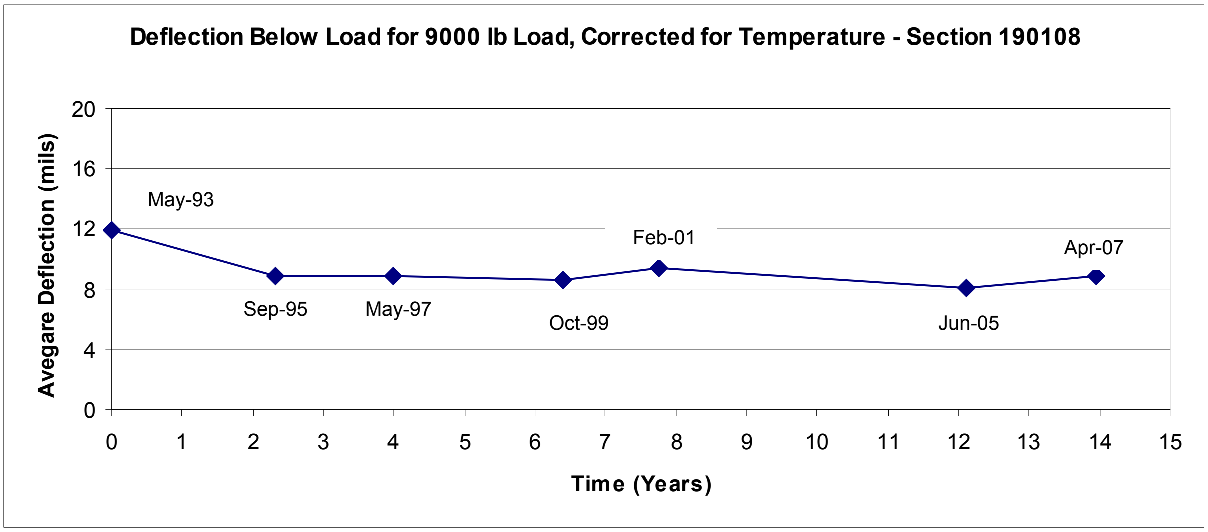

Figure 146. Graph. Average normalized deflection below 9,000-lb load, section 190108 (Iowa).

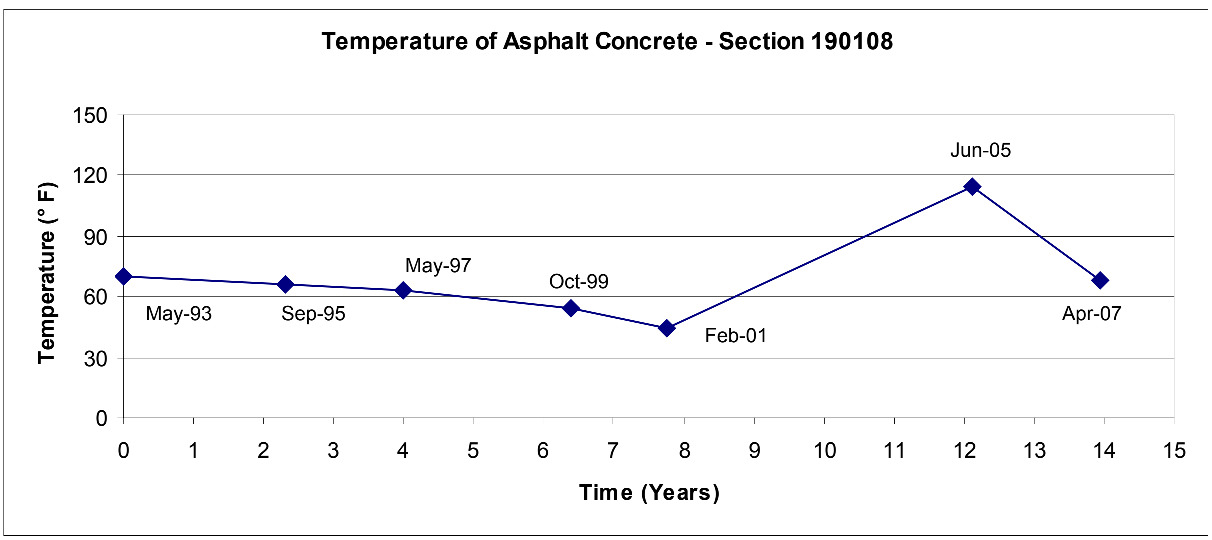

Figure 147. Graph. Mid-depth temperature of AC layer, section 190108 (Iowa).

D.2 GROUP 2 SECTIONS

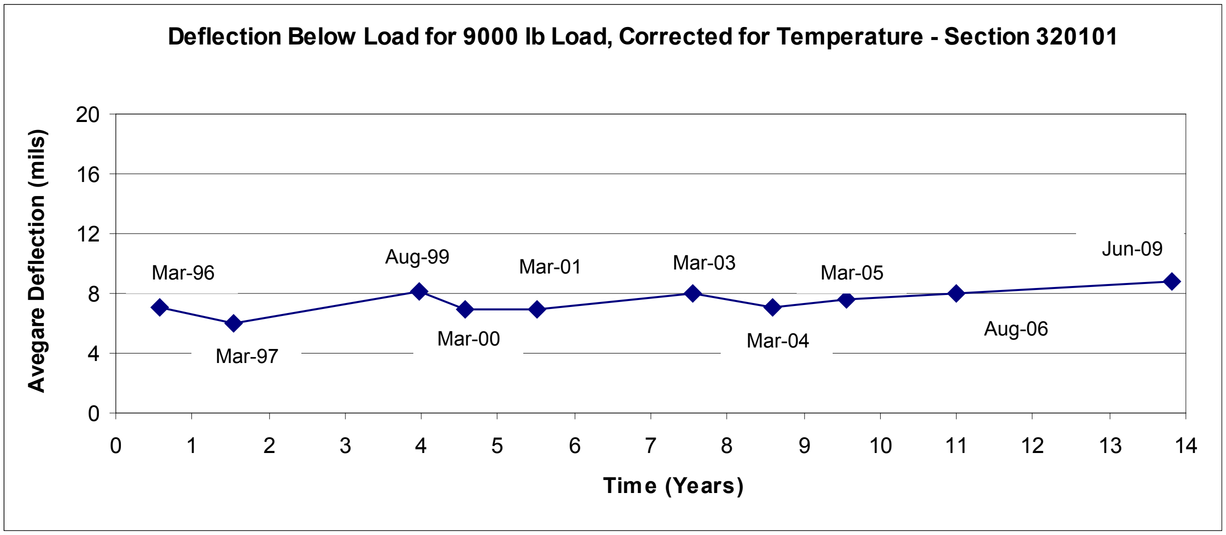

Figure 148. Graph. Average normalized deflection below 9,000-lb load, section 320101 (Nevada).

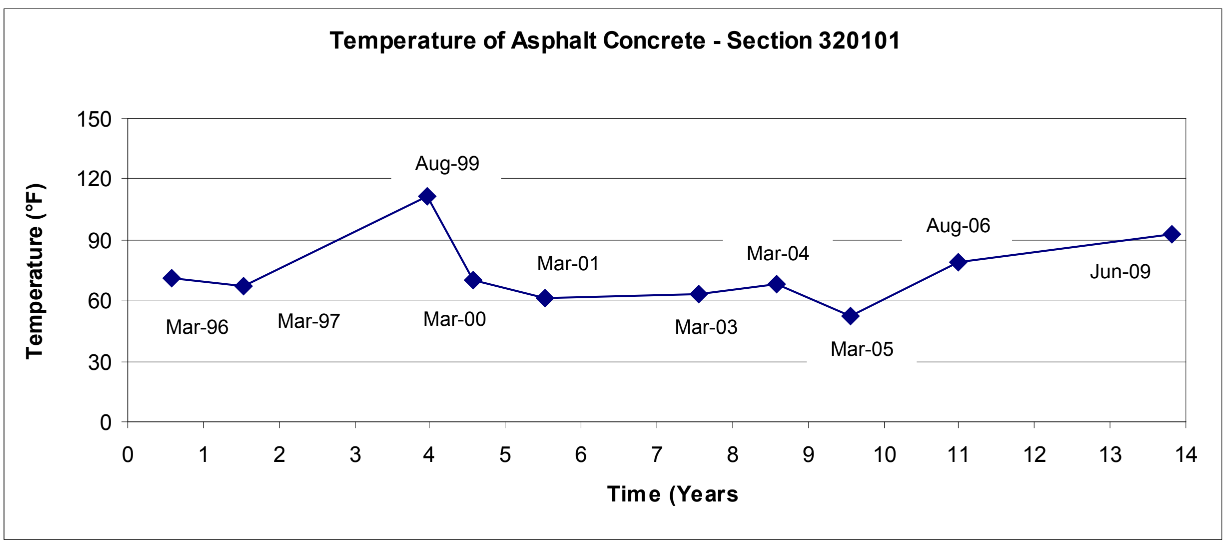

Figure 149. Graph. Mid-depth temperature of AC layer, section 320101 (Nevada).

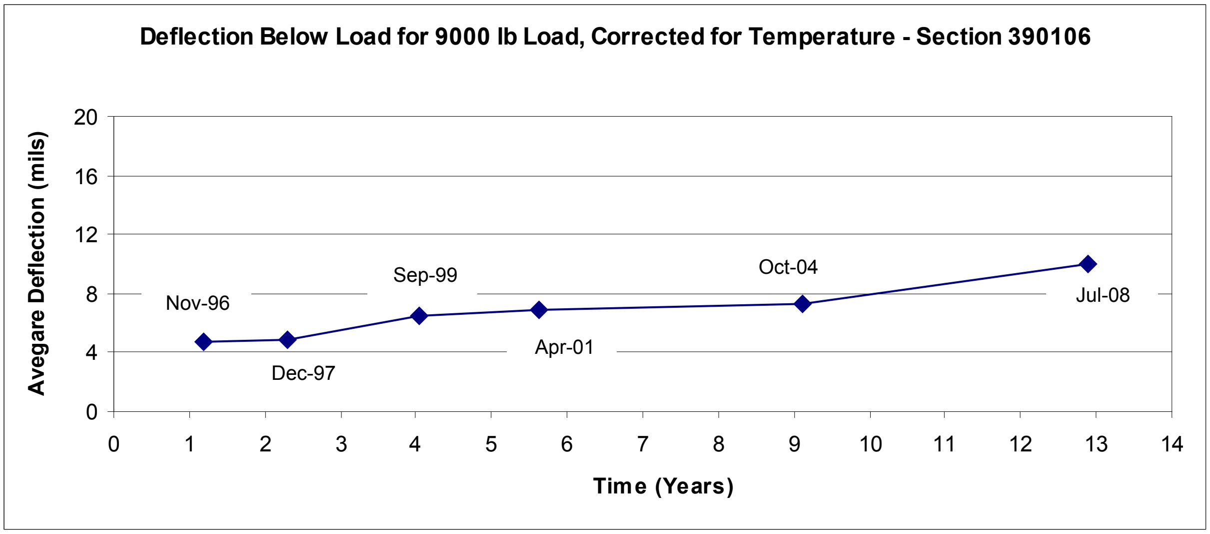

Figure 150. Graph. Average normalized deflection below 9,000-lb load, section 390106 (Ohio).

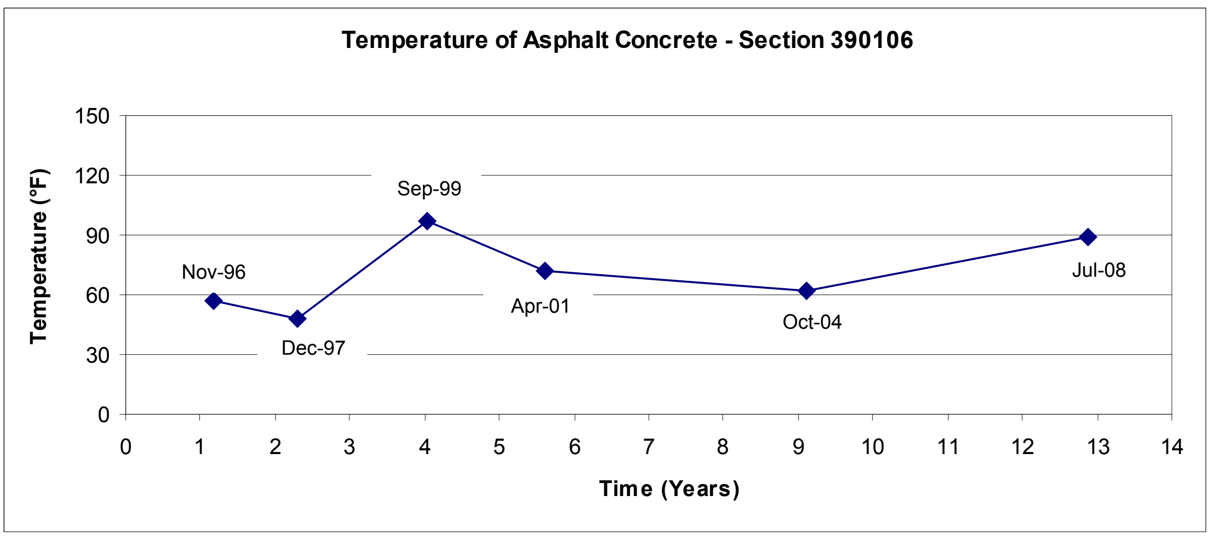

Figure 151. Graph. Mid-depth temperature of AC layer, section 390106 (Ohio).

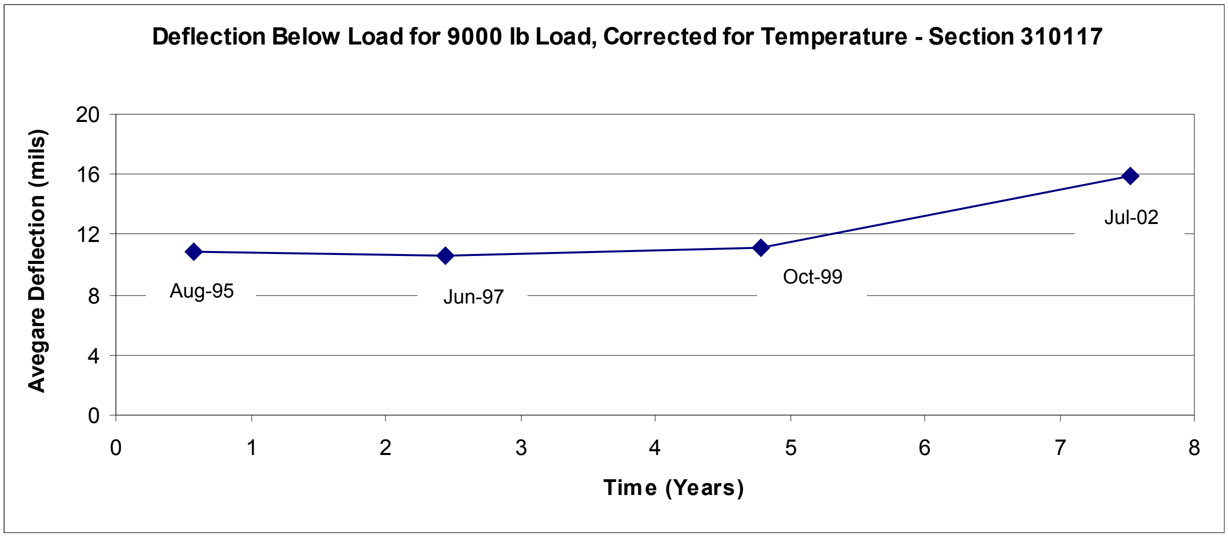

Figure 152. Graph. Average normalized deflection below 9,000-lb load, section 310117 (Nebraska).

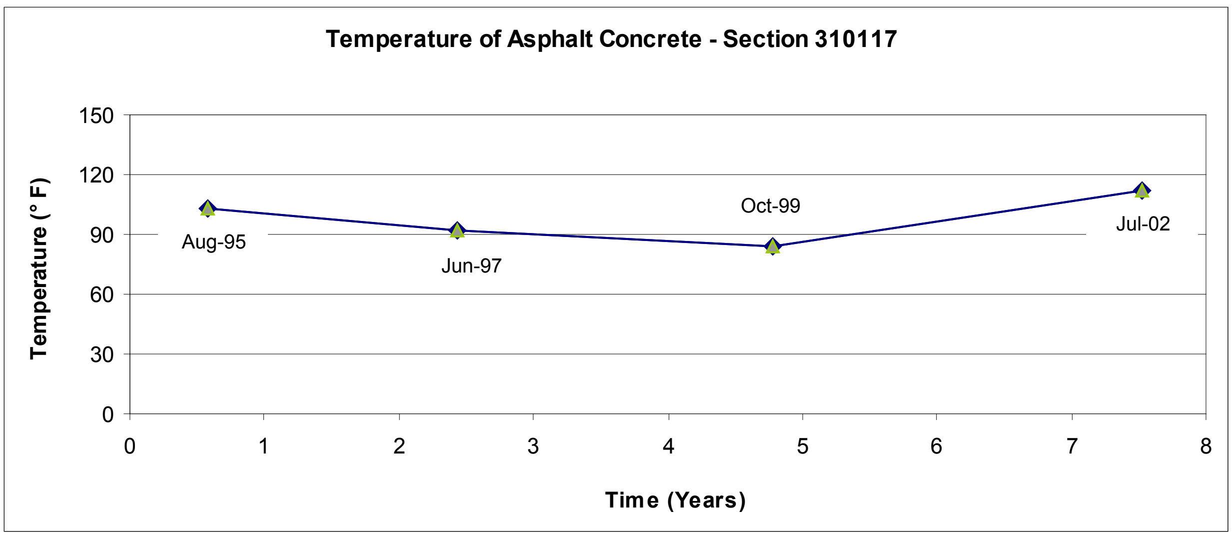

Figure 153. Graph. Mid-depth temperature of AC layer, section 310117 (Nebraska).

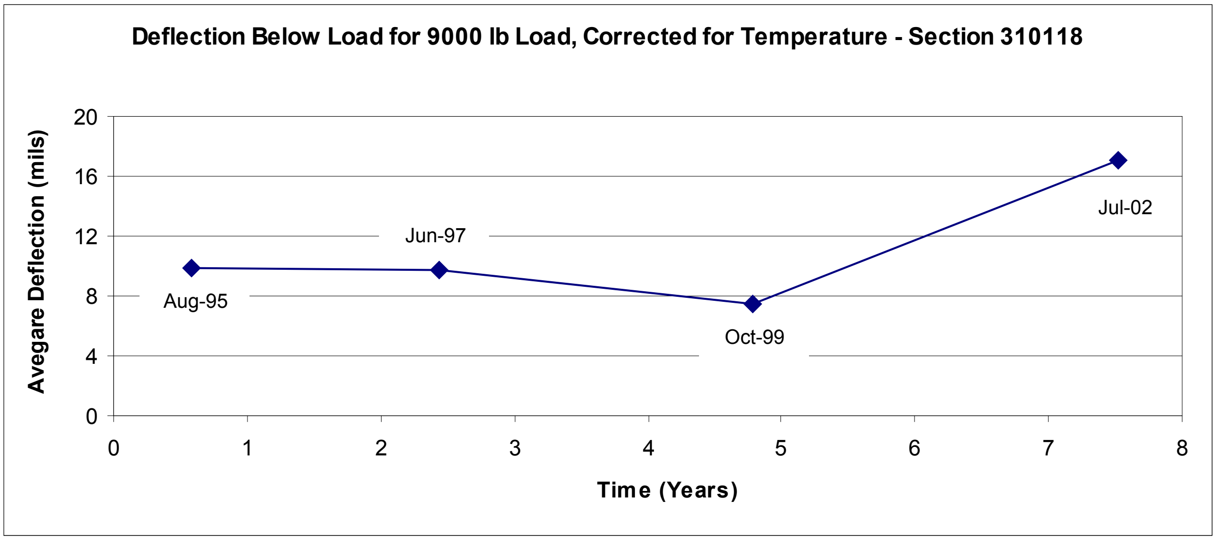

Figure 154. Graph. Average normalized deflection below 9,000-lb load, section 310118 (Nebraska).

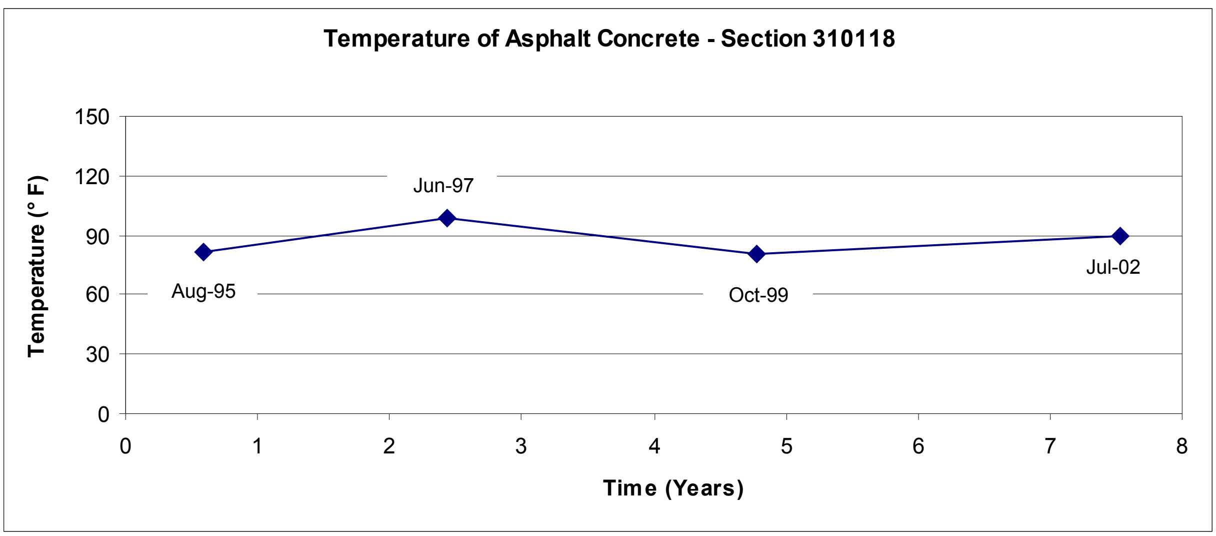

Figure 155. Graph. Mid-depth temperature of AC layer, section 310118 (Nebraska).

D.3 GROUP 3 SECTIONS

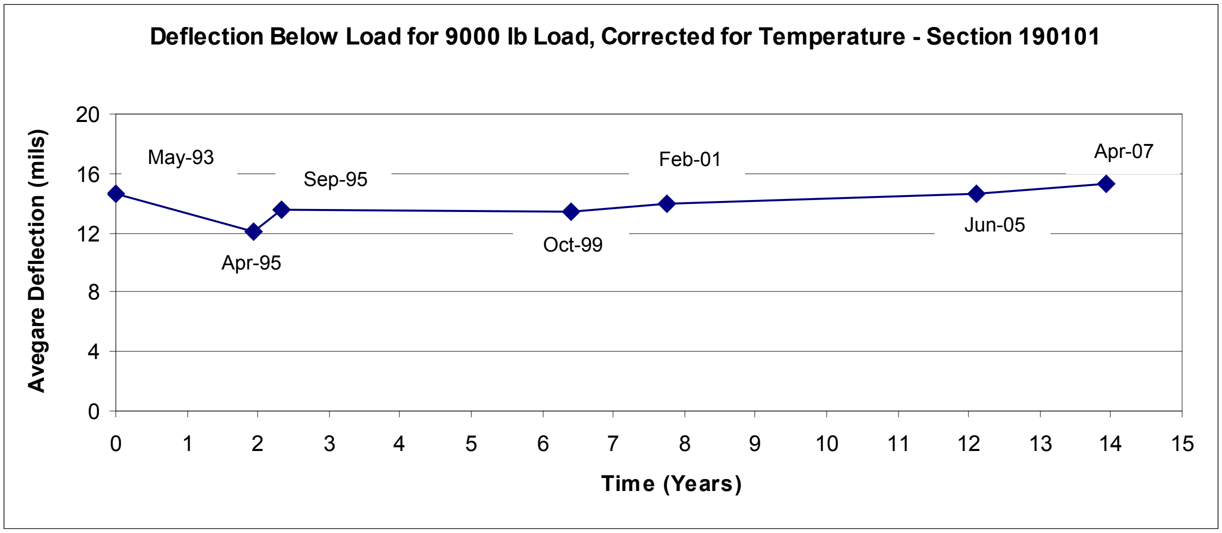

Figure 156. Graph. Average normalized deflection below 9,000-lb load, section 190101 (Iowa).

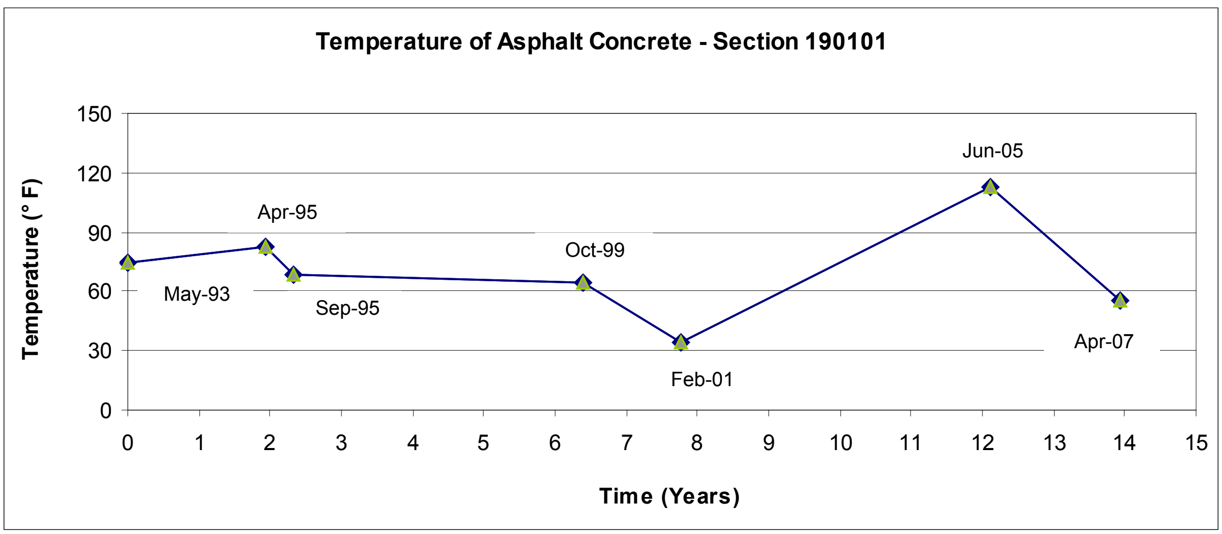

Figure 157. Graph. Mid-depth temperature of AC layer, section 190101 (Iowa).

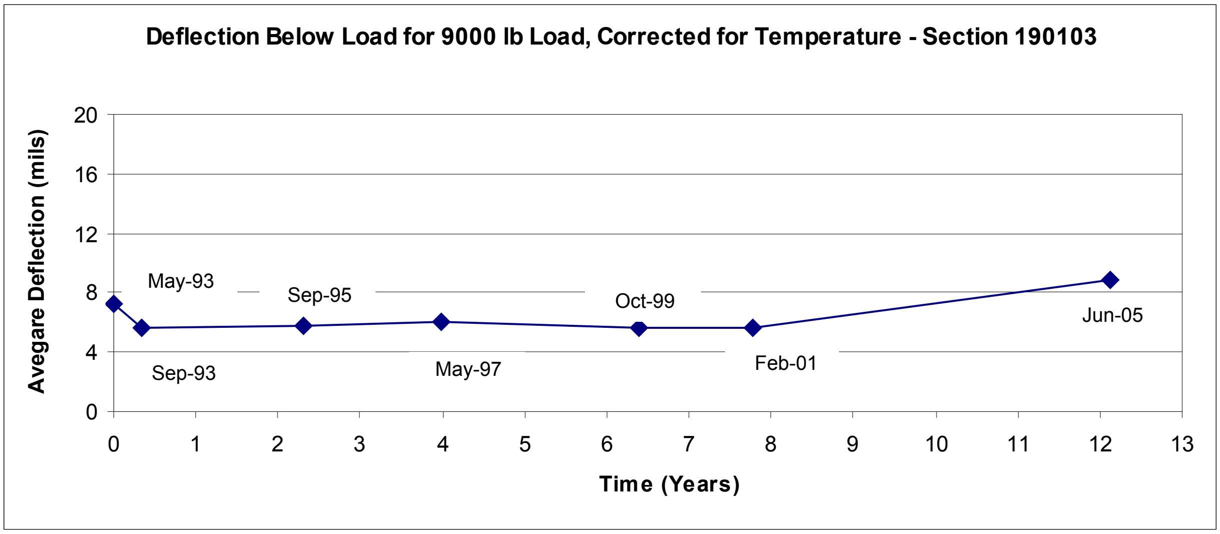

Figure 158. Graph. Average normalized deflection below 9,000-lb load, section 190103 (Iowa).

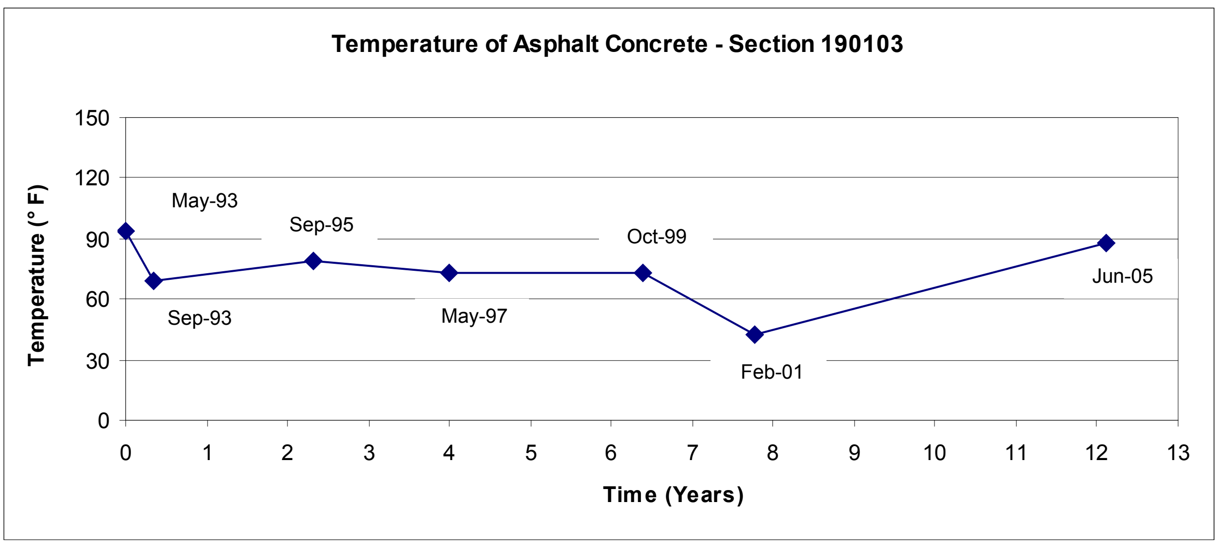

Figure 159. Graph. Mid-depth temperature of AC layer, section 190103 (Iowa).

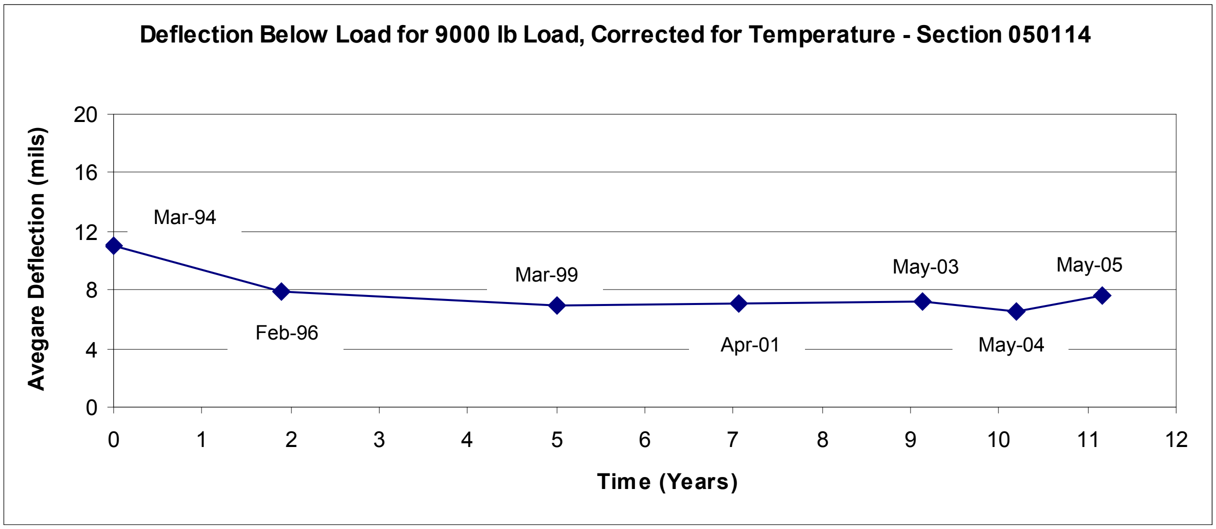

Figure 160. Graph. Average normalized deflection below 9,000-lb load, section 050114 (Arkansas).

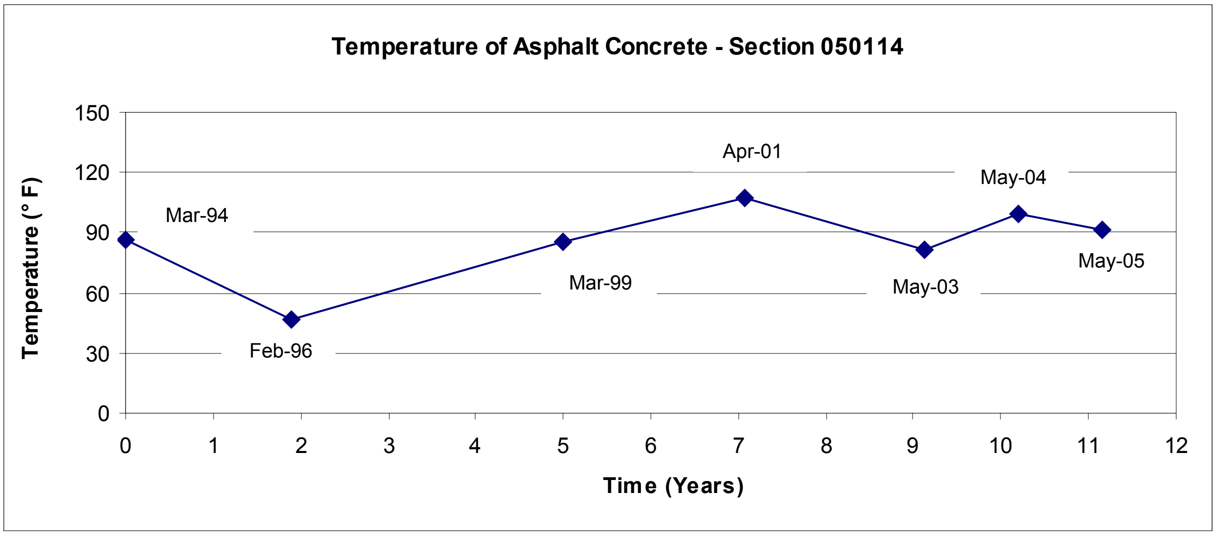

Figure 161. Graph. Mid-depth temperature of AC layer, section 050114 (Arkansas).

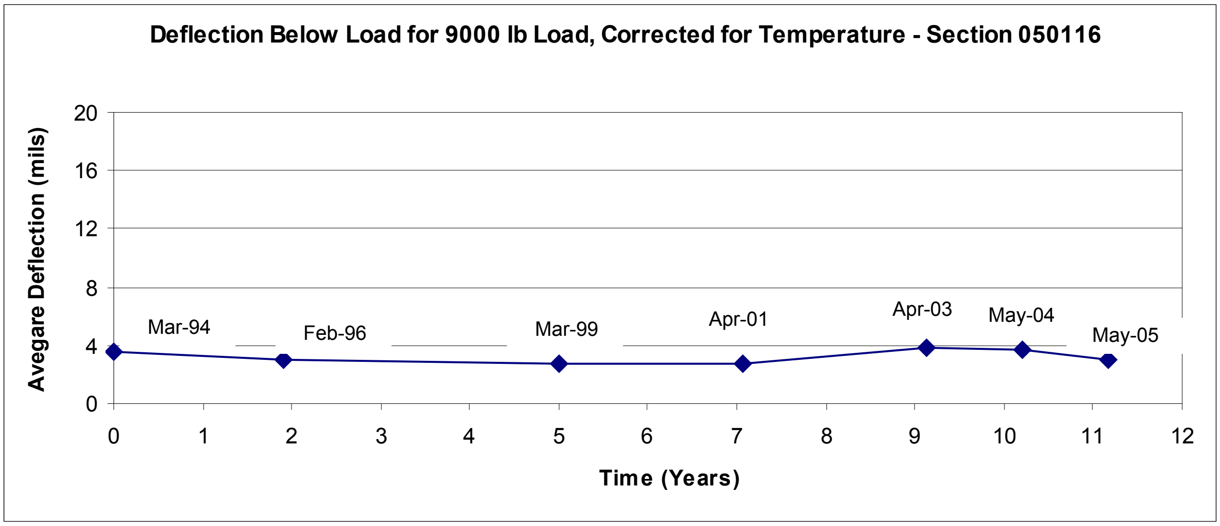

Figure 162. Graph. Average normalized deflection below 9,000-lb load, section 050116 (Arkansas).

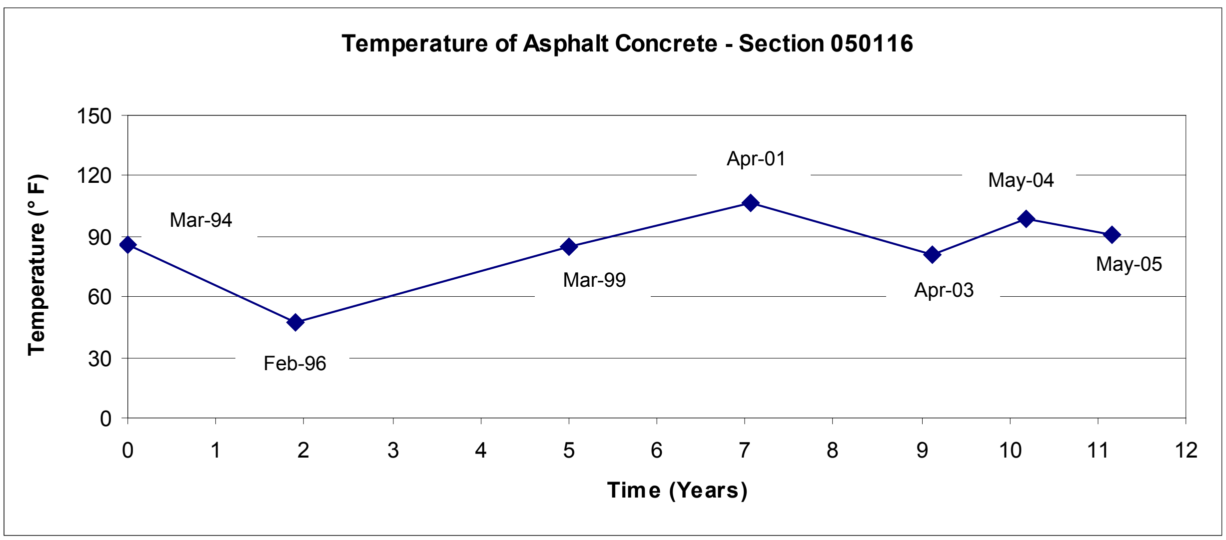

Figure 163. Graph. Mid-depth temperature of AC layer, section 050116 (Arkansas).

D.4 GROUP 4 SECTIONS

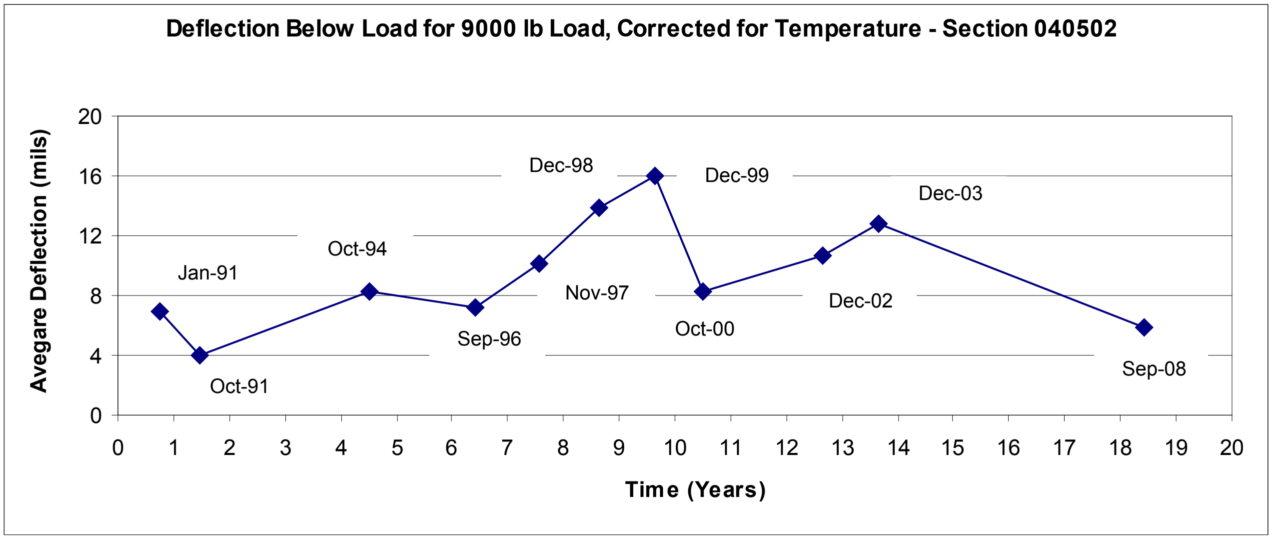

Figure 164. Graph. Average normalized deflection below 9,000-lb load, section 040502 (Arizona).

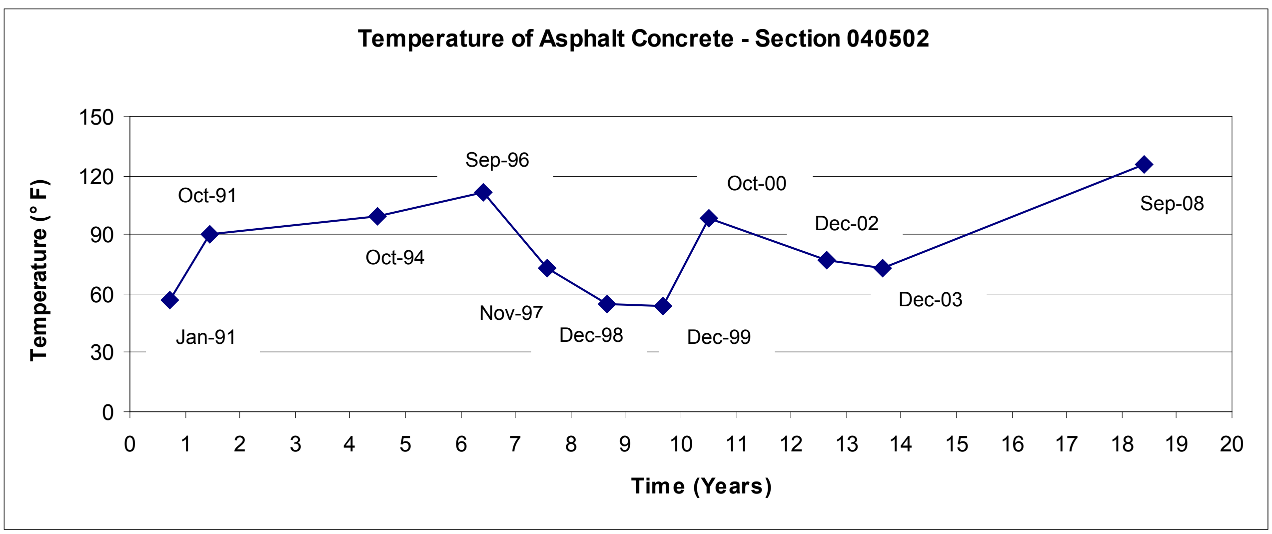

Figure 165. Graph. Mid-depth temperature of AC layer, section 040502 (Arizona).

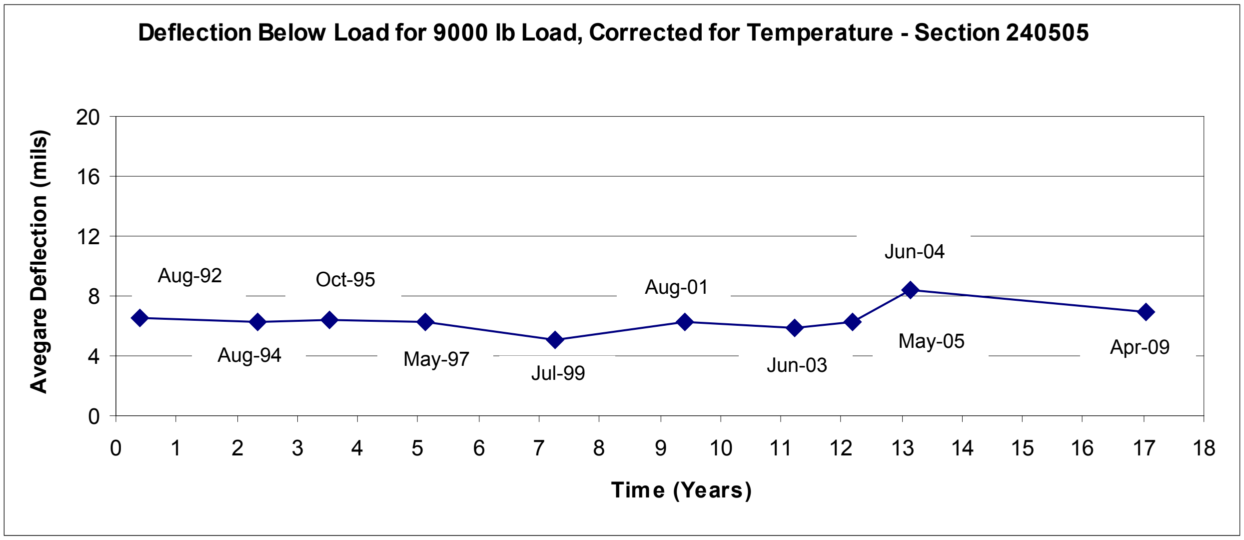

Figure 166. Graph. Average normalized deflection below 9,000-lb load, section 240505 (Maryland).

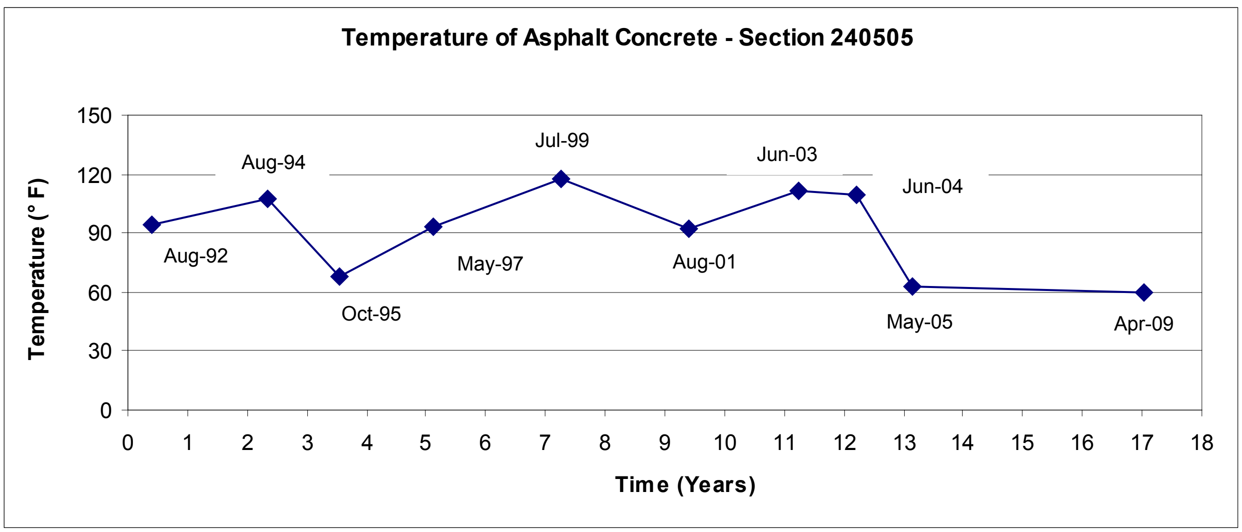

Figure 167. Graph. Mid-depth temperature of AC layer, section 240505 (Maryland).

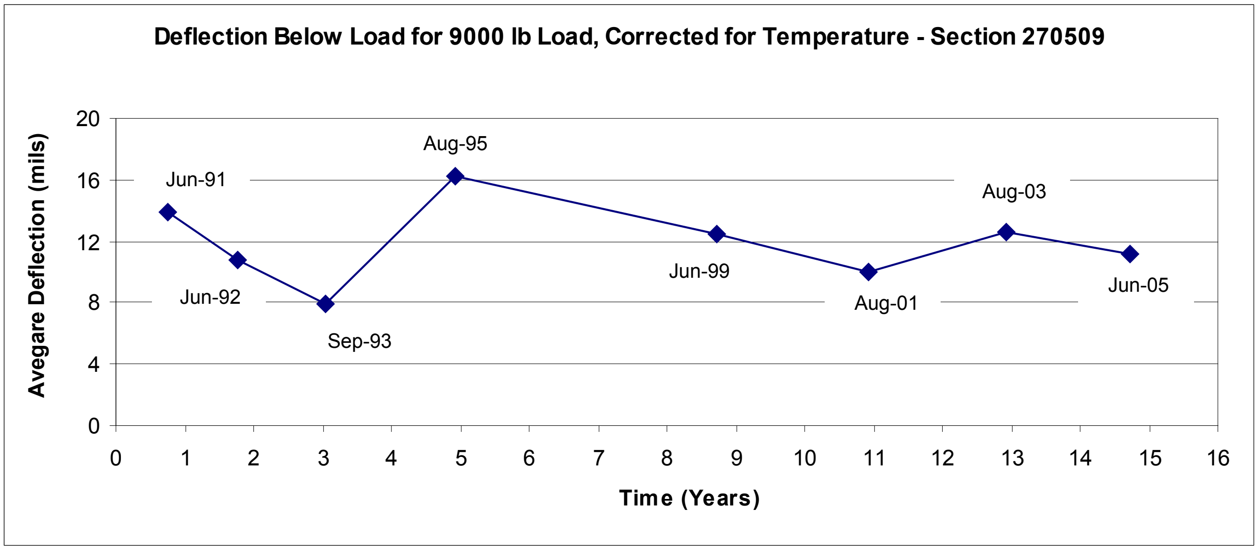

Figure 168. Graph. Average normalized deflection below 9,000-lb load, section 270509 (Minnesota).

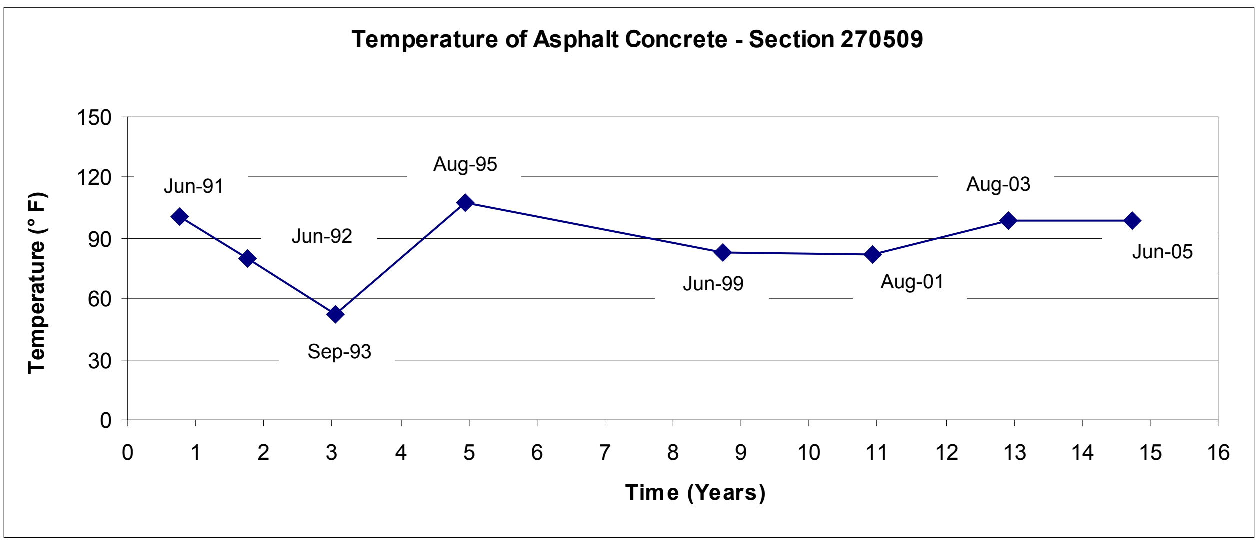

Figure 169. Graph. Mid-depth temperature of AC layer, section 270509 (Minnesota).

D.5 GROUP 5 SECTIONS

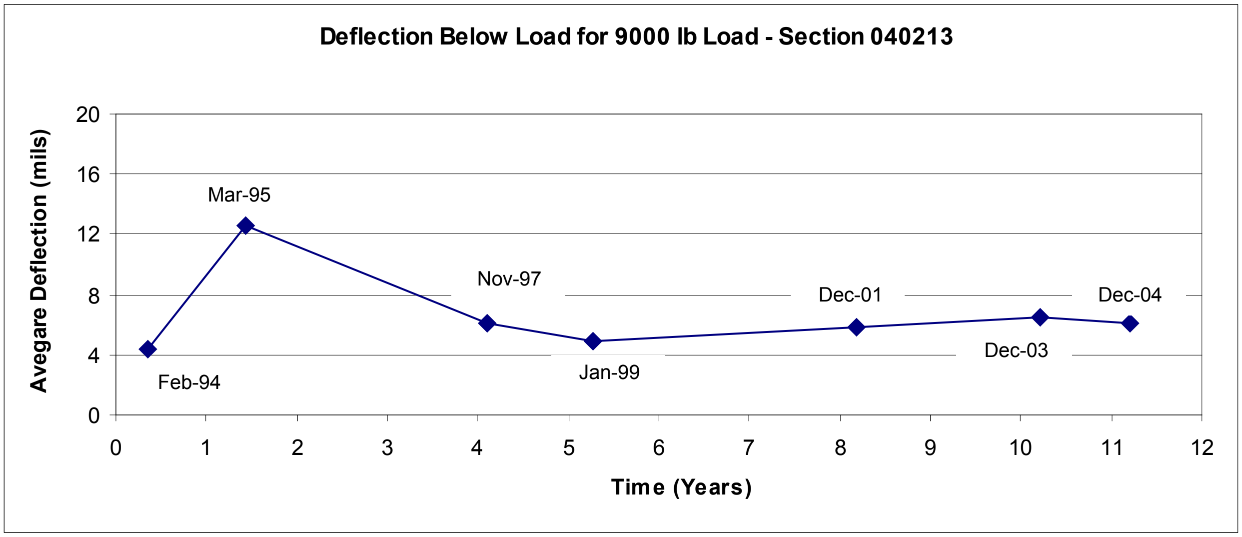

Figure 170. Graph. Average normalized deflection below 9,000-lb load, section 040213 (Arizona).

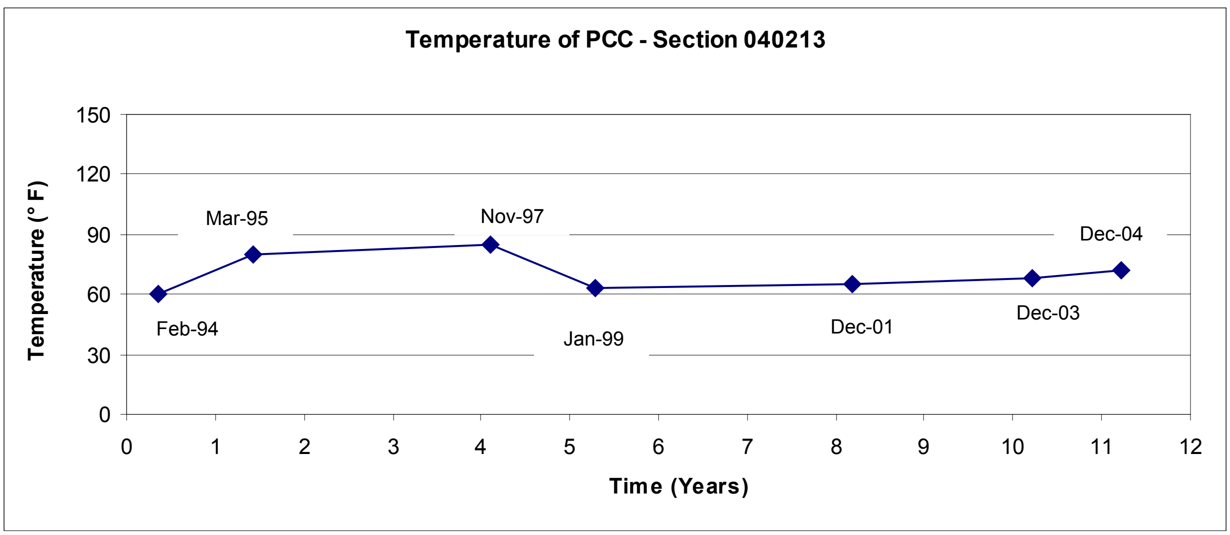

Figure 171. Graph. Mid-depth temperature of PCC layer, section 040213 (Arizona).

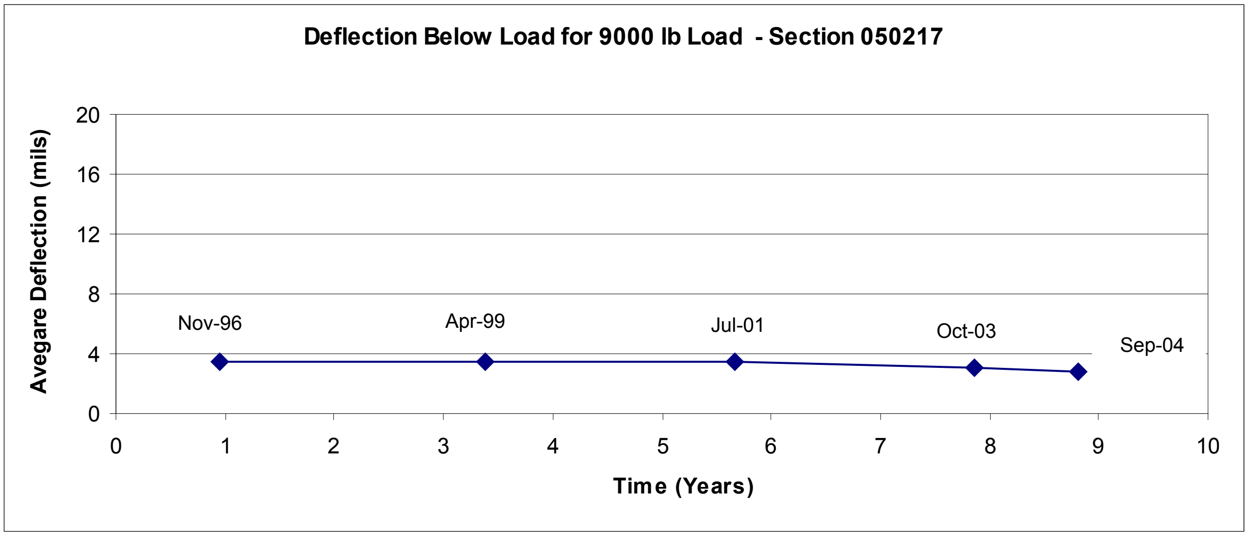

Figure 172. Graph. Average normalized deflection below 9,000-lb load, section 050217 (Arkansas).

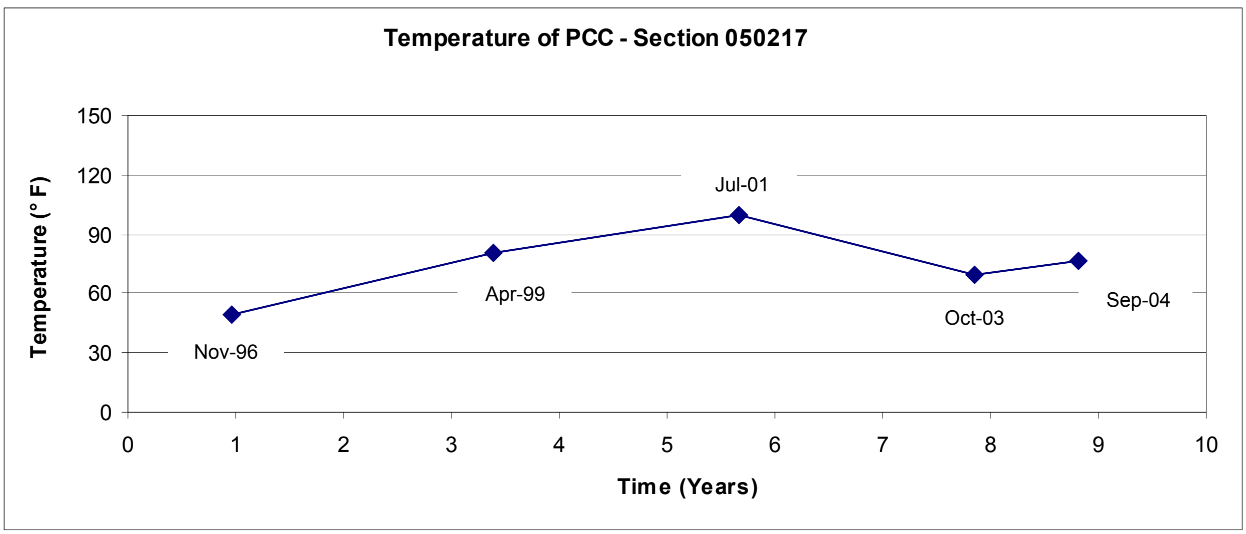

Figure 173. Graph. Mid-depth temperature of PCC layer, section 050217 (Arkansas).

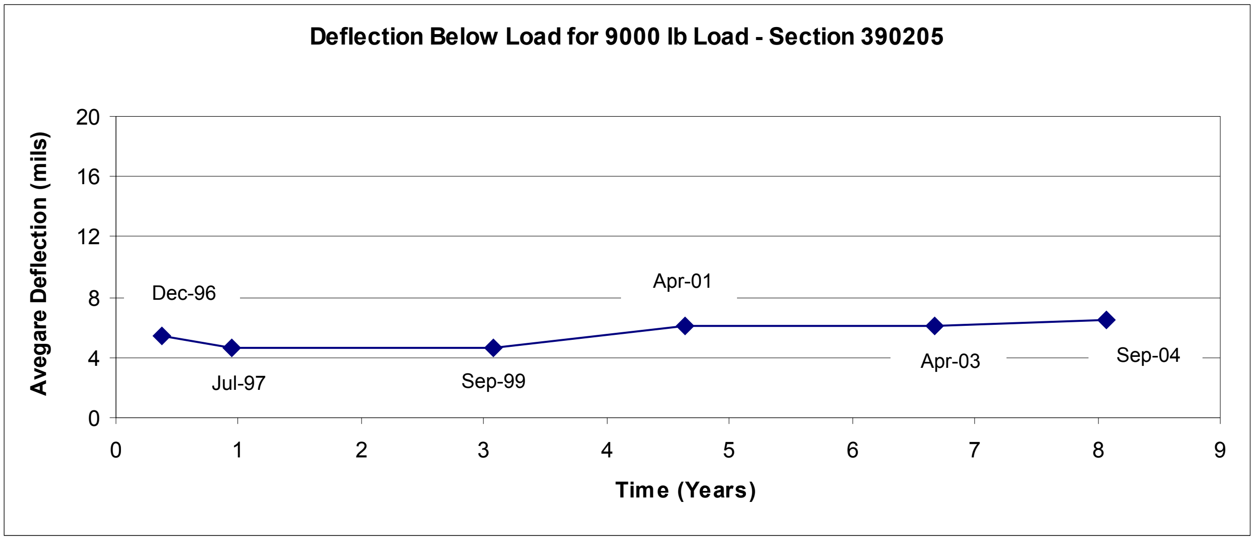

Figure 174. Graph. Average normalized deflection below 9,000-lb load, section 390205 (Ohio).

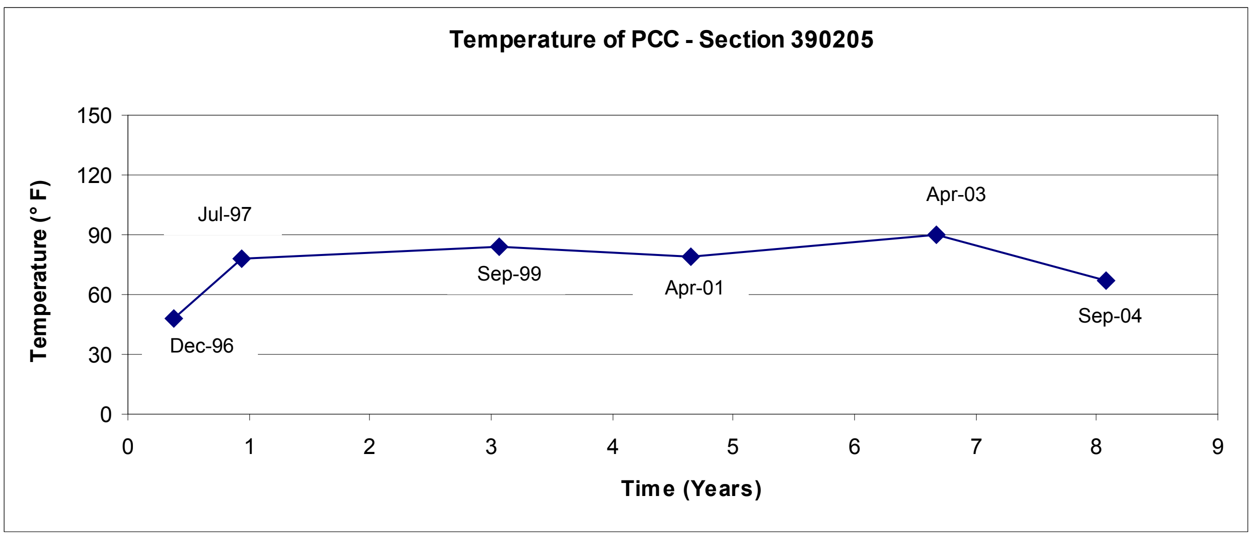

Figure 175. Graph. Mid-depth temperature of PCC layer, section 390205 (Ohio).

REFERENCES

1. Turner-Fairbank Highway Research Center. (2011). *How to Get LTPP Data*, Federal Highway Administration, Washington, DC. Obtained from: http://www.fhwa.dot.gov/research/tfhrc/programs/infrastructure/pavements/ltpp/getdata.cfm.

2. Boussinesq, J. (1885). *Application des Potentiels a l'etude de l'equilibre et du Mouvement des Solids Elastiques*, Gauthier-Villars, Paris, France.

3. Burmeister, D.M. (1943). "The Theory of Stresses and Displacements in Layered Systems and Applications to the Design of Airport Runways," *Proceedings, Highway Research Board*, *23*, 126–144.

4. Von Quintus, H. and Killingsworth, B. (1997). *Analysis Relating to Pavement Material Characterizations and Their Effects on Pavement Performance*, Report No. FHWA-RD-97-05, Federal Highway Administration, McLean, VA.

5. Zhang, Z., Manuel, L., Damnjanovic, I., and Li, Z. (2003). *Development of a New Methodology for Characterizing Pavement Structural Condition for Network Level Applications*, Report No. FHWA/TX-04/0-4322-1, Center for Transportation Research, University of Texas at Austin, Austin, TX.

6. Smith, J.T. and Tighe, S.L. (2004). "Assessment of Overlay Roughness in Long-Term Pavement Performance Test Sites: Canadian Case Study," *Transportation Research Record 1869*, Transportation Research Board, Washington, DC.

7. Perera, R.W. and Kohn, S.D. (1999). "International Roughness Index of Asphalt Concrete Overlays: Analysis of Data from Long-Term Pavement Performance Program SPS-5 Projects," *Transportation Research Record 1655*, Transportation Research Board, Washington, DC.

8. Buch, N., Chatti, K., Haider, S.W., Pulipaka, A.S., Lyles, R.W., and Gilliland, D. (2006). "Network-Level Evaluation of Specific Pavement Study-2 Experiment: Using a Long-Term Pavement Performance Database," *Transportation Research Record 1947*, Transportation Research Board, Washington, DC.

9. Chatti, K. (2006). *Effect of Design and Site Factors on Long-Term Performance of Flexible Pavements in SPS-1 Experiment*, Transportation Research Board 85th Annual Meeting, Transportation Research Board, Washington, DC.

10. Rauhut, J.B, Eltahan, A., and Simpson, A.L. (1999). *Common Characteristics of Good and Poorly Performing AC Pavements*, Report No. FHWA-RD-99-193, Federal Highway Administration, McLean, VA.

11. Federal Highway Administration. (2000). *Performance Trends of Rehabilitated AC Pavements*, TechBrief, Publication No. FHWA-RD-00-165, McLean, VA.

12. Federal Highway Administration. (1998). *What Makes Portland Cement Concrete (PCC) Pavements Rough?*, TechBrief, Publication No. FHWA-RD-98-148, McLean, VA.

13. Vepa, T.S, George, K.P., and Shekharan, A.R. (1996). "Prediction of Pavement Remaining Life," *Transportation Research Record 1524*, Transportation Research Board, Washington, DC.

14. Aultman-Hall, L., Jackson, E., Dougan, C.E., and Choi, S.N. (2004). "Models Relating Pavement Quality Measures," *Transportation Research Record 1869*, Transportation Research Board, Washington, DC.

15. Dewan, S.A. and Smith, R.E. (2002). "Estimating International Roughness Index from Pavement Distress to Calculate Vehicle Operating Costs for the San Francisco Bay Area," *Transportation Research Record 1816*, Transportation Research Board, Washington, DC.

16. Mactutis, J.A., Alavi, S.H., and Ott, W.C. (2000). "Investigation of Relationship Between Roughness and Pavement Surface Distress Based on WesTrack Project," *Transportation Research Record 1699*, Transportation Research Board, Washington, DC.

17. Lin, J.D., Yau, J.T., and Hsiao, L.H. (2003). *Correlation Analysis Between International Roughness Index and Pavement Distress By Neural Network*, Presented at the 82d Annual Meeting of the Transportation Research Board, Washington, DC.

18. American Association of State Highway and Transportation Officials. (2008). *Mechanistic-Empirical Pavement Design Guide, A Manual of Practice*, Interim Edition, Washington, DC.

19. Odoki, J.B. and Kerali, H.G.R. (2000). *HDM-4 Analytical Framework and Model Descriptions, Vol. 4*, Highway Development and Management, HDM-4 Series of Publications, World Bank, Washington, DC, and PIARC, Paris, France.

20. Sayers, M.W. and Karamihas, S.M. (1997). *The Little Book of Profiling: Basic Information About Measuring and Interpreting Road Profiles*, University of Michigan Transportation Research Institute, Ann Arbor, MI.

21. Sayers, M.W. (1999). "Profiles of Roughness," *Transportation Research Record 1260*, Transportation Research Board, Washington, DC.

22. Karamihas, S.M. and Senn, K. (2009). "Profile Analysis of Arizona Specific Pavement Studies 5 Project," *Transportation Research Record 2095*, Transportation Research Board, Washington, DC.

23. American Association of State Highway and Transportation Officials. (1993). *Guide for Design of Pavement Structures*, Washington, DC.

24. Rada, G.R., Prabhakar, V., and James, M. (2011). *Deflection Analysis of SPS-1 Sites (2011),* Draft FHWA Report, Federal Highway Administration, McLean, VA.

25. Karamihas, S.M. and Gillespie, T.D. (2002). *Smoothness Criteria for WIM Scale Approaches*, UMTRI Report 2002-37, University of Michigan Transportation Research Institute, Ann Arbor, MI.

26. Karamihas, S.M., Gillespie, T.D., Perera, R.W., and Kohn, S.D. (1999). *Guidelines for Longitudinal Pavement Profile Measurement*, Report No. 434, National Cooperative Highway Research Program, Washington, DC.

27. Byrum, C.R. (2005). "The Effect of Slab Curvature on IRI Values for Jointed Concrete Pavements," *International Journal of Concrete Pavements*, *1*(1), 23–32, International Society for Concrete Pavements, Cleveland, OH.

28. Karamihas, S.M., Gillespie, T.D., Perera, R.W., and Kohn, S.D. (2001). *Diurnal Changes in Profile of Eleven Jointed PCC Pavements*, Proceedings of 7th International Conference on Concrete Pavements, Orlando, FL.

29. Karamihas, S.M. and Senn, K. (2011). *Curl and Warp Analysis of the LTPP SPS-2 Site in Arizona*, University of Michigan Transportation Research Institute, Ann Arbor, MI.

BIBLIOGRAPHY

1. Agarwal, P.K., Das, A., and Chakroborty, P. (2006). "Simple Model for Structural Evaluation of Asphalt Concrete Pavements at the Network Level," *Journal of Infrastructure Systems*, *12*(1), 41–49, American Society of Civil Engineers, Reston, VA.

2. Ali, H. and Selezneva, O. (2000). "Seasonal Trends and Causes in Pavement Structural Properties," *Nondestructive Testing of Pavements and Backcalculation of Moduli: Third Volume*, ASTM International, West Conshohocken, PA.

3. Carvalho, R., Ayres, M., Tayabji, S., and Selezneva, O. (2010). *Impact of Design Features on Pavement Response and Performance in Rehabilitated Flexible and Rigid Pavements*, Report No. FHWA-RD-10-066, Federal Highway Administration, McLean, VA.

4. Carvalho, R., Stubstad, R., Briggs, R., Selezneva, O., Mustafa, E., and Ramachandran, A. (2011). *Simplified Techniques for Evaluation and Interpretation of Pavement Deflections for Network-Level Analysis*, Report No. FHWA-HRT-12-023, Federal Highway Administration, McLean, VA.

5. Chakroborty, P., Agarwal, P.K., and Das, A. (2007). *Simple Model to Predict Structural Condition of Asphalt Concrete Pavements at the Network Level*, Transportation Research Board 86th Annual Meeting, Transportation Research Board, Washington, DC.

6. Chatti, K., Buch, N., Haider, S.W., Pulipaka, A.S., Lyles, R.W., Gilliland, D., and Desaraju, P. (2005). "LTPP Data Analysis: Influence of Design and Construction Features on the Response and Performance of New Flexible and Rigid Pavements," *NCHRP Web Document No. 74*, National Cooperative Highway Research Program, Washington, DC.

7. Choi, J.H., Adams, T.M., and Bahia, H.U. (2004). "Pavement Roughness Modeling Using Back-Propagation Neural Networks," *Computer-Aided Civil and Infrastructure Engineering*, *19*(4), Wiley-Blackwell, Hoboken, NJ.

8. Corley-Lay, J.B. and Mastin, J. (2009). *Evaluation of LTPP Profile Data for Flexible Pavements*, Transportation Research Board 88th Annual Meeting, Washington, DC.

9. Evans, L.D. and Eltahan, A. (2000). *LTPP Profile Variability*, Report No. FHWA-RD-00-113, Federal Highway Administration, McLean, VA.

10. Federal Highway Administration. (1998). *Roughness Trends of Flexible Pavements*, TechBrief, Publication No. FHWA-RD-98-132, Federal Highway Administration, McLean, VA.

11. Fwa, T.F. and Setiadji, B.H. (2006). "Evaluation of Backcalculation Methods for Nondestructive Determination of Concrete Pavement Properties," *Transportation Research Record 1949*, Transportation Research Board, Washington, DC.

12. Guclu, A. and Ceylan, H. (2007). *Condition Assessment of Composite Pavement Systems Using Neural-Network-Based Rapid Backcalculation Algorithms*, Transportation Research Board 86th Annual Meeting, Transportation Research Board, Washington, DC.

13. Helali, K., Voth, M.D., Bekheet, W., Amenta, J.A. and VanDerHurst, P. (2006). *Development of Roughness Deterioration Models for National Park Service Network*, Transportation Research Board 85th Annual Meeting, Transportation Research Board, Washington, DC.

14. Jiang, Y.J. and Tayabji, S.D. (2000). "Evaluation of Concrete Pavement Conditions and Design Features Using LTPP FWD Deflection Data," *Nondestructive Testing of Pavements and Backcalculation of Moduli: Third Volume*, ASTM International, West Conshohocken, PA.

15. Jiang, Y.J. and Darter, M.I. (2005). *Structural Factors of Jointed Plain Concrete Pavements: SPS-2-Initial Evaluation and Analysis*, Report No. FHWA-RD-01-167, Federal Highway Administration, McLean, VA.

16. Karamihas, S.M. and Senn, K.A. (2009). *Detailed Profile Analysis on the Arizona SPS-5 Project*, Transportation Research Board 88th Annual Meeting, Transportation Research Board, Washington, DC.

17. Khazanovich, L., Darter, M., Bartlett, R., and McPeak, T. (1998). *Common Characteristics of Good and Poorly Performing PCC Pavements*, Report No. FHWA-RD-97-131, Federal Highway Administration, McLean, VA.

18. Ksaibati, K. and Mahmood, S.A. (2002). *Utilizing the Long-Term Pavement Performance Database in Evaluating the Effectiveness of Pavement Smoothness*, Mountain-Plains Consortium, Fargo, ND.

19. Kutay, M.E., Weaver, E., and Wiser, L.J. (2007). "Development of Transfer Functions for Spectral Compatibility of Inertial Profilers Used in Long-Term Pavement Performance Program," *Transportation Research Record 2005*, Transportation Research Board, Washington, DC.

20. La Torre, F., Domenichini, L., and Darter, M.I. (1998). *Roughness Prediction Model Based on the Artificial Neural Network Approach*, Fourth International Conference on Managing Pavements, University of Pretoria, Pretoria, South Africa.

21. Lee, D., Chatti, K., and Baladi, G.Y. (2002). "Development of Roughness Thresholds for Preventive Maintenance Action Aimed at Reducing Dynamic Loads," *Transportation Research Record 1816*, Transportation Research Board, Washington, DC.

22. Lee, D., Chatti, K., and Baladi, G.Y. (2002). "Roughness Thresholds for Smoothing Pavements as a Preventive Maintenance Action," *Transportation Research Record 1816*, Transportation Research Board, Washington, DC.

23. Moody, E.D. (1997). "Analysis of LTPP Profile Data for Jointed Concrete Pavement Sections," *Transportation Research Record 1570*, Transportation Research Board, Washington, DC.

24. Owusu-Antwi, E.B., Titus-Glover, L., and Darter, M.I. (1998). *Design and Construction of PCC Pavements, Volume I: Summary of Design Features and Construction Practices that Influence Performance of Pavements*, Report No. FHWA-RD-98-052, Federal Highway Administration, McLean, VA.

25. Park, K., Thomas, N.E., and Lee, K.W. (2007). "Applicability of the International Roughness Index as a Predictor of Asphalt Pavement Condition," *Journal of Transportation Engineering*, *133*(12), American Society of Civil Engineers, Reston, VA.

26. Perera, R.W., Byrum, C., and Kohn, S.D. (1998). *Investigation of Development of Pavement Roughness*, Report No. FHWA-RD-97-147, Federal Highway Administration, McLean, VA.

27. Perera, R.W., Byrum, C., Kohn, S.D., and Richter, C.A. (1997). *Roughness Characteristics of GPS Flexible Pavements in the LTPP Program*, Eighth International Conference on Asphalt Pavements, University of Washington, Seattle, WA.

28. Perera, R.W. and Kohn, S.D. (2002). "Issues in Pavement Smoothness: A Summary Report," *NCHRP Web Document 42*, National Cooperative Highway Research Program, Washington, DC.

29. Perera, R.W. and Kohn, S.D. (2001). "LTPP Data Analysis: Factors Affecting Pavement Smoothness," *NCHRP Web Document 40*, National Cooperative Highway Research Program, Washington, DC.

30. Perera, R.W. and Kohn, S.D. (2006). *Ride Quality Performance of Asphalt Concrete Pavements Subjected to Different Rehabilitation Strategies*, Airfield and Highway Pavements: Proceedings of the 2006 Airfield and Highway Pavement Specialty Conference, American Society of Civil Engineers, Reston, VA.

31. Rahim, A.M., Fiegel, G., Ghuzlan, K., and Khumann, D. (2009). "Evaluation of International Roughness Index for Asphalt Overlays Placed Over Cracked and Seated Concrete Pavements," *International Journal of Pavement Engineering*, *10*(3), Taylor & Francis Ltd., Abingdon, United Kingdom.

32. Raymond, C.M., Tighe, S.L., Haas, R., and Rothenburg, L. (2003). "Analysis of Influences on As-Built Pavement Roughness in Asphalt Overlays, Application Notes," *International Journal of Pavement Engineering*, *4*(4), Taylor & Francis Ltd., Abingdon, United Kingdom.

33. Ritcher, C.A. and Rauhut, J.B. (1989). *SHRP Plans for Nondestructive Deflection Testing in the Development of Pavement Performance Prediction Models*, First International Symposium on Nondestructive Testing of Pavements and Backcalculation of Moduli, ASTM International, West Conshohocken, PA.

34. Saleh, M.F. and Mamlouk, M.S. (2002). "Calibration of a Pavement Roughness Model Based on Finite Element Simulation," *International Journal of Pavement Engineering*, *3*(4), Taylor & Francis Ltd., Abingdon, United Kingdom.

35. Stoffels, S., Lee, W.S., and Bae, A. (2006). *Observed Effects of Subgrade Moisture on Longitudinal Profile*, Transportation Research Board 85th Annual Meeting, Transportation Research Board, Washington, DC.

36. Stubstad, R.N., Jiang, Y.J., and Lukanen, E.O. (2007). "Forward Calculation of Pavement Moduli with Load-Deflection Data," *Transportation Research Record 2005*, Transportation Research Board, Washington, DC.

37. Suthahar, N., Ardani A., and Morian, D.A. (2000). "Early Evaluation of Long-Term Pavement Performance Specific Pavement Studies-2, Colorado," *Transportation Research Record 1699*, Transportation Research Board, Washington, DC.

38. Teomete, E., Bayrak, M.B., and Agarwal, M. (2004). *Use of Artificial Neural Networks for Predicting Rigid Pavement Roughness*, 2004 Transportation Scholars Conference, Iowa State University, Ames, IA.

39. Tighe, S., Haas, R., and Li, N. (2001). "Overlay Performance in Canadian Strategic Highway Research Program's Long-Term Pavement Performance Study," *Transportation Research Record 1778*, Transportation Research Board, Washington, DC.

40. Titus-Glover, L., Owusu-Antwi, E.B., Hoener, T., and Darter, M.I. (1998). *Design and Construction of PCC Pavements, Volume II: Design Features and Practices that Influence Performance of Pavements*, Report No. FHWA-RD-98-127, Federal Highway Administration, McLean, VA.

41. Von Quintus, H.L., Eltahan, A., and Yau, A. (2001). "Smoothness Models for Hot-Mix Asphalt Surfaced Pavements: Developed from Long-Term Pavement Performance Program Data," *Transportation Research Record 1764*, Transportation Research Board, Washington, DC.

42. Von Quintus, H.L. and Simpson, A.L. (2003). *Structural Factors for Flexible Pavements—Initial Evaluation of the SPS-1 Experiment*, Report No. FHWA-RD-01-166, Federal Highway Administration, McLean, VA.

43. Von Quintus, H.L., Mallela, J., Jiang, J., and Buncher, M. (2007). "Expected Service Life of Hot-Mix Asphalt Pavements in Long-Term Pavement Performance Program," *Transportation Research Record 1990*, Transportation Research Board, Washington, DC.

44. Wang, K., Li, Q., Hall, K.D., and Elliott, R.P. (2007). "Experimentation with Gray Theory for Pavement Smoothness Prediction," *Transportation Research Record 1990*, Transportation Research Board, Washington, DC.

45. Wu, Z., Shekharan, R., Chowdhury, T., and Diefenderfer, B.K. (2009). *Development and Implementation of Network-Level Selection of Pavement Maintenance and Rehabilitation*

Strategy: Virginia Practice, Transportation Research Board 88th Annual Meeting, Transportation Research Board, Washington, DC.

46. Yin, H., Stoffels, S.M., and Antle, C.A. (2006). *Profile Data Variability in Pavement Management: Findings and Tools from LTPP*, Airfield and Highway Pavements: Proceedings of the 2006 Airfield and Highway Pavement Specialty Conference, American Society of Civil Engineers, Reston, VA.

47. Zoltan, G., Sidess, A., and Bonjack, H. (1992). "Rational Method for Selecting Maintenance Treatment Alternatives on the Basis of Distress, Structural Capacity and Roughness," *Transportation Research Record 1344*, Transportation Research Board, Washington, DC.

Recycled
Recyclable

HRDI-30/11-12(500)E